Estimation of Rotational Degrees of Freedom Using Spline Functions

By

Alvert Namasamu Ng'andu

B.Eng (UNZA), M.Sc. (Cranfield)

Thesis Submitted to the University of Nottingham for the Degree of Doctor of Philosophy

March

1995

Table of Contents

ABSTRACT

Structural Dynamics Modification work often requires the inclusion of rotational degrees of freedom in the modal data. These are not usually directly measurable because suitable transducers are not yet readily available. This work investigates the estimation of rotations from computed or measured translational data using spline functions for curve and surface fitting.

The estimation accuracy is found to depend on a number of factors including the spatial distribution of data points, the level of error in the original data and the degree of smoothing applied.

Analysis on beam and plate structures shows that an interpolating spline gives the best results on error-free data, but that some degree of smoothing is required when dealing with noisy data. It is shown that structural boundary conditions provide a useful basis for judging the level of smoothing required. For clamped structures, the approximation which minimises the slope at the clamped boundary is found to be acceptable. For free boundaries, the approximation which minimises the second derivative of the fit function there gives the best overall results.

The accuracy of the rotation estimates is found to depend on the general level of error in the original data but is influenced to a much lesser extent by the distribution of error between data points. The errors in the rotations from data with a maximum error of 1% of the largest modal translation are shown to be generally below 10% provided there are at least two measurement points between nodal lines for the highest mode of interest.

As a consequence of the errors in the rotations, the errors in the structural dynamics modification predictions are found to be broadly less than 5% when rotational errors are of the order of 10%. Further, it is shown that estimates of rotations which are within 20% of the correct value yield frequency prediction errors which are under 10%.

Thus, it is concluded that the proposed method is a quick, simple, versatile and effective tool for estimating rotations yielding comparable performance with existing methods on similar structures. An additional benefit is that there is no requirement for performing finite element analyses of the structure.

o0o

ACKNOWLEDGEMENTS

I wish to express my deep and sincere appreciation to many who have contributed to and during the preparation of this thesis.

First, to my Supervisors, Dr E J Williams and Dr C H J Fox, for their invaluable guidance, helpful criticism, instruction, patience and encouragement, all in a very friendly atmosphere, I say "Thank You". In the same breath, my gratitude goes to the Department of Mechanical Engineering at the University of Nottingham for making available the facilities for carrying out the research.

Credit and thanks must also go to the staff at the Cripps Computer Centre, University of Nottingham, for their advice and assistance during the development of the computer software used in the project.

I am further indebted to the University of Zambia for the financial support throughout the duration of this work without which this thesis would not have materialised.

I must also express my heartfelt gratitude to Steve Palmer for making his PC available for my use during the preparation of this thesis.

Finally, to my family, both immediate and extended, who have been wondering when it would all end: Shirley, your love, patience and support throughout were phenomenal; Milimo and Nchimunya, your forbearance when I could not be there for you was simply fantastic; The Thompson family, you gave me a home away from home; and Colette, you are the sister whose love and friendship I shall live to cherish. To you all and many more at Nottingham Central (for the spiritual fellowship), may the Good Lord bless and keep you always.

o0o

TO

MY FAMILY

particularly

my late father, J F Ng'andu; my mother, E M Ng'andu;

my late sisters-in-law, Dr G M Ngwengwe and Mrs I Mweendo

"THE FEAR OF THE LORD IS THE BEGINNING OF WISDOM"

(Proverbs 9:10)

NOMENCLATURE

c	-	coefficient of the spline approximation function
e_y	-	offset in y-direction
e_z	-	offset in z-direction
f_q	-	prescribed function value at point q
g	-	total number of knots in spline approximation function
k	-	degree of polynomial function
m	-	total number of measurement points
n	-	number of degrees of freedom
p	-	number of modes in the database
r	-	mode number of interest
$s(x)$	-	spline approximation function
w_q	-	weighting applied to the measurement point q
x_q	-	measurement point q
$M_q(y)$	-	normalised B-spline function in y-direction
N	-	total number of knots in spline function
$N_i(x)$	-	normalised B-spline function in x-direction
N_x	-	number of knots in x-direction
N_y	-	number of knots in y-direction
S	-	non-negative smoothing factor
$\{P_i\}$	-	force at structural point i
$\{q\}$	-	vector of modal space coordinates in the modal space of the modified structure
$\{u\}$	-	vector of physical space coordinates of the modified structure
$\{v\}$	-	mass-normalised vector of the modal space coordinates in the modal space of the modified structure
$\{x\}$	-	vector of physical space coordinates of the unmodified structure
$\{\delta_i\}$	-	displacement at structural point i
$[a,b]$	-	range upon which spline approximation function is defined
$[c]$	-	modal damping matrix
$[k]$	-	modal stiffness matrix
$[m]$	-	modal mass matrix

$[m_1]$ - modal mass matrix of the modified structure in the modal space of the unmodified structure

$[m_2]$ - modal mass matrix of the modified structure in the modal space of the modified structure

$[\Delta c]$ - modal modification damping matrix

$[\Delta k]$ - modal modification stiffness matrix

$[\Delta m]$ - modal modification mass matrix

$[I]$ - unit matrix

$[C]$ - physical damping matrix

$[K]$ - physical stiffness matrix

$[M]$ - physical mass matrix

$[Q]$ - displacement transformation matrix

$[W]$ - force transformation matrix

$[\Delta C]$ - physical modification damping matrix

$[\Delta K]$ - physical modification stiffness matrix

$[\Delta M]$ - physical modification mass matrix

$[\phi_1]$ - matrix of modal vectors of the unmodified structure

$[\phi_2]$ - matrix of modal vectors of the modified structure

$[\psi_1]$ - matrix of eigenvectors of the modified structure in the modal space of the unmodified structure

$[\Theta]$ - matrix of mass-normalised vectors of the modified structure in the modal space of the modified structure

δ_i - discontinuity jump in the k^{th} order derivative at the interior knot, λ_i

λ - knot in spline approximation function

γ - damping coefficient

θ, ε_q - weighted sum of squared residuals

ω - frequency of vibration

CHAPTER 1

INTRODUCTION

1.1 Dynamic Analysis and Modal Analysis

Historically, dynamics problems have been tackled by using 'rule-of-thumb' approaches in which the complexities of dynamic analyses have been circumvented through over-design. Solutions to vibration problems have therefore generally entailed 'beefing up' the structure [1]. In recent years however, high energy costs and more stringent consumer demands for performance and safety have necessitated the development of structural components that cost less, last longer, and are less expensive to operate, but carry greater loads, vibrate less and run more quietly. In order to be able to predict structural strength and reliability, today's dynamicist must anticipate, determine and satisfactorily control dynamic deflections, loads and stresses.

The dynamic properties of a structure can be defined by specifying either its mass, damping and stiffness distribution (Spatial Model) or its modes of vibration (Modal Model). Spatial Models are time consuming and difficult to formulate and are virtually impossible to verify without performing experimental tests [1]. In addition, the accuracy of the results is highly dependent on the modelling skills of the analyst. The Modal Model, which is usually experimentally derived, is on the other hand of particular importance and attraction to the analyst because its use does not require a knowledge of the physical mass, damping and stiffness distributions of the structure. It also lends itself to easy experimental verification and derivation, allows graphical presentation of the structural dynamic properties and easy comparison of the dynamic properties of different structures. A further benefit is that the effects of structural modifications can be easily investigated using the modal model. However, the modal model suffers from incompleteness due to limitations in the number of modes, the frequency range and the mode shape data which can be practically measured. The investigation which follows is an effort to address the latter of these limitations.

The term 'Modal Analysis' comprises a relatively wide range of research areas and applications but can be defined as the analytical (via the use of finite elements) or experimental analysis of the structural dynamic characteristics of a mechanical system in terms of its modal parameters

[2]. In general usage however, the term is used to refer to the process of extracting modal parameters from test data rather than analytically. The approach is dependent on the premise that the resultant response of a structure is made up of contributions of several individual responses, each contribution being dependent on the coupling between the natural modes of vibration.

Except for diagnostic techniques, it is true to say that, in all cases, the ultimate purpose for undertaking a modal analysis is to obtain a mathematical model of the structure [3,4]. However, the modal properties, besides being directly related to the structure's physical parameters, are useful in such a wide variety of applications that a classification will never be complete. Nevertheless some general fields of application will include [1,3,5-8]:

1. identification and evaluation of unexplained phenomena (trouble-shooting excessive vibrations),
2. verification, correlation and correction of analytical models,
3. structural integrity monitoring (as a non-destructive technique to assure structural integrity or to detect hidden faults),
4. development of dynamic models for use in active control algorithms,
5. development and validation of analysis procedures,
6. determination and prediction of dynamic forces or responses, and
7. generation of modal models for use in predicting the effects of modifications to the original structure.

The quality and quantity of the data taken from a modal test therefore depend on the subsequent use of that data. Some applications are more demanding in terms of the accuracy and completeness required than others. For comparison and correlation type applications, only accurate estimates of natural frequencies and descriptions of the mode shapes with just sufficient detail and accuracy to permit identification and correlation are required. Sub-structuring and predictive type applications, on the other hand, require accurate modal parameters and have the added constraints that the model should include all the coordinates of interest and should not be confined to certain individual modes since out-of-range modes will influence the behaviour of the structure in a given frequency range of interest [3,5,9]. The effect of error in the modal data in predictive type applications is an integral part of this study.

Significant advances in the area of modal analysis have been made over the past fifty years. The volume of this activity has increased over the last ten to twenty years in parallel with, and as a direct result of, the increase in the numerical capability available to both analysis and test. During this period, modal analysis has evolved from the role of verifying finite element models to the role of providing the modal database for predicting the dynamic characteristics of modified structures [10-12]. However, there are still significant problems which limit the use and accuracy of modal analysis in this role [13].

One of the most important considerations in a modal test is the number and selection of coordinates used. In the higher-level applications, the choice of the coordinates is dictated by the configurations of any modifications or attached components and is not simply a matter of including sufficient coordinates to generate a helpful display of the mode shape itself. In these applications, all coordinates at the points where attachments or modifications will be made must be included, and this means in the rotational as well as translational directions. Vibration is transmitted by moments as well as by forces, and compatibility in angular displacements must be maintained at junctions just as much as in translations. Not only are 50% of all coordinates rotations, but 75% of all frequency response functions involve rotational coordinates [8]. While the omission of such rotational information is not a restriction in the lower-level applications, it is crucial in the higher-level applications where the effects due to moments and rotations need to be included if the analysis is to be realistic [14]. Thus, the work contained in this thesis is aimed at addressing this limitation in modal analysis.

Another problem which limits the use of modal analysis is the assumption that damping in a system is proportional to mass and stiffness. However, it is known that some structures, such as rotating machinery, exhibit non-proportional damping and this leads to error in making predictions. This limitation is however not addressed in this work.

Although theoretically, a structure has an infinite number of modes, only a finite number of modes can be experimentally obtained. Therefore any higher-level application must use a truncated data base which will inevitably lead to some level of error. This problem has however received the attention of a large number of researchers [15-23] and is still an active area of investigation and is therefore not dealt with in this study.

1.2 The Present Study

1.2.1 Background to the Problem

The three basic assumptions that are made in order to perform an experimental modal analysis are linearity, time invariance and observability. While the linearity and time invariance assumptions have historically received the most attention, it is only recently that there has been increased activity in work related to observability. Observability means that the input-output measurements contain enough information to generate an adequate behavioral model of the structure [6]. This is particularly relevant since test data always describes an incomplete model of the structure as evidenced in at least three different ways. First, the data is normally limited to a minimum and maximum frequency as well as limited frequency and amplitude resolution. Second, the placement of the exciters and sensors must be adequate to spatially define the mode shapes independently from one another. Third, until very recently, no information has been available relative to local rotations due to a lack of suitable transducers.

The estimation of rotations has attracted increasing attention over the past decade. Traditionally, rotations had been estimated by measuring the translation of two closely spaced points [3]. The procedures involved were quite demanding, not least because they required the acquisition and subsequent processing of many different measurements made at different times and were therefore prone to error. Over the years, more elaborate techniques have been articulated. These have been dominated by two procedures namely, dynamic condensation and expansion methods which depend on the development of large finite element models of the structures [24-28] and therefore require large amounts of computation and are costly, and linear polynomial interpolation of shape functions [24,29-31]. The latter does not require a finite element model of the structure and also allows estimation of rotations (and translations) at any location on the structure without the need for additional measurements and is therefore simple, quick and cost effective. The use of this technique has however not realised its full potential due to the inability of polynomials to produce acceptable estimates of rotations for modes with complex mode shapes. In addition, there is no information available on the optimum spatial distribution of points to yield the best results. Further, although most structures can be analyzed in straight lines locally, there are some complex structures for which this simplification does not hold.

It must also be realized that work on transducers that permit the measurement of angular displacements has continued [32,33] and at least two prototypes have been successfully used by

several researchers [34-38]. However, not only is the knowledge and expertise in the use of these transducers in its infancy, they are also very expensive to acquire. In addition, if all degrees-of-freedom are measured as a matter of routine, it doubles the size of the problem. Although the task can be reduced if the locations at which the rotations are required are known before hand, this information is usually not available.

1.2.2 The Problem

The work detailed in this thesis discusses the estimation of rotational degrees-of-freedom using cubic B-spline curves and surfaces. The key questions which are addressed are:

1. **How accurate are the estimates of the rotations from the spline functions?** and

2. **What are the effects of errors in the rotations on the accuracy of the predictions of dynamic changes following structural modifications?**

Particular attention is therefore paid to the parameters which affect the performance of the fitters such as the selection of the coordinates, the optimum spatial distribution, the level of smoothing required and the level of error in the initial data. The question of the level of smoothing required is of particular importance since published work has concentrated on interpolation type approximations for estimating rotations..

The acceptability of the estimates of rotations thus obtained is investigated by performing structural dynamics modification predictions for a variety of case studies. In all cases, the effect of any errors in the estimates of rotations on the modal predictions is gauged by comparing the predictions based on the expanded databases with predictions based on exact or finite element rotations. In this way, other sources of error in the predictions are excluded. From the results of the analysis, guidelines on the optimal use of the proposed technique of estimating rotational degrees of freedom are formulated.

1.3 Lay-out of the Thesis

The remainder of this thesis is presented in five chapters.

Chapter 2 surveys the literature in the area of estimating rotations. The principles and techniques used hitherto are discussed in detail and their merits and demerits outlined. This not only provides a historical perspective, it also gives the current-state-of-the-art in this area. Thus, the place of the present work in the general body of knowledge in this area is established.

Chapter 3 deals with the theoretical development of B-splines and their application to the problem at hand. Only the relevant detail for the application at hand is presented. Subsequently, a discussion of the software which is developed is presented in the appendices.

Chapter 4 discusses the accuracy of the estimation of rotations and outlines the parameters required for optimum performance of the estimation technique for both curves and surfaces. Estimates of rotations obtained from error-free and noisy data are compared with corresponding exact or finite element data for beam-type and plate structures.

Chapter 5 presents a detailed discussion of the effects of errors in the rotations on the accuracy of the predictions of dynamic changes following structural modifications. Modifications used include lumped masses, springs and rib stiffeners. A brief treatise of Modification Theory is also presented.

Finally, Chapter 6 presents the guidelines for optimum performance of the proposed technique and summarises the general conclusions of the study. In addition, the chapter highlights some aspects which require further investigation.

o0o

CHAPTER 2

LITERATURE REVIEW

2.1 Introduction

Modal analysis began in the early days of the space program in the United States in the 1950's and grew out of the field of Mechanical Impedance Measurement based upon analogue, narrow-band spectrum analysis [39]. During the last two or three decades, the technique has become a popular and established tool for analysing structural dynamic behaviour in various industries. Among these, the aerospace and automotive industries have probably received the most attention followed by power generating facilities, offshore structures and various technologies including computers, railroad, nuclear power plants, and building for earthquake resistance. National and international research organisations and academic institutions have, however, been the major driving force behind new developments. The rapid growth and development of the subject has therefore generated an enormous quantity of literature, software and equipment which is now available to anyone wishing to use the technique. Even for those closely involved with the developments themselves, it has been very difficult to digest all the information and new ideas as they have emerged. For the relative beginner, the task of "keeping up" has been formidable indeed! [8].

This chapter will therefore not endeavour to give a detailed review of the enormous volume of information on all the many aspects of modal analysis which exists and is being generated today, but will concentrate on a review of the relevant literature in the area of estimating rotational degrees of freedom. The review will not only strive to provide a historical perspective to the subject, it will also give the current state-of-the-art in this area. Inadequacies which the present work is intended to fill will also be highlighted.

2.2 Methods of Estimating, or Obviating the Need for, Rotations

For years, experimental modal analysis (EMA) has had a number of deficiencies which make it difficult to compare its results with those of the analytical modal analysis. Not only has this made the utilisation of EMA results difficult, it has also made justification of

EMA impossible in all but the most important problems [39]. One of the most important of these limitations has been the absence of rotational degree of freedom information in experimentally derived data bases which has, in the first instance, severely limited the incorporation of more sophisticated elements, such as beams and plates, in structural dynamics modification (SDM) efforts. In the second instance, the lack of a means of adding the deficient angular degrees of freedom to the modal vectors has meant that finite element analysis (FEA) and EMA data bases are inconsistent.

When applying structural dynamics modifications which can be represented as point masses, or as linear, pin-jointed spring or damper elements, only a knowledge of the translational degrees of freedom is required and data from a conventional modal survey will suffice. However, structural modification procedures which use beam or plate elements require the inclusion of rotational degrees of freedom (RDOF) at structural attachment points to effect moment coupling.

Until recently, experimentally based modal models had been restricted to contain only translational degrees of freedom (TDOF) due to lack of appropriate sensors. While several commercial SDM systems contained provisions to utilise RDOF, few researchers and analysts used these facilities since it had not been possible to transduce the required measurements. Because rotations can be measured or calculated, a number of techniques have been developed to overcome the problem of the missing RDOF.

2.2.1 Analytical Techniques

Rotations have for a long time been estimated by measuring the translation of two closely spaced points [3]. The difference between these measurements divided by the distance between the points gives an estimate of the required rotation. The procedures involved are quite demanding, not least because they require the acquisition and subsequent processing of many different measurements made at different times and are therefore prone to experimental error. Furthermore, if the sites for the proposed modification are not known when the modal survey is performed, an additional translation needs to be measured for each RDOF with a consequent significant increase in the test time.

Special rib elements which span three points but couple only the translational freedoms have been derived [40]. This avoids the need for rotations and can provide acceptable accuracy (typically, less than 10% error in the frequency predictions) for trouble shooting purposes. However, it has been shown that more accurate predictions require the inclusion of the rotational freedoms in the modal data base.

In 1984, Yasuda et al [13] reported on a mass additive technique for the estimation of RDOF in which a rigid mass was added to the structure at the point of interest. The rigid body motion of the added mass was measured using six or more independent translational transducers. A least-squares procedure was then used to compute the rigid body motions from which the rotational and translational degrees of freedom were estimated at the attachment. Results from two applications yielded large errors (in excess of 100%) in the estimation of the rotational freedoms. These errors were attributed to modal truncation and mode coupling (or repeated roots).

An approach proposed by Martinez et al [41], involves predicting the RDOF using a finite difference approximation with synthesized frequency response functions at the proximate data points. Although the approach minimises the inaccuracies due to noisy data, the errors due to transducer size remain appreciably large. Thus, attempts to include RDOF from translational data by interpolation or beam additions can be successful only if extreme care is taken to minimise the effect of transducer size and weight [42].

The task of expanding measured mode shapes using analytically-derived properties has been the subject of a number of previous investigations and three different routes can be identified. The first approach (route 1) for mode shape expansion uses the mass and stiffness matrices of the analytical model to compute the missing degrees of freedom in the measured mode shape. This approach is equivalent to an inverse Guyan reduction where the slave coordinates are recovered in terms of the masters. The second route relies on the assumption that the measured mode shapes can be expressed as linear combinations of the predicted ones. The third alternative (route 3) involves the interpolation or extrapolation of the measured degrees of freedom to those of the full model.

O'Callahan, Lieu and Chou [24] have articulated several procedures for estimating rotational degrees from translational data of a model obtained from either an experimental modal test or an analytical finite element model. The procedures are grouped into two categories, namely; dynamic condensation/expansion methods (route 1 above) and polynomial interpolating shape functions (route 3 above). They argue that it is good practice to develop a finite element model of the structural system and that since such a model contains a much greater number of degrees of freedom than the number obtaining in a test, the system of equations can be condensed to a reduced set of degrees of freedom at which measurements will be made. For such a finite element method (FEM) model, the same condensation matrix can be used as an expansion matrix to generate RDOF at any specific node on the structure.

If a FEM model is not available, then a polynomial interpolating shape function can be used to estimate the desired RDOF. The discourse by O'Callahan et al [24] includes the following procedures:

.The dynamic condensation/expansion procedure in which the active degrees of freedom and the non-existent (desired) degrees of freedom are related by a transformation matrix which is dependent on frequency in a condensation process similar to the standard Guyan condensation procedure. The technique tends to work well in representing the mode shapes for a condensed system giving a maximum error level of less than 2.5% in RDOF estimation.

.The static condensation/expansion procedure. Here the condensation procedure is based only on the stiffness matrix and therefore the matrix transformation process is based on the elastic strain energy of the system. The resulting transformation matrix develops Guyan mass and stiffness matrices which represent a reduced/condensed model of the original system and can be used to expand all modal vectors to include the deleted (desired) degrees of freedom. The errors in the RDOF estimates are typically less than 4%.

.The substructuring model procedure. The procedure involves developing a sub-model of the region where the RDOF are to be determined using the FEM

substructuring element technique. Similar equations to those for the condensation/expansion process can be developed for the assembly of elements constituting the substructure (the super-element) for which condensation is performed on the internal degrees of freedom. The difference in this case is that the deleted degrees of freedom are related to a limited set of active degrees of freedom as well as a set of degrees of freedom at the boundaries of the element. This method is theoretically expected to produce similar RDOF estimates to those produced by the static condensation/expansion procedure above.

.Interpolating polynomial procedure. This procedure uses functions similar to the shape functions defined in finite element formulations of the mass and stiffness matrices that are used in the condensation/expansion estimation procedure. The approximation of RDOF thus produced is local, that is the approach becomes similar to the substructuring element approach but using only a line shape function which is differentiated. The procedure does not need a FE model of the structure and a RDOF estimate can be made at any location on the structure without the need for additional measurements.

From experimental investigations involving beam and plate structures, the authors conclude that the dynamic condensation/expansion procedure produces the best results when the FEM and experimental models are "fairly well tuned" to each other. Similar conclusions are made for the static condensation/expansion technique as the rotational inertia effects are very small, especially in a "very crude mesh" model. Both methods however require FEM models and large amounts of computation. Although the substructuring/shape function technique does not produce as good results as the first two methods (errors rise up to about 5% for the higher frequency modes), it requires a smaller amount of computational effort to compute the local RDOF. This is its best asset. The shape function technique is found to be adequate (up to about 18% error in RDOF estimates) and relatively efficient for the estimation of RDOF especially for the lower modes. It is however generally concluded that all the methods tend to produce poorer results as the frequency or mode number increases.

In 1986, O'Callahan et al [25,26] suggested another technique which involved developing a finite element model of the structure which was then combined with measured translational data to approximate a combined modal database of rotational and translational degrees of freedom. The method uses the modal matrix from the FE model and the experimental model to form an expansion matrix for the estimation of all system degrees of freedom relying on the assumption that the measured mode shapes can be expressed as linear combinations of the predicted ones (route 2). Measured translational data is used to generate rotational along with additional unmeasured translational degrees of freedom. The technique is fundamentally an expansion process from an equivalently reduced eigen-system obtained only from the active degrees of freedom of the experimental system to all system degrees of freedom. Experimental validation of the procedure revealed that the process produced "extremely good" results (up to 12% error in the rotation estimates) in estimating unmeasured TDOF and RDOF in the SDM procedure using a generalised beam (up to 2% error in the SDM predictions). The associated time and cost may not, however, be justified for many applications.

Lieven and Ewins [27] have evaluated three techniques of expanding experimental data to the full coordinate system of the analytical model; namely 'modeshape', 'MAC' and Kidder's technique. Their work has shown that the 'modeshape' expansion technique as proposed by O'Callahan et al above [25,26] can result in inaccurate expansion (based on a Modal Assurance Criterion (MAC) [43] comparison of the expanded and original (complete) data) given poor initial correlation between the analytical and experimental modeshapes. The 'MAC' expansion technique involves calculating the MAC between the measured and the analytical modes, adjusting the phase of each analytical mode to match its experimental counterpart, scaling the analytical eigenvectors to the same magnitude as the experimental ones, and applying the transpose of the MAC matrix to the phase adjusted, scaled analytical degrees of freedom to generate the unmeasured freedoms. The results have shown that it can be used to expand lower order modes and rotations accurately (MAC values were at least 0.950). However, further rationalisation is required to improve the expansion of the higher order modes. Kidder's technique (route 1), a physical expansion method which is effectively derived from an inverse Guyan reduction, has been shown to give the most consistent results for expansion (i.e., unit MAC values) although its accuracy depends on the validity of the original model and the ratio of master to slave degrees of freedom. However when either the

'modeshape' or 'MAC' technique is implemented, the user can choose to use either smoothed or 'raw' data in the master coordinates - an option which is not available when using Kidder's method.

A subsequent study [28] of the two techniques based on finite element data (Modeshape and Kidder's), which attempted to define their validity boundaries, revealed that while the quality of the expanded mode shapes seemed to be case-dependent, the modeshape technique had several advantages over the physical expansion method: there was no need to store global mass and stiffness matrices and the CPU power and storage requirements were several orders of magnitude smaller. In addition, the modeshape method was shown to work best for one dimensional structures with well-separated modes. However, although random errors did not seem to affect the quality of expanded mode shapes adversely, the complexity of a mode shape was a significant adverse factor for the quality of expansion.

It will be noted that the methods of estimating rotational degrees of freedom cited in references [24-28] stem from the area of model updating or tuning. The methods are thus seen to be indirect techniques since the object of model updating is to modify FE models in order to improve their correlation with test data. Thus, although there is a plethora of model updating techniques, the quality of the estimates of rotations which derive from them is generally only implied since the comparison indicators which are used (such as the MAC, orthogonality checks or FRF comparisons) do not explicitly indicate the accuracy of the estimates from point to point.

Mitchell-Dignan and Pardoen [29] further investigated the estimation of RDOF by using FE shape functions or interpolating polynomials according to FE methodology in conjunction with the modal parameters of the unmodified structure (route 3). One and two dimensional shape functions were used to estimate the translational and rotational degrees of freedom at any given location on a structure. Three types of elements were presented; namely a colinear element which utilises five colinear reference nodes, and two plate elements which use four and eight reference nodes respectively. Experimental tests showed that a refined nodal mesh is required for "RDOF estimates within realistic limits". The results indicated that the four node element produced the largest errors (typically up to 70% about the x-axis and 100%

about the y-axis) whereas the 8-node plate element (up to 32% about the x-axis and 60% about the y-axis) and the colinear element (up to 22% about the x-axis and 37% about the y-axis) produced much lower error levels. The errors in the predictions of the effects of rigidly attaching a rib to the plate were, in the main, less than 10% for all three types of elements thereby indicating that the predictions were not very sensitive to the errors in the rotations. It was also noted that an under-estimation of the RDOF resulted in a corresponding under-prediction of the modified frequencies.

Based on the third expansion alternative, a spatial curve fitting technique has been developed at Nottingham University [30]. In the technique, measured translational modal vectors are fitted with cubic and quadratic polynomials to provide local approximations to the mode shape function. The polynomial functions are then differentiated to give the required rotations. The method has been applied to structures made up of flat surfaces in which translational mode shape data had been measured on a rectangular grid. The fitting is carried out to groups of four adjacent points and the rotations are averaged at points where several fits provide individual estimates. In the three-dimensional case where the surface in question may not be aligned to the global axes, it is suggested that local axes can be defined which allow the two dimensional analysis to be employed. A simple coordinate transformation would then yield the required global rotations. The method has similar advantages to the interpolating polynomial procedure and it is also simple, quick and cost effective. Results from tests show that the accuracy of the RDOF estimate depends on the density of the original displacement measurements and also that the estimate improves with an increase in the number of measurement points between nodes. The tests suggest that an error of about 15% will be incurred if there are two dimensional points in between nodes, but that this drops to less than 5% if the density is increased to three measurement points between nodes. It is also shown that frequency predictions following a modification are relatively insensitive to errors in calculated rotations (at least for the cantilever and plate structures used in the tests). Although there are relatively few examples of this technique being applied to structural dynamics because of the problems associated with complex spatial descriptions and sudden changes of geometry, the main limitation is that polynomial fits are unable to produce acceptable rotations, and therefore acceptable modification predictions, for the more complex higher frequency mode shapes.

In 1986, Haisty and Springer [31] presented a method of estimating rotations which uses third-order spline curves to approximate the deflected shape of a vibrating structure. In the method, the classical boundary conditions for beam elements (i.e., fixed, pinned and free) were incorporated into the equation set and the rotational contributions to the deflection curve were obtained by differentiating the resulting spline curve equation. Although the method is both easy to apply and accurate, the paper reported the performance of the method for the first mode only. The performance of the technique for the more complex higher frequency modes is therefore not known and neither is the acceptability of the resulting rotations for the prediction of structural dynamics modification efforts.

In a more recent study, Waters and Lieven [44] have applied a modified surface spline to smooth out noise from measured data prior to expansion. Expansion was performed in conjunction with correlating analytical modes (from an FE model) on the basis of the mode shape disparity (indicated by the Modal Scale Factor) between the measured and analytical modes. The technique was developed for application to sparsely defined databases for which the results indicated that the modified surface spline was an "effective means" of expanding and smoothing experimental modeshapes. It is thus clear that surface splines were not used as a stand-alone technique for estimating rotations in this technique.

Other researchers [45] have suggested the use of a "rigid body mode enhancement method" in which RDOF are obtained by treating the part of the structure where the RDOF are required as a rigid body. In this way dependent degrees of freedom (which may be impossible to measure or may be required after performing the modal test) can be generated using constraint equations and a least squares solution technique as a post-processing technique which obviates the need for a FE model. The estimates of the RDOF gave a root mean square (RMS) error of 4.52%. This level of error was accompanied by a significant reduction (up to 80%) in the off-diagonal terms of the MAC matrix after processing by the proposed technique. The authors have therefore concluded that "good estimates" of rotations are obtained.

2.2.2 Experimental Techniques

Although translational measurements of dynamic response had dominated experimental modal analysis, a transducer that permitted the measurement of angular acceleration with similar ease was recently developed [32]. The transducer reported in this work was a product of the piezoelectric beam technology and is called the Translational-Angular Piezobeam (TAP) accelerometer. Evaluation of the functionality of the transducer revealed that it performed well and produced data which is qualitatively comparable to that obtained from translational transducers. The tests also revealed that alignment of the transducer in the correct measurement orientation was critical and had to be very precise to ensure consistency and precision.

In a separate effort to demonstrate the utility and limitations of the new transducer, Lang [34] concluded that although the new equipment is "very good", there was still a lot to be learnt in order to fully exploit it. Its utilisation was, in the opinion of this researcher, also seriously affected by the upper frequency limit of 2000 Hz. Results also showed that including rotational degrees of freedom during an initial modal search improves the odds of identifying all of the modes characterising a given bandwidth.

Other researchers [35,36] have since used the new equipment for model improvement and verification of the theoretically estimated rotational entries of mode shapes. The results have once again confirmed the potential of the new equipment.

In a more recent effort, Cafeo et al [33] have reported the development of a novel non-contacting measurement approach capable of simultaneously sensing one dynamic translation and two dynamic angular rotations. The system, based on the positional measurement of two collimated light beams reflected from a planar target, has been called the three-degree of freedom laser vibrometer. An evaluation of the transducer's dynamic performance in a modal test environment demonstrated the system's ability to produce high quality time and spectral data.

Subsequent work on the measurement and application of experimental rotational degrees of freedom for mode shape refinement using the data from the laser vibrometer has been

reported [37]. In the work, the authors have investigated several methods for combining the estimated translation and rotation data to refine the description of the mode shapes based on an integration method which used polynomial curve fitting methods incorporating both translational and rotational residues at each measurement point to define the mode shapes. The work reports the results of analysis performed on a cantilever beam. With regard to the accuracy of the estimates of the rotations from 5th order polynomial global curve fitting, their results showed that significant errors (rotation RMS errors of 0.479 for mode 1 and 0.369 for mode 2, where the RMS error is an average type of error indicator) may arise when trying to estimate rotational degrees of freedom from polynomial mode shapes developed from experimental translations. The results qualitatively implied that small amounts of noise in the translation were seen to produce large errors in the derived rotations. They therefore concluded that estimating rotations from noisy translational data may be "suspect unless the residue values are highly accurate and virtually noise free". On the other hand, including rotational data with the translational data in the fits yielded significant improvements in the estimates of rotations, namely 86% for mode 1 and 72% for mode 2, compared with simply using translations. Estimates of rotations from cubic spline interpolation gave a 9% improvement in mode 1 and a 13% degradation in the estimates when compared with estimates from 5th order polynomial global curve fitting thereby suggesting that the fit functions were picking up a lot of the noise from the initial data. Third order polynomial curve fitting with the rotational data included in the fits was seen to yield poorer results (52% and 67% degradation for modes 1 and 2 respectively when compared with the results from 5th order polynomial curve fitting) than those obtained from cubic spline interpolation. However, this effort did not consider the benefits of estimating rotations from noisy translations using a smoothing approximation. The sensitivity of modification predictions to such an approximant is therefore still not understood. The application of measured rotations to the prediction of structural modifications with beam elements however demonstrated that the data provided by the three-degree of freedom laser vibrometer was sufficiently accurate for the structural dynamics modification method to work well [38]. Notwithstanding the potential of the transducer, the capital outlay required for its acquisition may not be justified for some applications and establishments.

2.3 Key Points from the Literature Review

This chapter has discussed several techniques of estimating, or obviating the need for, rotations. The key points can be summarised as follows:

1. Although special elements which circumvent the need for rotations have been derived, more accurate SDM predictions require the inclusion of the rotations in the modal data base.

2. Recent developments in experimental techniques of including the rotations yield data which is sufficiently accurate to give acceptable SDM predictions. However, there are two main limitations:

   (a) In the case of the Translational-Angular Piezobeam transducer, the upper frequency limit is only 2000 Hz.
   (b) In the case of the laser vibrometer, the capital outlay required for its acquisition may not be justified for the majority of applications and establishments.

3. Three different routes, for each of which several techniques have been developed, can, in the main, be identified for analytically expanding measured mode shapes:

   Route 1. This method uses mass and stiffness matrices of the analytical model to compute the missing degrees of freedom and is equivalent to an inverse Guyan reduction.

   Route 2. This route relies on the assumption that the measured mode shapes can be expressed as linear combinations of the predicted ones.

   Route 3. This involves the interpolation or extrapolation of the measured degrees of freedom to those of the full model.

(a) Evidence from literature suggests that while all three routes generally give acceptable data, route 2 gives the best results, followed by route 1 and finally route 3. However, the time and cost requirements for route 2 techniques may not be justified for many applications.

(b) The main limitation for route 1 is the requirement for large amounts of storage and computation due to the need to store global mass and stiffness matrices.

(c) Route 3 does not require FE models and is relatively efficient for the estimation of RDOF especially for the lower modes. It therefore holds the best chance for the development of a relatively simple but quick and cost effective technique.

(d) All analytical methods tend to produce poorer results as the frequency or mode number increases.

(e) Techniques based on route 3 have not considered the estimation of rotations using smoothing approximations. In addition, and as far as this researcher is aware, only interpolants have been investigated.

2.4 Contribution to Knowledge of the Present Study

From the foregoing discussion, it is clear that although the advent of a transducer capable of measuring rotational freedoms may change the conventional experimental modal analysis technique, there still is a need for a simple and quick post measurement technique that can be used to generate the missing data as, when and where required. One technique which has shown such potential is the curve fitting approach. This work is therefore an effort to extend the capabilities of estimating rotations and any missing translations from translational modal data using curve or surface fitting. The ability to estimate rotations using surface fitting is of particular interest since except for one or two references, the majority of the work available in the literature reports analysis on beam-type structures while claiming that the methods can also be used for plate-type structures. The investigation will concentrate on spline functions and will endeavour to establish the validity boundaries with regard to the estimation of rotations and their acceptability in predicting structural dynamics modification efforts.

o0o

CHAPTER 3

CURVE AND SURFACE FITTING

3.1 Introduction

Curve fitting is concerned with the mathematical representation of smooth continuous relationships between one physical variable (the dependent variable) and another or others (independent variable(s)). Curve fitting is itself a term used to refer collectively to interpolation and approximation [46]. The problem of interpolation is finding a mathematical curve or surface that passes exactly through a set of prescribed points, whereas the problem of approximation is finding a curve or surface that passes near a set of points (or is representative of some underlying relationship). In a mathematical sense, interpolation problems are probably easier to solve, but in a practical sense approximation is generally more important.

Curve fitting problems occur in many scientific and engineering applications which may be theoretical or experimental. There is however no general rule for assigning a specific function to a data set. The data must therefore be studied critically, and here the standard texts give little guidance beyond stern warnings to be cautious. It is not caution that is missing however, boldness in conjecture and persistence in follow-up are much more important [47].

Generally, many functions could represent a data set, but the user must often decide the most suitable function in accordance with some criteria [48]:

.Well-known functionality. In some cases the mathematical relationship between variables is well-known.

.Graphical representations. In the case of correlation functions of one (or two) independent variables, it is very useful to plot *y vs x* on cartesian, semilogarithmic or logarithmic coordinates. The curve shapes are then compared with elementary standard functions and often the most suitable function is selected.

.Statistical criteria. When a fitting function is chosen and the correlation is performed, statistical parameters allow consideration of the validity of the fit. Parameters such as deviations, correlation coefficient, significance tests, can be used.

In a typical curve fitting exercise, there exists an array of data that is to be represented mathematically by some analytical function. It is generally expected that fitting will provide information both about the equation constants estimated and about the limitations on future use of the equation with these constants.

This chapter deals with requirements and criteria for curve and surface fitting and the choice of functions for the problem at hand. The theoretical background of spline functions, on which the work reported in this thesis is based, is also discussed. An overview of the implementation of splines to the problem of estimating rotational degrees of freedom, which is the major thrust of the work, and the subsequent software development is also given.

3.2 Criteria for Curve and Surface Fitting

Certain considerations must be made before the choice of an appropriate curve fitting technique for a particular problem is made. There are no universal answers here but the technique chosen should depend on the nature of the data, the nature of the phenomenon modelled (as far as it is known), and the characteristics of the technique considered by the user to be the most important [48]. Some of the general characteristics include:

1. **Differentiability of the fitted curve.** This is a measure of the smoothness of the fitted curve. A curve is 'very smooth' if it has 'many successive derivatives at every point'.
2. **Confidence in the data.** If the user has sufficient confidence in his data to demand that the fitted curve must contain (or interpolate) every data point, then he must focus on interpolation schemes for his fits. If on the other hand, there is a sizeable experimental error that enters in a random way which if possible should be smoothed out of the fitted curve, then judgement is to be exercised in assessing the degree of smoothing to be applied and the choice of smoothing procedure. This aspect is dealt with in more detail in later parts of this work.

3. **Global versus local techniques.** If the data at a given point influences the nature of the fitted curve at distant points then the fitting technique will have to be global rather than local. This depends on the user's knowledge of the physical phenomenon being modelled and on the density of data points.

4. **Computational effort.** This is easily understood and its significance will depend on the magnitude of the computation involved. Generally, it is clear that, for either spline or polynomial techniques, the computational effort increases rapidly with the degree of the fitted curve. In addition, fitting techniques that are local in nature will generally offer significant computational advantages over global techniques.

5. **Convergence.** This is a consideration that is much more for the mathematician than anybody else. However, the study of convergence does give valuable insights into curve fitting problems and can provide some further information on the choice of procedure. While convergence is of greater importance in approximation work than it is in interpolation, there is generally a trade-off to be considered between the rate of convergence and the volume of computation.

6. **Visual criteria.** In some applications, such as the one treated in this work, a major difficulty in designing curve and surface fitting techniques is the formulation of clear criteria for acceptability. In such cases, a graphic display of a fitted curve can be utilized to apply visual criteria after which the curve can then be modified accordingly.

3.3 Fitting Functions

In any study of curve and/or surface fitting there is one class of functions that play a supremely important role. Polynomials are used for approximation because they can be evaluated, differentiated, and integrated easily and in finitely many steps using just the basic arithmetic operations of addition, subtraction and multiplication [49,50]. Polynomials are ideal for representing relatively uncomplicated relationships, and (at least for polynomials of low or moderate degree) yield compact representations of the data. However, if the function to be approximated is badly behaved anywhere in the interval of approximation, such as sudden changes in curvature, then the approximation is poor everywhere [50]! This is one

of the essential limitations of polynomial approximation. Also, for more complicated relationships one is usually tempted to increase the degree of the polynomial in order to improve the fit. 'Higher degree' does not, however, necessarily mean or equate to 'good' as values of the higher degree polynomials exhibit oscillatory behaviour and large swings [49]. In addition, there may not be sufficient data to determine all the coefficients properly, and thus the effort of calculating the polynomial is increased and the tendencies towards unboundedness are exacerbated. In their work on curve fitting with polynomials, Cox and Hayes [51] have, as a very rough general rule, indicated that the degree of the polynomial to be fitted should not be taken above a value equal to half the number of data points. Therefore polynomials are really quite inappropriate for general use as approximating functions [52].

Lancaster and Salkauskas [49] have indicated that one way of avoiding high-degree polynomials is to join adjacent pairs of data points (or knots) with polynomials of some degree, different from point to point, perhaps, and to make sure that where these join, a certain amount of smoothness (the function and many of its derivatives are continuous across these knots) is achieved. These **piecewise polynomials** or **splines** offer greater hope for success. Among the many advantages of spline approximation is local control of the curve which allows modification of a data point with only a small region of the curve affected. Another important consideration is that such representations are more numerically stable and are usually computationally efficient since they require a lower degree polynomial for the same fit performance. For these reasons therefore, this work uses splines as the fitting functions.

The precision of spline approximations depends mainly on the choice of the number of knots and their locations. It might be expected that one can approximate the true (but unknown) response function as closely as possible by adding more knots. For measurement data, however, this is not necessarily true. As the number of knots increases, deviations between spline estimates and measurements will decrease accordingly. However, as the dimension of the spline approaches the number of data points, the accuracy of the function approximation decreases since the function will tend to reflect the errors associated with the measurement. Thus the number of knots used in approximations must be limited to avoid the problem of

overfitting [53]. In addition, for a specified number of knots, the accuracy of spline approximation is also influenced by the distribution of knots [50] as is shown later.

3.4 Theoretical Development of Splines

Polynomial spline functions (or simply polynomial splines or splines) have diverse application. They have been used to provide solutions to mathematical problems in interpolation, data and function approximation, ordinary and partial differential equations, and integral equations in many scientific and engineering applications including instrumental calibration, sonar signal analysis, highway visualisation, terrain following, computer aided design and plant growth analysis [54]. A more recent application has been in the extraction of rotational degree of freedom information from modal test data [31,55]. As a result of recent improvements in measurement techniques using laser velocimetry [32,33], spline surfaces have found application in smoothing the measured data in order to improve the quality of the data. The data thus processed is subsequently used for model updating in modal analysis [56] (thus ensuring better FE modelling) and in mechanical intensity (power flow) computations in which the velocity fields are represented as spline surfaces [57].

In the 1970's, the use of splines transformed approximation techniques and theory because of their suitability and convenience for computer calculations. In more recent years the availability of computationally efficient routines has greatly contributed to their popularity. One of their most desirable properties is that they provide optimal theoretical solutions to the estimation of functions from limited data and give good balance between smoothness and flexibility. Moreover, it has been shown that splines occur naturally in the analysis of many approximation methods [52].

3.4.1 Representation of Spline Functions: *B*-Splines

While a polynomial spline of degree k is generally understood to be a kind of piecewise polynomial function of degree k on some (finite or infinite) interval with $k-1$ continuous derivatives there [50], the question of representation, especially in computational dealings, is of primary importance [54]. Splines can be represented in terms of a basis (i.e., as a linear combination of certain basis splines, just as polynomials can be expressed as linear combinations of certain basis polynomials such as Chebyshev or Legendre polynomials).

Such a representation is used in preference to the redundant one consisting of a set of polynomial pieces together with continuity conditions at the joints.

Only three kinds of bases for spline spaces have actually been given serious attention; those consisting of truncated power functions, of cardinal splines and of *B*-splines. Truncated power bases are known to be open to severe ill-conditioning [54], while cardinal splines are difficult to calculate [49,52]. By contrast, bases consisting of *B*-splines (which are linear combinations of the truncated power functions) are well-conditioned at least for up to the twentieth order [54]. Such bases are also local (compact) in the sense that at every point only a fixed number (equal to the order) of *B*-splines is non-zero. *B*-splines are also quite easily evaluated using their definition as a divided difference of the truncated power function [58]. *B*-splines were first introduced by Schoenberg [59] and a comprehensive compendium of many of their algebraic properties can be found in [54] and [60].

Because splines have for a long time been widely used to approximate response functions from measured data, their theoretical development and evaluation is well-documented [59-64]. The implementation of splines which is used in this work is heavily dependent on algorithms developed by Dierckx [58,65,66]. The following sections give only a summary of the detail contained therein.

3.4.2 Curve Fitting

Given a strictly increasing sequence of real numbers
$a = \lambda_0 < \lambda_1 < \ldots < \lambda_g < \lambda_{g+1} = b$ a spline function $s(x)$ of degree k with knots λ_i, $i = 1,2,\ldots,g$; is a function defined on the range $[a,b]$ having the following two properties:

(i) In each interval $[\lambda_i, \lambda_{i+1}]$, $i = 0,1,\ldots,g$; $s(x)$ is given by some polynomial of degree k or less (3.1)

(ii) $s(x)$ and its $k-1$ derivatives of orders $1,2,\ldots,k-1$ are continuous everywhere in the range $[a,b]$ (3.2)

Consequently, a smoothing spline approximation $s(x)$ to the set of function values f_q at the points x_q, $q=1,2,\ldots m$, $x_q < x_{q+1}$, in the *B*-spline representation is given as

$$s(x) = \sum_{i=-k}^{g} c_i N_{i,k+1}(x) \tag{3.3}$$

where $N_{i,k+1}$ denotes the normalised B-spline and c_i are the coefficients of the spline function. Such an approximation attempts to find a compromise between the following conflicting objectives:

(i) the prescribed values f_q should be fitted closely enough (closeness of fit).

(ii) the approximating spline should be smooth enough, in the sense that the discontinuities in its kth derivative are as small as possible (smoothness).

Formulation of this criterion mathematically requires some measure of smoothness and some measure of closeness of fit. For the latter, the sum of squared residuals, θ, is used while for the former, the sum of the squares of the discontinuity jumps, δ_i, in the kth order derivative of $s(x)$ at the interior knot, λ_i, is used. The approximation criterion is therefore formulated mathematically as follows:

$$\textit{minimise} \qquad \eta = \sum_{i=1}^{g} \delta_i^2 \tag{3.4}$$

subject to the constraint

$$\theta \leq S \tag{3.5}$$

where S is a given, non-negative constant which controls the extent of smoothing and therefore is called the smoothing factor.

3.4.2.1 The Choice of Knots

In the placement of knots in the fit functions, the knots are located inside the intervals $[\lambda_i, \lambda_{i+1}]$ with the largest sum of squared residuals. In addition, the knots are added only in those intervals which have at least one interior data point and allowance is made for more than one knot to be located in the interval $[\lambda_i, \lambda_{i+1}]$. The object of the strategy is simply to add knots at that part of the approximation interval where the fit is particularly poor.

Therefore, because the knots are only added and not relocated, the sum of squared residuals decreases with each knot addition.

If $S=0$, the requisite number of knots is known in advance, i.e., $g=m-k-1$. In that case the necessary knots are located immediately, at the data points if the degree k is odd and midway between the data points if it is even.

3.4.3 Surface Fitting

In the surface fitting problem, a closed rectangular domain $D=[a, b] \times [c, d]$ is given. Consider the strictly increasing sequence of real numbers

$$a = \lambda_0 < \lambda_1 < \ldots < \lambda_g < \lambda_{g+1} = b \tag{3.6}$$

and

$$c = \mu_0 < \mu_1 < \ldots < \mu_h < \mu_{h+1} = d \tag{3.7}$$

then the function $s(x,y)$ is called a spline k in x and l in y, with knots λ_i, $i=1,2,\ldots,g$ in the x-direction and μ_j, $j=1,2,\ldots,h$ in the y-direction, if the following conditions are satisfied:

(i) On any subrectangle $D_{ij}=[\lambda_i, \lambda_{i+1}] \times [\mu_j, \mu_{j+1}]$, $i=0,1,\ldots,g$; $j=0,1,\ldots,h$; $s(x,y)$ is given by a polynomial of degree k in x and l in y. (3.8)

(ii) All derivatives $\partial^{i+j} s(x,y)/\partial^i x\, \partial^j y$ for $0 \le i \le k-1$ and $0 \le j \le l-1$ are continuous in D. (3.9)

Such a spline can be expressed in terms of the normalised B-splines as

$$s(x,y) = \sum_{q=-k}^{g} \sum_{r=-1}^{h} c_{q,r}\, M_{q,k+1}(x)\, N_{r,l+1}(y) \tag{3.10}$$

where $M_{q,k+1}(x)$ and $N_{r,l+1}(y)$ are the normalised B-splines, respectively defined on the knots

$$\lambda_q, \lambda_{q+1}, \ldots, \lambda_{q+k+1} \quad (\lambda_{-k}=\ldots=\lambda_{-1}=a; \quad \lambda_{g+2}=\ldots=\lambda_{g+k+1}=b)$$

and

$$\mu_r, \mu_{r+1}, \ldots, \mu_{r+l+1} \quad (\mu_{-l}=\ldots=\mu_{-1}=c; \quad \mu_{h+2}=\ldots=\mu_{h+l+1}=d)$$

A similar approach to the curve fitting case is used for the iterative solution of the constrained minimisation problem for the approximation $s(x,y)$ to a set of data points (x_q, y_q, f_q) for $q=1,2,...,m$. However, while knots are added at that part of the approximation domain where the fit is particularly poor (i.e., where the residuals are largest) as before, only one knot is added during each successive iteration because here the dimension of the spline grows much faster. Indeed, if a single knot is placed in the x-direction, the number of B-spline coefficients increases by $(h+l+1)$ ($(g+k+1)$ if a knot is added in the y-direction). The consequences are:

(i) on the one hand, that the sum of squared residuals, possibly decreases rapidly, but

(ii) on the other hand, that the time for solving the least-squares problem may go up very fast.

3.5 Weighting of Data Points

An important question to be considered before starting the curve fitting is whether the data points are of the same or different accuracy, and whether they should be assigned different 'weights' in the fitting process. Very often the data points will all be of equal, or nearly equal, accuracy, or can be so regarded. The weights will then all be taken equal to unity, and the question then becomes trivial, as is the case in the work reported in this thesis.

However, if the data values f_q $(q=1,2,...,m)$ of the dependent variable are of substantially differing (absolute) accuracies, then appropriate weights must be applied during the curve fitting so that those values known to be more accurate have a greater influence on the fit than others. These weights should be calculated from estimates of the absolute accuracies of the f_q-values, expressed as standard deviations, probable errors or by some other measure which has the same dimensions as f_q. Specifically, for each f_q the corresponding weight, w_q, should be inversely proportional to the accuracy estimate of f_q. For example, if the percentage accuracy is the same for all f_q, then the absolute accuracy of f_q is proportional to f_q (assuming f_q to be positive, as it usually is in such cases but not in the application in this work) and so $w_q=K/f_q$, for $q=1,2,...,m$, for an arbitrary positive constant K. (This definition of weight is stressed because often weight is defined as the square of that used here.)

Finally it may be remarked that weights need usually be determined only quite roughly and it is often sufficient simply to estimate values from a general knowledge of the physical situation from which the data arise.

With the inclusion of the weights, w_q, the least-squares spline approximation $s(x)$ or $s(x,y)$ to the set of data points (x_q, f_q) or (x_q, y_q, f_q) has the property that it minimises the weighted sum of squared residuals, ε_q, for $q=1,2,...,m$, where for curve fitting

$$\varepsilon_q = \sum_{q=1}^{m} w_q [f_q - s(x_q)]^2 \tag{3.11}$$

and for surface fitting

$$\varepsilon_q = \sum_{q=1}^{m} w_q [f_q - s(x_q, y_q)]^2 \tag{3.12}$$

3.6 Choice of the Degree of the Spline Functions

Although any continuous function can be approximated by a spline function of degree k, provided that the spacing between the knots is sufficiently small, approximation by splines of degree greater than three is rare. One of the main reasons is that increasing the degree of the spline normally makes the localisation properties poor, because the tails of the cardinal (basis) functions decay at a slower exponential rate. Another reason is that there are many reliable algorithms that are available for approximating by cubic splines. In addition, even though large values of k provide more smoothness and higher accuracy, they reduce the amount of flexibility [52] and increase the cost of computation.

The history of the past fifteen to twenty years shows that cubic splines are the most widely used. Amongst the many advantages that cubic splines have is the property that they provide a suitable balance between flexibility and accuracy. They also offer a good compromise between efficiency (computation time, memory requirements) and quality of fit. This work therefore employs only cubic spline curves and surfaces for curve and surface fitting.

The smooth cubic spline approximation $s(x)$ to the set of data points $(x_q f_q)$, with weights w_q, for $q=1,2,...m$ in the B-spline representation is therefore given as

$$s(x) = \sum_{i=1}^{N-1} c_i N_i(x) \tag{3.13}$$

where N_i denotes the normalised B-spline defined upon the knots $\lambda_i, \lambda_{i+1}, ..., \lambda_{i+4}$ and N is the total number of knots. The knots $\lambda_5, ..., \lambda_{N-4}$ are the interior knots, which divide the approximation interval $(x_1 ... x_m)$ into $N-7$ intervals. The coefficients c_1, $c_2, ..., c_{N-4}$ are then determined as the solution of the following constrained minimisation problem:

$$\text{minimise} \qquad \eta = \sum_{i=5}^{N-4} \delta_i^2 \tag{3.14}$$

subject to the constraint

$$\theta = \sum_{q=1}^{m} \epsilon_q^2 \leq S \tag{3.15}$$

where δ_i stands for the discontinuity jump in the 3rd order derivative of $s(x)$ at the interior knot λ_i, ε_q denotes the weighted residual $w_q(f_q - s(x_q))$, and S is the non-negative smoothing factor.

The corresponding expression for the bivariate spline function is given as

$$s(x, y) = \sum_{i=1}^{N_x - 4} \sum_{j=1}^{N_y - 4} c_{ij} M_i(x) N_j(y) \tag{3.16}$$

3.7 Implementation in the Numerical Algorithms Group Library

The methods described in the preceding sections have been implemented in the Numerical Algorithms Group (NAG) [67] suite of subroutines and are available as subroutines E02BEF and E02DDF for curve and surface fitting respectively. In both cases, apart from the set of data points (x_q, f_q) (or (x_q, y_q, f_q) for surface fitting) with the corresponding weights w_q, the

user merely has to provide the smoothing factor S, to control the trade-off between closeness of fit and smoothness of fit, as measured by the sum of squares of residuals, θ. For curve fitting, provision is made for fitting in more than one direction, but for surface fitting, only a single out-of-plane translation is allowed.

If the weights have been correctly chosen as discussed in section 3.5 above, the standard deviation of $w_q f_q$ would be the same for all q, equal to σ, say. In this case, choosing the smoothing factor S in the range $\sigma^2(m \pm \sqrt{2m})$ (where m is the number of data points), as suggested by Reinsch [62], is likely to give a good start in the search for a satisfactory value. If nothing is known about the statistical error in f_q, each w_q can be set equal to one and S determined by an iterative search. In this connection, it is useful to note that if S is too small, the spline approximation is too wiggly and picks up too much noise (overfit); if S is too large the spline will be too smooth and signal will be lost (underfit) [65,66]. In the extreme cases the algorithms return the least-squares polynomial if S is very large and an interpolating spline if S is equal to zero.

In the iterative search for a solution, for each positive value of S, a suitable knot set is built up (starting with no interior knots) and the corresponding spline is fitted to the data by least-squares with the weighted sum of the squares of the residuals, θ, computed. If $\theta > S$, new knots are added to the knot set to reduce θ at the next stage. The new knots are located in intervals where the fit is particularly poor. Eventually $\theta \leq S$ and at that point the knot set is accepted. This acceptable solution has $\theta = S$ within a relative tolerance of 0.001 [67].

3.8 Implementation of NAG Spline Subroutines for the Estimation of Rotational Degrees of Freedom

In Chapter 2, it was indicated that the rotational degrees-of freedom and any other unmeasured data can be estimated by approximating the mode shapes of a structure using a mathematical function such as a cubic spline curve or a cubic spline surface. The resulting function is then differentiated to give the required data. In this work, NAG routines E02BEF and E02DDF have been incorporated into a procedure (**AUGFITTER**) in which the spline functions obtained from curve (or surface) fitting are differentiated and evaluated, using NAG subroutines E02BCF for curves and E02DEF for surfaces, to give the required rotations and any other missing data. Full details of the program **AUGFITTER** and the associated flowchart are given in Appendix 1.

CHAPTER 4

ACCURACY OF THE ESTIMATES OF ROTATIONS

4.1 Introduction

In the last twenty years, experimental modal analysis has evolved from the role of verifying the results of finite element analysis (FEA) to a new, more demanding role of providing the modal data for the analysis of the dynamic effects of structural changes. The prediction of the effects of structural changes to the dynamic properties of a structure, more commonly known as Structural Dynamics Modification (SDM), has received the attention of a large number of researchers over the past decade. This concentrated effort has culminated in the availability of several sophisticated techniques which, in turn, has given rise to increased popularity of the use of SDM as an inexpensive and quick tool in solving structural vibration problems. However, it is known [68,69,70] that the accuracy of the SDM predictions depends on the accuracy of the original modal data.

Until very recently, experimentally based modal models have been restricted to contain only translational displacements. These translational displacements represent only three of the six degrees of freedom (DOF) present at each point on the structure. The other three, the rotations, have not historically been included in modal tests for a number of reasons. Firstly, they are not normally needed to display modeshape data. Secondly, rotational transducers have not been commonly available and thirdly, with the available methods, routine measurement of rotations has doubled the problem size in terms of time and storage space. While a knowledge only of the translational displacements is adequate for structural dynamics modifications in the form of lumped masses, or pin-jointed spring or damper elements, modifications which require moment coupling at points of attachment such as beams and plates, require the inclusion of rotational degrees of freedom in the modal data.

In recent years, several investigators have studied various techniques for estimating rotations using both experimental and analytical procedures as shown in Chapter 2. Amongst the analytical techniques, the alternative of curve and surface fitting has some

attractive advantages in that it is quick and cheap, does not require prior knowledge of the modification sites, unmeasured displacements can also be estimated from the fit functions and random errors in the measured displacements can be smoothed by the fit function.

In Chapter 3, the general requirements and criteria for curve and surface fitting were presented along with a brief theoretical background of splines. This chapter discusses the accuracy of the estimates of rotations from spline curves and surfaces. Integral to the treatise is a discussion of the parameters which control the performance of the estimation technique and their effects on the performance. Quantitative comparisons of the estimates of rotations from analytical and simulated experimental databases with corresponding analytical or finite element data for beam and plate structures are included. The chapter also discusses the problem of optimising the estimation method for the best rotations; best being understood in the context of the best predictions following a modification. In this regard, optimisation of the estimation process is discussed further in Chapter 5.

4.2 Parameters Controlling the Accuracy of the Estimates of the Rotations

In Chapter 3, it was indicated that the precision of spline approximations depends mainly on the choice of the number of knots and their locations. It was also intimated that appropriate weights must be applied during the curve fitting so that those data values known to be more accurate have a greater influence on the fit than others. If nothing is known about the statistical error in the data values, the optimum value of the smoothing factor, S, is determined by an iterative search. The value of S resulting from such a search fixes the number of knots in the fit. The value of S is itself dependent on the number of measurement points and their location on the structure and the level of error in the data values. The parameters which control the accuracy of the estimates of the rotations can therefore be itemised as:

(a) the smoothing factor, S, which, in turn, controls the number of knots in the fit function,

(b) the number of measurements points and their location on the structure,

(c) the level of error in the data, and

(d) the weighting of the data points.

In the sections which follow and with the exception of the weighting of the data points, discussion of the effects of the rest of the parameters on the accuracy of the estimates of rotations is presented by way of several case studies.

4.3 Curve Fitting Performance - Cantilever Beam

In this investigation, the estimation of rotations was explored using a mild steel cantilever beam, 500mm long, 25.4mm wide and 12.7mm deep. The cantilever beam was chosen because it provides different but most commonly used boundary conditions. Thus, it allows the investigation of the performance of the estimating method for different end conditions. The discussion initially considers the performance of the proposed technique on error-free data. The insights gained here are used in the subsequent analysis on noisy data to establish the bounds of application.

4.3.1 Fit Performance On Error-free Data

4.3.1.1 Effect of the Smoothing Factor or Number of Knots on the Estimation of Rotations

The cantilever beam was initially modelled using ten two-noded beam finite elements and translational and rotational modal data for the first nine flexural modes was obtained from finite element (FE) computation. Estimates of rotations were also obtained by curve fitting the 'error-free' finite element translational data with the spline function as described in Chapter 3 with all data points carrying the same weight. For the purposes of this study, this data was taken to be sufficiently accurate since the errors in the translations when compared with exact values were less than 0.1%. In order to study the effect of the number of knots on the estimates of the rotations, computations were performed for several internal knot conditions, namely; 0, 1, 3, 6 and 7 internal knots, the former being the least-squares polynomial fit and the latter the interpolating spline.

Figure 4.1 shows, for the fifth mode, the improvement in the estimates of the rotations as the fit was tightened. The trends for the other modes were similar. It will be seen that the best estimator of rotations was the interpolant. In addition, it was evident that the accuracy of the estimates of rotations depended on the spatial description of the mode shapes provided by the initial data. This was shown by the deterioration in the performance of the estimator with

increase in the mode number for the same fit. While the approximation technique was able to provide acceptable estimates of rotations away from the boundaries once the underlying modeshape function had been picked up (with 6 knots here), it was unable to truly represent the modeshape functions at and near the boundaries. This led to large errors in the estimated rotations.

Figure 4.2 shows the error between the calculated and exact rotations (normalised with respect to the largest FE rotation) for the fifth flexural mode of the cantilever using the six-internal knot fit results. For measurement points 3 to 9, the errors in the rotations were found to be of the order of 5%. The figure also clearly shows the relationship between the error values and the mode shape. Generally, errors in the calculated rotations were largest at or near the points of inflection of the mode shape; a result repeated for all the other modes. The errors for the two points nearest the ends were, however, found to be higher. This was attributed to the inability of the relatively loose fit functions to truly represent the mode shape functions at the ends. This result was consistent with results obtained using conventional polynomials [30].

The average errors for points 3 to 9 for the first nine modes of the cantilever for the six-internal knot fit are shown in Figure 4.3. As the mode number increases, the spatial description of the mode shape from the translational data deteriorates and the error in the computed rotations increases as might be expected. Alternatively, this means that in order to obtain better accuracy for the higher modes, a tighter fit must be used as the mode number is increased. In other words, no single fit is suitable for all the modes in a given data set.

Yet another way of viewing the error data in Figure 4.3 is to plot it against the number of points between nodes, as shown in Figure 4.4. The smoothness of the curve suggests that such data might be used as a guide to identify the number of measurement points required for a given level of accuracy. For example, if the measurement density provides two points between nodes, then an error of the order of 6% on the normalised scale for this level of smoothing (six internal knots) might be expected in the calculated rotations. Obviously the level of accuracy would be expected to improve with reduced smoothing (e.g., using the interpolant) for this 'error-free' data.

4.3.1.2 Effect of the Measurement Point Density and Distribution on the Estimates of Rotations

As a preamble to this section, it must be stated that in the implementation of spline curve and surface fitting in the NAG library, there are no recommendations on the number and location of data points to be used. Only the lower limits of 4 and 16 data points for curve and surface fitting, respectively, are given. It is also apparent from the preceding section that the accuracy of the estimates of rotations especially at and near the boundaries, is heavily dependent on the number and location of points in the database. The number and location of data points, in tandem with the value of the smoothing factor supplied, in turn, control the number and location of the knots in the resulting fit function.

Evidence from literature asserts that the accuracy of an approximation depends on the number and location of the knots in the fit and on the behaviour of the function underlying the data [66]. Powell [52] has shown that while any continuous function can be approximated by a spline provided that the spacing between the knots (and hence between points) is sufficiently small, increasing the number of knots, generally improves the accuracy of the approximation, the limiting case being the approximation which picks up too much of the noise in the translations. His work has also indicated that although changes in knot spacing can give large gains in efficiency, error control is more difficult when there are frequent changes in knot (and hence data point) spacing. He concludes that a successful compromise is to keep each knot spacing for several consecutive intervals (distance between knots), and to allow only halving and doubling where the knot spacing changes.

Published work [58,61] and this author's own experience on the use of the NAG spline and curve fitting subroutines confirm that not all data points in a database are used as knot locations. Even when interpolating, the results showed that the two points adjacent to the ends are never used as knot locations. However, the presence of these points on one hand, improves the representation (modelling) of the structure there while exaggerating the presence of any error in the data on the other hand. The results also indicate that the addition of knots always begins at mid-span and subsequent knots are then added away from mid-span towards the ends as the smoothing factor is reduced. Dierckx [58] has also shown that the fit produced by spline approximation becomes unreliable in regions, especially near the

boundaries, where there are no data points. This situation is accentuated if the smoothing factor becomes very small.

Empirical insights into the effect of varying point density and location were gained by studying the performance of the estimation technique on different size databases. An interpolation was performed on exact data from the Euler-Bernoulli solution of the equations governing cantilever vibrations for databases with point densities varying from 4 to 20. In all cases, the data points were equi-spaced along the cantilever.

The variation of the modulus of the error in the computed rotations at the ends of the beam (normalised to the largest rotation for each mode) for the first five flexural modes of the cantilever is shown in Figures 4.5 and 4.6. The dips in Figure 4.6 reflect a sign change in the error values due to the use of a logarithmic scale on the y-axis. Since at least four points are required to specify the cubic spline used to approximate the translational mode shape, no results exist for databases with less than four points. It is important to note that generally and for each mode, the largest error in the calculated rotation occurred at the points where the rotation was close to zero i.e., near the fixed end and at or near the nodal points. By contrast, at points where the rotation was not close to zero, the normalised error was typically at least an order of magnitude less than the maximum error. This fact should permit reasonable estimates of rotations to be obtained without requiring the utilisation of a large number of base points.

As would be expected, the largest errors occurred in the highest mode and this determined the choice of the number of points. It was shown in the previous section that if there are at least two measurement points between nodes, a maximum error of less than 10% would be expected in the calculated rotations. In this case, this spacing was satisfied with 16 points for mode 5 and resulted in a maximum error of less than 3% in the calculated rotations.

The use of equi-spaced data gave discrepancies in the computed rotations at the ends of the beam, even with an interpolating spline (Figure 4.1). Figure 4.7 shows the improvement with the addition to the original 11-point database of a mid-point value in each end interval (Δ). However, while the fixed end was satisfactorily modelled, there was still notable discrepancy

(3.4% error) in the tip rotation. By adding a further two points near each end, thereby expanding the database to 17 points (∇ in Figure 4.7), the error in the tip rotation was reduced to 0.027%. Thus, it is seen that once the spacing which satisfies the requirement for at least two measurement points between nodal lines is met, the ends need to be treated differently by adding extra points to improve the representation there.

4.3.2 Fit Performance on Simulated Experimental Data

In order to provide the background and justification for the method used in simulating experimental modal data from analytical data, it is necessary to understand the main sources of error in measurement and their effects on experimental modal data.

4.3.2.1 Sources of Error in Frequency Response Function Measurements

It has already been stated that the accuracy of Structural Dynamics Modification predictions depends on the accuracy of the original modal data. Experimental modal data is derived from frequency response function (FRF) measurements which are susceptible to numerous sources of error such as inexact equipment calibration, excessive signal noise, misinterpretation of data, incorrect transducer location, inappropriate treatment of structural non-linearities and the use of inappropriate modal identification algorithms [71]. These sources of error manifest themselves as one or more of the following errors [72] in the resulting modal data:

(a) global calibration errors; due to improper scaling,

(b) localised calibration errors; due to improper use or calibration of transducers or the signal conditioning system,

(c) modal scaling errors; due to different amplitude scaling between modes in the database,

(d) geometry truncation errors; due to misinterpretation of the mode shapes of the structure as a result of spatial aliasing, and

(e) modal truncation errors; due to the exclusion of significant modes of vibration.

These experimental errors are more commonly categorized as either random or systematic (bias) errors and several researchers have directed their efforts at attempts to reduce the levels of these errors in order to extract accurate modal parameters from tests. Random error is defined as error in the estimation process which produces variations about the true value.

This variance is reduced as the number of samples increases. Bias error, on the other hand, is defined as any error that precludes the estimation of the true FRF even with an infinite number of samples.

In their work on FRF estimates, Bendat and Piersol [73] have shown that the estimation of an FRF using estimates of the power spectral and the cross-spectral density functions, which is the most common scheme, will generally involve bias errors from a number of sources, namely:

(i) bias inherent in the estimation procedure which is usually negligible compared to other bias and random errors,

(ii) bias resulting from violations of the basic assumption that the system is a constant parameter system. Even when the constant parameter assumption is valid, the linearity assumption is often violated and this results in bias error,

(iii) bias in the power and cross-spectral density estimates used in the estimation of the FRF. Although this bias can be significant at frequencies where spectral peaks occur, it can be suppressed by making the resolution bandwidth sufficiently narrow to accurately define peaks in the spectra,

(iv) bias due to extraneous measurement noise in the measured input which does not actually pass through the system, and

(v) bias due to the contributions of other unmeasured inputs to the measured output. These unmeasured inputs will be correlated with the measured input since unmeasured inputs which are not correlated with the measured input do not cause bias error since they appear as uncorrelated extraneous noise at the output. They do, however, contribute to the random error in the FRF estimates.

Transducer noise which is not correlated with the input gives rise to localised random errors which can be eliminated (or at least controlled) by sufficient averaging. However, all real world measurements contain some noise.

Mitchell and Wicks [74] have shown that bias error is often significantly greater than the random error since it is more difficult to control. Mitchell et al [75] have also indicated that

bias error in FRF measurements will yield residue values which are biased in the direction of the bias error, i.e., positive bias gives larger residue estimates (and hence larger vector components) than the actual values and vice versa. Contributions from Allemang et al [76] on this subject have shown that modes with small peaks in the FRF measurement suffer most in the presence of bias error and that this is a local rather than a global effect. Their work also shows that bias due to non-linearity is localised to the excitation location due to overestimation of the compliance at that point.

4.3.2.2 Simulation of Experimental Modal Data from Analytical Data

From the foregoing discussion, it is clear that any simulation of experimental modal data must be dominated by bias since in practice, random error is small in comparison to bias error. However, since random error can only be minimised and not completely removed, the simulation must also allow a random distribution of the error. The object is to produce simulated modal data which is representative of real experimental modal data. Most simulations that have been reported in literature have merely added random noise to analytical data without taking account of the bias element. The justification for this has usually been that the experimentalist is expected to control most sources of bias error in a modal test. In this work however, the presence of bias error in real experimental modal data is deemed important enough to be reflected in any simulation.

Therefore, in this work, simulation of experimental data was achieved by adding to each translational displacement value in the database a random value between 0% and 1% of the largest translational component in the mode. The decision to use a maximum of 1% of the largest modeshape component was based on the level of error which was introduced to the modeshape components relative to the local value. Higher proportions of the largest modeshape component were found to yield large errors relative to the local value especially for small modeshape vector values. While larger errors are possible, the 1% level of error was therefore taken to be representative of the error level in real experimental data. Although 1% was the maximum error relative to the largest modeshape component of a mode, it must be understood that it was not the maximum percentage error relative to the local value of the modeshape component.

The addition of noise was done in a biased manner such that negative displacements had negative errors added to them and vice versa. In this way the simulated experimental modal vectors were sensitive to noise as they would be in a real measurement situation; the largest components of the mode shape, which have the largest dynamic range would suffer the least from the effects of noise whereas the components of the mode shape which have the least dynamic range would suffer the most from the effects of the noise.

4.3.2.3 Representative Error Level

Simulated experimental data was generated as described above for the cantilever beam described earlier using the 17-point model described in section 4.3.1.2. Representative plots of the original analytical modal vectors and the simulated experimental modal vectors are shown in Figure 4.8a and 4.8b for the second and fifth modes of the cantilever. It will be seen that, generally, the differences in the data are small. Since the experimental modal data set had known error, the performance of the fit function in terms of the estimates of rotations could be easily studied and related to the level and pattern of the errors in the experimental modal data.

Estimates of rotations were computed from this data by curve fitting with all the data points equally weighted. Translational and rotational modal data for the first ten flexural modes was also obtained from the Euler-Bernoulli solution of the analytical expression for the cantilever. Exact translational data was used to allow comparison of the performance of the estimating technique on noisy and error-free data. The exact rotational data was used as the basis for comparison.

In order to provide an understanding of the performance of the fit function, several computations, starting with the least-squares fit through to the interpolant, were performed on both exact and seeded data. It was envisaged that the conclusions from this investigation would facilitate the automation of the optimisation process for the best rotations from the estimation technique. This has to be understood in the context that the fitting routines, as they are available in the NAG Library, are formulated purely to handle translational data and not for the accurate estimation of derivatives.

While the full approximating criteria as specified in the NAG library [67] were met quite early in the search (relatively large values of S) with satisfactory fits to the translational data, the fits from which the estimates of the rotations were acceptable were, in all cases, obtained with much smaller values of the smoothing factor. There was however no obvious empirical relationship between the value of S for which the translations were acceptable and that which yielded the best rotations. This necessitated the establishment of some acceptability criteria for the computed rotations. Boundary conditions of the structure were seen as the prime criteria in this regard. This was due to the fact that it was more difficult to obtain good results at the ends of the fitting range than in the middle. It was also envisaged that the use of boundary conditions would provide a means of judging the acceptability of the estimates of the rotations for structures for which analytical solutions were not available.

Another important consideration in optimising the search for the best fit was whether the optimum fit had to be the absolute mathematically accurate fit (i.e., little (under 0.5% error) or no discrepancy with the analytical solution) or whether in fact only a 'ball park' estimate (within 20% of the exact value) would be adequate for SDM calculations. This aspect could however only be clarified by considering the sensitivity of the errors in the structural dynamics modification predictions to the errors in the rotations and is dealt with in the next chapter.

The main objectives for performing this analysis were therefore:

(i) to compare the performance of the estimation process on simulated experimental data with the performance of the same fits (same control parameters) on analytical error-free data,

(ii) to investigate the effect of varying the smoothing factor, S, on the estimates of the rotations for a fixed number of knots in the fit function especially at the ends of the cantilever beam when compared with exact rotations, and

(iii) to study, for the fit function, the behaviour of the first derivative (the rotation) at the fixed end and the second derivative at the free end of the cantilever with change in the smoothing factor. These derivatives are the governing boundary conditions for a cantilever beam.

Preliminary examination of the results revealed that while the curve fitting routine was capable of yielding acceptable estimates of rotations up to the mode before which the requirement of at least two measurement points between nodal lines was violated (mode 6 in this case), it was immediately clear that the main challenge would be automation of the optimisation process in accordance with the main controlling parameters. This summary examination also revealed that for the same number of knots, there was considerable change in the rotation estimates with change in the smoothing factor and that this variation was, as expected, largely at the ends of the structure, particularly at the fixed end. This observation was evident for both analytical and seeded data. It will also be noted that for the fundamental mode, the best approximation was the fit with the least number of internal knots (i.e., zero) since any addition of knots to the fit function for this mode picked up a lot of the noise in the translations. This is illustrated in Figure 4.8c and is consistent with the fact that the number of knots required to adequately represent the mode shape function increased with rise in mode number.

(a) Comparison of the Fit Performance on Seeded Data Against Performance on Exact Data

When comparing the performance of an approximating technique on different data sets, it is important to realise that for the comparison to be valid, parameters which are not the focus of the investigation must be maintained constant. This was found to be especially critical in this work since for the same number of knots, a different value of the smoothing factor was in fact a unique solution which satisfied the full fitting criteria as specified in the library routine [67] and therefore resulted in a unique set of rotations.

Figure 4.9 shows representative sets of rotations derived from interpolating the seeded data for modes 2 and 5. In order to aid comparisons, the exact values are also plotted in the figures. It is immediately apparent that the interpolant was an inappropriate estimator of rotations from seeded data since this fit function tended to pick up a lot of the noise from the initial data particularly at the ends of the cantilever. This gave rise to another important consideration: that although a dense distribution of data points everywhere on the structure was desirable for analytical data, the same was not particularly desirable for experimental

data. The determination of an optimum fit would therefore have to take account of an optimum distribution of points on the structure especially near the boundaries.

Figure 4.10 shows the comparison of the estimates of rotations from exact and noisy data for a fixed number of knots as the value of S was altered. The approximation based on error-free data was used as the basis for comparison. It will be seen that the performance of the estimation method on both data sets was very similar (a welcome observation) as highlighted by the small values of the discrepancies, the largest discrepancy being at the fixed end of the cantilever. The much larger discrepancy seen at mid-span for mode 2 was attributed to the proximity of an internal knot there the effect of which lead to a sign change in the rotation estimate at that point.

A more detailed view of the variation in the discrepancy in the computed rotation at the ends of the beam is presented in Figure 4.11. It is apparent that the discrepancy in the computed rotations was greater at the root than at the tip. In addition, the results indicated that, as would be expected, for the same controlling parameters, the errors in the estimates from noisy data were some-what greater than the errors in those from exact data. This is generally indicated by the positive signs of the discrepancy values. The plummeting trend of the discrepancy at the fixed end was attributed to the greater rate of change in the computed rotations from noisy data there as the smoothing factor was reduced.

The key conclusion which can be drawn from this comparative analysis is that, for the same controlling parameters, the performance of the estimation technique on both data sets is very similar although discrepancies become more pronounced as the mode number is increased. It is however expected that this may not be the case for data with a much higher level of noise.

(b) Effect of Varying the Smoothing Factor on the Computed Rotations

The variation of the error in the computed rotations (compared with exact rotations and normalised to the largest rotation) for varying S while keeping the number of knots fixed is shown in Figure 4.12 for modes 2 and 5. It is seen that the largest errors are at the ends of the beam such that satisfying a given error tolerance at the ends will invariably result in equal

or better accuracy elsewhere. With the exception of the interpolating spline (S=0.0), the general trend is for the errors to reduce as S is reduced. The fact that the interpolating spline is an unsuitable estimator of rotations from noisy data can be seen, for example for mode 5, at the tip, where the error using this fit ($\triangledown$) is greater than when using S=0.003 ($\diamond$). It is therefore apparent that there must be an optimum combination of S and number of knots which minimises the largest error in the computed rotations.

Figure 4.12b highlights a feature which was not seen from the computations for mode 2 (Figure 4.12a) which were based on a looser fit (only one internal knot). For mode 2, the computed rotations follow the expected trend, i.e., the largest rotation is computed at the free end of the beam, while in the case of mode 5, which is a tighter fit (9 internal knots), the rotations are seen to follow the expected trend until a certain value of the smoothing factor is reached. Beyond this value, the largest rotation is computed one or two points before the tip. This feature was observed to have some relationship with the optimisation of the estimation method. The characteristic was also evident in computations on simulated data for other modes where a relatively tight fit was used.

Examples of the variation in the normalised error in the rotations at the ends as the smoothing factor is varied are shown in Figure 4.13. For mode 5 (Figure 4.13b), the error in the tip rotation is zero for S=0.003 while the error in the root rotation is lowest for S≈0.0. The minimax optimum condition is at S=0.0006. In situations where rotations would be required at many locations on the structure, this approximation would minimise the largest error in the range since it has already been shown that at this level of smoothing, the errors in the rotations away from the boundaries are already lower than those at the boundaries (see Figure 4.12b). While the data for mode 2 does not provide for a similar analysis, it is apparent that the trend is similar and that similar conclusions would not be far-fetched. It will also be noted that once the approximation is in the 'ball park' of the optimum fit (S=0.002 for mode 2 and S=0.003 for mode 5 in this case), the error in the computed rotations is below 10% on the normalised scale.

(c) Fit Performance vis-à-vis Cantilever Boundary Conditions

It was intimated earlier that the structural boundary conditions were considered to be potentially useful criteria for optimising the estimation method. Figure 4.13 provides valid evidence for the premise that a good estimator of the rotations would be one which gave the least error in the computed rotation at the root of the cantilever. Although the plots indicate that the best rotations are obtained from relatively tight fit functions in as far as the zero first-derivative requirement at the root is concerned, they do not provide any information about the zero second-derivative requirement at the free end which is the governing boundary condition at that end.

Figure 4.14 shows two possible scenarios of the behaviour of the second derivative at the free end which were observed. When these plots are viewed in the light of Figure 4.13, it is quite clear that the value of S at which the boundary condition at the tip was met was much larger than the value for which the boundary condition at the root was met. The results in Figure 4.13 also suggested that the estimates of the rotations could be improved if the smoothing factor was further reduced from the value which satisfied the tip boundary condition. These observations lead to the conclusion that the value of S for which the approximation minimises the errors in the computed rotations everywhere on the beam must lie between the values at which the boundary conditions are satisfied.

An interesting characteristic which accompanied the fulfilment of the tip boundary condition was that computations based on values of the smoothing factor smaller than the value at which the tip boundary condition was met invariably produced rotations whose maximum was predicted one or two points away from the free end, i.e., there was a change in the orientation of the rotations. This was considered a useful additional criterion for identifying the optimum fit.

4.3.2.4 Worst Case Scenario Analysis

In order to optimise the performance of the estimation method, it became necessary to simulate the worst case scenario which could arise from measurement. The optimum fit arising from such a database would clearly satisfy databases with less severe patterns of error in the translations.

The previous section used data with a random set of bias errors. The worst case of such a contamination would consist of the full (1% in this case) error being utilised. Thus, worst case scenario simulated experimental data was generated for the beam previously described using the seventeen-point model by adding 1% of the maximum modal vector component in the exact database to every other point on the structure. This method of seeding gave rise to two patterns of seeding which would be the limiting cases for the error levels, namely: one for which the error was added to the tip and then to every other point on the beam except the fixed end, and the other for which the tip carried no error. These seedings are hereafter referred to as the 1-0-1-0- and the 0-1-0-1- worst case scenarios and are shown in Figure 4.15 for the first mode of the cantilever.

An attempt was made to establish how far removed the representative error level simulation described earlier was from either of the worst case limit cases. In order to do this an interpolation was performed on the limit cases, the representative error level and exact analytical data with equal weighting for all the data values. The results, shown in Figure 4.16 for modes 1, 2 and 3, indicate that the representative error level leaned toward the error-free condition. However, it must be pointed out that this is true only for the distribution of errors used here and may not hold for all random distributions. The results also confirm the very low sensitivity of the computed rotations to the errors in the translations away from the boundaries. This is seen in the very similar estimates of the rotations from the three databases. The behaviour of the second derivative was also examined for these databases and the details are given in Table 4.1 for the first two modes. The results reveal the high sensitivity of the second derivative at the free end to the errors in the translations for the worst case seedings. This is highlighted by the multiple sign changes in the second derivative from the worst case databases evident even for the first mode. In addition, the sign changes, for mode 1 at least, show some relationship with the pattern of the seeding of the translations.

In an attempt to optimise the performance of the estimation technique on the worst case databases, rotations were computed from these for the first five flexural modes of the cantilever. A cursory examination of the fit results revealed that even for these worst cases, the estimator was capable of returning acceptable estimates of the rotations (typically less than 10% error) although this was usually after diligent searching. The results also indicated that,

as in the case of the representative error level, a good fit was characterised by a change in the orientation of the rotations at the free end. That is, the largest rotation was estimated at the point adjacent to the tip. Also, as in the case of the representative error level, the best approximation for the fundamental mode was the fit without any internal knots.

Figure 4.17 shows a selection of fits to mode 5 of the beam using the 0-1-0-1- data. As in the case of the error-free data, once the under-lying trend for the modeshape function was picked up by the fit (here, when using more than 16 knots), the addition of more knots (and consequent further reductions in the value of S) had little effect on the computed rotations away from the boundaries.

(a) Optimisation Based on the Boundary Conditions

It was shown in the previous section that the errors in the rotational estimates are not minimised everywhere at once and an optimum approximation which minimised the overall errors in the rotations for the representative error level data set was found. In the case when the exact solution is unknown, it is reasonable to use zero rotation at a clamped boundary as the target value for the approximation. At a free (or simply-supported) boundary, the appropriate target would be zero second derivative of the displacements.

In order to test the generality of the method, rotations were computed for the first five modes of the cantilever using fits based on a range of numbers of knots, each spanning a range of values of the smoothing factor, S, seeking combinations which satisfied the boundary conditions at the ends of the beam.

Figure 4.18 shows the first derivative at the root and the second derivative at the tip for modes 2 (9-knot fit) and 5 (17-knot fit). The similarity in the corresponding values for the two databases shows that the criteria are not very sensitive to the pattern of bias error seeding; a very desirable feature for applications in practice when the actual errors are unknown.

Figure 4.18 also shows that, as was the case previously (Figure 4.13), the free end boundary condition was satisfied with a larger value of S than that required for the root boundary

condition. This was true for the other modes in the database and also for both databases. In addition and perhaps surprisingly, it was found that for mode 5, the approximations based on minimising the second derivative at the free end (S=0.013 or S=0.020) do not correspond to zero error in the tip rotation (S=0.001 from Figure 4.13). Indeed the approximation based on zero rotation at the fixed end was more accurate than either.

Table 4.2 shows the comparison of the calculated rotations at the ends of the beam in the region bounded by the approximations which satisfied the boundary conditions for 0-1-0-1-data. In the table, the value of S decreases as one goes from (e) to (a), (e) being the value of S which satisfies the tip boundary condition and (a) that which satisfies the root boundary condition. It will be found that the optimum value of S is, for all modes, closer to the value satisfying the root boundary condition; confirming the result of Figure 4.13. Graphical evidence for this is presented in Figure 4.19 in the form of error plots using data from three approximations, namely; the approximations at which the boundary conditions were met and another approximation in mid-range.

From the foregoing, it will be realised that identification of the optimum requires a significant amount of computation, something which would not be justified in practice. It is concluded therefore that combinations which satisfy the root condition are sufficiently close to the true optimum for practical purposes.

(b) Optimisation Based on the Sum of the Squares of the Data Values and the Smoothing Factor

One of the main objectives in the search for an optimum estimator of the rotations was an attempt to relate the smoothing factor for the approximation at which the fitting criteria were met with regard to the translations and the smoothing factor from which the best estimates of rotations were derived. Although the NAG routines, as available in the NAG Library, are not automated for acceptance of an approximation (it is the responsibility of the user to establish his criteria for acceptance based on his knowledge of the underlying function), it was envisaged that establishment of some empirical relationship between the two approximation conditions would eliminate some of the effort expended in the search of the optimum approximant of the rotations.

An attempt was made, using 0-1-0-1- data, to establish an empirical relationship between the sum of the squares of the data values, the value of the weighted sum of squared residuals from the least-squares polynomial fit and the value of S at which the minimum second derivative at the tip (which is in the 'ball-park' of the optimum) occurred. This was done by determining the factors by which the sum of the squares of the data values would need to be divided to provide the least-squares polynomial fit and the minimum tip second derivative approximation. The analysis was performed on three databases, namely; the 17 point model previously described (Model 1), a 17 point model with the points near the boundaries equidistant from each other (Model 2) and a 15 point model again with the points near the boundaries equidistant from each other (Model 3). Although the difference in the point density is small, addition of even a single point to a model has a significant effect on the performance of the technique as was shown earlier. It was envisaged that these databases would provide some insight into the effect of varying point locations and densities on the magnitudes of the factors relating the three approximation conditions.

The results from this analysis, shown in Table 4.3, indicate that the factor by which the sum of the squares of the data values would need to be divided in order to provide the value of S for the least-squares fit significantly dropped, with increase in mode number. The magnitudes of the factors were seen to be lower for the smaller database. The factors which related the sum of the squares of the data values to the value of S at which the second derivative condition at the tip was satisfied did not however, follow any ordered pattern. This was attributed to differences in the parameters which control the approximations at which the second derivative condition for each mode was met, particularly the number of knots in the fit function. The number of knots for the least-squares polynomial fit was, on the other hand, the same for all modes (i.e., eight external knots, no internal knots). Despite the lack of a definite trend in the factors, the results still provide a useful threshold divisor of 160, from model 2, from which the search for the optimum approximant could be initiated. This value however only applies to the particular structure and level of error used in this case and may not apply for a different structure.

(c) Optimisation Based on First Order Difference Computations

In this approach, it was presumed that the results from a first order difference (FOD) computation before any fitting was performed could give an indication of the level of smoothing which would be required for the given level of error in the translational data. This was based on the understanding that the FOD calculation removes the mean effect and highlights the point-to point variation of the estimate of the rotation. Thus, it was envisaged that FOD estimates of rotations could give a feel of the orders of magnitudes of the rotations i.e., if the FOD estimates differed wildly from an initial approximation using curve fitting, this would give an indication of how far this initial approximation from fitting was from the optimum. It must also be understood here that in order to provide reasonably accurate estimates, FOD computations would require at least two data points between nodal points. This is consistent with the conclusion drawn earlier in this work.

Typical results of the FOD analysis on four different beam models, for modes 1 and 5, are given in Tables 4.4 to 4.7 using the exact, 0-1-0-1- and 1-0-1-0- databases. The exact analytical rotations are also included as a comparison base. The results indicate that a high level of smoothing would be required for the first mode for the 15 and 17 point models when worst case databases are used. This was shown by the multiple sign changes in the FOD calculation of the rotations and buttresses the earlier observation that the best approximation for the fundamental mode was the least-squares polynomial fit. No spurious sign changes were however seen for the other modes although there were irregularities in the magnitudes of the computed rotations especially near the boundaries and at or near the points of inflection of the mode shapes. Although this is not specifically dealt with in this work, it is envisaged that the level of the magnitudes of these irregularities could also be used as an indicator of the level of smoothing required.

(d) Effect of the density and spacing (location) of data points on the structure on the estimates of rotations

The data from the computations on the 17, 15 and 13 point worst case databases used in the optimisation analysis described in the previous section was also used in this investigation. The analysis revealed that for a small database, a tighter fit (smaller value of S) was required to produce comparable performance with an approximation from a larger database. The

results also indicated that for the same fit (same controlling parameters), the calculated translations and rotations deriving from the larger database were better. This was not unexpected since a larger database allows for better modelling of the structure.

The fluctuation in the calculated rotations near the boundaries is shown in Figure 4.20 and 4.21 for modes 1 and 5 respectively. It will be noted that for mode 1, the accuracy of the rotations deteriorates as the value of S is reduced. This provides further confirmation that the least-squares fit is the best estimator of rotations for the fundamental mode. On the other hand, it is evident from Figure 4.21 that, for the higher frequency modes, as the value of the smoothing factor was reduced, the models with the higher density of points near the ends of the cantilever yielded less fluctuation in the estimated rotations there than the 13-point database.

Comparison of the performance on the two 17-point databases revealed that the approximation from the database with evenly spaced points near the boundaries gave better estimates of rotations (in both form and magnitude) than the same approximation on the database with unevenly spaced base points near the boundaries. This observation was also confirmed by the estimates of the rotations from first order difference computations.

The sensitivity of the estimation technique to a much closer spacing of the data points was investigated by modelling the cantilever beam with 41 equidistant points. This reduced the spacing of the data points by a factor of four. The results confirmed that, from the optimum fit, there were no spurious fluctuations of the rotations anywhere on the structure. This outcome is explained by the fact that the knots of the fit function were not placed at consecutive data points (i.e., the fitting routine had more data points to choose from when locating the knots and thus the knots were located at the points at which the fit was particularly poor). In the case where the value of the smoothing factor was small enough to pick up the noise in the translational data, there were no fluctuations in the computed rotations in the mid-section of the beam as seen from previous analyses.

It can therefore be concluded that equidistant spacing of the data points on the structure in modelling is desirable. However, locating points close together in the database demands a

higher level of smoothing which in turn leads to higher levels of error in the estimated rotations. Assuming that there are already two points between nodal lines, a halving of the spacing near the boundaries provides a good compromise between good representation of the structure and good estimation of the rotations there. Finally, in order to avoid having to use very tight fits which may lead to unreliable results especially near the boundaries, the database should be made as large as possible. These conclusions must always be viewed in the light that there must be at least two measurement points between nodal lines.

4.3.3 Fit Performance on Real Experimental Data

The results presented so far on curve fitting noisy data have considered simulated experimental data. The real test however, is its applicability to real experimental data. Appendix 3 demonstrates the performance of the proposed technique on real experimental data. The discussion which is presented in Appendix 3 is based on a cantilever beam database which does not follow the criteria developed in the preceding sections on optimising the performance of the proposed method. Thus, the results presented merely demonstrate the performance of the technique on real experimental data albeit on a database which is less than ideal and do not provide any new insights.

In the appendix, it is shown that the errors in the estimates of the rotations from the approximation which minimises the errors in the rotation at the fixed end are, in the main, less than 10%. This very welcome observation is consistent with the observations made in the preceding discussions on error-free and simulated experimental data and thus confirms the capability of the proposed technique for smoothing noisy data. The appendix proceeds to demonstrate the acceptability of the estimates of rotations for structural dynamics modification work.

4.4 Surface Fitting Performance

Although most structures can be analyzed in straight lines locally, there are some complex structures for which the straight-line simplification does not hold. Part of the effort in this work was therefore directed at investigating the performance of bicubic spline surface fitting to the problem of estimating rotations from translational modal data. In addition, and so far as this researcher is aware, there has not been any published work on the use of surface fitting

for estimating rotations from translational data. It was therefore envisaged that this endeavour would provide new insights in this regard. To this end, different plate-like structures were investigated, namely; a free-free plate and a cantilever plate. In each case, translational and rotational modal data was obtained using finite element analysis. Rotations at every point on the structures were also obtained using the bicubic-surface fitting estimation technique described in Chapter 3. It must be noted that since only one out-of-plane direction can be used, only the rotations about in-plane axes were calculated.

It must be understood from the outset that extensional vibrations in which motion is only in the plane of the plate can also occur in plate structures. However, as this type of vibration is associated with high frequencies and has less practical significance than transverse vibrations, it is not considered in this work.

Tests on the performance of the surface fitting method indicated that, in general, the calculated translations and rotations from a curve fit were more accurate than those from a surface fit. This was due to the greater smoothing effect in a surface fit arising from the requirement to include the weights (effects) of the points adjacent to each measurement point since each point is inherently dependent on not only two but four adjacent points. In addition, due to the failure of the fitter to adequately model the boundaries as seen in the curve fitting case, the estimates of the rotations were better away from the boundaries of the structure than at the boundaries. The results also revealed that, generally and as a result of smoothing, large errors in the calculated translations were not necessarily associated with large errors in the computed rotations at those locations where the large errors in the translations occurred. As in the case of curve fitting, the best estimator of the rotations from error-free translational data was the interpolant.

Comparison of the relative accuracy of the computed in-plane rotations showed that the relative accuracy of the estimates of the rotations about the in-plane axes was heavily dependent on the relative dimensions of the structure. This was attributed to the way the fitting algorithm added knots to the fit function. In the algorithm used, the knots are always added in the x-direction to start with. That is, in the search for the fit which satisfies the fitting criteria, knots are added alternatively in the x and y directions of the plane starting

with the x-direction. The approximation is therefore able to pick up the trend in the underlying function in the x-direction before this is done for the y-direction. However, in the case where the number of knots in the fit function is the same in both directions, the underlying function is picked up better in the direction of the shorter dimension. Thus, the relative dimensions of the structure in the x-y plane are an important consideration here as they have a bearing on the measurement point density (and hence knot location) in each direction, i.e., a short dimension is modelled better than a longer dimension when the same number of measurement points in each direction is used. It may finally be remarked that, as would be expected, the accuracy of the computed rotations improved with increase in the number of measurement points on the structure.

4.4.1 Fit Performance on Error-free Data

4.4.1.1 Free-Free Plate

For this enquiry, a free-free mild steel plate, 152mm long, 300mm wide and 5.5mm deep, was modelled using a 5 x 5 grid of measurement points thereby producing 16 four-noded thin plate elements. Translational and rotational modal data for the first 20 modes (including the rigid body modes) was obtained from FE analysis. Figure 4.22 shows the FE translational mode shapes for the first four flexural modes. Estimates of the rotations were also obtained by surface fitting the finite element translational data with all data points carrying the same weight from three approximations namely; the least-squares fit (no internal knots), one knot in either of the in-plane directions and one knot in each of the in-plane directions. A representative set of results for the first four modes is shown in Figures 4.23 to 4.26 in the form of rotational modeshapes (the results for the other modes were similar).

It is apparent from the figures that the accuracy of the estimates of the rotations improved with a tighter fit albeit with some departure from this trend for mode 2. While the improvement in the performance was not unexpected, the accuracy of the estimates was also seen to be dependent on the complexity of the mode shapes. The average error in the estimated rotations at all points was observed to be very small (less than 2%) for the rigid body modes. The errors in the estimates of the rotations for the flexural modes were however much higher, rising beyond 100% for the higher frequency modes. The errors were seen to rise not simply with an increase in mode number but rather, with increase in the complexity

of the deformed shape. It is also particularly important to note that here, unlike in the case of curve fitting, approximations using relatively large values of the smoothing factor (i.e., high level of smoothing) are capable of returning reasonable estimates of rotations. In addition, it is seen that in a surface fit, the under-lying trend of the mode shape function is picked up with relatively fewer points in the model than in the case of curve fitting and thus the spacing requirement determined there is less critical here.

Figure 4.27 presents the performance of the interpolating spline. It will be seen that, as in the case of curve fitting, the interpolant returns the best approximation from error-free data. In this case, the maximum error in the estimates of rotation was around 70% for the higher frequency modes. It is also particularly interesting to note that the estimates of rotations about the y-axis are superior to those about the x-axis. This is due to the fact that although the number of knots in both directions is the same during interpolation (9 in this case), the x-direction is modelled better than the y-direction because it is the shorter of the two dimensions.

In the analysis on curve fitting, it was shown that addition of a mid-point near the boundaries had a dramatic effect on the estimates of rotations there since addition of the extra point improved the representation of the structure (Figure 4.7). Figure 4.27 also presents the comparison of the performance of the interpolant on the 25-point model with a model in which a mid-point was added near the ends (thereby expanding the database to 49 points). The data is presented in the form of rotational mode shapes. Once again the results exhibit the dramatic improvement in the quality of the estimates of rotations, the maximum error being around 20% for the higher frequency modes.

4.4.1.2 Cantilever Plate

A mild steel cantilever plate of dimensions 500mm long, 150mm wide and 5mm deep was used here. The finite element model, from which translational and rotational modal data for the first 10 modes was derived, consisted of 140 thin-plate elements (36 x 5 grid of measurement points) thus yielding 900 degrees of freedom (thin-plate elements do not have a rotational DOF about the out-of-plane axis) of which 25 were grounded. This idealisation is shown in Figure 4.28. In addition to providing further insights into the performance of the

surface approximant on different boundary conditions, this type of structure was specifically chosen in order to provide a basis for comparing curve and surface fitting. The mode shapes for modes 3, 4, 7 and 8 are shown in Figure 4.29.

In this case, three approximations were used namely; fit with at least one internal knot in both directions, fit with at least two internal knots in both directions and the interpolant. Initial examination of the results revealed features not unlike those which had been seen in the curve fitting case. The comparison of the estimates of the rotations from the first two approximations with FE rotations is shown in Figures 4.30 and 4.31 in the form of rotational mode shapes. The results show the expected improvement in the estimates of the rotations with reduction in the smoothing factor. In addition, the results indicate the poor performance of the estimator in the regions adjacent to the boundaries as was seen in the case of curve fitting. This is shown in detail in Figure 4.32 in which the errors in the rotations (normalised to the largest rotation for each mode) are presented in the form of modeshapes and error plots. Although it was clear from the data that the approximation using at least two internal knots in both directions still produced appreciable discrepancies, the magnitudes of the errors in the rotations were generally less than 20%. In the proximity of the boundaries however, the errors were higher. A particularly noteworthy characteristic which is apparent is the inferior quality of the estimation of the rotations about the y-axis to that of those about the x-axis. However, this is not surprising since the rotations about the y-axis were higher than those about the x-axis.

The results from the interpolating approximation which are shown in Figure 4.33, indicate the significant improvement of the estimates of the rotations over the approximations with a higher level of smoothing. The error in the rotations is also seen to be much lower in the region near the boundaries. In fact, the magnitude of the errors in the rotations was less than 5% for rotations about the x-axis and less than 1.5% for rotations about y-axis. Thus, it is seen that the approximation returns better estimates of rotations about the y-axis than about the x-axis as was the case for the free-free plate when interpolation was used. This is however explained by the fact that during interpolation in this case, the number of knots in the x-direction is much higher than that in the y-direction since this is dependent on the number of measurement points in each direction, which in this case, is higher in the x-

direction. Therefore, the location of knots in the x-direction is better optimised than in the y-direction. Thus, the under-lying modeshape function is better represented by the fit function in this direction thereby leading to superior estimates of rotations about the y-axis. When this observation is viewed in the light of the results seen for smoothing in the case of the free-free plate, it may be concluded that in any exercise in which surface fitting is used to estimate the rotations, the choice of the orientation of the structural global axes will be determined by the end-use of the data.

4.4.2 Fit Performance on Real Experimental Data

The discussions presented so far have considered the performance of the surface approximant on error-free data. The real test, however, is its performance on real experimental data. The modal data for a plate-like structure which was used in this case was not consistent with the findings about optimising the performance of the estimation method. Thus, the discussion of the performance of surface approximation on real experimental data is included in Appendix 3. The presentation also provides insights into the treatment of a multi-surface structure, especially at the joint lines, where the user must decide which rotational entries to retain since the approximation necessarily produces more than one set of rotations at the joint line.

It is shown in the appendix that the estimates which must be retained at the joint line are those from the approximation on the larger of the planes which constitute the structure. The appendix also considers the accuracy of SDM predictions based on the expanded data.

4.5 Curve Fitting Versus Surface Fitting

In order to compare the relative performance of curve fitting approximation against surface fitting approximation, two cases were considered comprising of a cantilever beam, 500 x 25.4 x 12.7mm, and a cantilever plate, 500 x 150 x 5mm. In each case, the longest dimension was modelled with 36 equidistant measurement points and translation and rotational modal data was obtained from the analytical solution, in the case of the beam, and from finite element analysis, in the case of the plate. The complete plate model consisted of 180 measurement points on a 36 x 5 grid. Estimates of the rotations were also obtained by curve and surface fitting the appropriate data-set using the interpolating approximation. The comparison of the

performance of the two approximants is summarised in Figure 4.34 for the first two bending modes of the structures in the form of error plots. The relative performance of the surface approximation at the free edge and at mid-section is also highlighted.

The results show the superior overall performance of the curve fitter over the surface fitter. The errors in the rotations from the curve fitter were at least several orders of magnitude better than those from surface fitting. What is less apparent for surface fitting is the expected observation that the estimates of rotations away from the boundaries are superior to those at the boundaries. This was however amply illustrated in Figures 4.32 and 4.33. The comparison of the performance of curve fitting with surface fitting provides useful guidance to the user of the technique about the choice of the fitting method to be used depending on the end-use of the expanded data.

4.6 Real vis-à-vis Complex Modal Data

Although all the analyses in the investigations reported in this work were based on real modal data, this researcher acknowledges the existence of complex spatial descriptions of structural mode shapes. This is especially the case in the analyses involving rotating machinery or proportionally-damped structures. While most commercially available modal analysis systems are capable of handling the resulting complex modeshape descriptions, post-processing analysis usually either assumes that the mode shapes are 'almost' real valued and therefore disregards the imaginary parts or ignores any phase angles which are not 0 or 180 degrees. This is in part based on the assumption that most real physical world structures exhibit classical or light damping and therefore have damping forces which are insignificant when compared to the inertial and restoring forces.

In their investigation into modeshape expansion techniques, Imregun and Ewins [28] have however shown that it is unlikely that acceptable results can be obtained from an expansion of markedly complex modeshape vectors to those of the full model. Their results have not only indicated that complex mode shapes cannot be expanded accurately using assumed real mode shapes, they have also shown that the use of complex modal data deteriorates the quality of the expansion. In as far as the estimation of unmeasured data (both rotations and translations) from measured translations using curve and surface fitting is concerned, it can

therefore be inferred that the user of this technique must exercise great caution in instances where the mode shapes are markedly complex as the resulting expansion may be grossly erroneous. Although this aspect is not dealt with in this work, it is reasonable to surmise that both curve and surface fitting may be used with complex modes. This could be done by separately treating real and imaginary parts of the displacements and then combining the resulting rotations to provide the complex rotations.

4.7 Closing Discussion

One of the tests for ascertaining the performance of a new technique is to compare its performance against other techniques. To this end, the performance of other techniques of estimating rotations must be known. In Chapter 2, the discussion of each estimating technique included, where possible, the performance levels. It was shown there that the most accurate techniques were those which required the development of finite element models [24,25,26,28] and the 'rigid body enhancement method' [45] which did not require an FE model. While the performance of these techniques was very good (up to 5% error in the rotations), the associated time, storage requirements and cost could not be justified for many applications.

The spline curve and surface fitting method proposed in this work is a cheaper, simpler and quicker technique which has been shown to yield errors of less than 10% from noisy data provided there are at least two measurement points between nodal lines. While errors may not be directly comparable due to differences in the structures and database sizes (and the absence of database size information and/or structural dimensions in some cases), the proposed method generally offers better performance than previous 'modeshape' techniques which yielded errors of between 15% and 100% on error-free data [13,24,29,30]. In addition, this level of performance is comparable with at least one of the FE based methods [25,26] which yielded errors of up to 12% in the estimated rotations. In this instance, comparisons are valid since at least four of the published sets of results [13,24,25,30] all considered a cantilever beam using error-free data, albeit with different dimensions and database sizes. The plate study [29] considered a cantilever plate also using error-free data with a similar database size as that used on the free-free plate in this work although the dimensions of the plate used were not cited. Thus, the comparisons given here should not be taken to be

absolute but should be treated as loose indicators of the performance of the proposed technique.

This chapter has also shown that the proposed method is versatile and offers the freedom to either smooth or interpolate the data. In the circumstances where interpolation is desirable, the analysis has shown that the method offers errors of less than 5% provided the spatial description of the structure allows for adequate representation of the structure, especially near and at the boundaries. In addition, the choice between curve and surface fitting offers further flexibility in the application of the method provided it is remembered that curve fitting offers superior performance.

4.8 General Concluding Remarks

The analyses reported in this chapter lead to the following conclusions:

1. The best estimator of rotations from error-free translational data is the interpolant.
2. The accuracy of the estimates of the rotations depends on the spatial description of the mode shapes provided by the measured translations. Typically, errors in the rotations are generally below 10% provided there are at least two measurement points between nodal lines.
3. Generally, fit functions are unable to truly represent the modeshape functions at the boundaries. This leads to large errors in the estimates of the rotation at and near the boundaries. In order to compensate for this, a dense distribution of measurement points near the boundary is desirable when dealing with error-free data.
4. For plate structures, the accuracy of the estimates of rotations is dependent on the orientation of the structural global axes and the modelling of the structure with regard to the density of measurement points in each planar direction. However, the accuracy of the estimates ultimately depends on the level of smoothing used in the approximation. The required level of smoothing depends on the particular problem and the values of the smoothing given in section 4.3.2.4 for beams make a good starting point in the search.
5. Generally, estimates of the rotations from a curve fit approximation are more accurate than those from a similar (i.e., same controlling parameters) surface fit approximation.

6. The complexity of a mode shape is a significant adverse factor for the quality of expansion. The quality of augmentation deteriorates rapidly as mode shapes become more complex (i.e., as mode number increases), particularly as the condition for spatial aliasing is reached.

7. The accuracy of rotational estimates depends on the level of error in the initial translational data. The higher the level of error in the initial data, the higher the level of smoothing required. In the absence of smoothing, the approximation will carry high errors while too much smoothing will lose the under-lying modeshape function. Thus, an optimum must be found which minimises the error in the estimates of rotations.

8. When dealing with noisy data,

   (a) the optimum estimator of the rotations is the approximation which satisfies the structural boundary conditions. This occurs at a value of the smoothing factor which is much smaller than that at which the full approximating criteria for the translations are met.

   (b) equidistant spacing of the data points is desirable. However, a dense location of points, especially near the boundaries, leads to high errors in the estimation of the rotations. Having satisfied the requirement of two measurement points between nodal lines, a halving of the spacing near the boundaries provides a good compromise between good representation of the structure and the risk of picking up the noise in the initial data.

   (c) in order to avoid using very small values of the smoothing factor (i.e., very tight fits) which may lead to unreliable results, especially near the boundaries, the database should be made as large as possible with regard to the number of measurement points.

   (d) the first order difference computation is a good indicator of the level of smoothing required for a given level of error in the translations and a given distribution of points on the structure. This information is provided by the number of sign changes between nodal lines and the irregularities in the magnitudes of the computed rotations resulting from the calculation. This gives guidance to the user of the proposed technique about where the search for an optimum may be initiated.

(e) the accuracy of the estimates of the rotations is not very sensitive to the pattern of error in the initial data.

(f) large errors in the calculated translations are not necessarily associated with large errors in the computed rotations at those locations due to the effect of smoothing.

9. Although this work has not considered the treatment of complex data, caution must be exercised in the application of the proposed technique in instances where the modal data is markedly complex as the resulting expansion may be grossly erroneous. Thus, this aspect calls for further investigation.

o0o

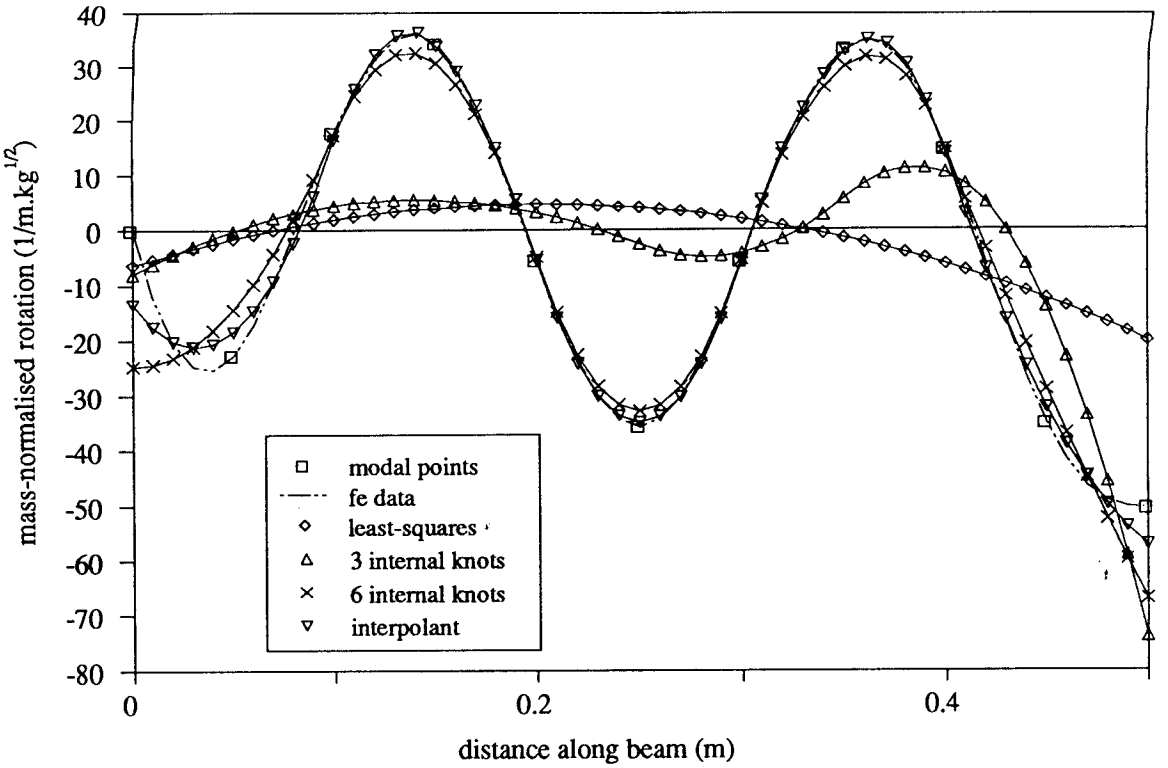

Figure 4.1: **Comparison of the rotation mode shapes for the fifth mode of the steel cantilever (11 point model)**

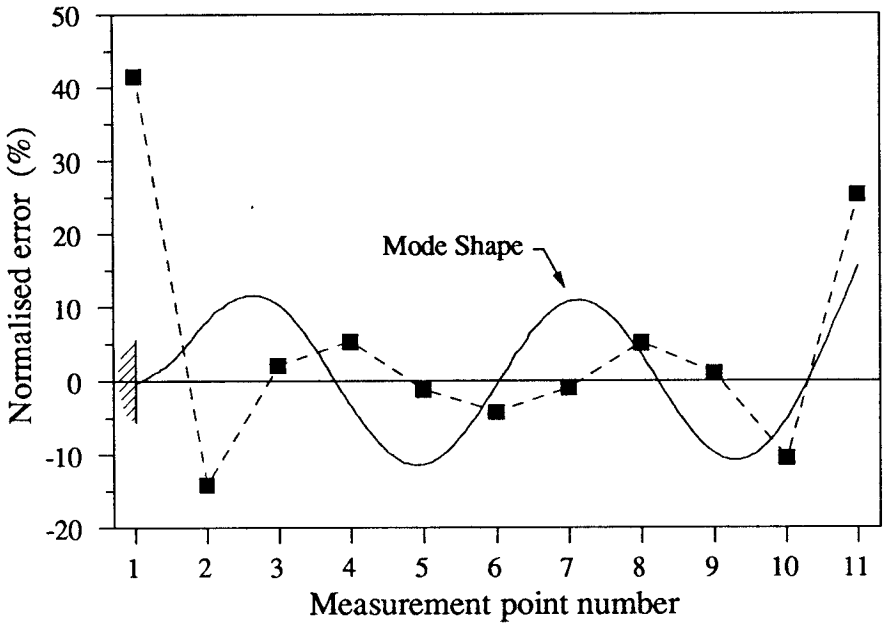

Figure 4.2: Normalised Mode Shape and Error in Calculated Rotations for the Fifth Flexural Mode of the Steel Cantilever

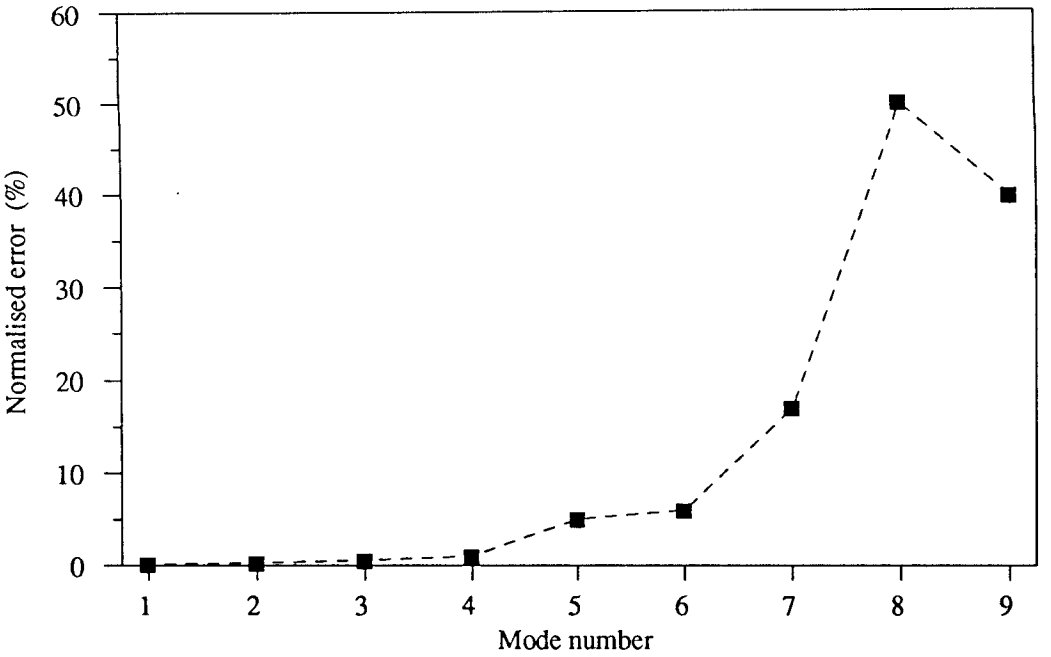

Figure 4.3: Normalised Error in Calculated Rotations for the Steel Cantilever

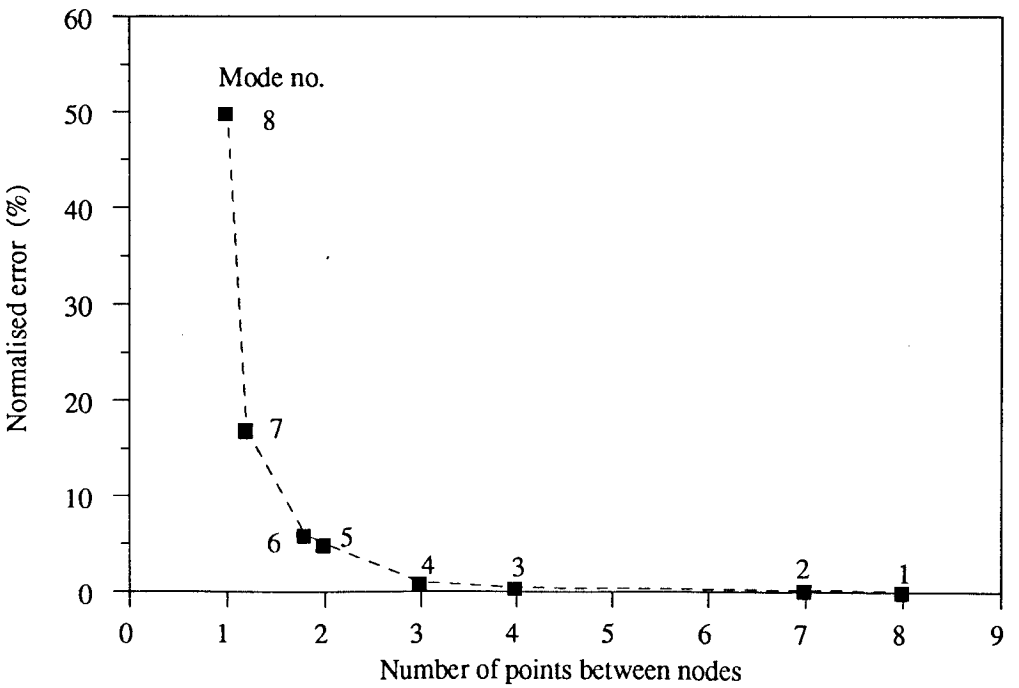

Figure 4.4: Normalised Error in Calculated Rotations vs Number of Points Between Nodes

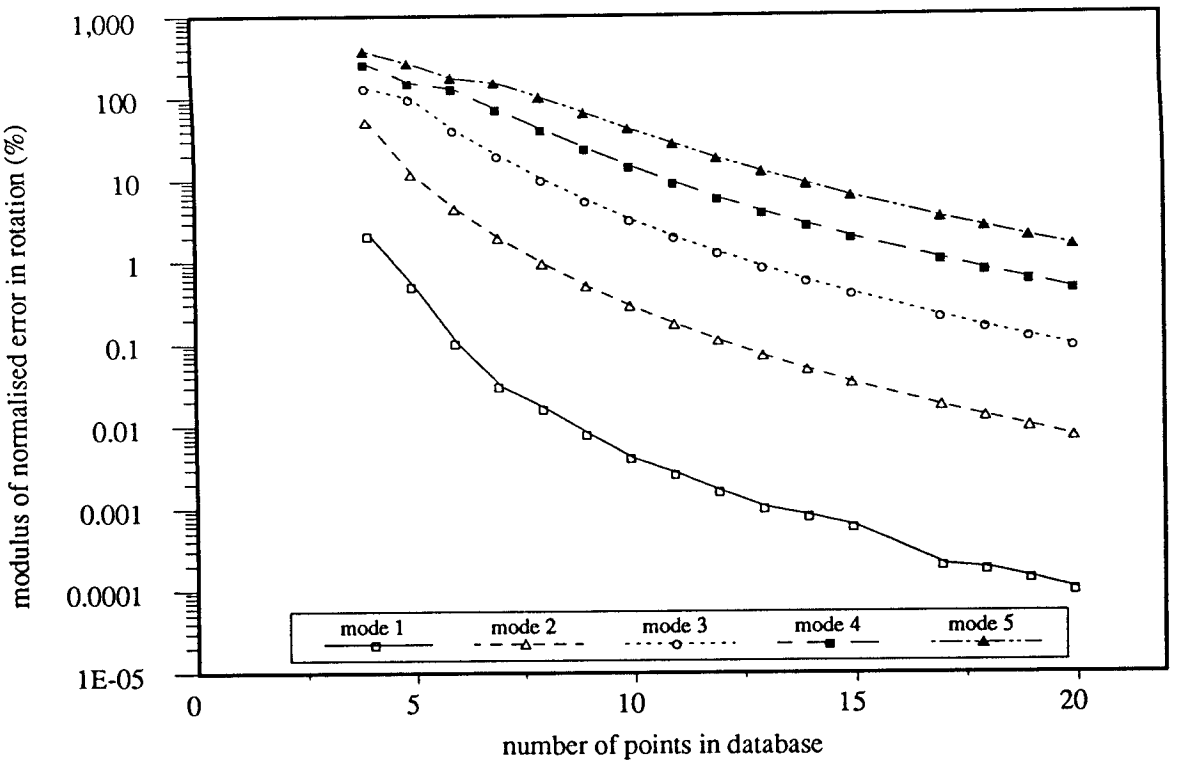

Figure 4.5: **Variation of the error in the computed rotations at the root with change in point density**

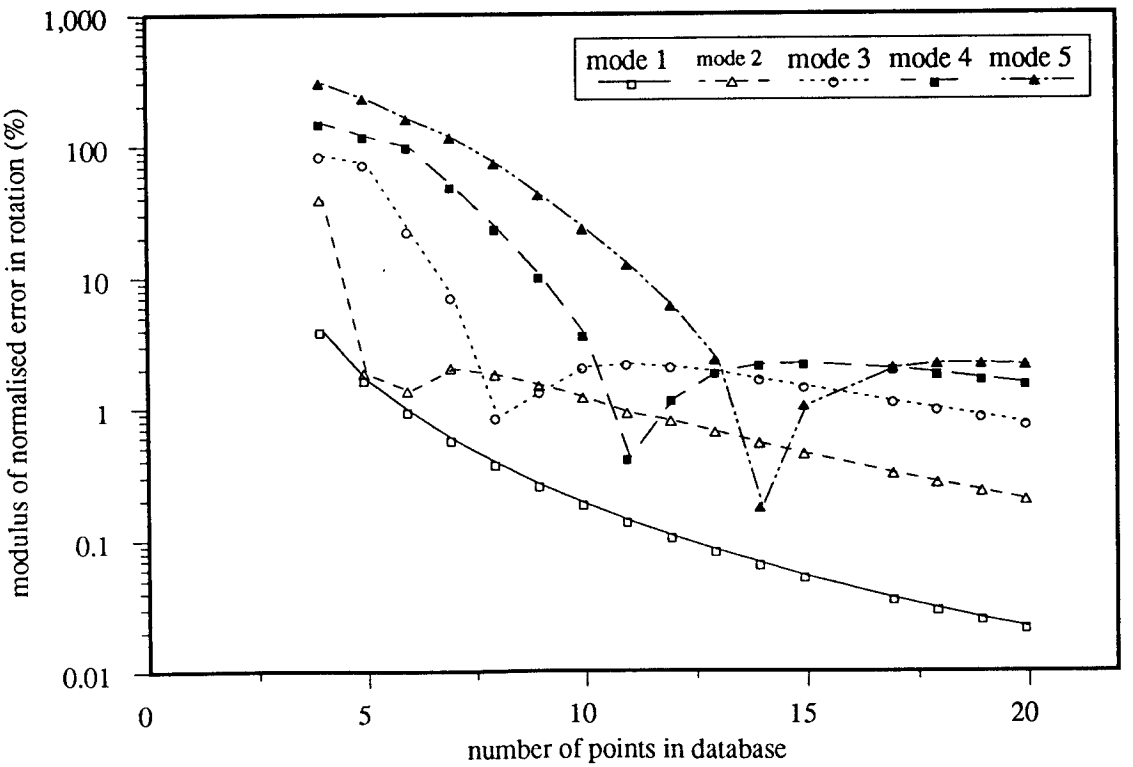

Figure 4.6: **Variation of the error in the computed rotations at the tip with change in point density**

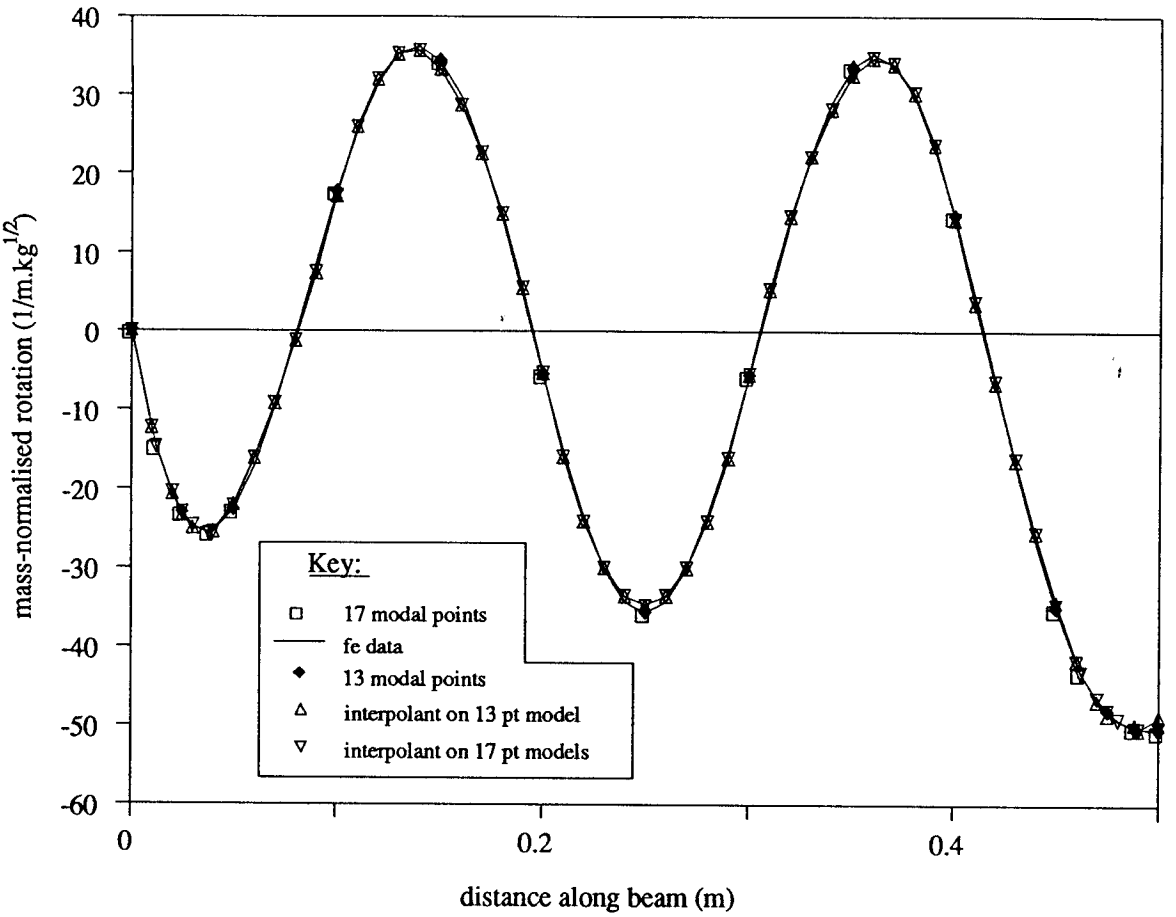

Figure 4.7: **Comparison of the rotation mode shapes for the fifth mode of the steel cantilever (13 and 17 point models)**

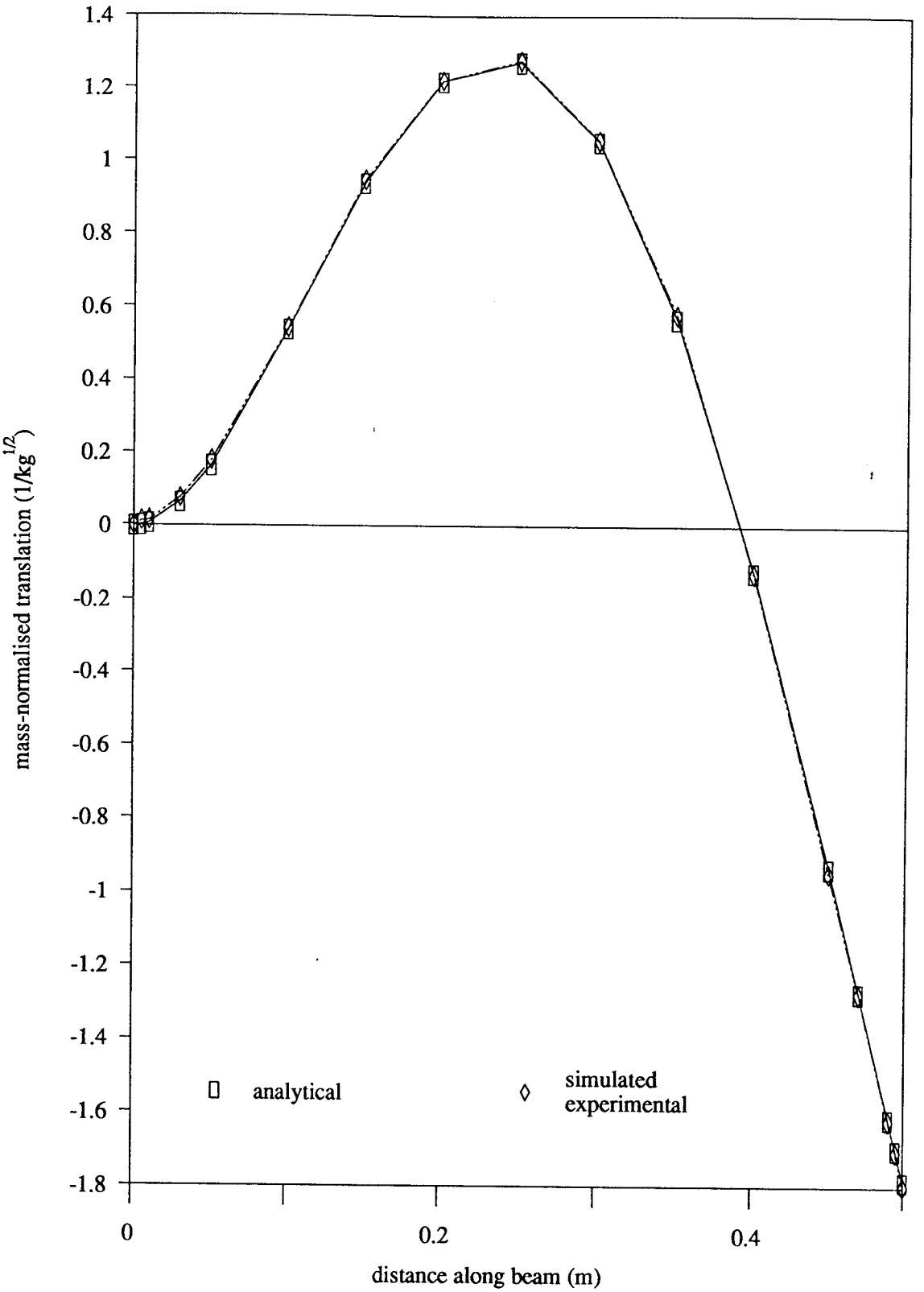

Figure 4.8a: **Comparison of the Simulated Experimental Mode Shape with the Analytical Mode Shape (mode 2) for the Steel Cantilever**

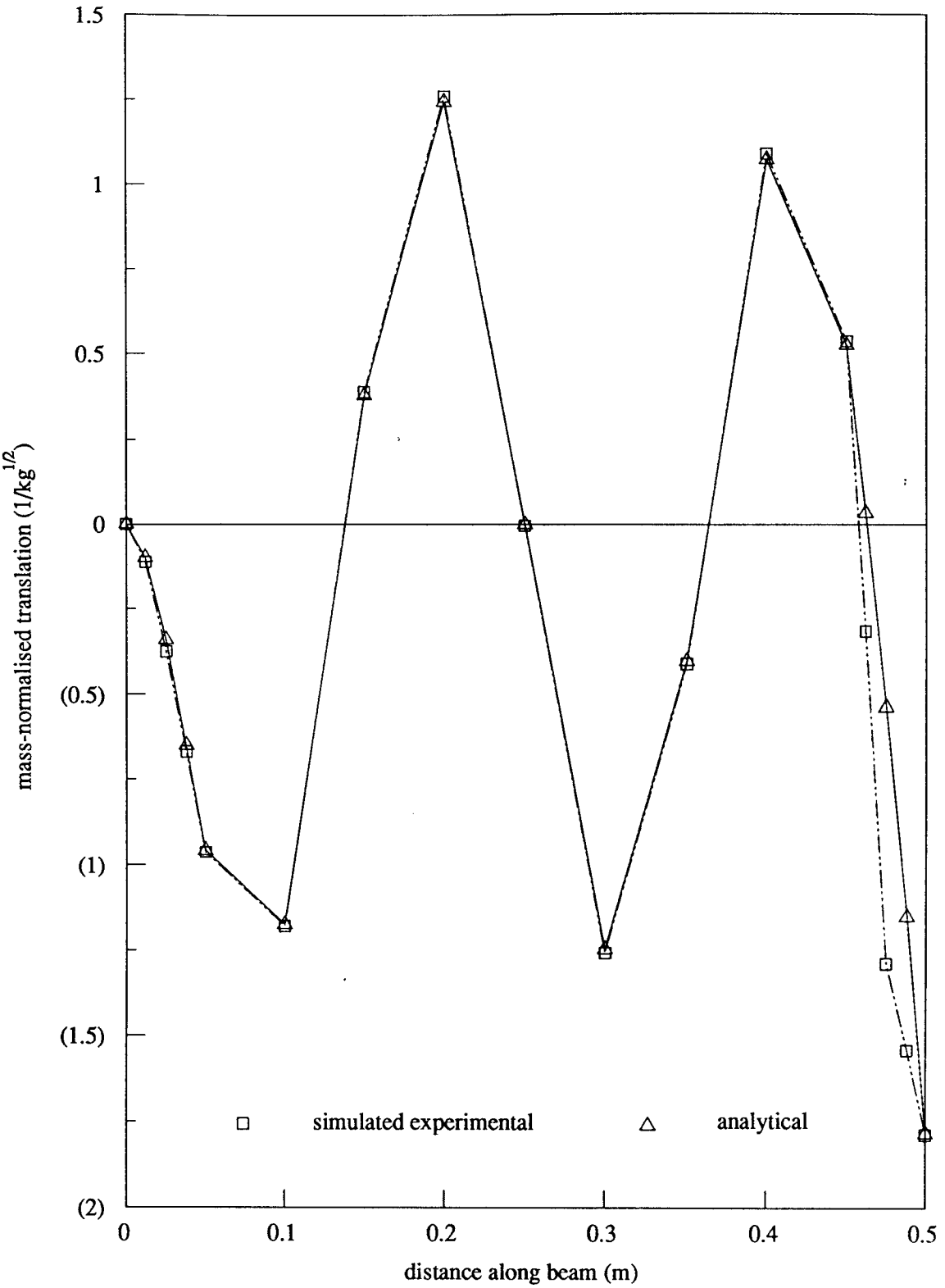

Figure 4.8b: **Comparison of the Simulated Experimental Mode Shape with the Analytical Mode Shape (mode 5) for the Steel Cantilever**

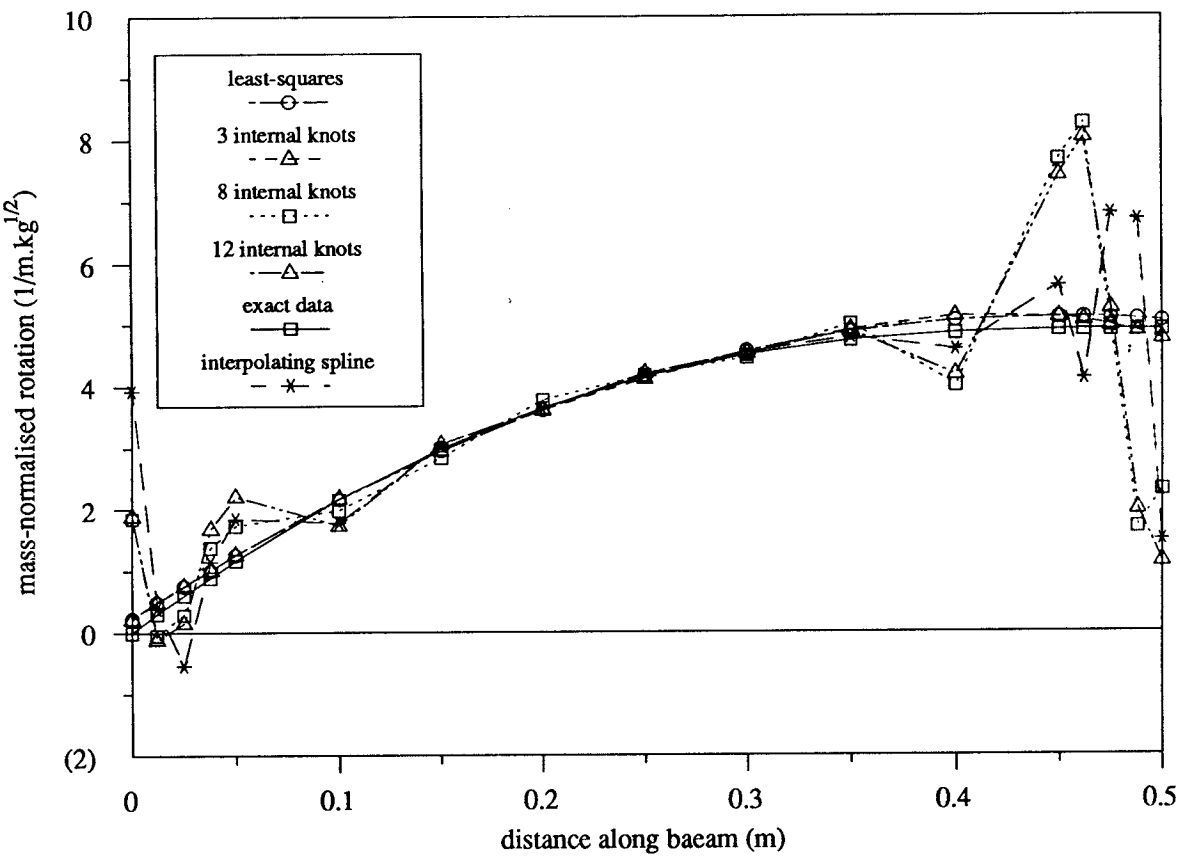

Figure 4.8c: **Comparison of the rotation mode shapes for the first mode of the steel cantilever from several fits on the simulated experimental data with representative error level**

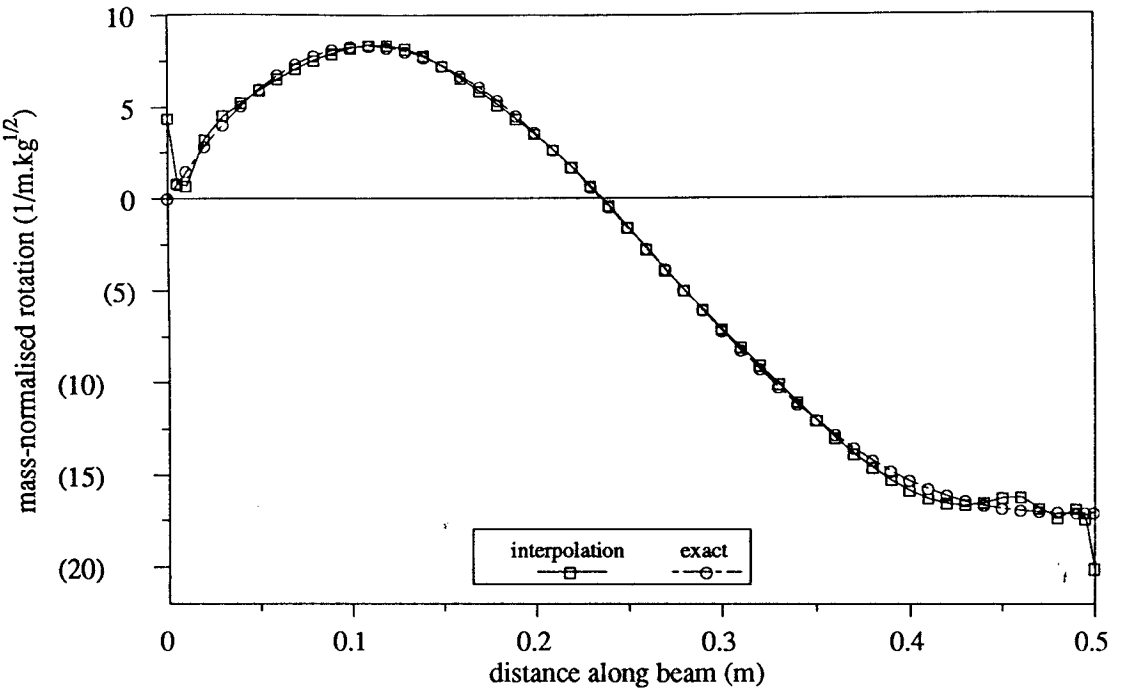

(a) mode 2

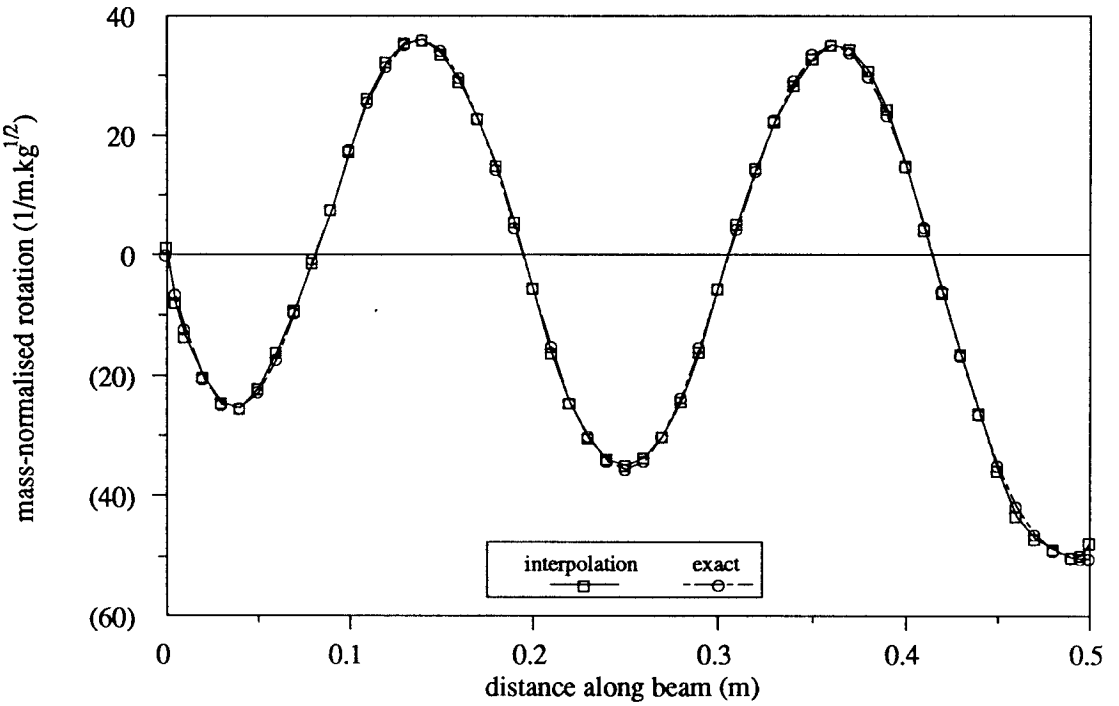

(b) mode 5

Figure 4.9: **Comparison of rotation mode shapes for the Steel Cantilever: Exact Data against Interpolation on Simulated Experimental Data**

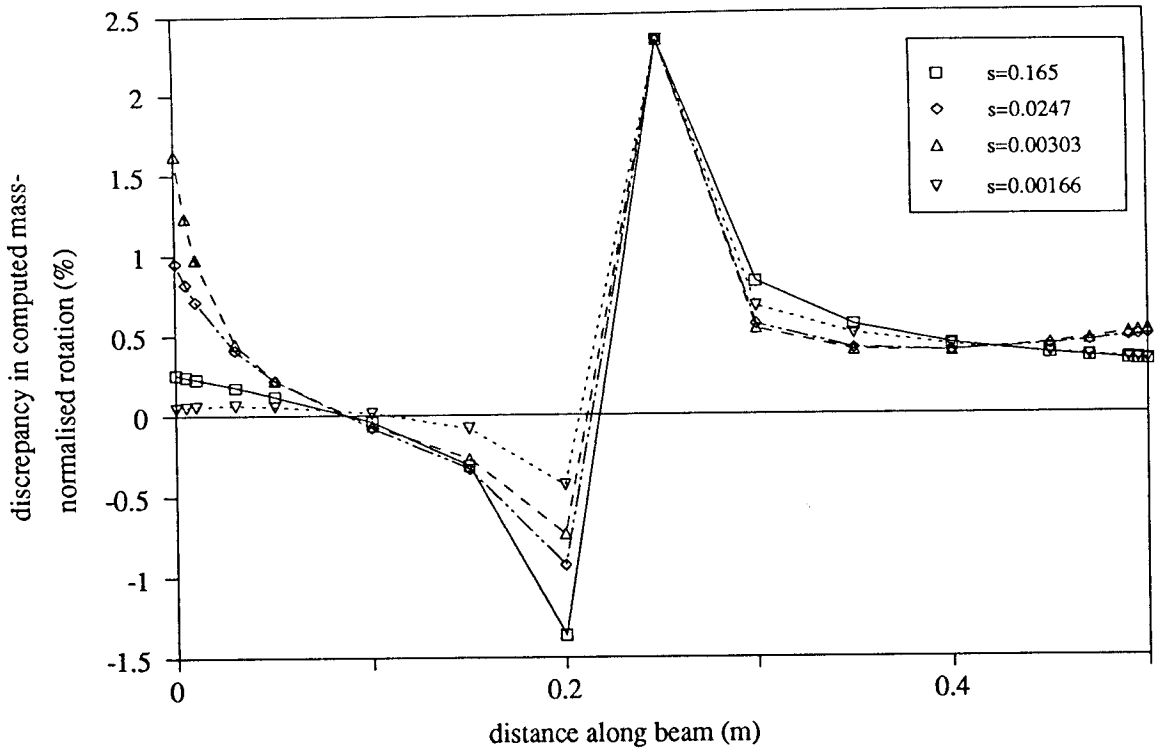

(a) mode 2, 9 knot fit

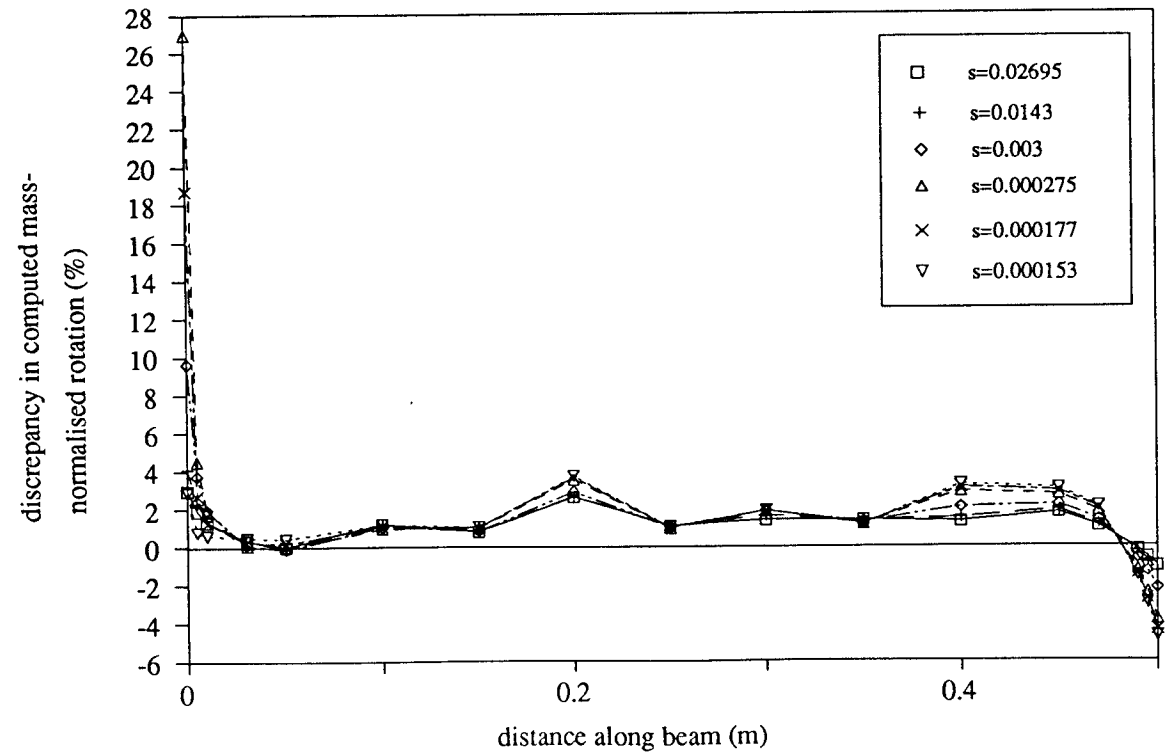

(b) mode 5, 17 knot fit

Figure 4.10: **Discrepancy in the Computed Rotations from approximations on Simulated Experimental and Exact data for the Steel Cantilever**

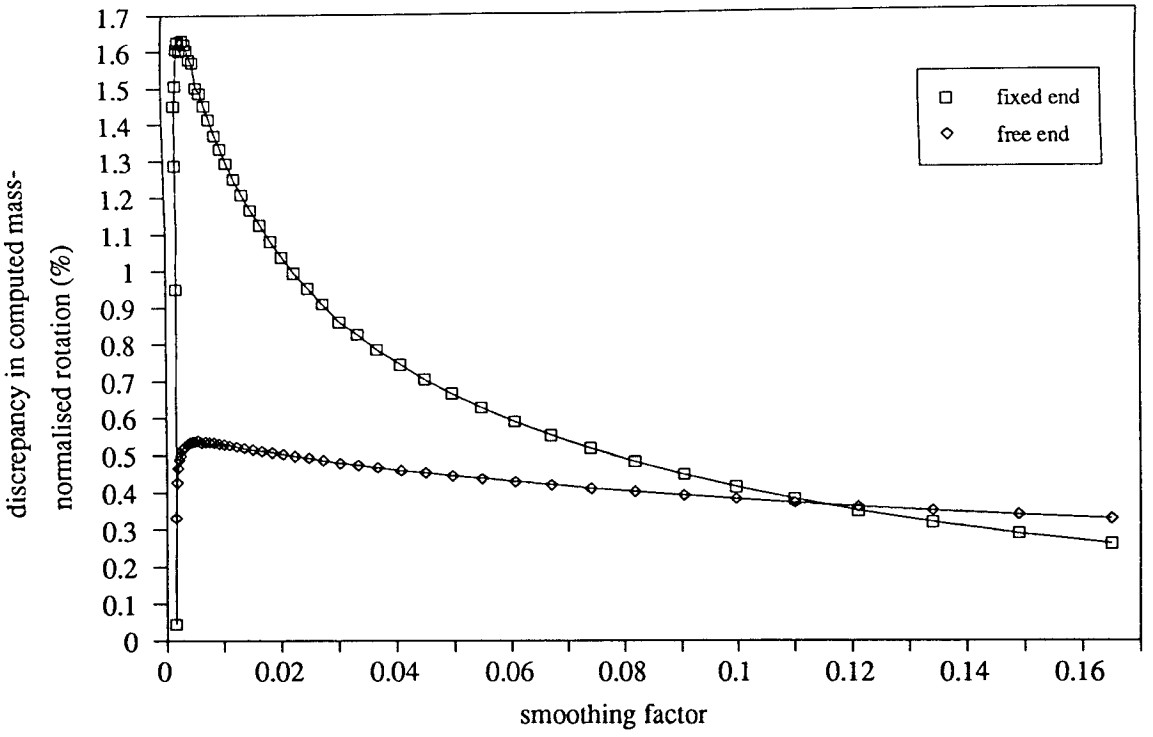

(a) mode 2, 9 knot fit

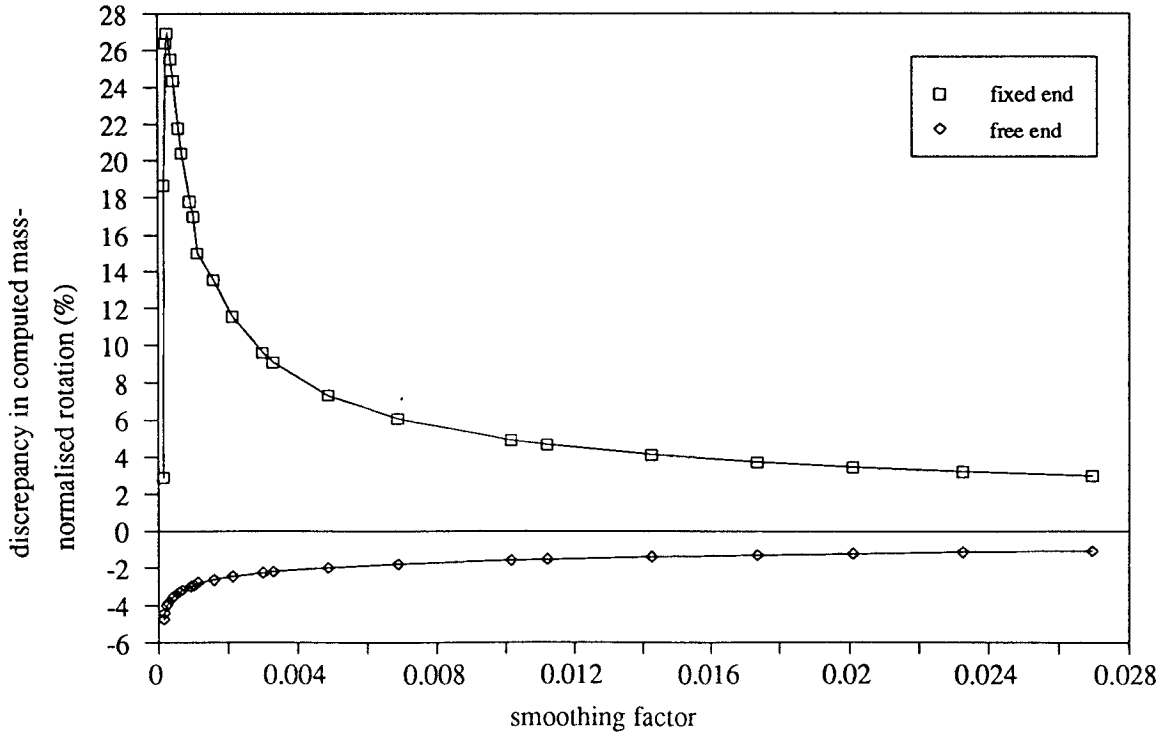

(b) mode 5, 17 knot fit

Figure 4.11: **Discrepancy in the Computed Rotations from Approximations on Simulated Experimental and Analytical Data at the ends of the Steel Cantilever**

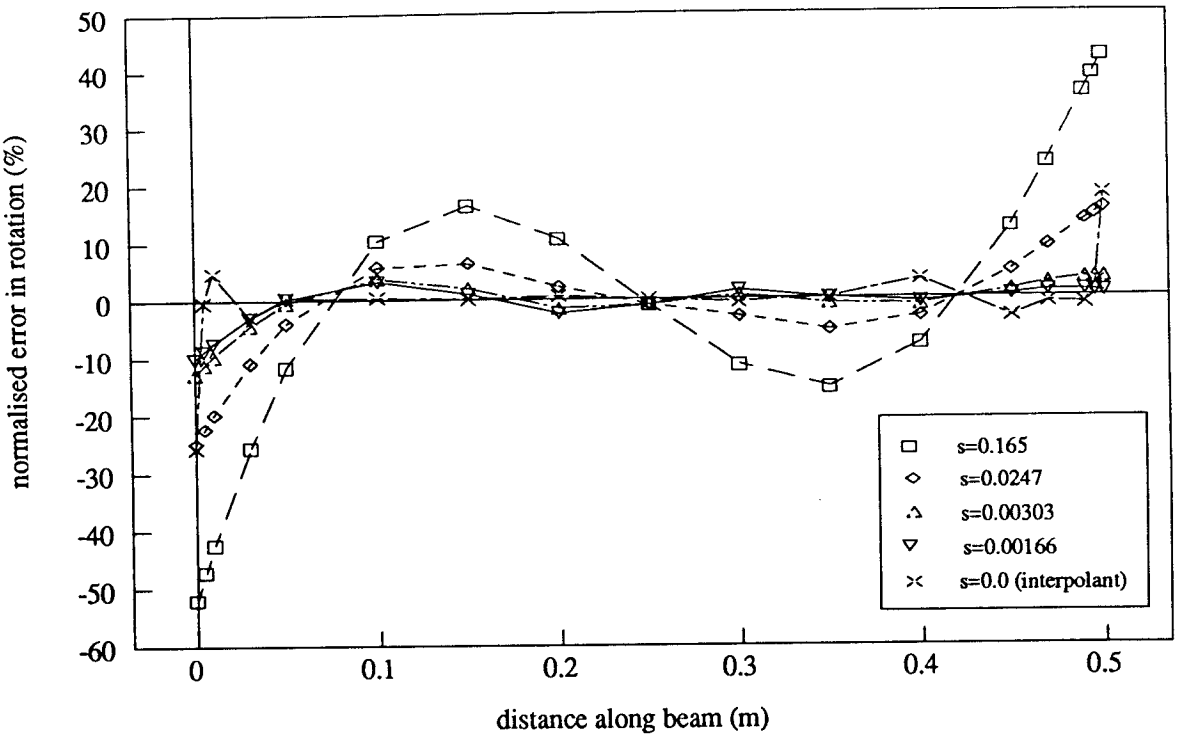

(a) mode 2, 9 knot fit

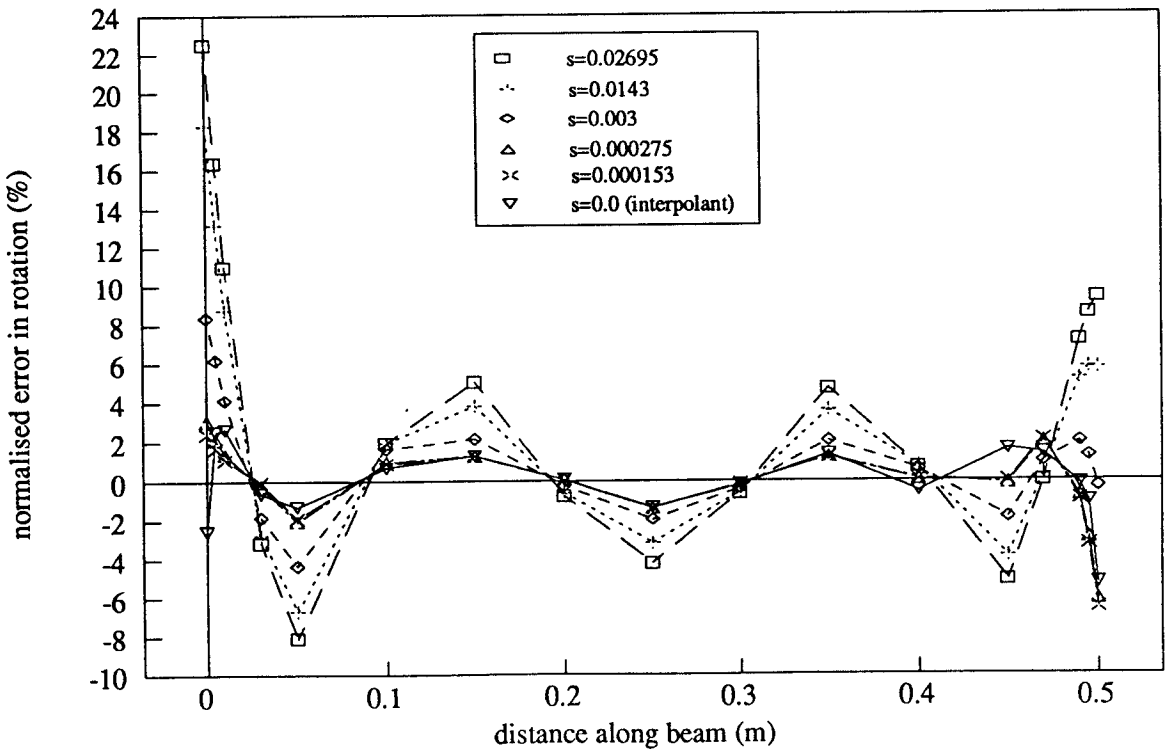

(b) mode 5, 17 knot fit

Figure 4.12: **Errors in the Computed Rotations from Several Approximations on Simulated *data for the Steel Cantilever***

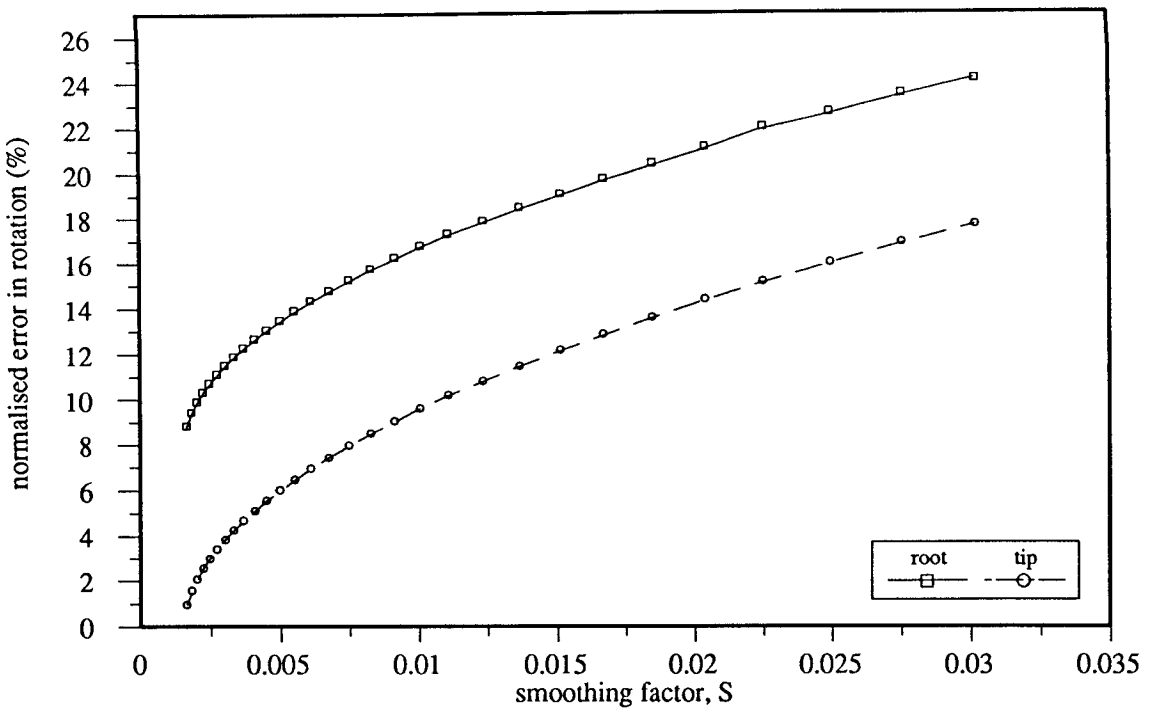

(a) mode 2

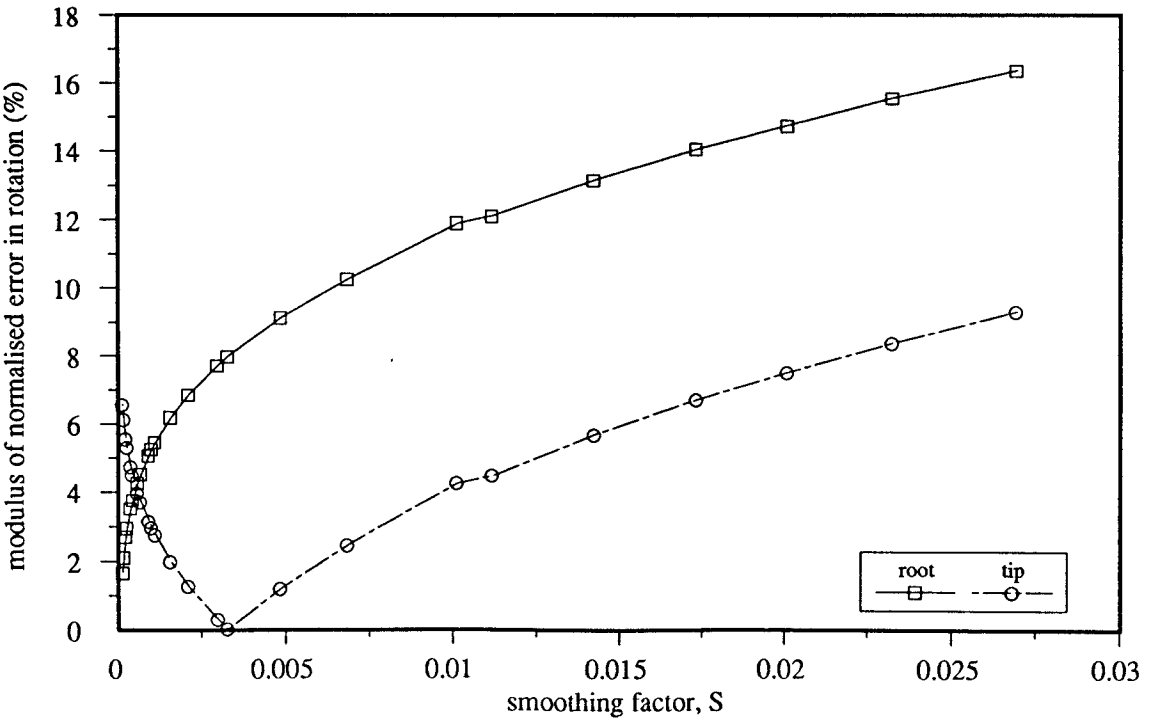

(b) mode 5

Figure 4.13: **Variation of the Error in the Computed Rotations for modes 2 and 5 from Simulated Experimental Data at the ends of the Steel Cantilever with Change in the Smoothing Factor**

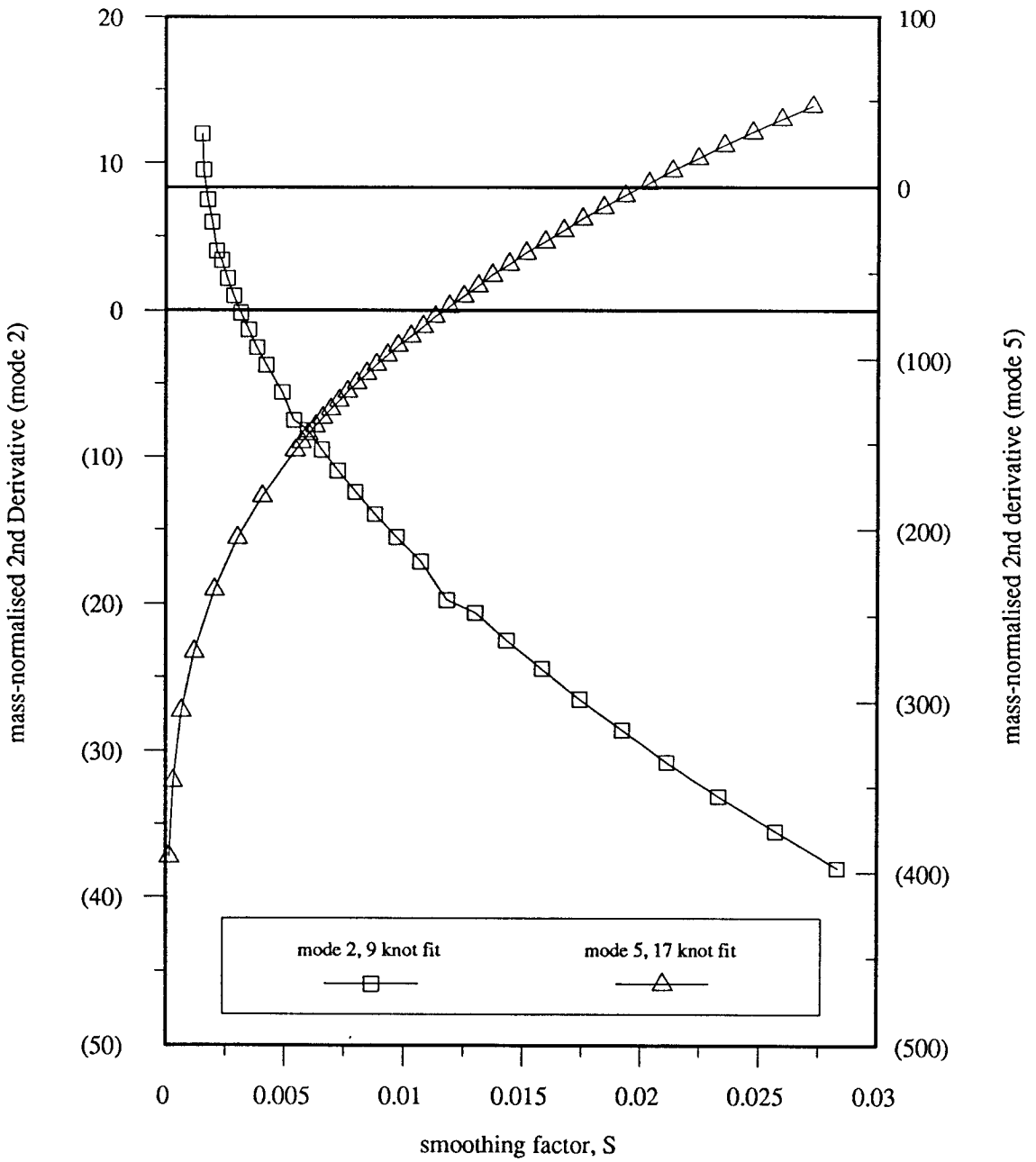

Figure 4.14: **Characteristic Behaviour of the Second Derivatives of the Fit Functions at the free end of the Steel Cantilever with change in the Smoothing Factor**

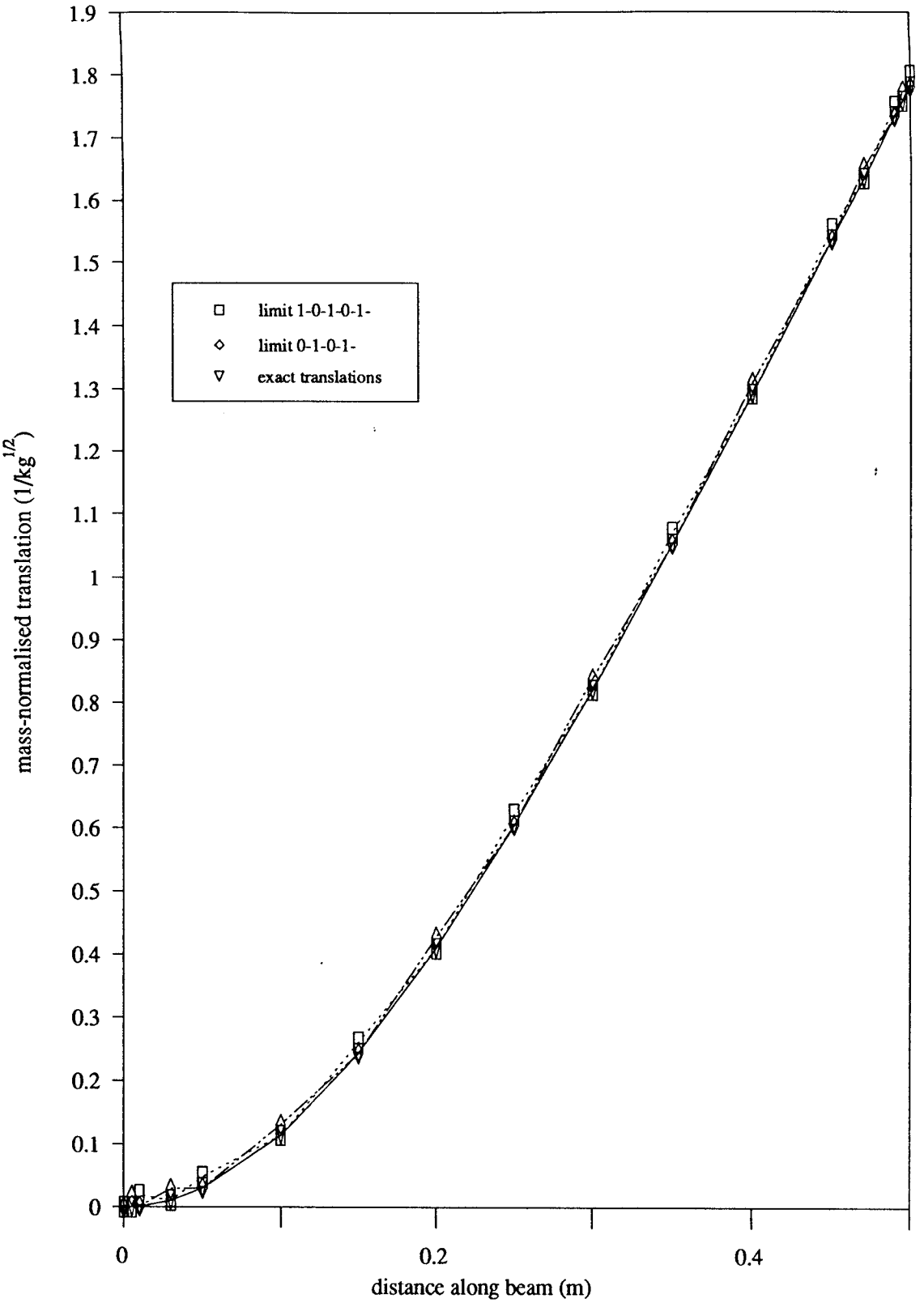

Figure 4.15: **Worst Case Scenario Error Seedings of the First Translational Mode Shape of the Steel Cantilever with Exact Translations Superimposed**

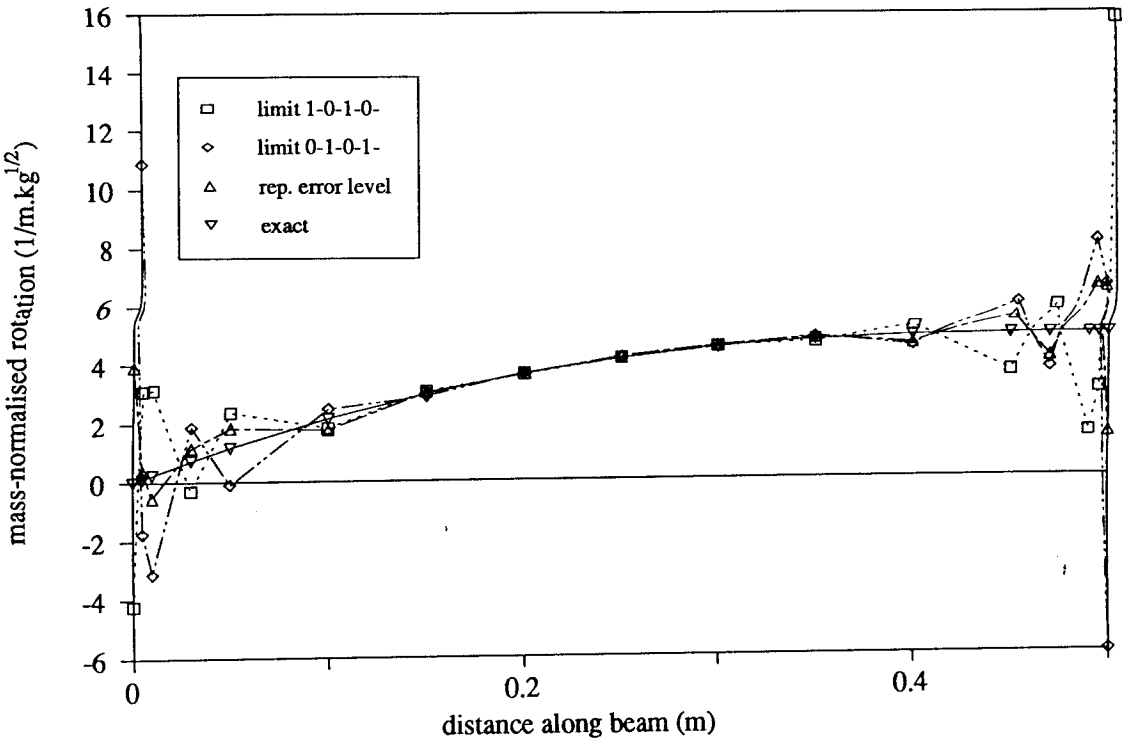

(a) mode 1

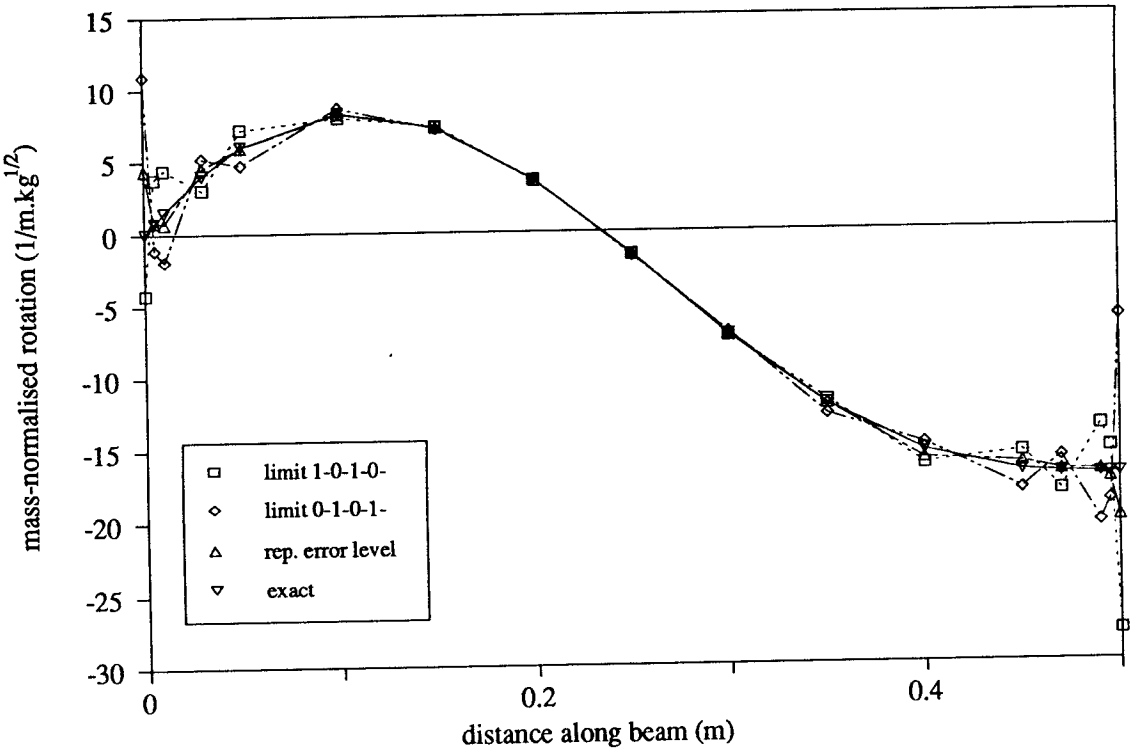

(b) mode 2

Figure 4.16: **Comparison of the Estimated Rotations from Worst Case Scenario and Representative Error Levels using the Interpolating Spline against Exact Data for the Steel Cantilever**

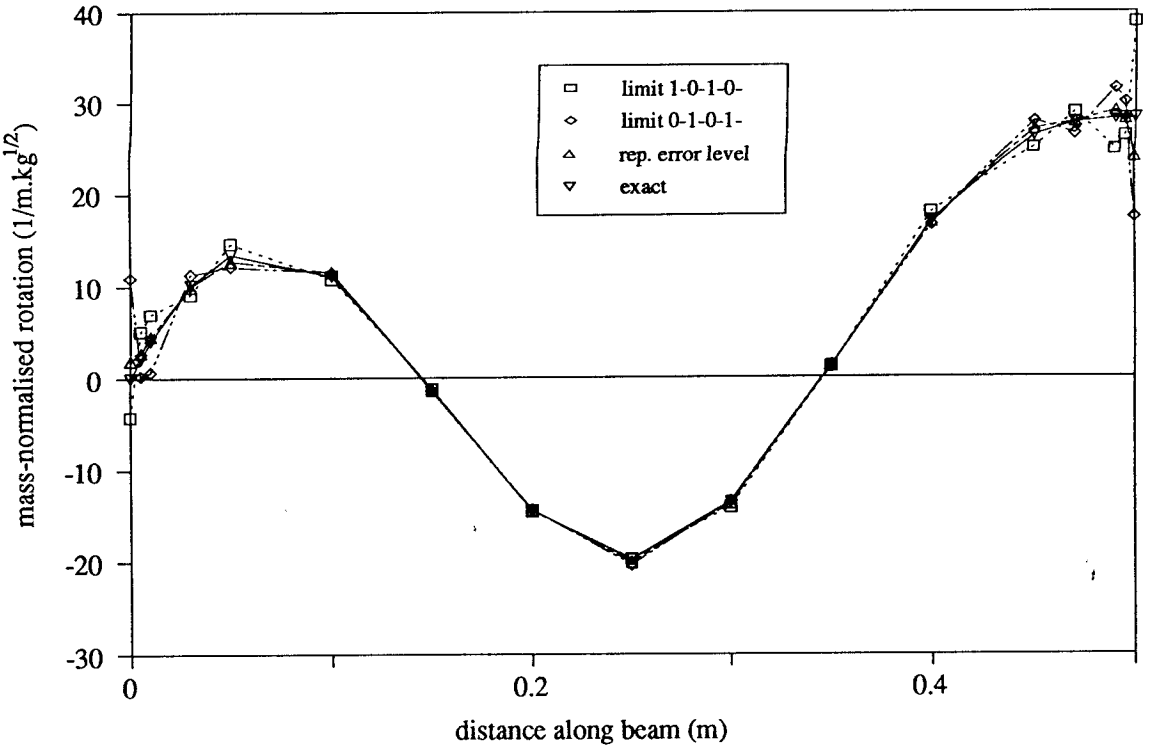

(c) mode 3

Figure 4.16: **Comparison of the Estimated Rotations from Worst Case Scenario and Representative Error Levels using the Interpolating Spline against Exact Data for the Steel Cantilever**

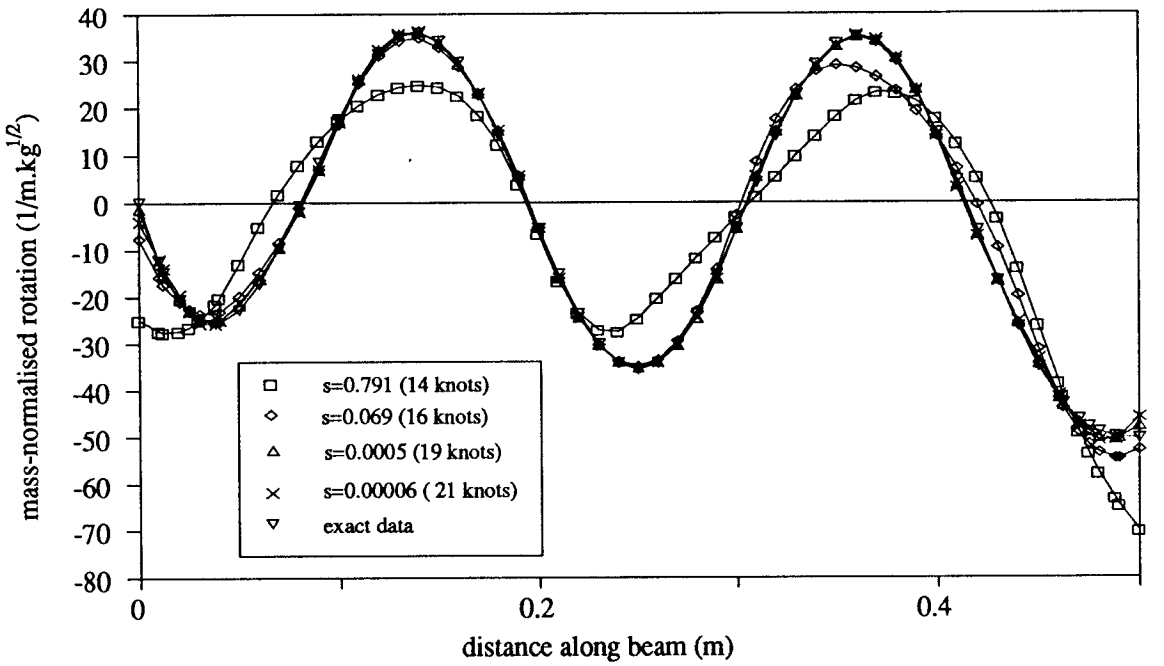

Figure 4.17: **Comparison of the rotation mode shapes for the fifth mode of the steel cantilever from several fits on 0-1-0-1-data**

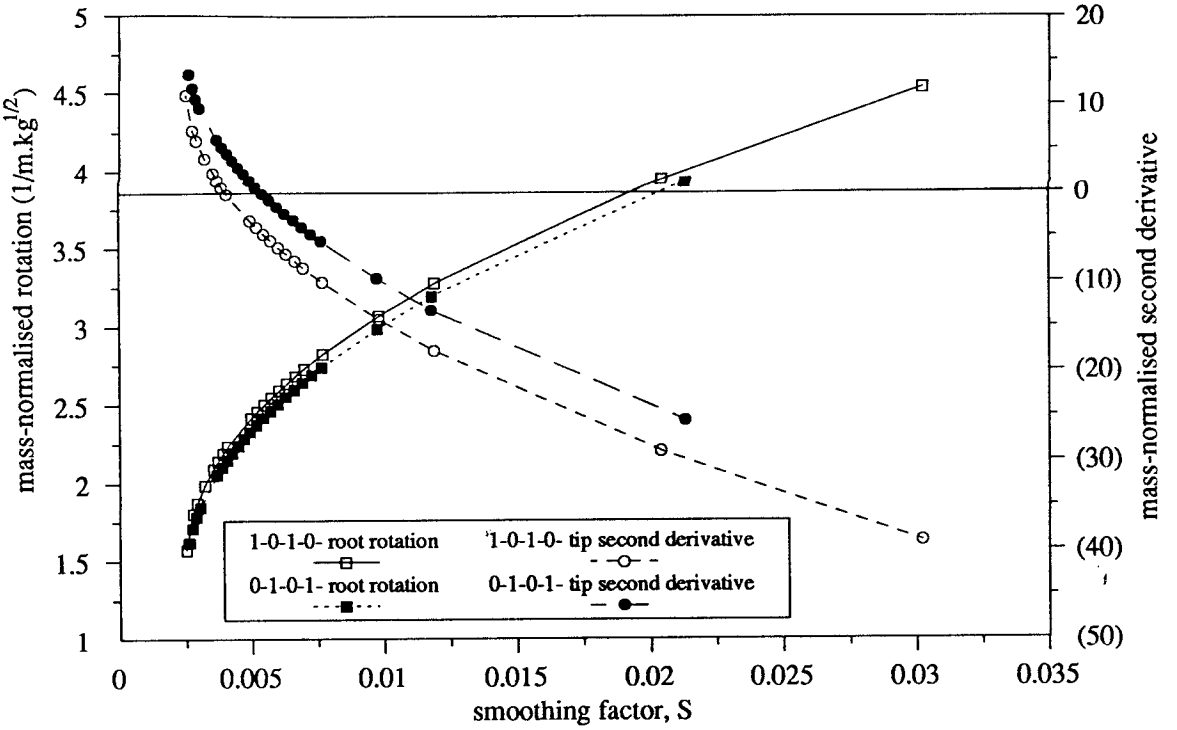

(a) mode 2, 9 knot fit

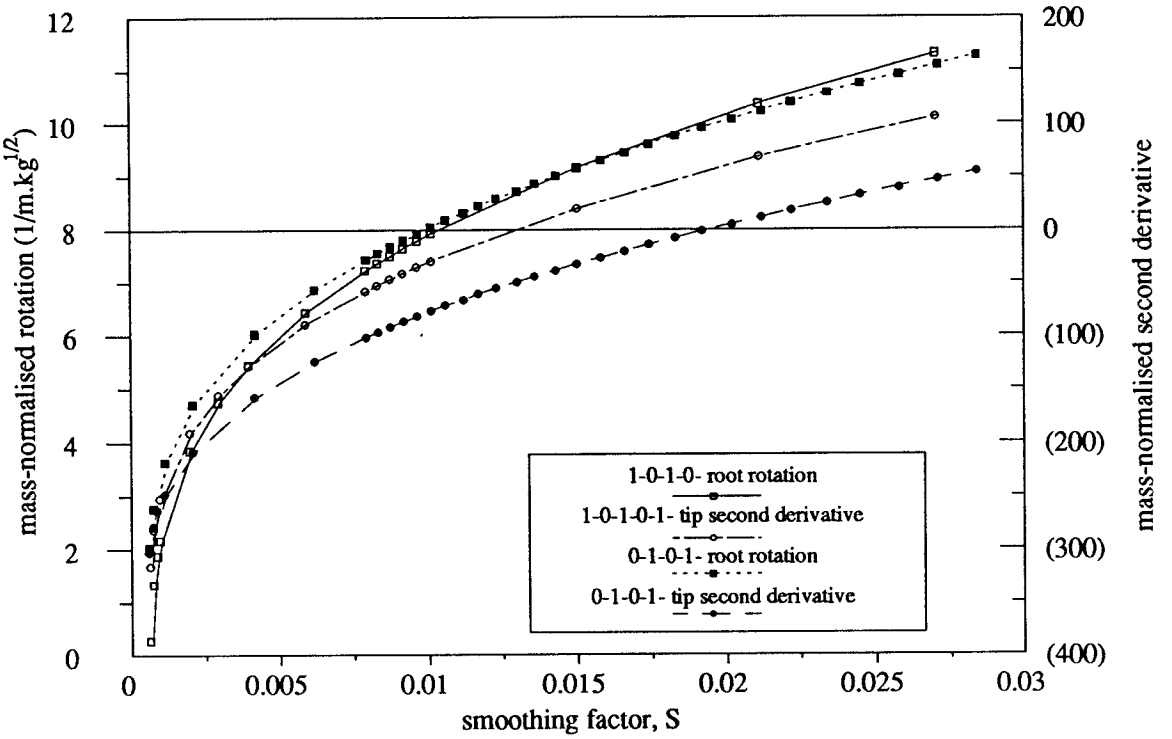

(b) mode 5, 17 knot fit

Figure 4.18: **Variation of the First and Second Derivatives of the fit Functions at the ends of the Steel Cantilever with change in the Smoothing Factor**

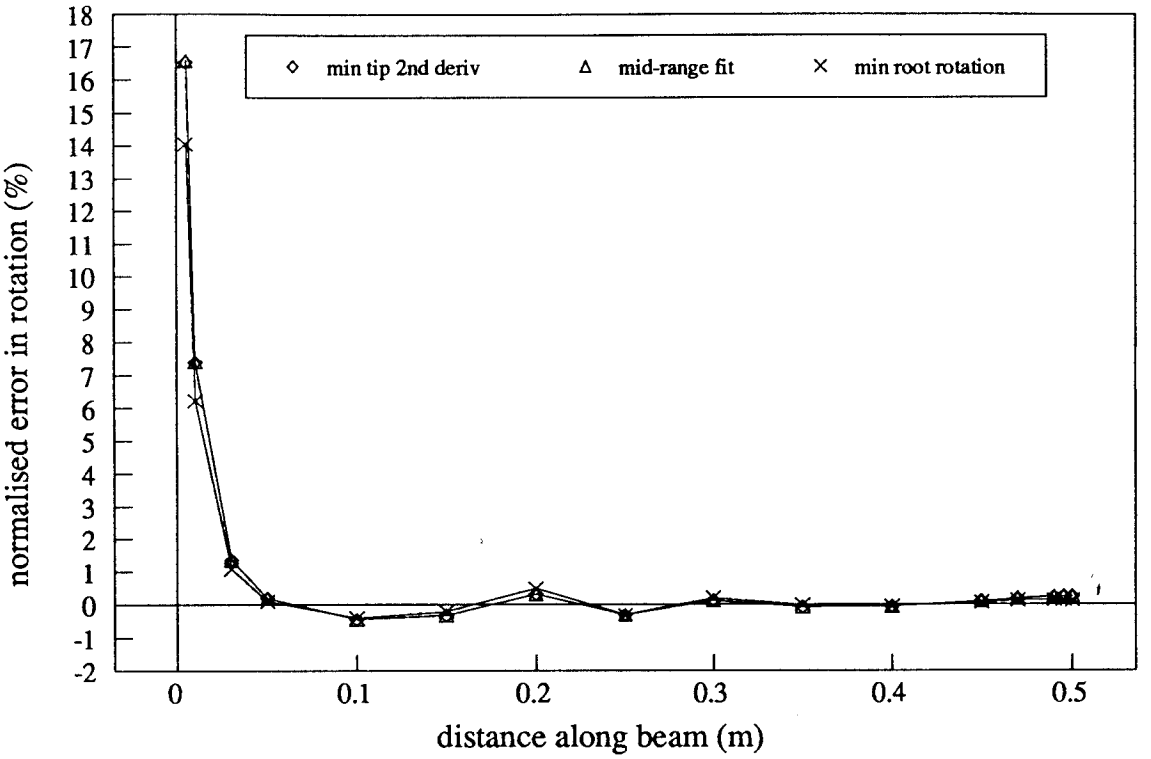

(a) mode 2

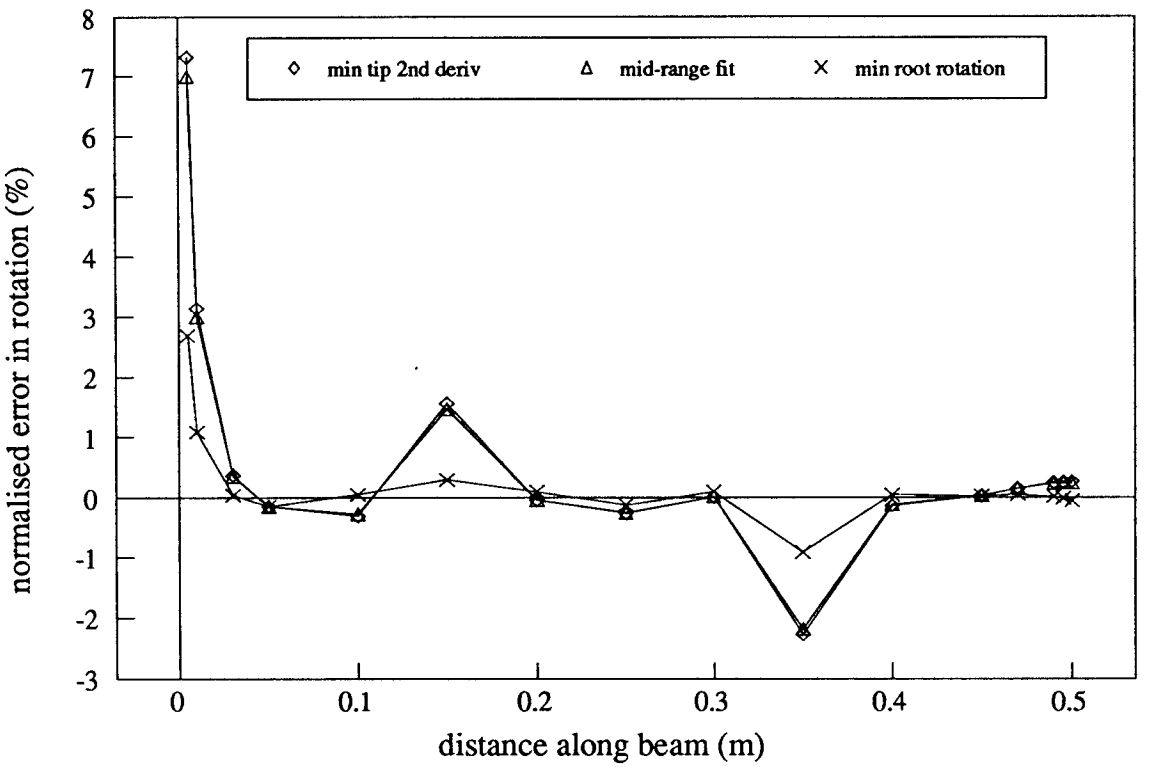

(b) mode 3

Figure 4.19: **Errors in the Estimated Rotations from Several Approximations on 0-1-0-1- Data for the Second and Third Modes of the Steel Cantilever**

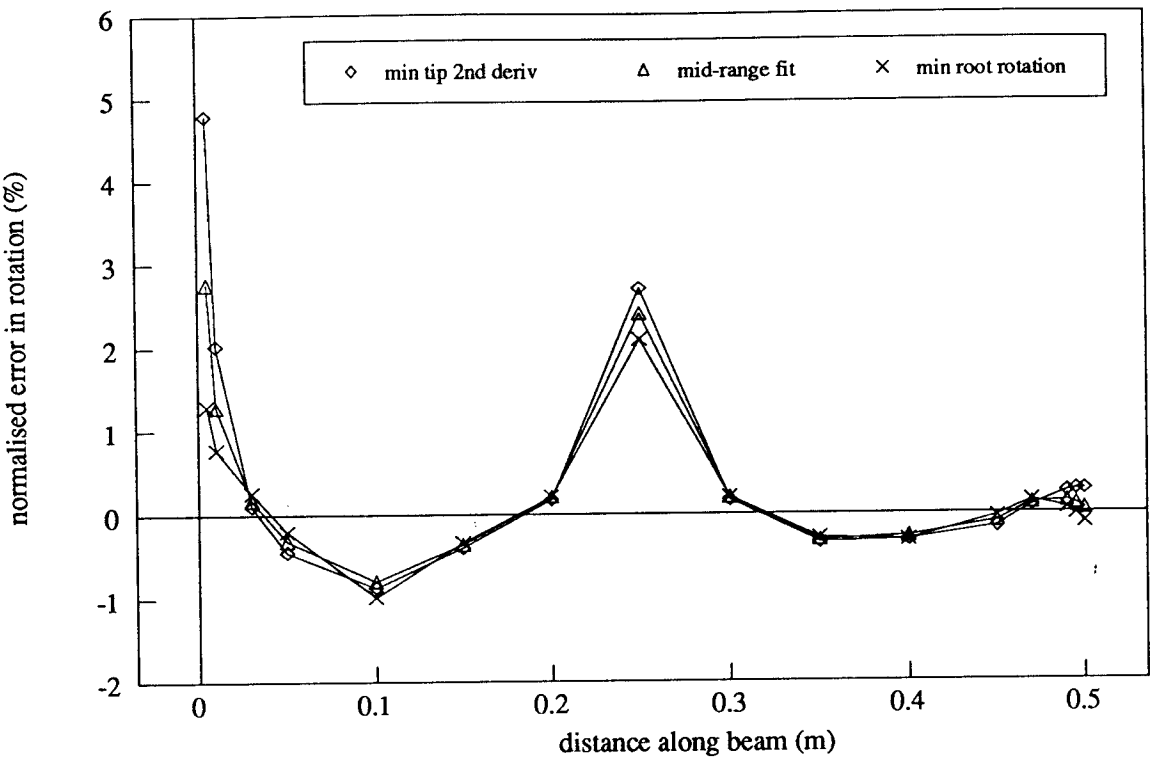

(c) mode 4

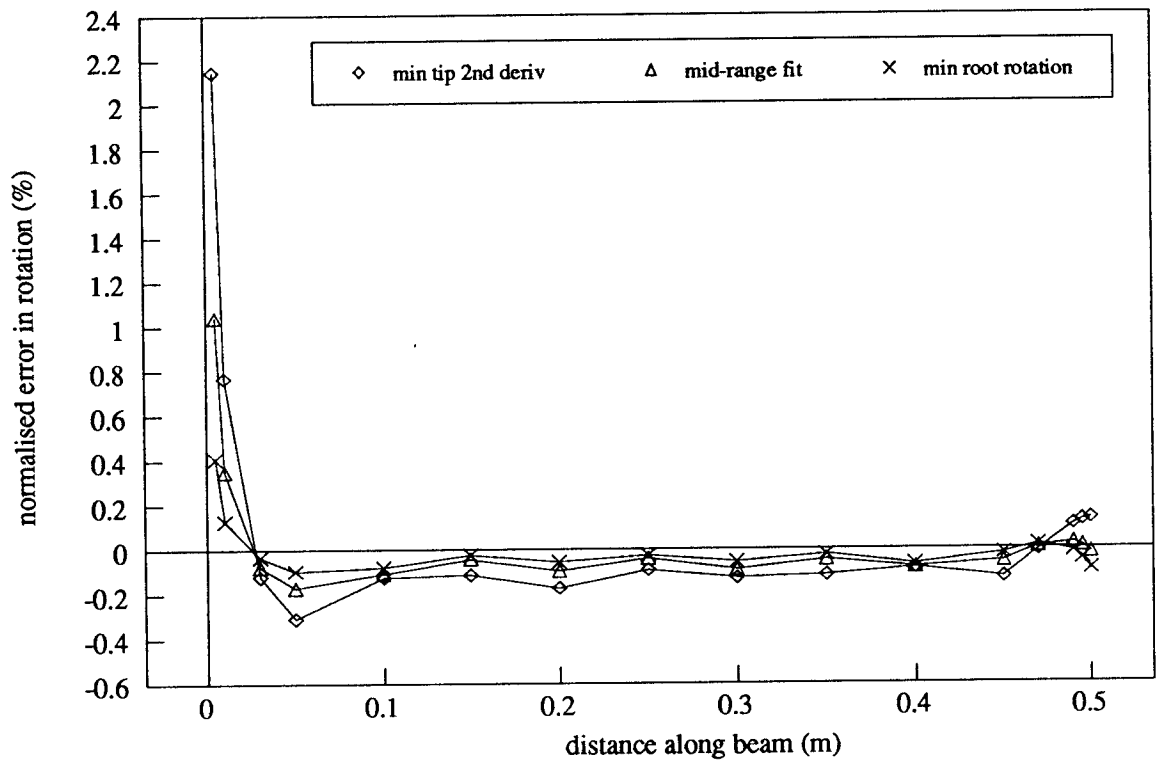

(d) mode 5

Figure 4.19: **Errors in the Estimated Rotations from Several Approximations on 0-1-0-1- Data for the Fourth and Fifth Modes of the Steel Cantilever**

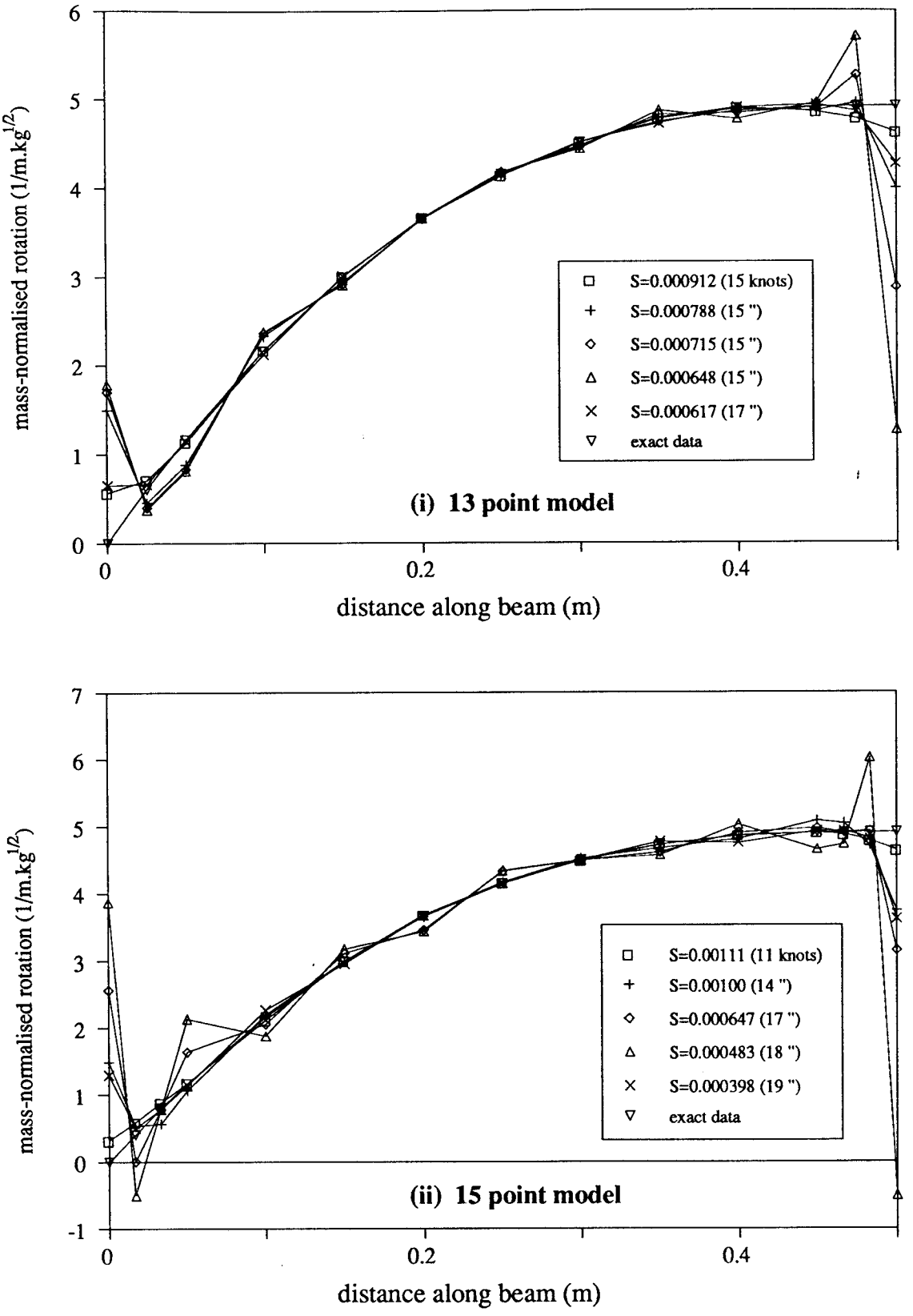

Figure 4.20a: **Effect of Varying Model Size on the Estimation of the First Mode of the Steel Cantilever from 0-1-0-1- Data**

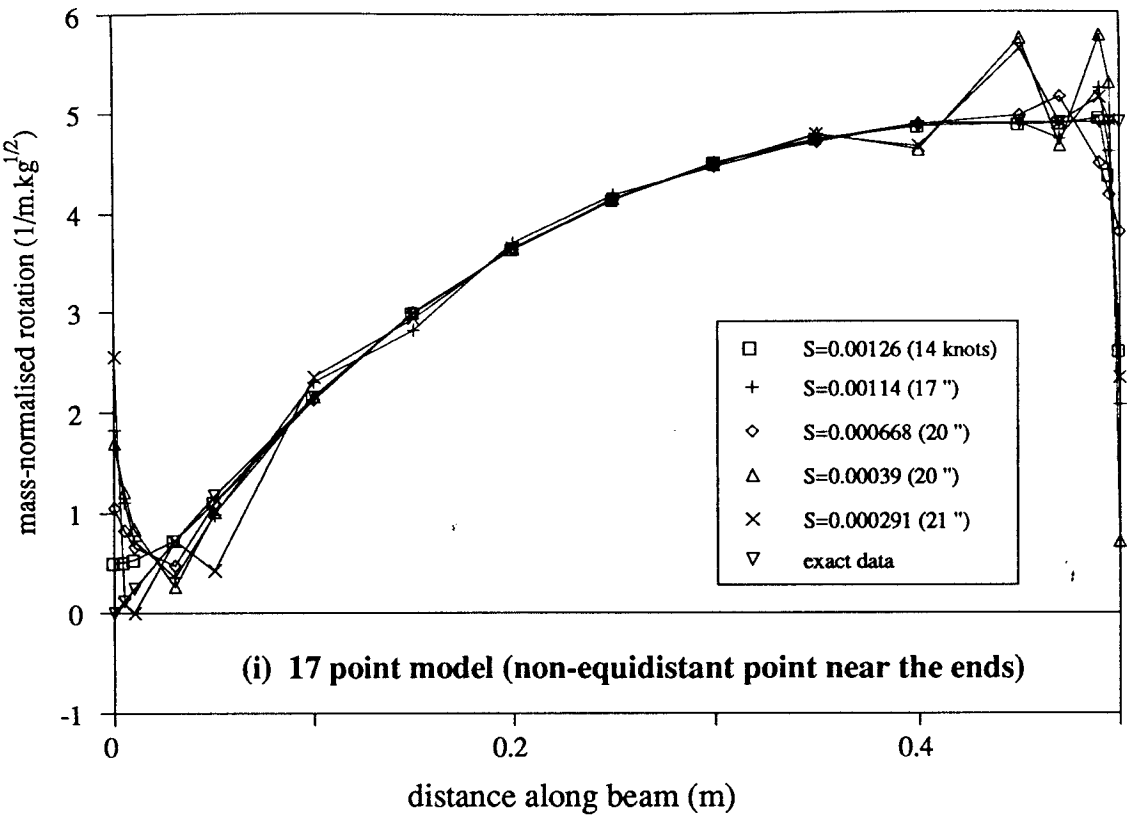

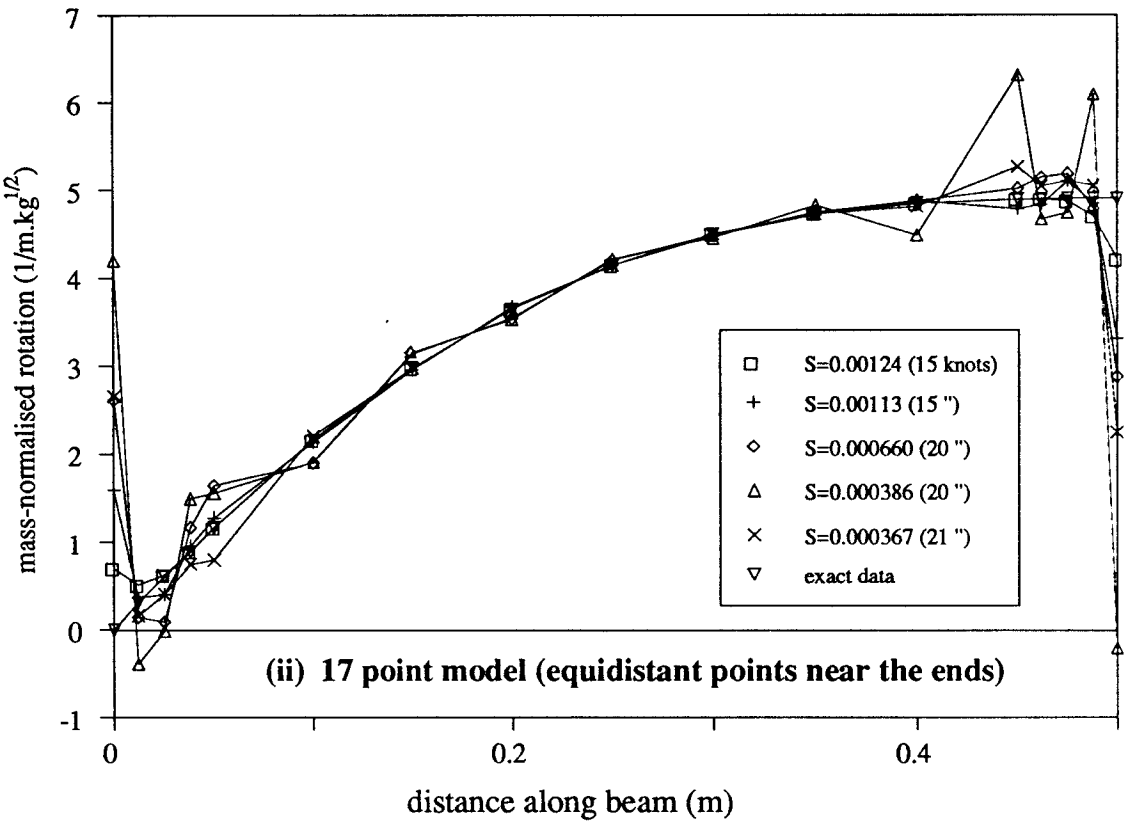

Figure 4.20b: **Effect of Varying Model Size on the Estimation of the First Mode of the Steel Cantilever from 0-1-0-1- Data**

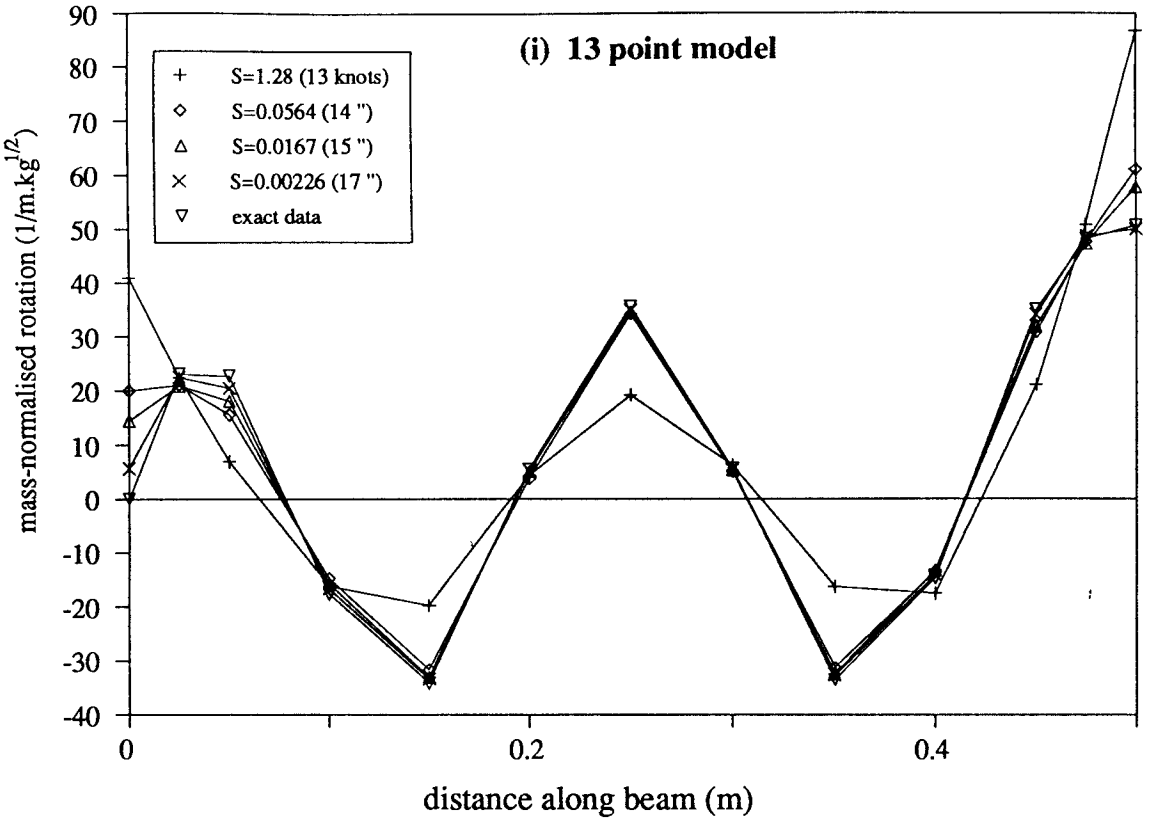

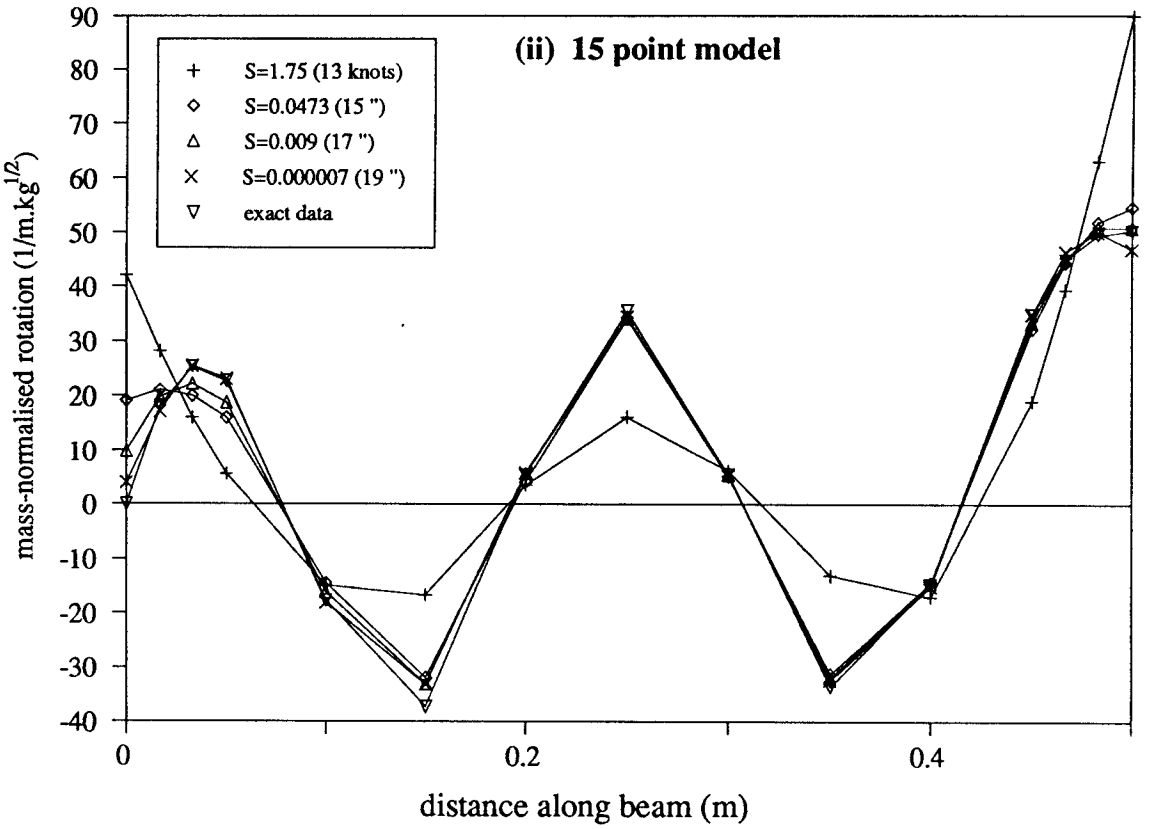

Figure 4.21a: **Effect of Varying Model Size on the Estimation of the Fifth Mode of the Steel Cantilever from 0-1-0-1- Data**

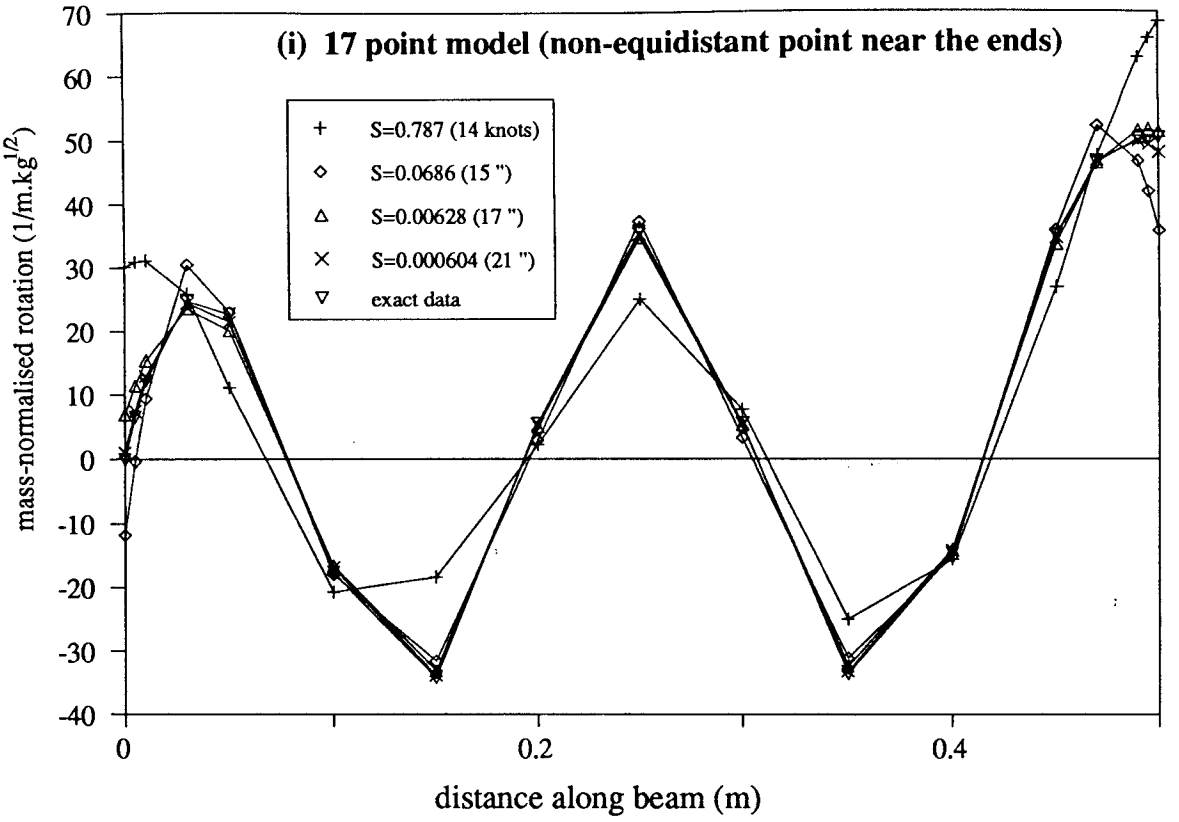

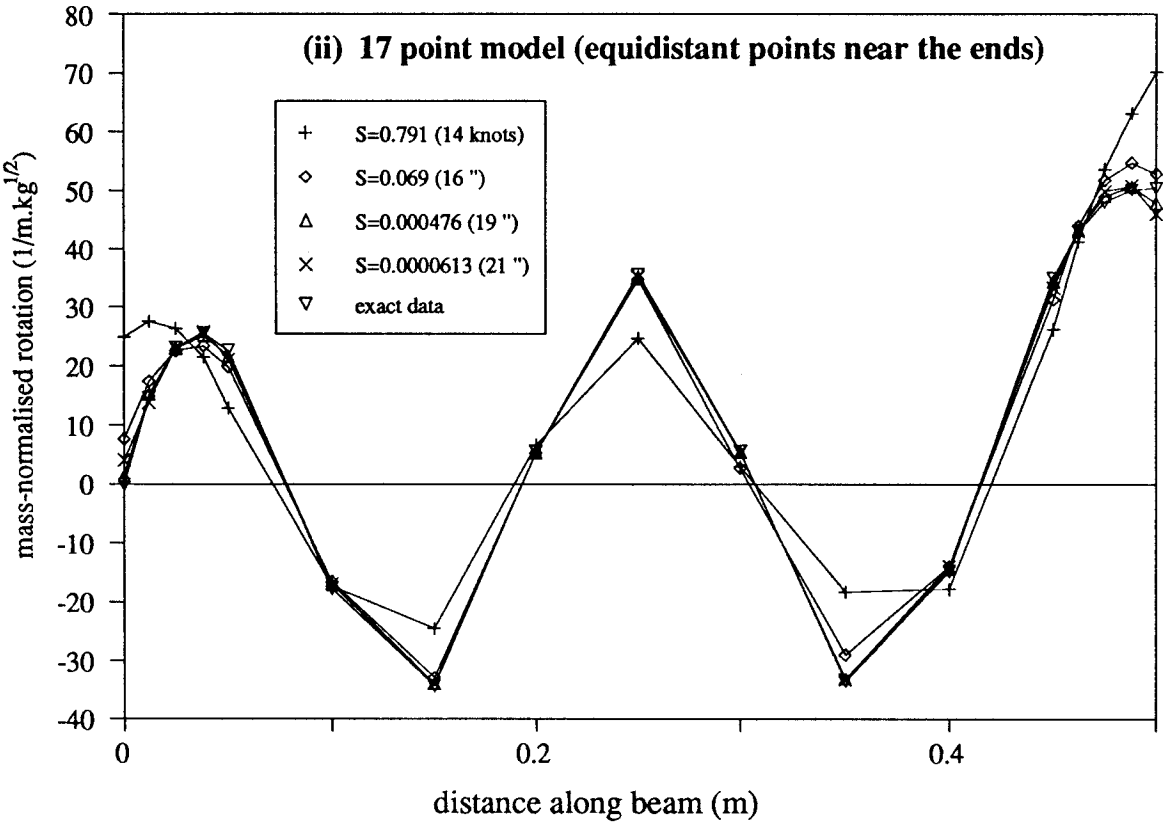

Figure 4.21b: **Effect of Varying Model Size on the Estimation of the Fifth Mode of the Steel Cantilever from 0-1-0-1- Data**

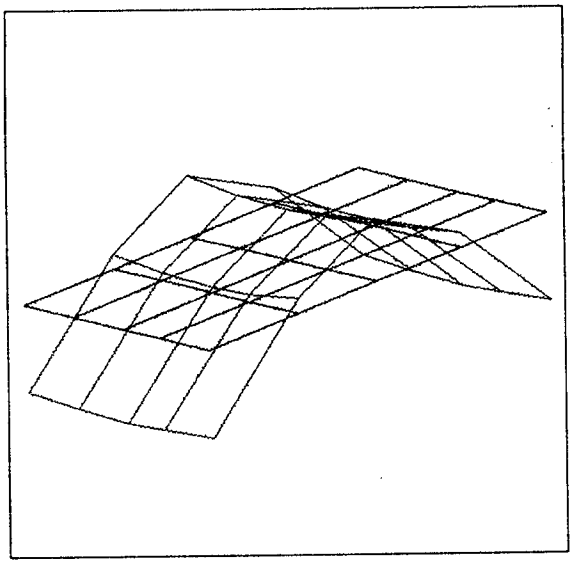

Mode 1, 328.5 Hz

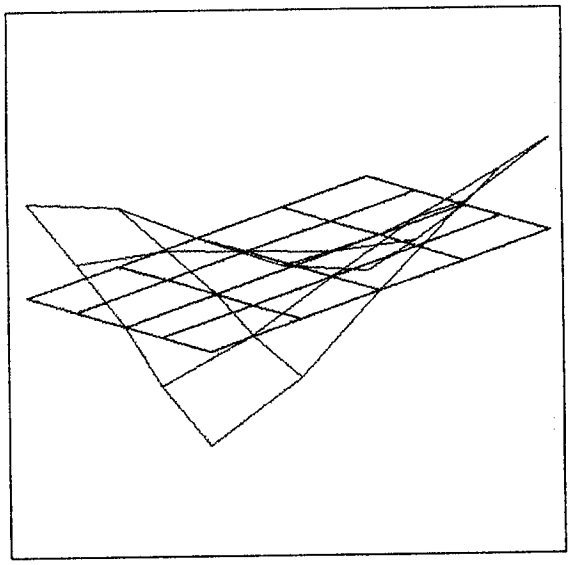

mode 2, 401.0 Hz

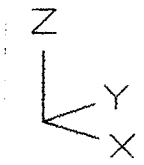

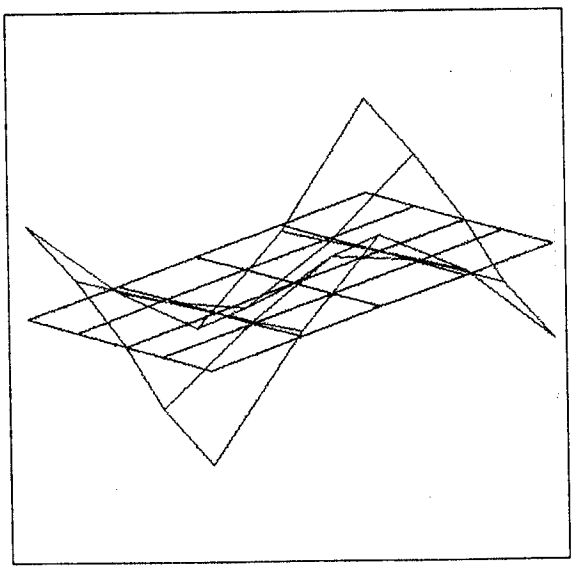

mode 3, 886.1 Hz

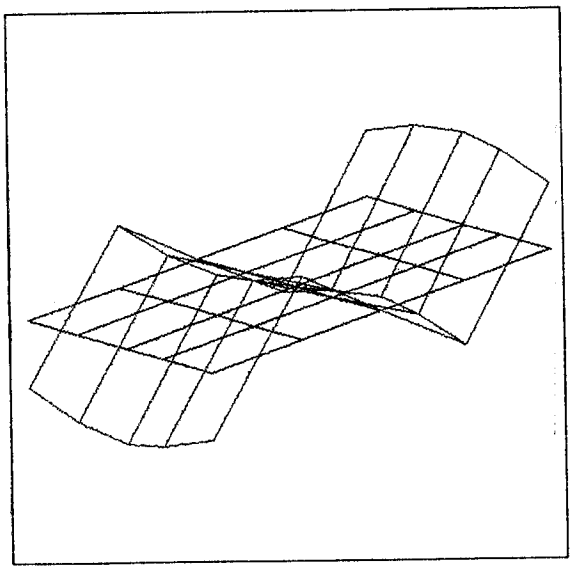

mode 4, 921.4 Hz

Figure 4.22: **Translational Modeshape Plots for the Flexural Modes of the Unmodified Free-free Plate**

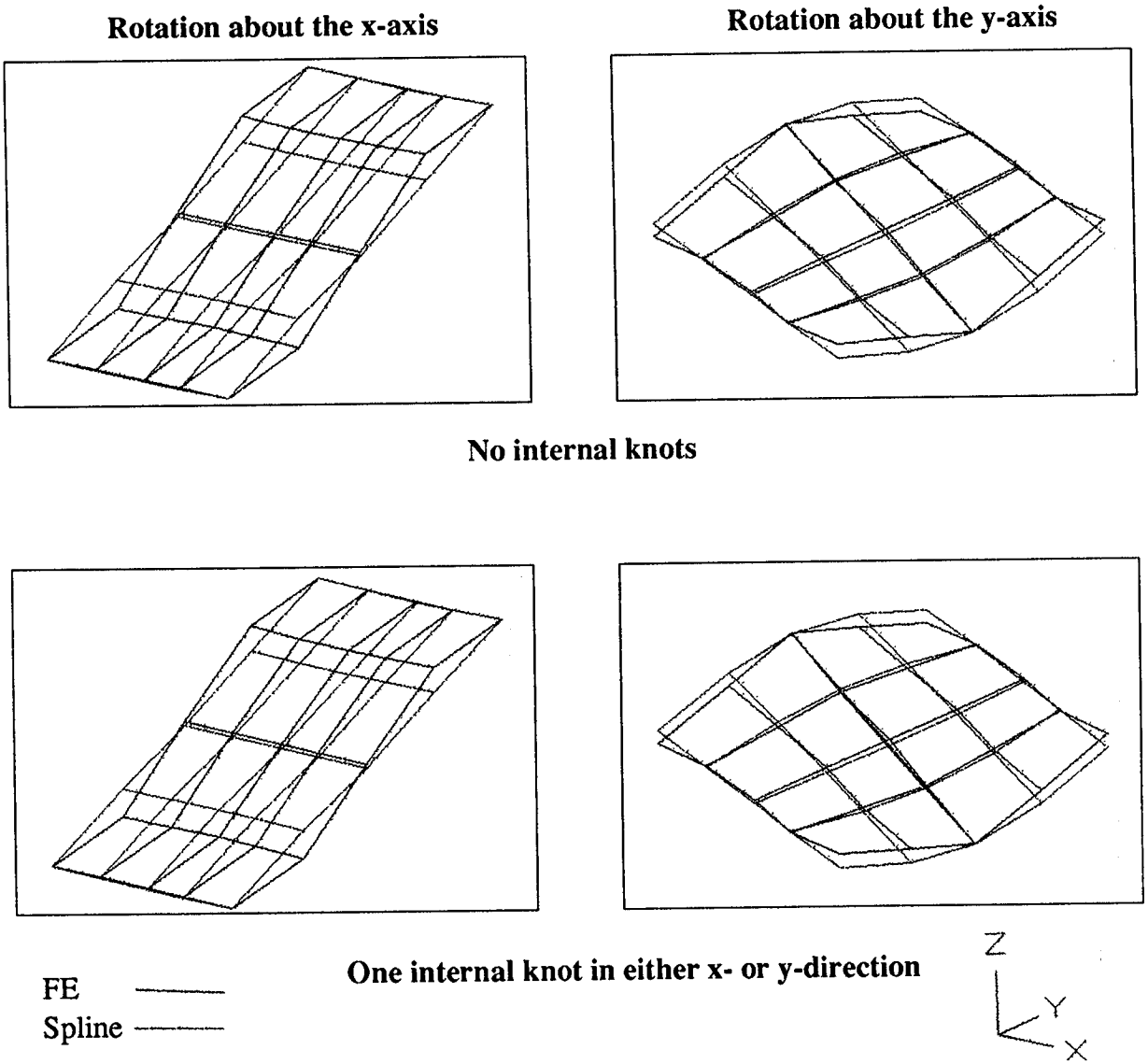

Figure 4.23: **Comparison of Rotational Modeshape Plots from Several Approximations with FE Modeshapes for the First Mode of the Free-free Plate**

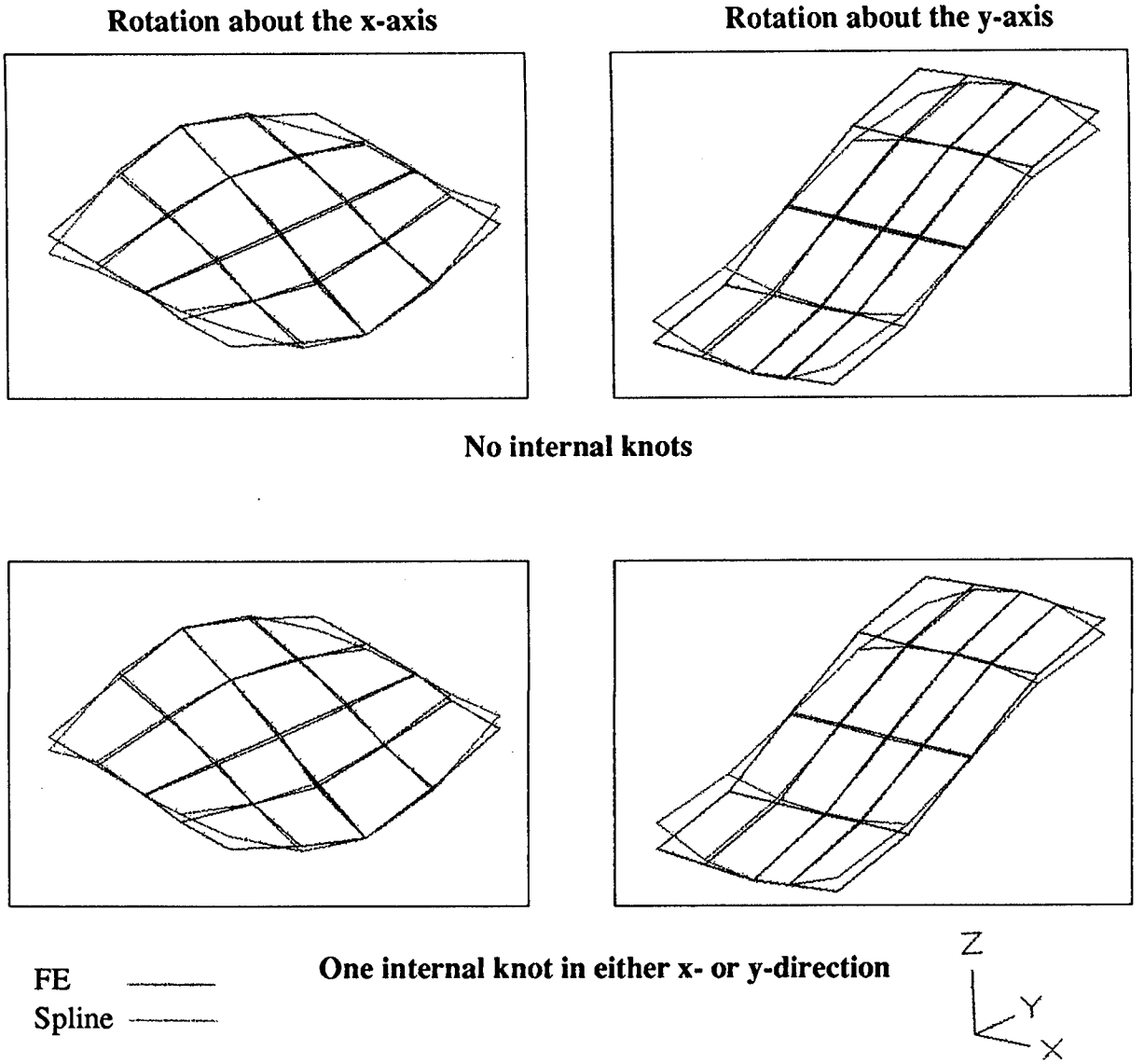

Figure 4.24: **Comparison of Rotational Modeshape Plots from Several Approximations with FE Modeshapes for the Second Mode of the Free-free Plate**

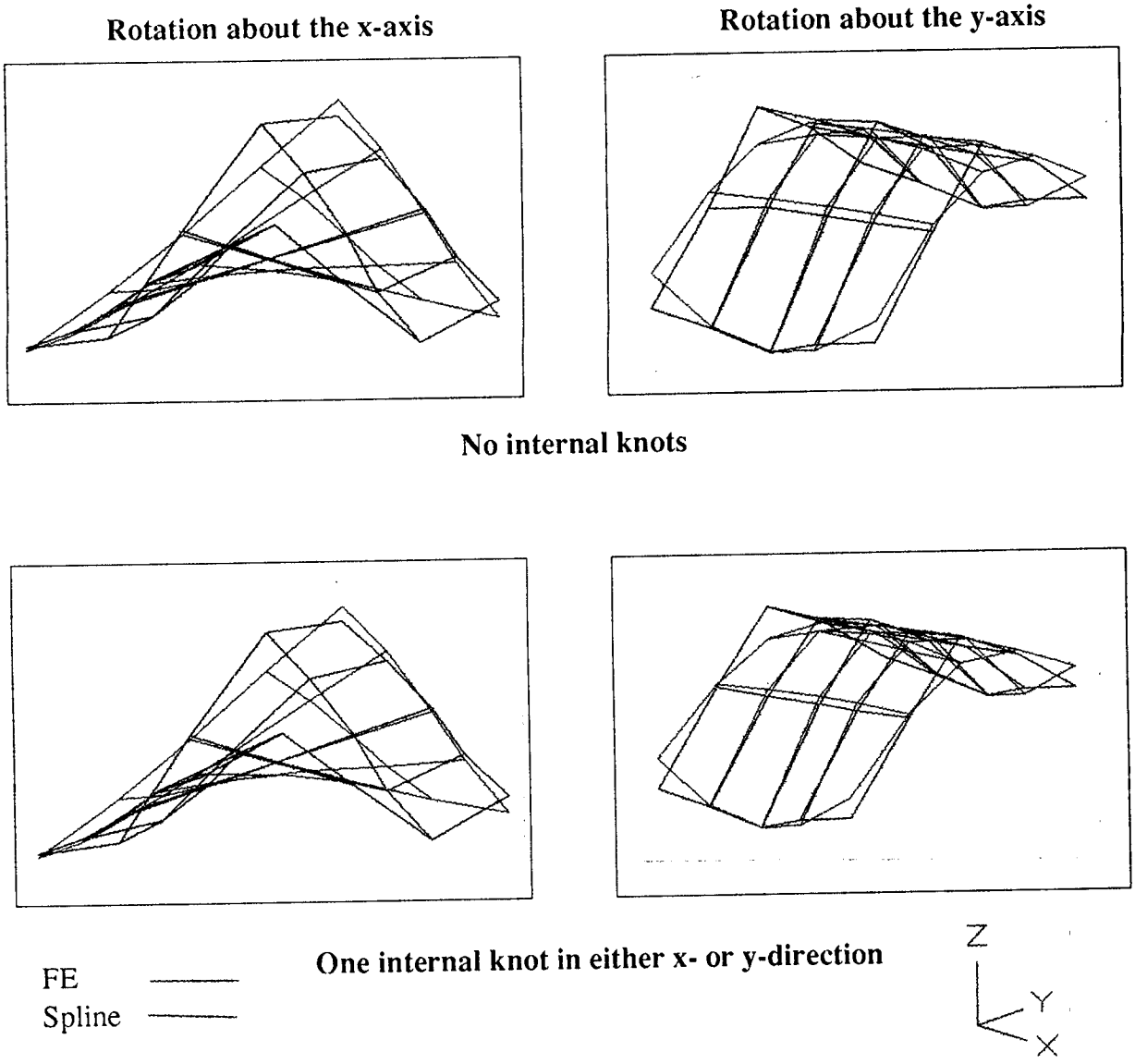

Figure 4.25: **Comparison of Rotational Modeshape Plots from Several Approximations with FE Modeshapes for the Third Mode of the Free-free Plate**

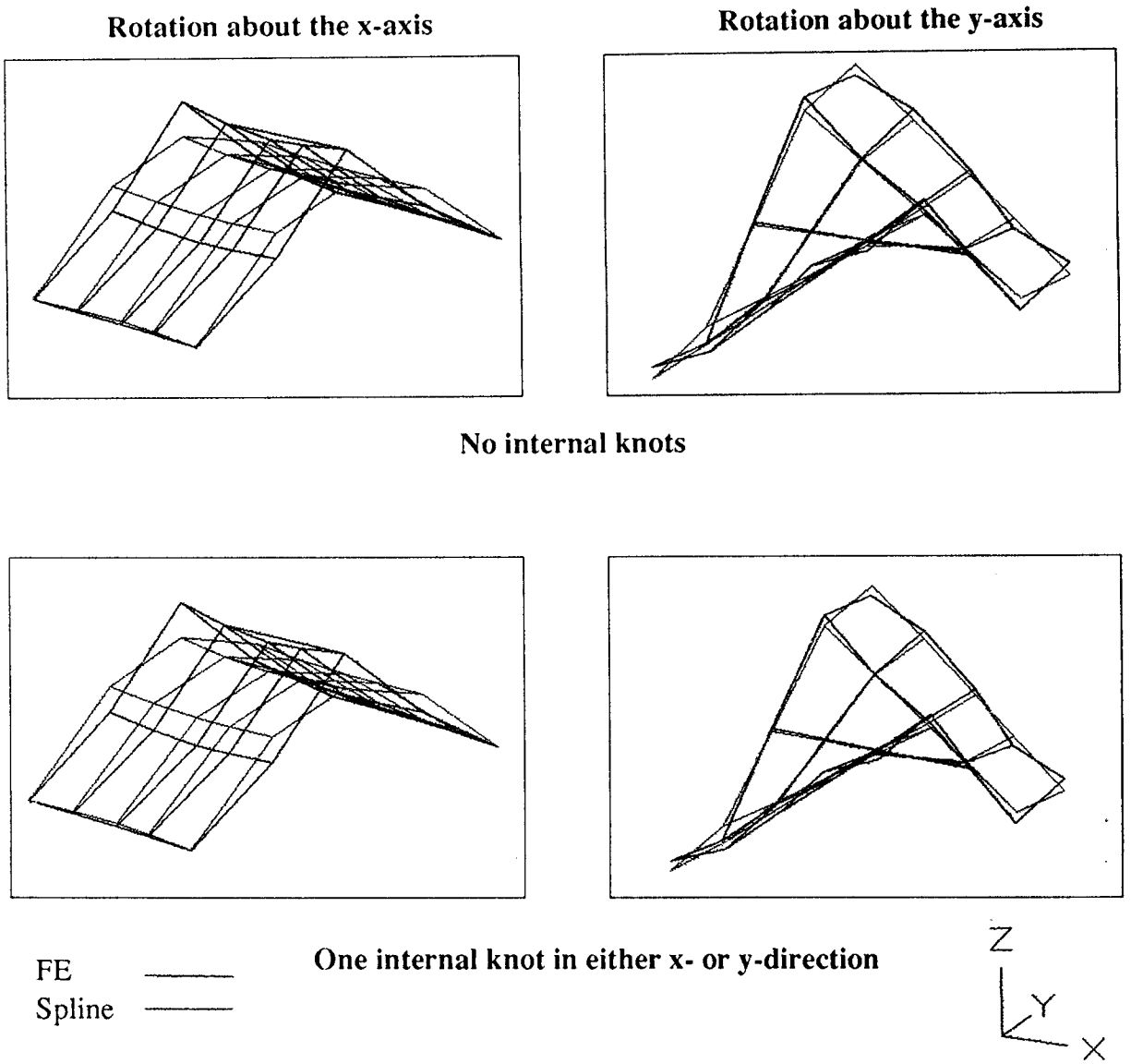

Figure 4.26: **Comparison of Rotational Modeshape Plots from Several Approximations with FE Modeshapes for the Fourth Mode of the Free-free Plate**

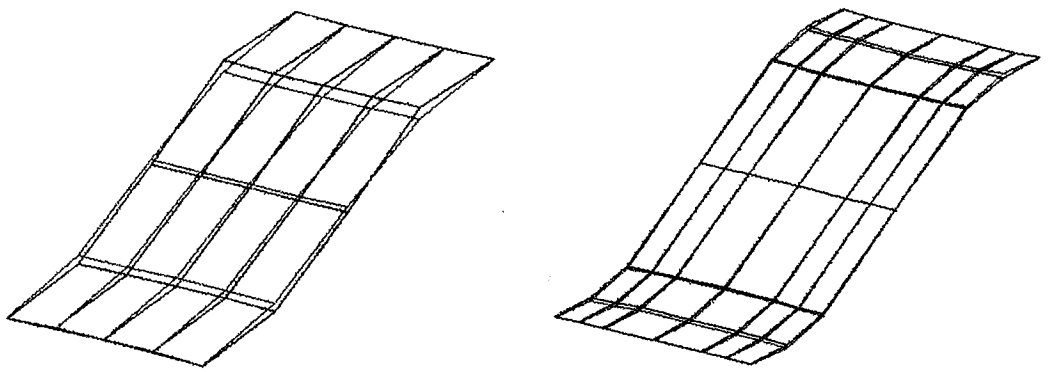

mode 1

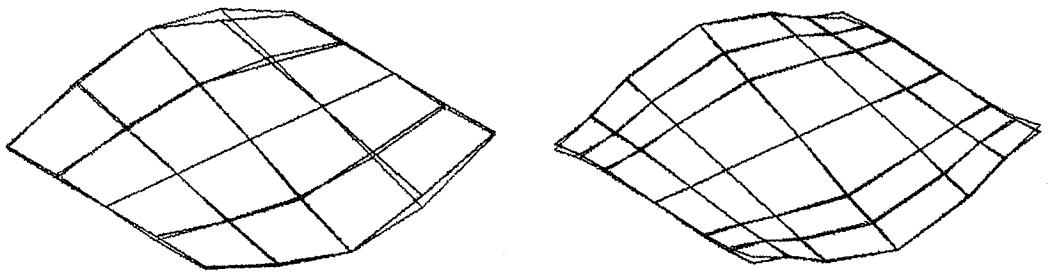

mode 2

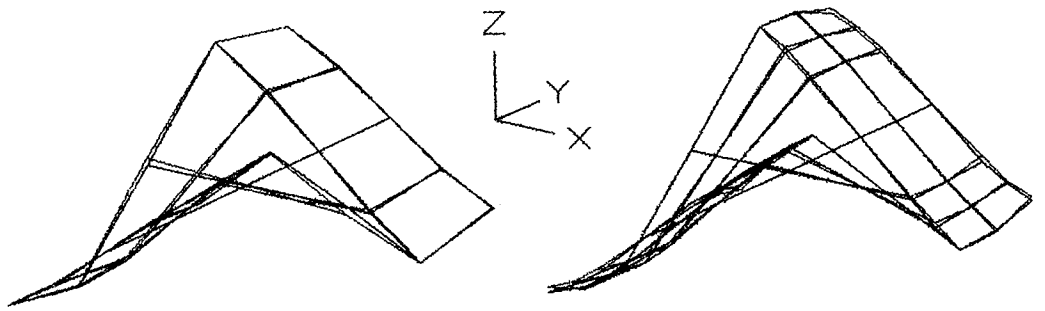

mode 3

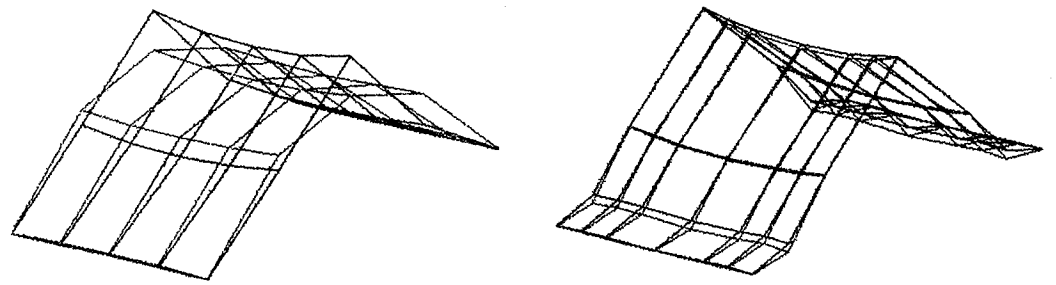

mode 4

FE ——
Spline ——

25-point model **49-point model**

Figure 4.27a: **Effect of introducing a mid-point near the boundaries on the performance of the surface fit using the interpolant (rotation about the x-axis)**

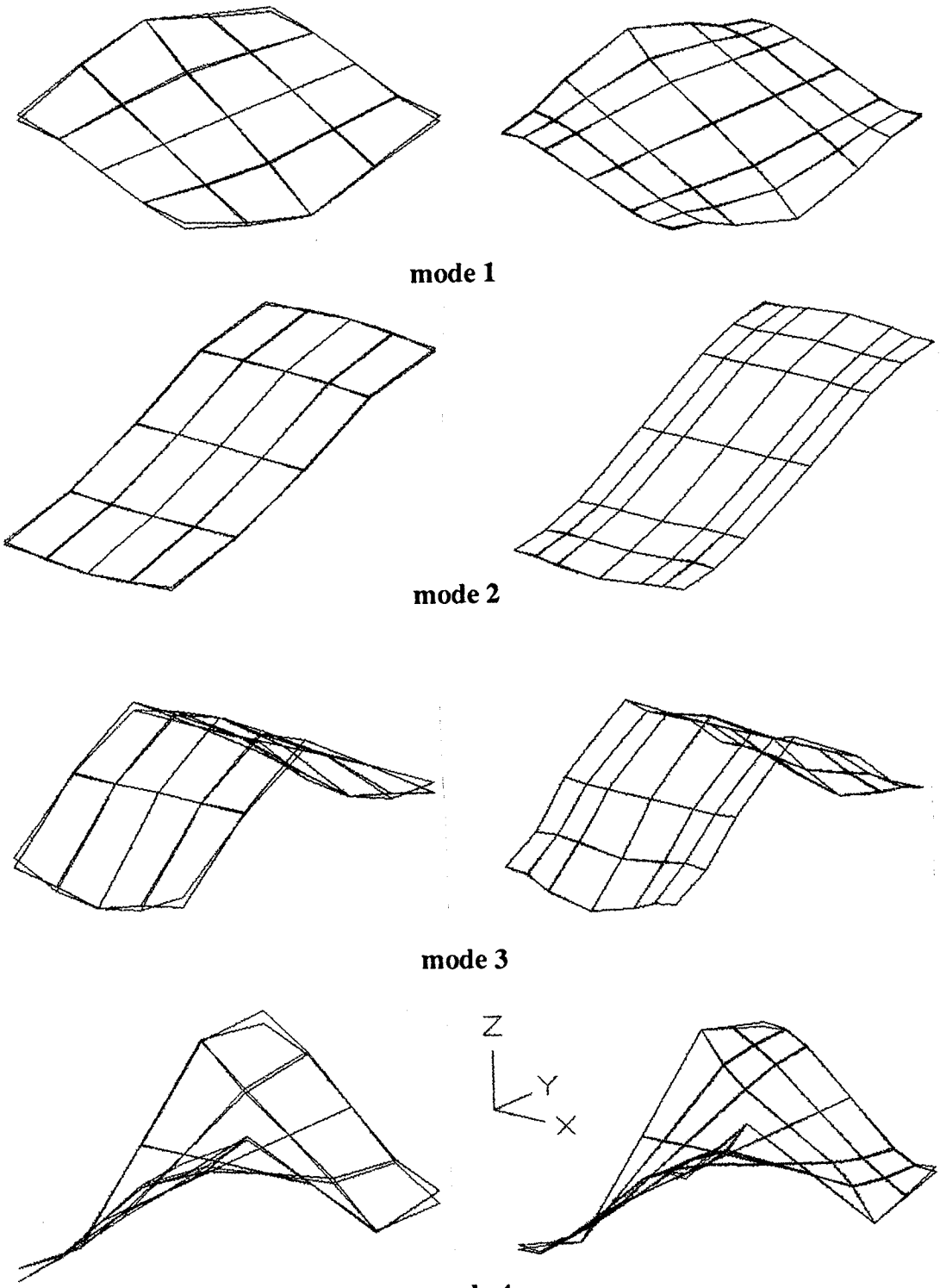

Figure 4.27b: **Effect of introducing a mid-point near the boundaries on the performance of the surface fit using the interpolant (rotation about the y-axis)**

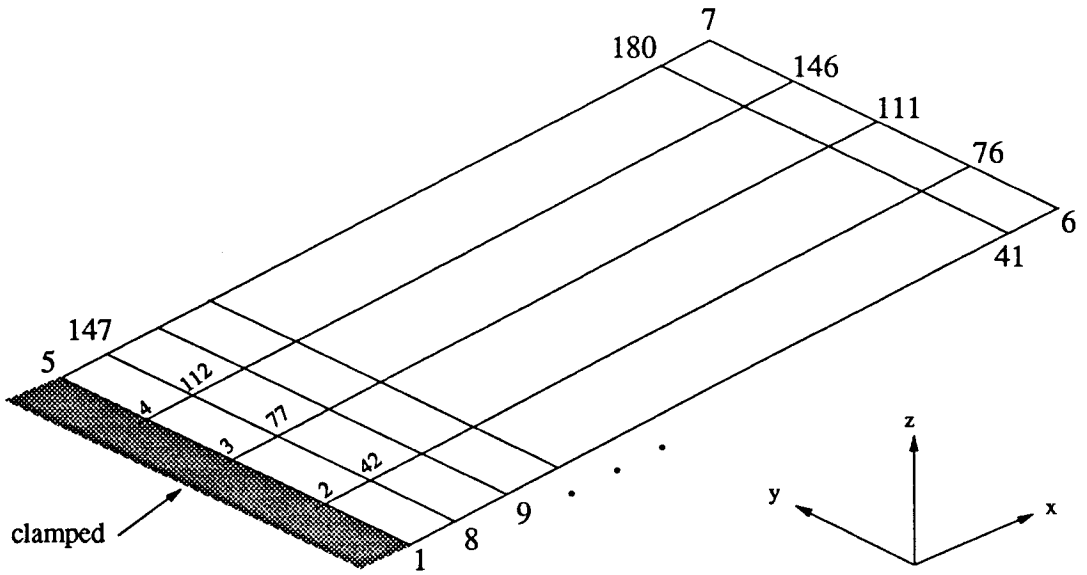

Figure 4.28: **Idealisation of the Cantilever Plate**

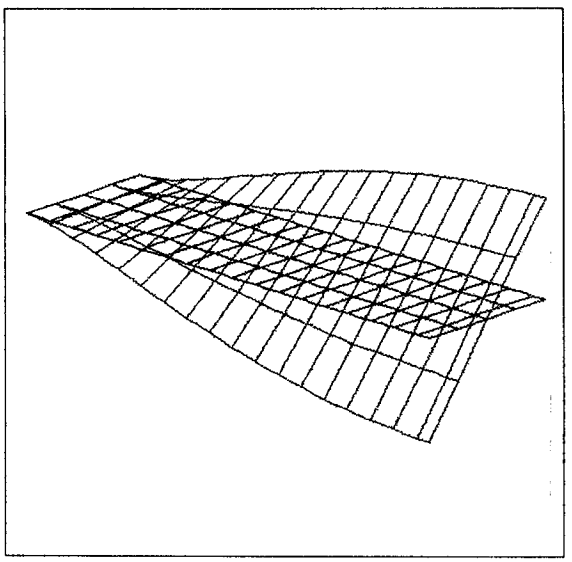

mode 3, 126.1 Hz

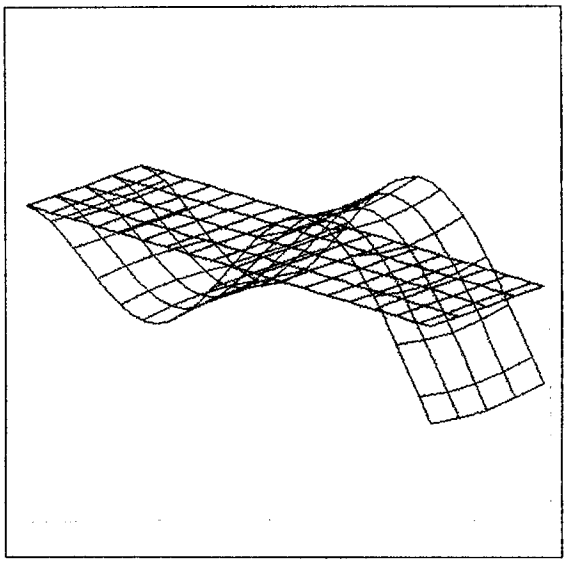

mode 4, 330.7 Hz

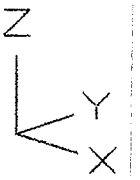

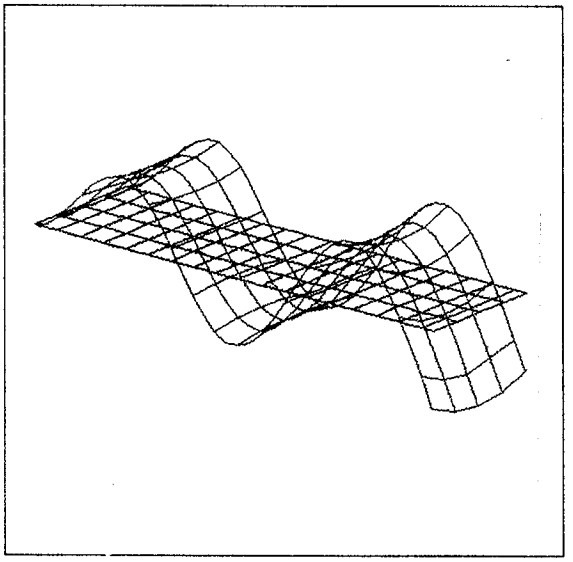

mode 7, 654.3 Hz

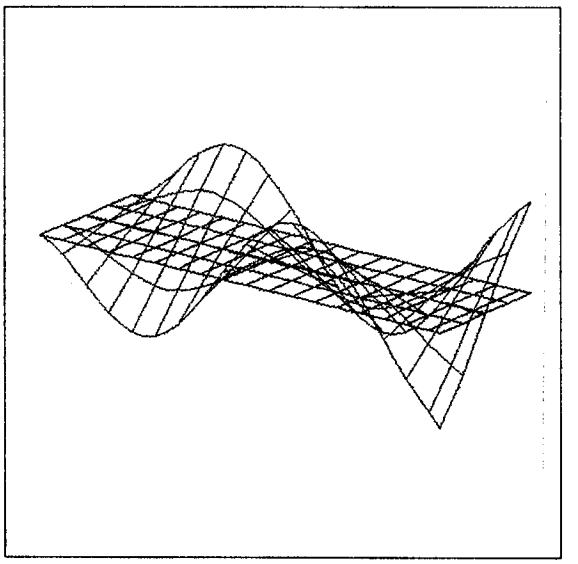

mode 8, 707.3 Hz

Figure 4.29: **Translational Modeshape Plots for the Flexural Modes of the Unmodified Cantilever Plate**

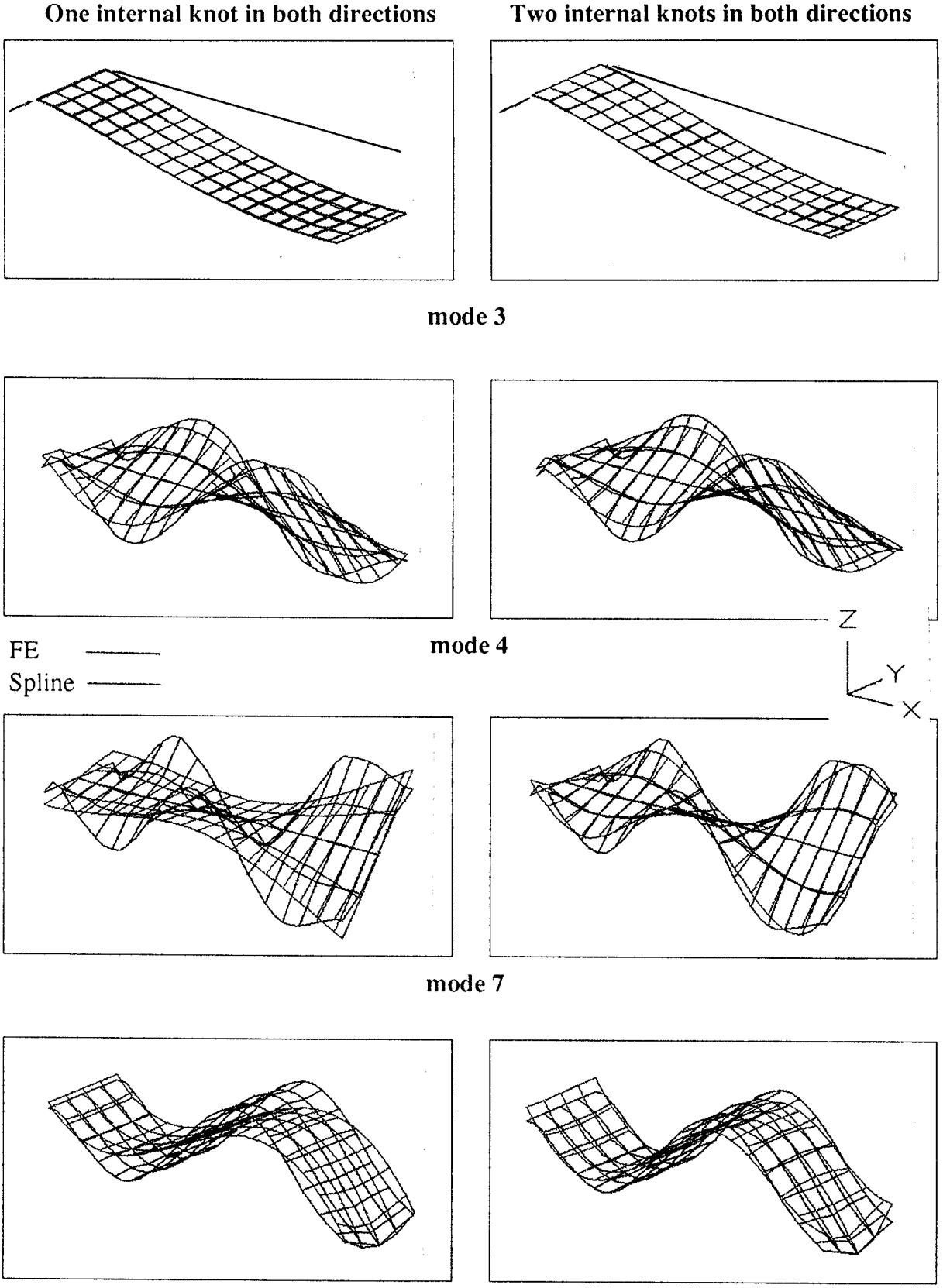

Figure 4.30: **Comparison of Calculated Rotational Modeshapes (Rotations about the x-axis) with FE Modeshapes for the Cantilever Plate**

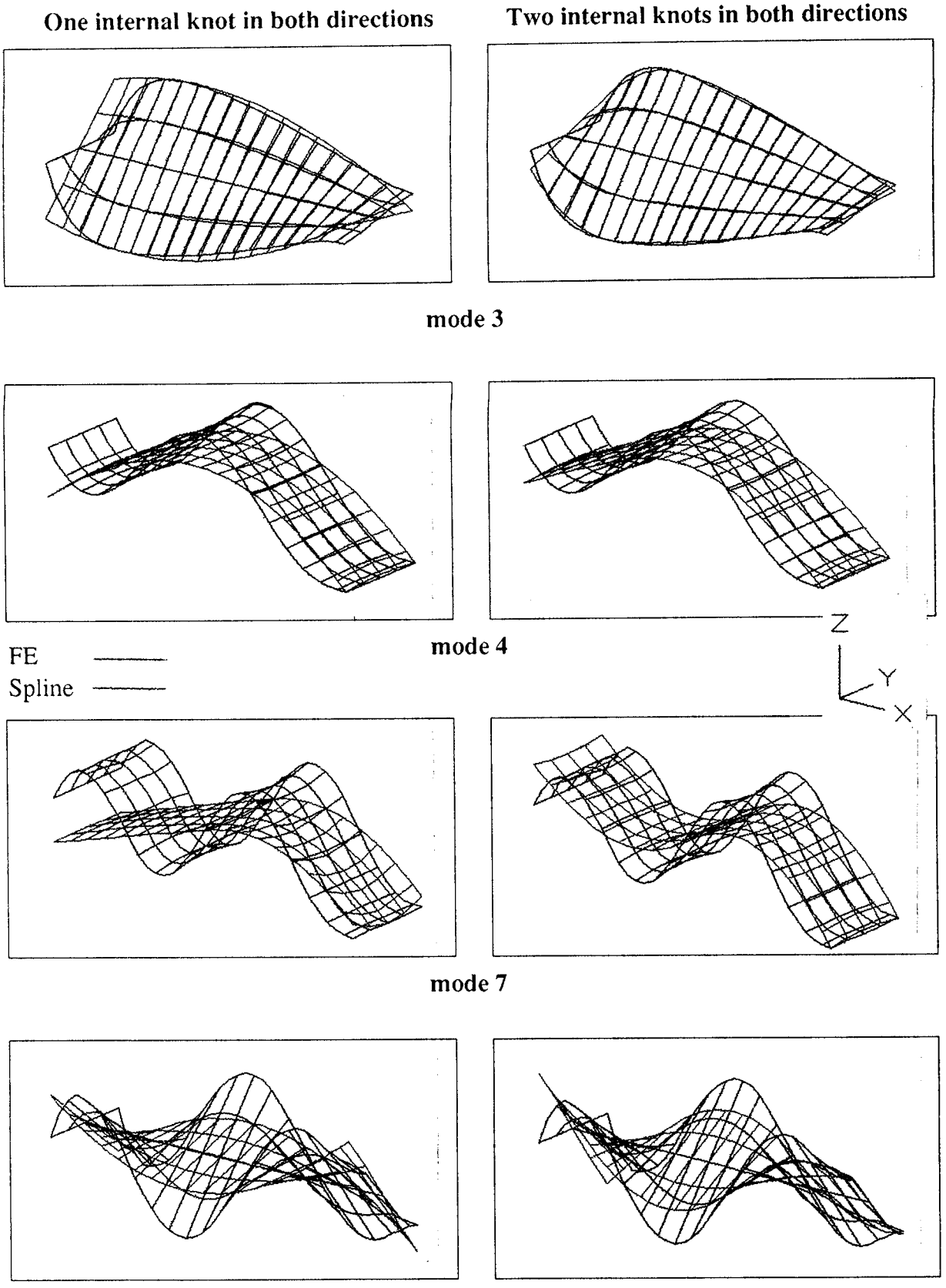

Figure 4.31: **Comparison of Calculated Rotational Modeshapes (Rotations about the y-axis) with FE Modeshapes for the Cantilever Plate**

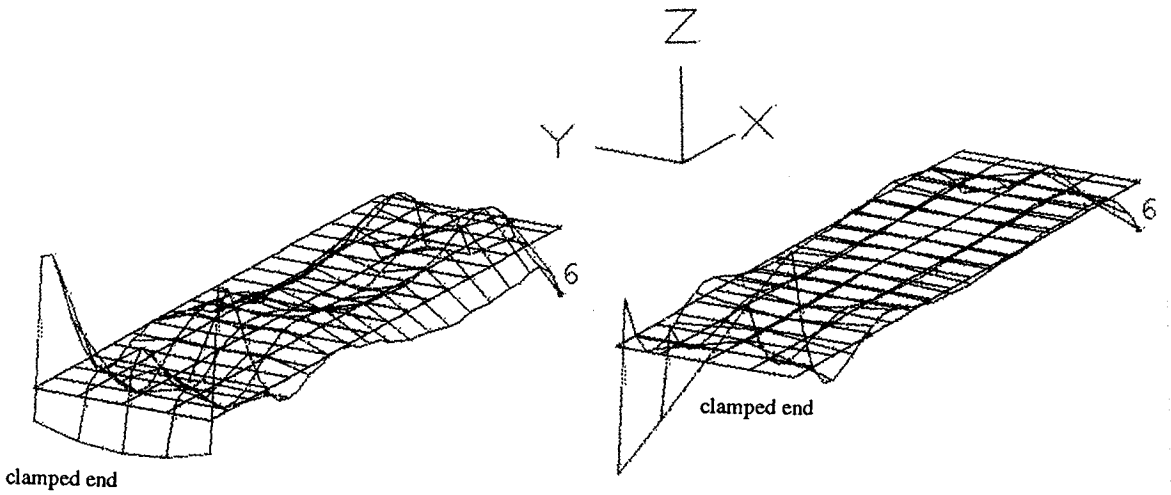

rotation about x-axis **rotation about y-axis**

error 'modeshapes'

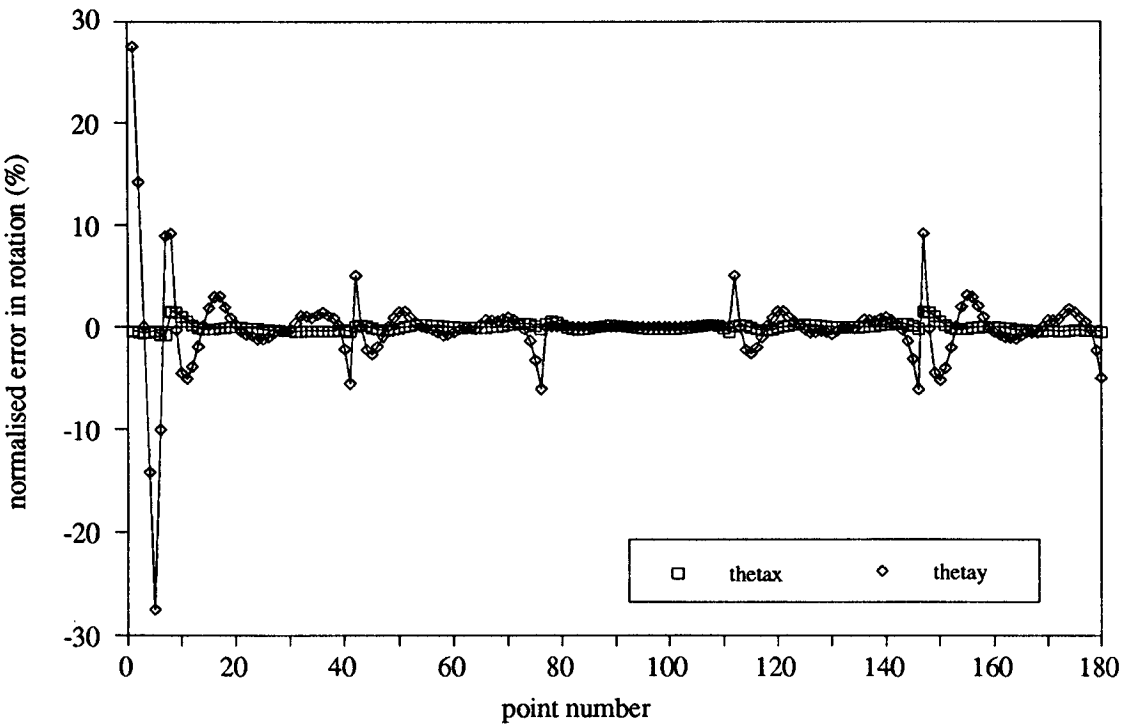

Figure 4.32a: **Comparison of the Surface Fit Performance about the in-plane axes for the Third Mode of the Cantilever Plate using a fit with two internal knots in each direction**

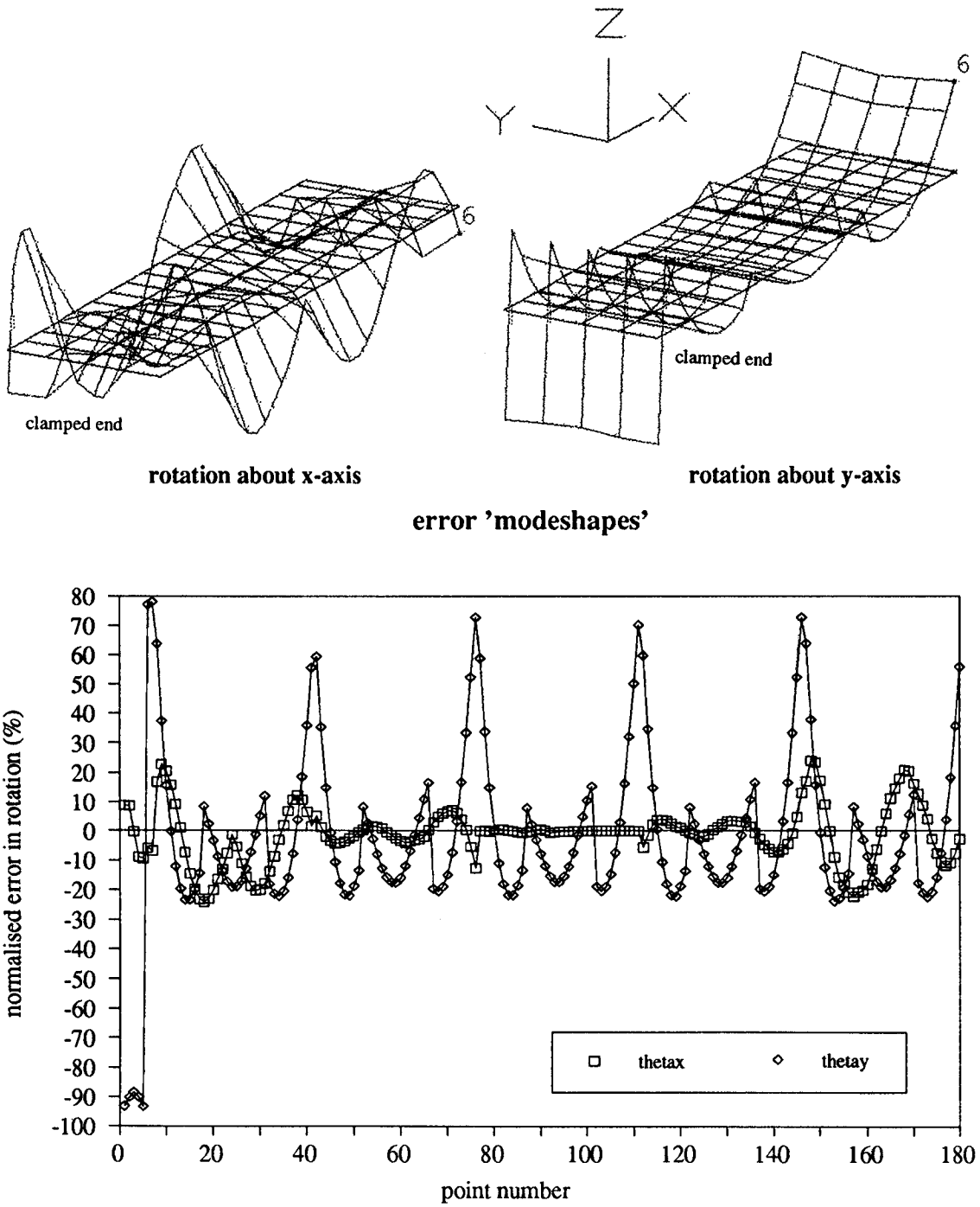

Figure 4.32b: **Comparison of the Surface Fit Performance about the in-plane axes for the Fourth Mode of the Cantilever Plate using a fit with two internal knots in each direction**

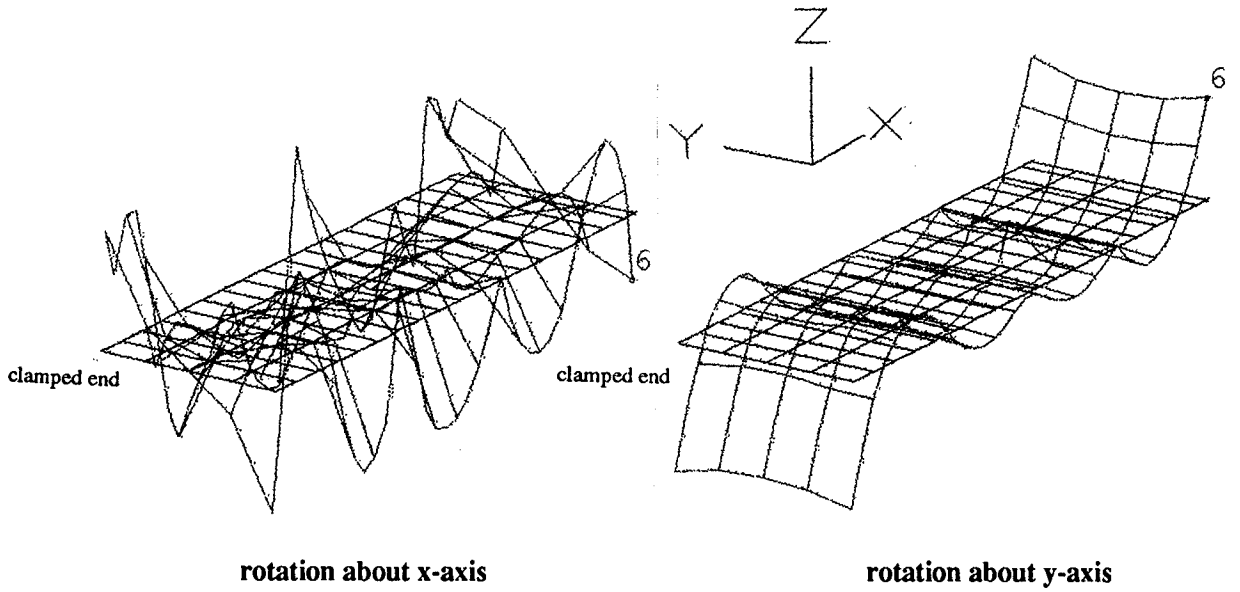

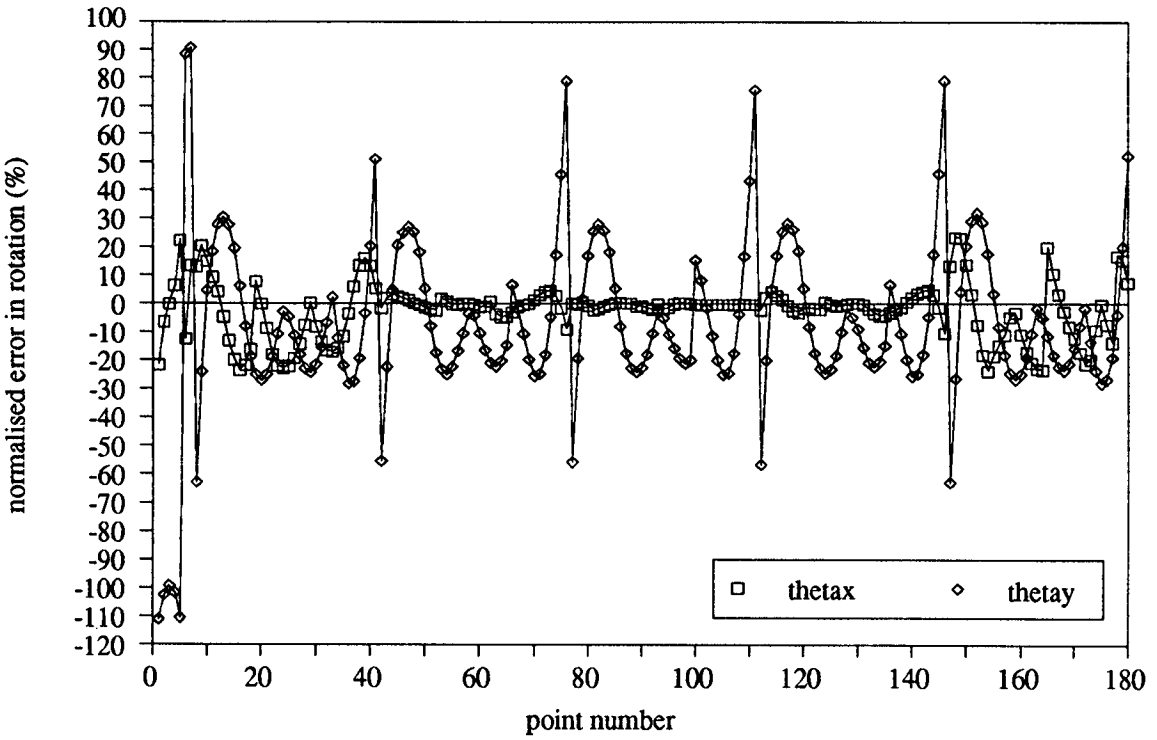

Figure 4.32c: **Comparison of the Surface Fit Performance about the in-plane axes for the Seventh Mode of the Cantilever Plate using a fit with two internal knots in each direction**

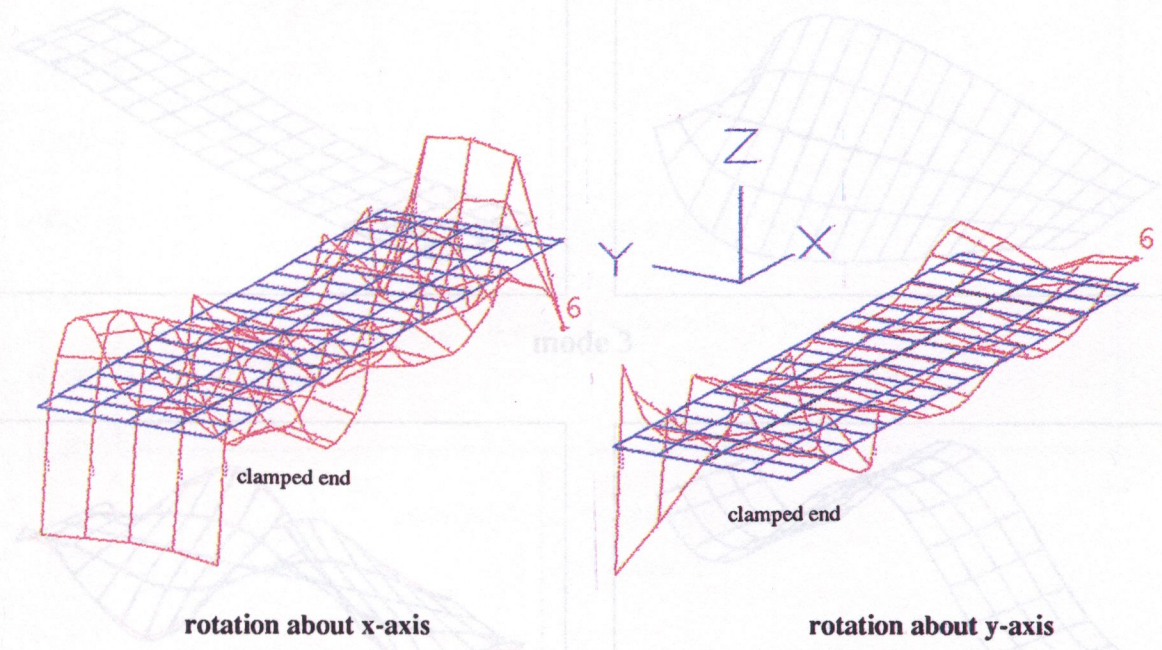

error 'modeshapes'

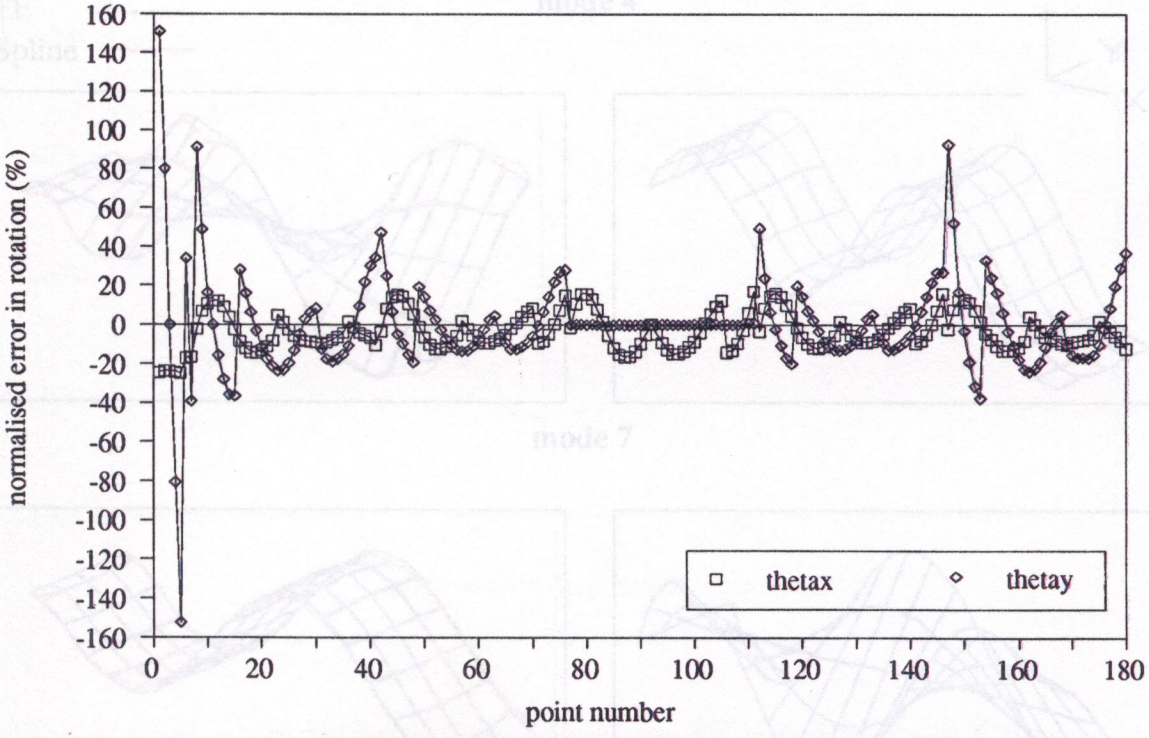

Figure 4.32d: **Comparison of the Surface Fit Performance about the in-plane axes for the Eighth Mode of the Cantilever Plate using a fit with two internal knots in each direction**

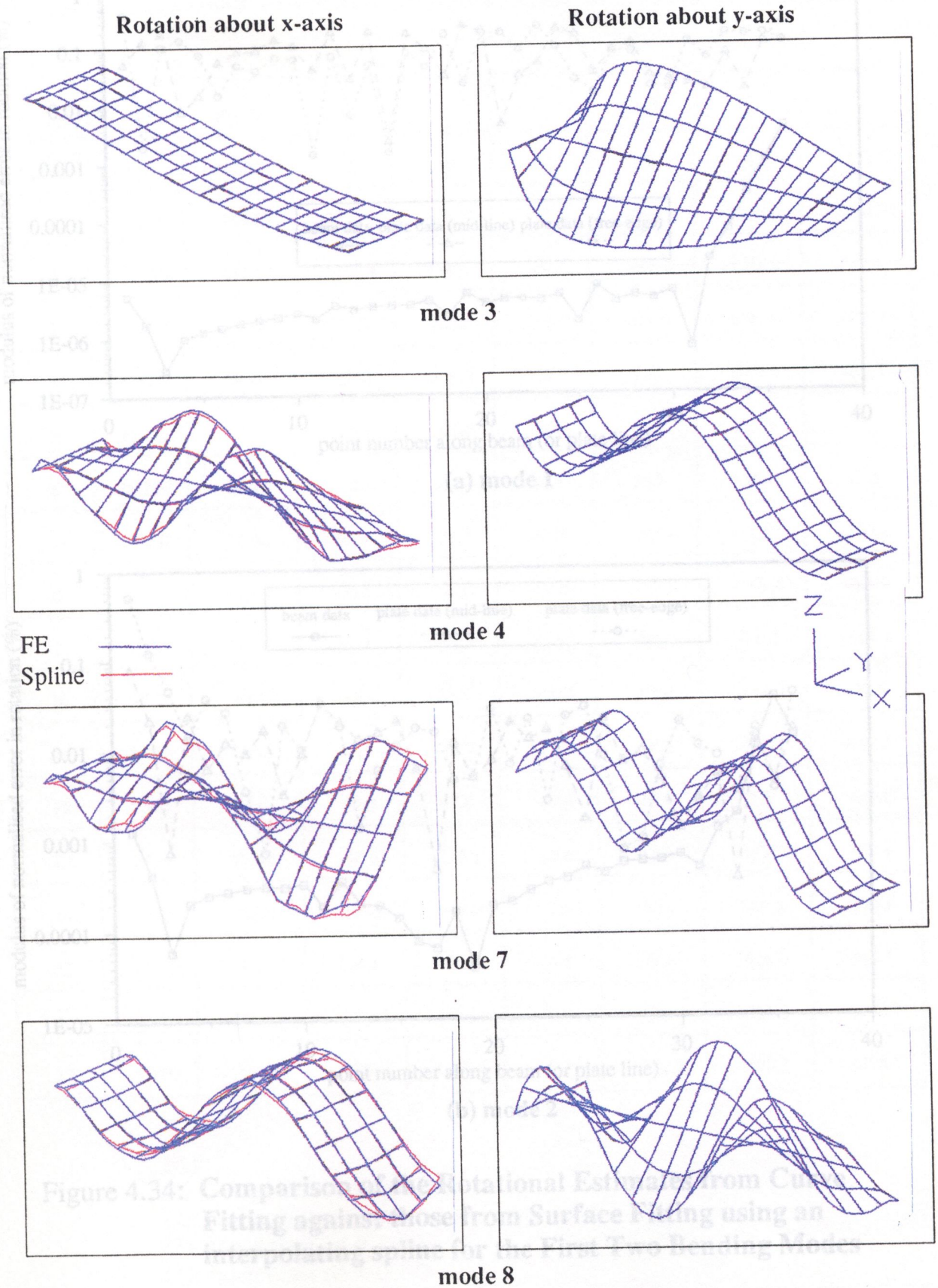

Figure 4.33: **Comparison of Rotational Modeshapes from an Interpolating Spline Surface with FE Modeshapes for the Cantilever Plate**

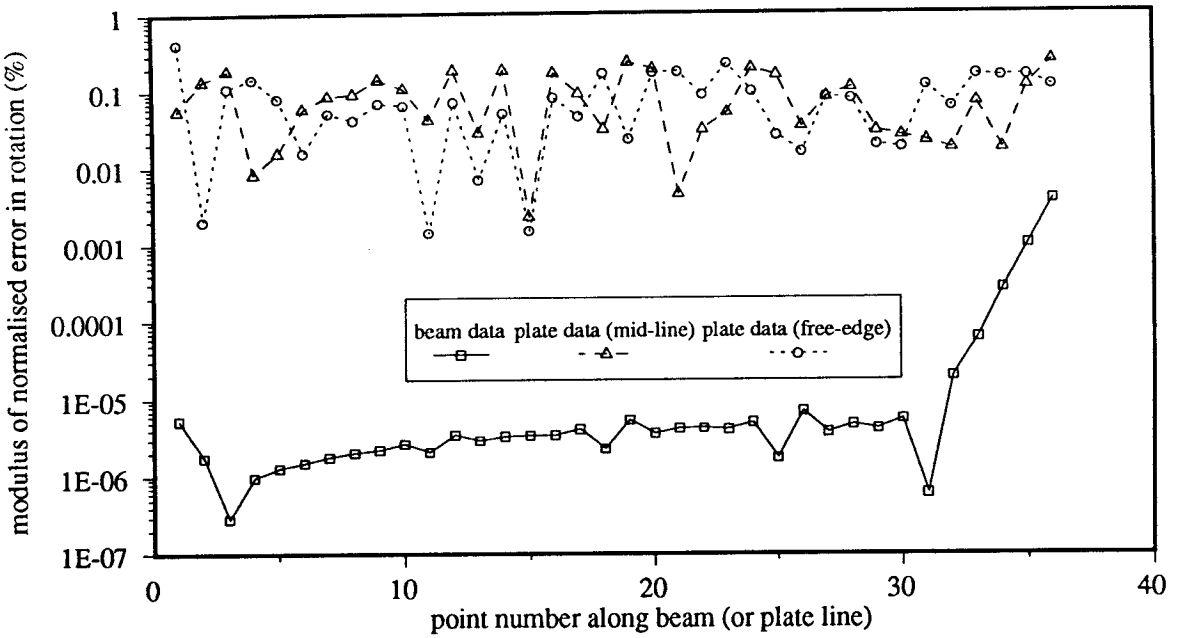

(a) mode 1

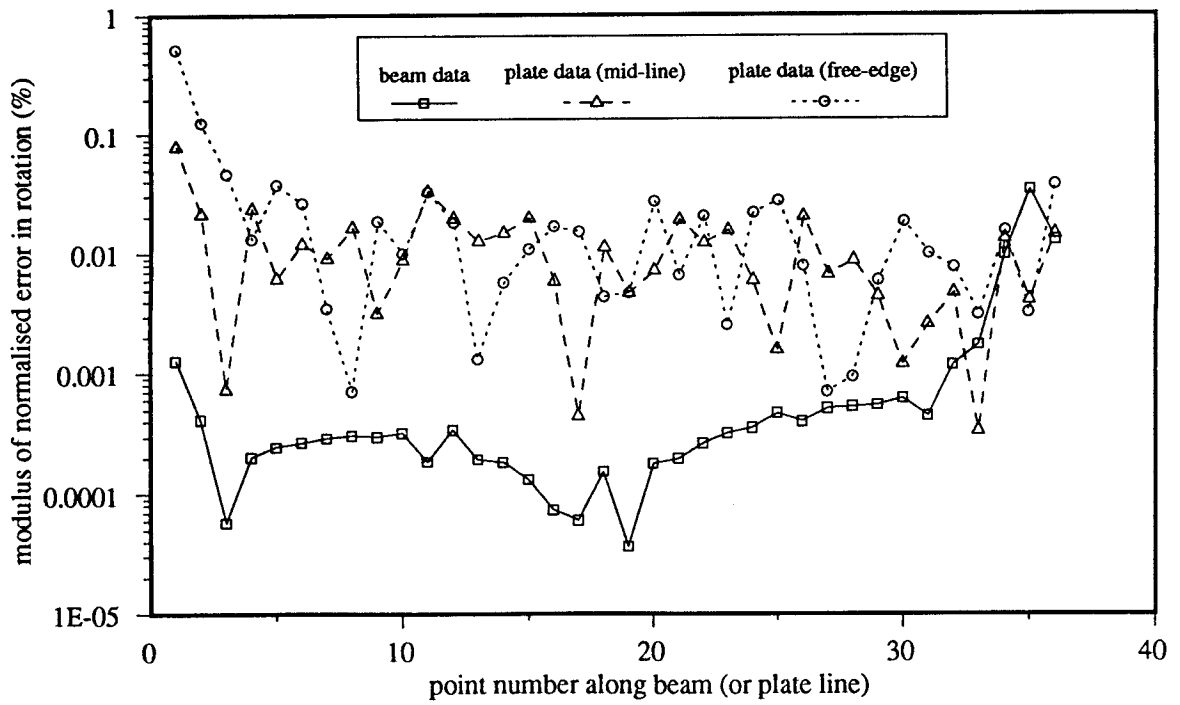

(b) mode 2

Figure 4.34: **Comparison of the Rotational Estimates from Curve Fitting against those from Surface Fitting using an interpolating spline for the First Two Bending Modes**

Table 4.1: Behaviour of the 2nd Derivative of the Interpolant on Simulated and Exact Data.

	mode 1				mode 2			
point	(1)	(2)	(3)	(4)	(1)	(2)	(3)	(4)
1	25.078	-966.02	-3654.7	2198.8	157.2	-1050.2	-3522.6	2330.9
2	24.733	-447.46	-1401.8	738.0	149.6	-369.2	-1276.8	862.9
3	24.387	71.39	851.2	-722.8	142.1	311.9	968.9	-605.1
4	23.007	98.14	-350.0	-375.3	112.2	72.1	-260.9	464.5
5	21.626	-28.96	152.1	-105.6	82.0	66.3	212.5	-45.1
6	18.189	26.23	-48.1	83.6	10.1	25.9	-56.1	75.5
7	14.808	24.86	63.9	-34.1	-51.4	-65.0	-2.5	-100.1
8	11.547	-1.90	-33.1	56.1	-94.6	-83.9	-138.2	-50.5
9	8.489	24.58	52.2	-35.2	-114.2	-120.7	-74.5	-156.2
10	5.731	-10.47	-38.9	50.3	-109.1	-99.0	-138.9	-70.9
11	3.381	19.96	52.5	-45.7	-83.7	-98.9	-89.8	-109.1
12	1.544	-27.65	-64.7	67.8	-47.0	-52.9	7.5	-69.1
13	0.374	69.42	130.8	-130.1	-13.6	38.0	-139.7	100.4
14	0.153	-220.82	-372.9	-372.9	-5.5	-99.2	366.4	-374.0
15	0.004	488.91	826.8	826.8	-0.3	98.1	-826.6	824.7
16	0.005	-530.95	-1426.5	-1426.5	-0.2	-326.1	1426.3	-1426.7
17	0.006	-1550.82	-3679.8	3679.8	-0.1	-750.2	3679.2	-3678.1

Key:
(1) Interpolant on Exact Data
(2) Interpolant on representative error level
(3) Interpolant on 0-1-0-1-
(4) Interpolant on 1-0-1-0-

Table 4.2: Comparison of the Computed Rotations from Various Approximations in the Region Bounded by the Limiting Conditions Using 0-1-0-1- Data for the Steel Cantilever Beam

	(a)		(b)		(c)		(d)		(e)	
mode	(1)	(2)	(1)	(2)	(1)	(2)	(1)	(2)	(1)	(2)
2*	2.099	-0.020	2.459	0.042	2.459	0.042	2.459	0.042	2.459	0.042
3	1.979	-0.013	2.957	0.012	4.935	0.068	5.155	0.079	5.155	0.079
4	1.660	-0.046	2.494	-0.029	4.908	0.020	9.302	0.111	9.302	0.111
5	2.055	-0.047	2.910	-0.038	4.997	-0.010	9.772	0.064	9.929	0.067

Key:

* Data for the first mode is omitted since the best fit for this mode was the least-squares polynomial

(a) 0.0<root rotation<2.1

(b) 2.1<root rotation<3.0

(c) 2.4<root rotation<5.0

(d) 2.4<root rotation<9.9

(e) approximation based on minimum second derivative at the free end

(1) Mass-normalised rotation at the fixed end of the cantilever

(2) % error in the rotation at the free end

Table 4.3 Relation Between the sum of the Squares of the Data Values and the value of S for the Least-Squares fit and the Fit which Minimises the Second Derivative at the free end of the Cantilever

	model 1		model 2		model 3	
mode	(1)	(2)	(1)	(2)	(1)	(2)
2	89.6	3002	84.5	2936	80.7	5913
3	17.9	803	14.7	662	14.3	821
4	1.7	221	1.5	160	1.4	4805
5	1.7	770	1.5	624	1.4	1297

Key:

(1) Sum of the squares of the data values divided by the weighted sum of squared-residuals for the least-squares fit.

(2) Sum of the squares of the data values divided by the value of S for the fit at which the second derivative at the free end is minimised.

Key for Tables 4.4 to 4.7.

(1) First-Order Difference (FOD) Calculation on Analytical Data
(2) FOD on 0-1-0-1- data base
(3) FOD on 1-0-1-0- data base
(4) Exact Analytical data

Table 4.4: Comparisons of the Computed Rotations from First-Order Difference Calculations for the 13 point Model

Distance along Beam (m)	mode 1				mode 5			
	(1)	(2)	(3)	(4)	(1)	(2)	(3)	(4)
0.025	0.306	1.020	0.306	0.605	13.631	14.345	13.631	23.107
0.050	0.890	0.177	1.603	1.168	24.688	23.974	25.401	22.710
0.100	1.680	2.036	1.323	2.163	4.364	4.721	4.008	-17.676
0.150	2.590	2.233	2.946	2.988	-31.059	-31.415	-31.415	-34.266
0.200	3.331	3.688	2.974	3.647	-17.305	-17.662	-16.949	5.494
0.250	3.910	3.553	4.267	4.148	24.871	25.227	25.227	35.650
0.300	4.337	4.694	3.980	4.503	24.942	25.299	24.586	5.660
0.350	4.627	4.270	4.984	4.731	-16.923	-17.279	-16.566	-33.543
0.400	4.800	5.157	4.444	4.854	-29.463	-29.820	-29.820	-14.694
0.450	4.883	4.526	5.240	4.902	10.928	11.285	10.572	34.973
0.475	4.906	5.619	4.192	4.908	42.515	43.228	43.228	47.972
0.500	4.909	4.195	5.622	4.909	49.779	49.066	50.492	50.416

Table 4.5: Comparisons of the Computed Rotations from First-Order Difference Calculations for the 15 point Model

Distance Along Beam (m)	mode 1				mode 5			
	(1)	(2)	(3)	(4)	(1)	(2)	(3)	(4)
0.017	0.206	1.276	0.206	0.408	10.015	11.085	10.015	18.169
0.033	0.605	-0.465	1.674	0.798	22.664	21.594	23.734	25.388
0.050	0.984	2.054	-0.086	1.168	24.800	25.869	23.730	22.710
0.100	1.680	1.323	2.036	2.163	4.364	4.008	4.721	-17.676
0.150	2.590	2.946	2.233	2.988	-31.059	-31.415	-31.415	-34.266
0.200	3.331	2.974	3.688	3.647	-17.305	-16.949	-17.662	5.494
0.250	3.910	4.267	3.553	4.148	24.871	25.227	25.227	35.650
0.300	4.337	3.980	4.694	4.503	24.942	24.586	25.299	5.660
0.350	4.627	4.984	4.270	4.731	-16.923	-16.566	-17.279	-33.543
0.400	4.800	4.444	5.157	4.854	-29.463	-29.820	-29.820	-14.694
0.450	4.883	5.240	4.526	4.902	10.928	10.572	11.285	34.973
0.467	4.905	3.835	5.975	4.907	40.465	41.535	41.535	45.033
0.483	4.908	5.978	3.838	4.909	47.760	48.830	46.690	49.641
0.500	4.909	3.839	5.979	4.909	50.217	49.147	51.287	50.416

Table 4.6: Comparisons of the Computed Rotations from First-Order Difference Calculations for the 17 point Model - Non Equidistant Points near the Boundaries

Distance along Beam (m)	mode 1				mode 5			
	(1)	(2)	(3)	(4)	(1)	(2)	(3)	(4)
0.005	0.155	1.581	0.062	0.125	3.396	6.962	3.396	6.624
0.010	0.458	-0.969	3.752	0.247	9.516	5.950	13.082	12.240
0.030	0.750	2.176	-0.405	0.721	19.818	20.709	18.926	24.786
0.050	1.031	-0.396	1.838	1.168	24.853	23.962	25.745	22.710
0.100	1.680	2.036	1.323	2.163	4.364	4.721	4.008	-17.676
0.150	2.590	2.233	2.946	2.988	-31.059	-31.415	-31.415	-34.266
0.200	3.331	3.688	2.974	3.647	-17.305	-17.662	-16.949	5.494
0.250	3.910	3.553	4.267	4.148	24.871	25.227	25.227	35.650
0.300	4.337	4.694	3.980	4.503	24.942	25.299	24.586	5.660
0.350	4.627	4.270	4.984	4.731	-16.923	-17.279	-16.566	-33.543
0.400	4.800	5.157	4.444	4.854	-29.463	-29.820	-29.820	-14.694
0.450	4.883	4.526	5.240	4.902	10.928	11.285	10.572	34.973
0.470	4.904	5.797	4.013	4.907	41.341	42.232	42.232	46.373
0.490	4.907	4.017	5.800	4.909	48.841	47.950	49.733	50.240
0.495	4.909	8.475	1.343	4.909	50.332	53.899	46.766	50.393
0.500	4.909	1.343	8.475	4.909	50.411	46.844	53.977	50.416

Table 4.7: **Comparisons of the Computed Rotations from First-Order Difference Calculations for the 17 point Model - Equidistant Points near the Boundaries**

Distance Along Beam (m)	mode 1				mode 5			
	(1)	(2)	(3)	(4)	(1)	(2)	(3)	(4)
0.012	0.155	1.581	0.155	0.308	7.860	9.287	7.860	14.672
0.025	0.458	-0.969	1.884	0.605	19.403	17.976	20.829	23.107
0.038	0.750	2.176	-0.677	0.892	24.821	26.247	23.394	25.580
0.050	1.031	-0.396	2.457	1.168	24.554	23.128	25.981	22.710
0.100	1.680	2.036	1.323	2.163	4.364	4.721	4.008	-17.676
0.150	2.590	2.233	2.946	2.988	-31.059	-31.415	-31.415	-34.266
0.200	3.331	3.688	2.974	3.647	-17.305	-17.662	-16.949	5.494
0.250	3.910	3.553	4.267	4.148	24.871	25.227	25.227	35.650
0.300	4.337	4.694	3.980	4.503	24.942	25.299	24.586	5.660
0.350	4.627	4.270	4.984	4.731	-16.923	-17.279	-16.566	-33.543
0.400	4.800	5.157	4.444	4.854	-29.463	-29.820	-29.820	-14.694
0.450	4.883	4.526	5.240	4.902	10.928	11.285	10.572	34.973
0.462	4.904	6.331	3.478	4.906	39.264	37.837	40.690	43.042
0.475	4.907	3.481	6.334	4.908	45.767	47.193	47.193	47.972
0.488	4.909	6.335	3.482	4.909	49.228	50.656	47.802	50.078
0.500	4.909	3.482	6.335	4.909	50.330	48.904	51.757	50.416

CHAPTER 5

EFFECTS OF THE ERRORS IN THE ROTATIONS ON THE ACCURACY OF THE STRUCTURAL DYNAMICS MODIFICATION PREDICTIONS

5.1 Introduction

The problem of determining the dynamic properties of a structure following a modification has received the attention of a large number of investigators in the last 15 to 20 years. In this regard, several structural modification and reanalysis techniques have been developed. In the majority of these techniques, the known parameters of the original unmodified structure are used to compute the new eigenvalues and eigenvectors of the modified design. In addition, the modified problem is usually solved with a much smaller number of degrees of freedom than the original system. Published work has however shown that the accuracy of the predictions of the dynamic behaviour of the modified structure depends on the accuracy of the original mode shape and frequency data [29,70]. Accuracy here is taken to mean the presence of error in the original modal data and/or the truncation error that is introduced by the inability to be able to describe the dynamics of a complex structure in simple terms over a limited frequency range. It is the effect of the former type of error on the predictions which this chapter will address.

Experimental errors in the measured mode shape vectors arise from broadly two sources, namely; calibration errors which may manifest themselves as incorrect magnitudes of the resulting modal vectors or errors due to geometry deficiency which give rise to spatial aliasing or the absence of some degrees of freedom at the measurement points. While it is known that the presence of error in the modeshape coefficients at modification attachment points will introduce errors in the predicted dynamic behaviour [68,69,70,77], most of the published work has only investigated the effect of missing rotational freedoms, of errors in the translational vector components and of errors in the frequencies of the unmodified structure. Although the literature is not entirely silent on the subject of the effect of errors in the rotations on the predictions, most references on this phenomenon merely point out the

presence of error in the predictions based on computed rotations but fail to relate the magnitude of the error in the predictions to the magnitude of the error in the rotations.

Although methods for expanding modal data to include all the freedoms at all the measurement points abound, the acceptability of a given level of error in the rotations and the suitability of the technique generally should be judged by its ability to predict the dynamic effects of structural modifications. Obviously, the better the approximating method of the rotations is, the better the SDM predictions. This chapter therefore considers the accuracy of the predictions of dynamic changes following structural modifications based upon modal databases expanded using spline curve and surface fitting as discussed in the preceding chapter. A brief exposition of modification theory precedes the discussion of the errors in the predictions due to modifications involving lumped masses, a rotational spring and rib stiffeners on beam and plate-like structures. To this end, the chapter endeavours to establish how the type, location and severity of the modification affect the accuracy of the predictions. A discussion of the sensitivity of the predictions to changes in the rotations is also included. This attempts to establish how large an error in the estimated rotations is "acceptable". In addition, an attempt is made to relate the magnitude of the errors in the rotations to the magnitude of the errors in the predictions using lumped-mass modification as a case study.

5.2 Structural Dynamics Modification Methods

Structural dynamics modification computations can be performed using either modal or physical coordinates. One advantage of the modal space approach over the physical space approach is that only the eigenvalues and eigenvectors of the unmodified structure are needed. In addition, all the matrices are normally considerably reduced in size thus greatly reducing computational time and memory requirements. On the other hand, use of the physical approach requires the stiffness, mass and damping matrices of the unmodified structure. In studying the accuracy of the predictions from the two approaches, several researchers [68,69] have shown that, in general, modal truncation was a significant limitation to the method. The results showed that the errors in the predictions did not seem to be related to the severity of the modification but rather to the absence of certain key descriptor modes in the databases. That is, the prediction was hampered by modal truncation and not modification severity. In addition, O'Callahan and Chou [78] demonstrated that truncation errors could be very severe

if the structure was severely modified, such as changing to a clamped end boundary condition from a free end boundary condition or adding a large stiffness, unless a near complete modal database is used in the analysis.

The foundation of all the structural dynamics modification methods is that the eigenvectors of the unmodified structure form a complete vector basis from which the motion of any modified structure can be described. Depending on the form of the modification, SDM methods can be classified into three main categories, as follows:

- techniques based on small modifications
- techniques based on localised modifications
- techniques based on global modifications

Techniques based on small modifications borrow heavily from Rayleigh's Method [79] and are founded on the premise that for small modifications, the mode shapes do not significantly change. Variants of the approach lead to sensitivity-type formulations of the problem. Techniques based on localised modifications are essentially available as the Local Eigenvalue Modification Procedure [10] in which the eigenvalues of the modified structure are functions of the modified mode shapes and the unmodified natural frequencies. In their investigations on global structural modifications, Luk and Mitchell [12] considered a variety of methods, namely; modifications performed in physical coordinates, modifications performed in both physical and modal coordinates and modifications performed in modal coordinates. Their work showed that the last method, which they called the Dual Modal Space Method (DMSM), was the most efficient. For this reason, this method was used to predict the dynamic behaviour of the modified structures in the case studies investigated in this work.

5.2.1 The Dual Modal Space Method

In the method, any number of mass, stiffness and damping modifications can be presented simultaneously as a global change to the modal mass, stiffness and damping matrices of the unmodified structure defined in the modal space of the unmodified structure (so-called modal space 1). The dynamics of the unmodified structure can be described in physical space by a set of homogeneous second-order differential equations in the form

$$[M]\{\ddot{x}\} + [C]\{\dot{x}\} + [K]\{x\} = \{0\} \tag{5.1}$$

These equations are transformed into modal space 1 using the relationship

$$\{x\} = [\phi_1]\{q\} \tag{5.2}$$

where $[\phi_1]$ is the matrix of eigenvectors of the unmodified structure scaled to give unit modal mass and yield

$$[m]\{\ddot{q}\} + [c]\{\dot{q}\} + [k]\{q\} = \{0\} \tag{5.3}$$

If the mode shapes are scaled to give unit modal mass and classical damping is assumed, the modal space matrices become,

$$[\phi_1]^T[M][\phi_1] = \begin{bmatrix} \ddots & & \\ & I & \\ & & \ddots \end{bmatrix}$$

$$[\phi_1]^T[C][\phi_1] = \begin{bmatrix} \ddots & & \\ & 2\gamma\omega & \\ & & \ddots \end{bmatrix} \tag{5.4}$$

$$[\phi_1]^T[K][\phi_1] = \begin{bmatrix} \ddots & & \\ & \omega^2 & \\ & & \ddots \end{bmatrix}$$

This gives

$$\begin{bmatrix} \ddots & & \\ & I & \\ & & \ddots \end{bmatrix}\{\ddot{q}\} + \begin{bmatrix} \ddots & & \\ & 2\gamma\omega & \\ & & \ddots \end{bmatrix}\{\dot{q}\} + \begin{bmatrix} \ddots & & \\ & \omega^2 & \\ & & \ddots \end{bmatrix}\{q\} = \{0\} \tag{5.5}$$

When modifications of mass, stiffness and damping are applied to the structure, equation (5.1) can be rewritten in the form

$$[M+\Delta M]\{\ddot{x}\} + [C+\Delta C]\{\dot{x}\} + [K+\Delta K]\{x\} = \{0\} \tag{5.6}$$

Transforming this into modal space 1 gives

$$[[I] + [\Delta m]]\{\ddot{q}\} + \left[\begin{bmatrix} \ddots & & \\ & 2\gamma\omega & \\ & & \ddots \end{bmatrix} + [\Delta c]\right]\{\dot{q}\}$$

$$+ \left[\begin{bmatrix} \ddots & & \\ & \omega^2 & \\ & & \ddots \end{bmatrix} + [\Delta k]\right]\{q\} = \{0\} \tag{5.7}$$

where [Δm], [Δc] and [Δk] are the modification matrices transformed into modal space 1. The solution of (5.7) gives the eigenvalues and eigenvectors $\{q_1\}$ of the modified structure defined in modal space 1. These vectors can be readily transformed back into physical space coordinates using

$$\{u\} = [\phi_2]\{q\} \tag{5.8}$$

The eigenvectors of the modified structure initially have unknown scaling. These initial solution vectors can be assembled into a modal matrix $[\psi_1]$ which can be used to transform the modal mass of the modified structure, $[m_1]$, from modal space 1 into modal space 2, which is the modal space of the modified structure as follows

$$[m_2] = [\psi_1]^T [m_1] [\psi_1] \tag{5.9}$$

$[m_2]$ will be a diagonal matrix, but its elements, m_{2r}, will not, in general, be equal to unity. These elements can however be used to scale the initial modal space 1 vectors, $\{q_1\}$, to give unit modal mass:

$$\{v_1\}_r = \frac{1}{\sqrt{m_{2r}}}\{q_1\}_r \tag{5.10}$$

When the scaled $\{v_1\}_r$ vectors are assembled into a new modal matrix, $[\Theta_1]$, the final modal matrix, $[\phi_2]$, containing the modal vectors of the modified structure scaled to unit modal mass can be generated:

$$[\phi_2] = [\phi_1]\,[\Theta_1] \tag{5.11}$$

For a structure with n degrees of freedom and a data set with p modes, $[\phi_1]$ and $[\phi_2]$ will be (n x p) matrices and $[\psi_1]$ and $[\Theta_1]$ will be (p x p) matrices.

It should be noted from equation (5.11) that the mode shapes of the modified structure are formed as linear combinations of the unmodified mode shapes weighted by the modal space solution vectors. Therefore, the initial model must include not only a sufficient number of modes, but must also contain the correct modes [9] for the type and location of the modification(s) to be made. The accuracy of the results can be expected to depend on the type, magnitude and location of the modification and the accuracy of the initial modal data as will be shown in later parts of this chapter.

In order to use the Dual Modal Space Method, two procedures, namely; MODS and EIGEN were written. The procedure MODS served two purposes. Firstly, it was used to process and format geometry, display and modal data for the fitting procedure, AUGFITTER. Secondly, MODS was used to generate the modification mass, damping and stiffness matrices according to the type and location of the modification. These matrices would then, along with the augmented modal data following expansion, be submitted to the procedure EIGEN for the formulation and solution of the new eigenvalue problem in modal space. Full details of each procedure along with an overview of the entire system of procedures, and the associated file manipulation are given in Appendix 1.

5.3 Modifications On the Cantilever Beam

The modifications used in these investigations were restricted to a lumped mass (with and without rotational inertia), a rotational spring and a rib stiffener. The choice of these types of modifications was governed by the fact that they provided different scenarios when relating the errors in the predictions to the errors in the rotations. While lumped mass and spring

modifications depend only upon the rotation and translation at the location where the modification is made, a rib modification links the translations and rotations at several points on the structure.

5.3.1 Mass Modifications

The base structure used in this study was a steel cantilever beam, 500mm long, 25.4mm wide and 12.7mm wide.

For the discussions which follow in the next two sections, the beam was modelled with ten two-noded beam finite elements for which modal data (frequencies and mode shapes) was obtained from finite element analysis for the first nine flexural modes. For the purposes of this study, this data was taken to be sufficiently accurate since the errors in the rotations were very small (less than 0.5% when compared with exact values). Much more importantly, the effect of these discrepancies on the predictions is removed since, in the analysis, the comparison base is the modal prediction based on the unseeded data. In order to understand how a given level of error in the rotations affected the predictions, errors in the predicted frequencies were investigated for a range of lumped mass modifications at the free end of the cantilever in which the mass was kept constant at 0.2 kg (representing approximately $^1/_5$ of the mass of the beam) while the rotational inertia associated with it was varied.

In the interpretation of the results which follow, the approach adopted was similar to that used by Tayeb [70]. A non-dimensional indicator of the severity of modification, the Inertia Modification Ratio (IMR), was defined as the ratio of the added moment of inertia to the total inertia of the beam (about an axis perpendicular to the beam and passing through one of its ends). The effect of the modification on the resulting frequencies was expressed in terms of the percentage error in the modal prediction of frequencies from modal data with the given error in the rotation when compared to the modal prediction based on unseeded FE data. Therefore, a negative percentage error indicated an under-prediction whereas positive percentage errors indicated over-prediction. In this way, the effect of a given error in the rotations was directly related to the magnitude of the error in the modal prediction.

5.3.1.1 Understanding the Modification

From the outset and in order to properly interpret the results, the nature of the lumped mass modification with increase in the value of the rotational inertia must be understood. Figure 5.1 shows the behaviour of the predicted frequencies from error-free data with increase in the value of IMR. It is seen from the figure that the effect of the mass modification with increasing IMR is to drop the frequencies of vibration. The higher frequency modes settle down at their constant levels at lower values of the IMR than the lower frequency modes. The results indicate that, generally, further increase in IMR beyond 10 has no appreciable effect on the frequency for each mode. However, it will be seen that the fundamental frequency was still dropping even for the largest IMR value used which was equivalent to an inertia value of 3.0 kgm^2 (roughly 100 times greater than the inertia of the beam itself). When this is viewed in the light of the movement of frequencies from those of the clamped-free condition to the clamped-clamped condition, the continuing drop in the fundamental frequency is then understood to be in keeping with the expectation that further increase in the IMR value would see the fundamental frequency drop to zero while the rest of the frequencies would settle at around those of the clamped-clamped condition. However, in this case neither the mass nor the inertia are large enough for this condition to be reached. Instead, an intermediate condition, which is close to the clamped-sliding condition, is achieved. In Figure 5.1, the exact clamped-sliding frequencies are included as asymptotic lines to illustrate this. Observation of the mode shapes, a representative set of which is given in Figure 5.2 for an IMR value of 114.5, in fact confirms the restriction in the slope at the free end.

An examination of the relative contributions of the original modes to the new modes following modification according to equation (5.11), indicated that, from an IMR value of 0.01, contributions from the original modes to the modes immediately downstream become increasingly significant. For example, the largest contributor to the new mode 5 is the original mode 4 and that to mode 6 is the original mode 5. This is representatively illustrated in Table 5.1 for mode 5. This fact is critical in understanding the effect of an error in the modeshape vector of a given mode on the predictions of frequency as will be shown in the next section.

For the purposes of the discussion which follows, it has to be acknowledged that use of a nine-mode database would produce significant modal truncation errors in the predictions as demonstrated in Figure 5.3. Figure 5.3 shows an increase in the error of the prediction with increase in mode number and the severity of modification. It will also be seen from the figure that the errors in the predictions for each mode level off at the IMR value where the frequency values were no longer transient (see Figure 5.1). Figure 5.3 indicates that for a given modification, the error in the modal prediction of frequency increases with increase in the mode number; an observation which is consistent with modal truncation. This problem is however dealt with by using a modal prediction based on error-free data as the basis for comparison. In this way, any error introduced in the predictions based on seeded data is directly related to the error introduced in the modal data since only one parameter is varied at a time.

5.3.1.2 Relation Between the Magnitude of the Error In the Rotations and the Magnitude of the Error in the Predicted Frequencies

In the following sections, an attempt is made to relate the magnitude of the errors in the rotations with the magnitude of the errors in the predictions of frequency. At the same time, the effect of a given level of bias error at selected rotational degrees of freedom is also established. In each of the cases which are presented, a 10% bias error was introduced at the tip rotation for a particular mode of the beam. This level of bias was chosen in order to exaggerate the effects on the predictions.

(a) Discussion of the Results from the case of the Error in the Tip Rotation of the First Mode of the Database

Figure 5.4a summarises the effect of mass modification at the free end of the cantilever using a modal database which has a +10% error introduced into the FE tip rotation of mode 1 on the predicted frequencies of the modified structure. It is clear that, for small amounts of inertia addition, the frequencies of the new structure are still very close to those of the unmodified structure. However, as the inertia is increased, the error in the modal prediction for the first two modes is seen to rise up to a level which remains constant in spite of further increases in the IMR value. While the frequency of the first mode is seen to be under-predicted, that for mode 2 is over-predicted. The errors in the prediction of the frequencies

of the rest of the modes (modes 3-9) in the database however remain virtually unchanged. A closer examination of the errors in the predicted frequencies revealed that in fact the frequencies for modes 3 to 9 were generally slightly under-predicted with a fall in the magnitude of the error as the mode number was increased. While the magnitude of the errors in the predicted frequencies beyond mode 2 were less than 0.2% and diminishing, the errors for the first two modes, which were the largest, were just under 7%. The overall effect of the seeding therefore was to introduce some flexibility into the modified structure resulting in an under-prediction of the frequencies of all the modes in the structure except for the mode adjacent to the first mode, which initially had the noise.

An alternative way of viewing the effect of the +10% error in the tip rotation for mode 1 was to consider the relative contributions of the original modes to the new modes. It will be seen from Figure 5.2 that the new mode 2 is very similar in shape to the old mode 1. This observation is borne out by the fact that the relative contributions of the original modes 1 and 2 to the new mode 2, shown in Figure 5.5, are such that the contribution from mode 1 becomes dominant beyond an IMR value of 0.1. This explains why the new second mode is significantly more sensitive to the error introduced to the tip rotation of the first mode than the rest of the modes in the database to which the contributions from mode 1 were an order of magnitude lower. Thus the presence of error in the tip rotation of the first mode was seen to 'contaminate' the prediction of the adjacent mode. On the other hand, the error-free tip rotations in the other modes had a 'diluting' effect on the original error. This was signified by the magnitude of the error in the prediction of the frequency of the first mode which was less than the magnitude of the error in the tip rotation. The observation is in agreement with the findings reported by Tayeb [70] from his investigations on the effect of errors in the initial translations and frequencies on the predictions.

Figure 5.4b shows the effect of the same modification but this time using a database with a -10% error in the FE tip rotation of the first mode. This time the behaviour of the errors in the predicted frequencies is seen to be reversed to that seen for the case when a +10% error was introduced in the tip rotation of the first mode. This seeding therefore has, except for the second mode, a stiffening effect on the modified structure. The relative magnitudes of the errors are however similar. This was a heartening observation as it suggested that while

the sign of the error in the rotation affected the resulting frequencies in a particular manner (under-prediction or over-prediction), the magnitudes of the errors in the predicted frequencies were unaffected. In both Figures 5.4a and 5.4b, at severe modification (IMR greater than 10 for this system), the error in the frequencies for mode 1 and 2 is seen to even out to around 6.5%.

While the behaviour of the relative modal contribution values is consistent with the assertion that the new modes are formed as linear combinations of the old ones according to equation (5.11), it does not offer any insights into either the manner of the predictions (i.e., the over-prediction of the second mode frequency for the case of a +10% error in the tip rotation of mode 1 or the reverse for a -10% error), or the magnitude of the error in the prediction of frequency (6.5% in this case). The explanation is thus qualitative rather than quantitative.

In order to provide further insight into the contribution of the error in the rotations to the errors in the predictions, the modification mass matrices in modal space (from equation (5.7)) were examined. This examination revealed that in the transformation of the modification matrices from physical to modal space, as required by the dual modal space method according to equation (5.4), the presence of any error in any modal vector component of a given mode was reflected only in the elements of that mode in the modal space modification matrix (i.e., the row and column for that mode). For example, the error in the tip rotation of the first mode was reflected in the elements of mode 1 only in the modal space mass modification matrix (i.e., only the first row and the first column of the matrix reflected the error). It must also be noted that the use of equation (5.4) produces symmetrical modal space modification matrices which are however not diagonalised.

A summary of the errors in the modal space modification mass matrix elements as a result of -10% and +10% errors in the tip rotation of the first mode is presented in Figure 5.6. It is immediately seen from the error plots that the largest error which was introduced in the elements of the mass matrix was in the element on the leading diagonal (m_{11}). This error is seen to increase rapidly as the IMR value is increased. The error in the off-diagonal elements however levels off at about 10% as the IMR value is increased beyond 1.0. In the case of the leading diagonal element, the rise in the error continues up to around 18% (nearly twice

the error originally introduced in the rotation) at an IMR value of 10. When this large error in the leading diagonal is viewed in the light of the errors in the frequency predictions, the 'dilution' effect of the error-free rotations is apparent. This is indicated by the magnitude of the error in the predicted frequencies as shown in Figure 5.4 (about 6.5% for modes 1 and 2 and lower than 0.2% for the rest). However, it must be understood that there is no suggestion of a quantifiable link between the errors in the modification mass elements and the resulting predictions as will be shown later in this section.

An attempt to trace the errors from source to effect indicated that the initial error in the modal vectors was initially amplified to around 18% in the leading diagonal element, m_{11}, only (the error was around 9% in the elements for the adjacent mode i.e., m_{12} and m_{21} and insignificant ($\approx 0\%$) in most) when the eigen problem was transferred to modal space using equation (5.7). This amplified effect was however reduced to around 6.5% in the solution process when simplifying the characteristic equation and solving for the frequencies. While such a sensitivity analysis is possible for a 2 degree of freedom problem, it is not amenable to problems with larger numbers of degrees of freedom.

The relationship between the magnitude of the error in the tip rotation for mode 1 and the magnitude of the error in the modal prediction of frequency is presented in Figure 5.7 for an IMR value of 114.5. The plots for the other levels of modification severity were similar. It will be seen from the figure that there exists a reasonably linear relationship between the level of error at the modification location and the level of error in the prediction of frequency. This is particularly attractive since it offers guidance in estimating the accuracy of a prediction for a known level of error at the modification location for the modification under investigation. Analysis for the case of increasing under-estimation of the rotation at the tip yielded similar magnitudes of the prediction error but with all the modes, except the second mode, over-predicted as was shown earlier.

An alternative way of viewing the data is presented in figure 5.8 in which the effects of 'contamination' and 'dilution' are clearly demonstrated. The scale on the y-axis is non-dimensional and represents the relative error in the prediction of frequency as the ratio of the percentage error in the prediction of frequency to the percentage error in the rotation at the

free end of the beam. A particularly interesting feature which is evident from the figure is the level of 'contamination' of the second mode with increase in the level of error in the tip rotation. It will be seen that the relative error in the frequency prediction is higher for the second mode for magnitudes of the error in the tip rotation of 5% and above. It is also interesting to note that, for the first mode, the relative error in the prediction of frequency actually drops as the level of error in the tip rotation is increased. For example, for the IMR value of 114.5 (Figure 5.8b), the relative error in the prediction ranges from about 0.8 for a 1% error in the tip rotation to 0.4 for a 100% error in the tip rotation. There is however no obvious explanation for this behaviour. In addition, the results also indicated that, as would be expected, the range of the relative error in the prediction of frequency for the first two modes reduced as the IMR was reduced (compare Figures 5.8a and 5.8b).

(b) Discussion of the Results from the case of the Error in the Tip Rotation of the Last Mode of the Database

In this case, a ±10% error was introduced in the tip rotation of the ninth mode. The results are presented in Figure 5.9 in the form of error plots with increasing severity in the modification. As the IMR value is increased, the error in the predicted frequencies is seen to rise for all modes until the stable state is reached at an IMR value of around 0.01. However, the increase is moderate when compared to the cases where the error was introduced to the tip rotation of the first mode. As would be expected, the error in the predicted frequencies of the ninth mode, which had the initial error, is seen to be the largest (about 1.9%). However, in contrast to the cases investigated before, contamination of the adjacent mode (mode 8) is much less in this case (only about 0.65% error in the prediction). This is however not surprising since the effect of the error in mode 9 on the prediction would be to contaminate the mode immediately downstream (higher frequency) than the mode immediately upstream (lower frequency). Figures 5.9a and 5.9b also show the 'dilution' of the effect of introducing the error. This is reflected by the reduction in the error in the predicted frequencies as one goes down to the fundamental mode of the database. The error in the predicted fundamental frequency (furthest from the mode with the initial error) is, as would be expected, very small (below 0.2%).

The relative contributions of the original modes to the new modes were, in this case, observed to follow a different pattern even though the new frequencies were under-predicted as in the case of the +10% increase in the tip rotation of the first mode. Here there was increased contribution from the original mode 9 to all the new modes except to the new mode 9 to which the contribution was reduced. Figure 5.10 presents the modal contributions to the new mode 9 from modes 8 and 9 which were the key contributors. It will be seen that although the original mode 9 was still the main contributor to the new mode 9, there was a significant contribution from the old mode 8 beyond an IMR value of 0.01. This explains why the error in the frequency prediction of mode 9 was much lower than the 10% error initially introduced into its tip rotation. The associated reduction in the error in the predictions of frequency upstream of mode 9 (i.e., lower frequency modes) is also a consequence of the reduction in the contributions from mode 9 to the other modes.

The overall effect of the seeding was to introduce flexibility into the new structure and hence the general under-prediction of the frequencies. This was not unexpected as it was consistent with previous observations in which the rotation was over-estimated.

The results from the corresponding analysis on the effect of seeding the largest tip rotation in the database with a -10% error are summarised in Figure 5.9b. A reversal of the behaviour, but with the same orders of magnitude of the error in the predicted frequencies is immediately apparent. Examination of the relative contributions of the original modes to the new modes also confirmed the reversal in the behaviour.

Figure 5.11 summarises the error in the elements of the modal modification mass matrix for a positive bias error in the tip rotation. It will be seen that contrary to observations from the case of bias error in the tip rotation of the first mode, the mass elements were over-predicted although the resulting predictions of frequency were consistent with those seen for a +10% error in the tip rotation of mode 1, i.e., under-prediction of the frequencies. It is also particularly interesting to note that in this case, the error in the leading diagonal element, m_{99}, is higher (>20%) than that seen for the leading diagonal element, m_{11}, for the case with the error in the tip rotation of the first mode (<19%). When this is viewed in the light of the corresponding error in the frequency prediction which is lower than that seen for the case of

the bias error in the tip rotation of the first mode, it confirms the qualitative nature of the explanation of the effect of the modification on the prediction of frequency alluded to earlier.

The smaller errors in the predictions resulting from this seeding when compared with the case when the noise was added to the tip rotation of the first mode suggests that the predictions of the low frequency modes are more sensitive to the errors in the rotations than are predictions of the high frequency modes.

From the smoothness of the error curves and the similarities in the magnitudes of the errors in the predicted frequencies as shown in Figures 5.4 and 5.9, it may be concluded that an over-prediction of the rotation at the modification location will result in an under-prediction of the frequencies following a mass modification. On the other hand, if the value of the rotation is under-estimated, the resulting frequencies will be over-predicted. This is consistent with qualitative expectations since a restriction in movement (translational or rotational) suggests higher stiffness and hence higher frequency while the reverse is true for excessive movement. It is also clear from the foregoing discussion that a given level of error in the rotations does not necessarily translate into the same level of error in the predicted frequencies. The errors in the frequencies are seen to be much lower than the errors in the rotations. This is however not surprising since error was introduced in only one mode shape vector component. The other error-free components tended to moderate the influence of the single error.

(c) Discussion of the Results from the Case of the Error in the Tip Rotation of the Fifth Mode of the Database

Figure 5.12 summarises the effect of introducing a +10% error in the tip rotation of the fifth mode in the database. In this case, it will be noted that the seeding leads to an under-prediction of the frequencies of the low frequency modes up to the mode which initially had the error. On the other hand, the frequencies for modes 6-9 were over-predicted. However, it will be seen that the error in the prediction of the sixth mode was the largest.

While the complexity of a sensitivity analysis on the quantitative effect of the error in the tip rotation on the predictions of frequency leaves a void on the discussion of Figure 5.12, the

relative magnitude of the errors in the prediction of the sixth mode can be attributed to the dominance of the relative contribution from the original mode 5 to the new mode 6. This is illustrated in Figure 5.13a from which it is apparent that the new mode 6 has a relatively smaller contribution from the original mode 6 beyond an IMR value of 0.005. Since the bias error was in the original mode 5, the relatively larger error in the prediction of the sixth mode is therefore not unexpected. It should also be remarked that the relative contributions from the other modes in the database were all less than 0.1 each except that from mode 7 which was about 0.17.

The variation of the relative contributions to the new mode 5 from modes 4 and 5 is presented in Figure 5.13b. It will be noted that the new mode 5 is made up of predominantly the original modes 4 and 5 beyond an IMR value of 0.007 with mode 4 being the dominant contributor. It is therefore not surprising that the error in the prediction of the fifth mode is less than the error in the prediction of the sixth mode.

The particular under-prediction of the frequencies of the modes upstream of mode 5 and the over-prediction of the frequencies of the modes downstream of mode 5 is in this case however not linked to the over-prediction of the modification modal mass elements which is shown in Figure 5.14. Comparison of Figure 5.14 with Figure 5.12 does not reveal any direct correlation between the two. It does, nevertheless, highlight the 'dilution' effect of the error-free rotations on the predictions which is indicated by the much smaller errors (less than 3%) in the predictions. What is of particular interest however is the fact that the largest error in the mass elements was in the leading diagonal element, m_{55} (about 21%), while the rest all levelled off at just under 10%. It is once again evident that while the higher magnitude of error in the prediction of the frequency of the mode upstream of the mode with the initial error can be explained in terms of equation (5.11), the manner and actual magnitude of the resulting prediction cannot be similarly dealt with.

(d) Discussion of the Results from the case of the Error in the Tip Rotations of all the Modes in the Database

Figure 5.15 presents the effect of introducing a +10% error in the tip rotations of all the modes in the database on the predicted frequencies. Although under-prediction of the

frequencies is the common feature for all modes, it is clear that the relative magnitude of the under-prediction cannot be easily related to the pattern and level of seeding. It is also evident that the magnitudes of the errors in the predictions of frequency bear no correlation with those seen when the error was introduced in the tip rotation of a single mode. The plot instead reveals a peaking of the errors in the predicted frequencies, but at different IMR values for each mode. However, when Figure 5.15 is viewed in conjunction with Figure 5.1, it will be seen that the IMR values at which peaking of the errors in the predicted frequencies for modes 2 to 9 occurs are consistent with the IMR values at which the predicted frequencies drop as a result of the mass modification. In other words, the largest magnitudes in the errors are seen in the region where the frequencies are transient from one steady state to another. In the region where the frequencies are stable (Figure 5.1), the errors were very low (less than 1%). In the case of the fundamental mode, the continuing rise in the error is also consistent with the continuing drop in the fundamental frequency as the IMR value is increased.

The variation of the errors in the predictions shown in figure 5.15 was attributed to a change in the mix of the original modes in the formation of the new modes when the seeded database was used. This is clearly illustrated in figure 5.17 for modes 1, 5 and 9 where the variation of the discrepancy in the relative modal contributions to the new modes when comparing the modal predictions based on unseeded and seeded databases is shown. It is clear that at low IMR values, the changes in the modal contributions are very small. However, as the IMR value is increased, there are significant differences in the mix of the old modes in forming the new modes. These differences however diminish with further increases in the IMR value beyond 10 for all modes except the fundamental mode for which the discrepancies are observed to settle at around 10%. Thus, it is clear that introduction of the error in all tip rotations introduced a variable truncation error in the predictions which was manifest in the particular pattern of the errors in the predictions.

It has already been shown that for the tip mass modification, the relative modal contributions to the new modes are dominated by the contribution from the mode immediately upstream of the mode of interest. While this still holds in this case, there does not seem to be any correlation between the relative modal contributions and the resulting frequency predictions. The errors in the modal modification mass matrix elements, typically shown for mode 5

elements in Figure 5.16 (the plots for the other modes were similar), also do not suggest any correlation between these and the errors in the predictions of frequency. In this case, the errors in the mass elements all level off at around 18% unlike in the cases when the error was introduced in the tip rotation of an individual mode, i, where the largest error in the prediction of the mass elements was at the leading diagonal element, m_{ii}.

Notwithstanding the foregoing, the results indicate that the new fundamental mode suffers most from the seeding while the highest frequency mode, mode 9, is least affected. This confirms that predictions for the low frequency modes are more sensitive to errors in the rotations than are predictions for the higher frequency modes. This is however not surprising since an error in the tip rotation of a low frequency mode has a more significant effect on the mode shape than an error in the tip rotation of a high frequency mode. This is because there are more sign changes in the slope for the higher modes which tends to dilute the effect of the error on the modeshape as a whole.

In the foregoing discussions of the effect of an error in the rotation entries at the tip of the cantilever, an attempt was made to trace the errors from source to effect. While the data indicates that errors in the rotations have an effect on the frequency predictions, it is clear that although the effect is quantitative, it is not directly quantifiable. This is manifestly shown by the absence of a link between the errors in the rotations and the errors in the modal mass matrix elements on one hand, and the errors in the modal modification mass matrix elements and the errors in the resulting frequency predictions on the other. This is attributed to the difficulties which are associated with sensitivity analysis for systems involving more than two degrees of freedom.

5.3.1.3 Effect of Errors in the Rotations on the SDM Predictions

(a) Analytical Data

In this series of tests, a mass of 0.2 kg having a moment of inertia of 0.3 kgm^2 was added to the free end of the cantilever described in the previous section but modelled with 61 equidistant measurement points. The inertia value is roughly 10 times that of the beam itself (i.e., IMR $\approx$ 11) and was chosen to exaggerate the effects of any errors in the calculated rotations. The effect of such a large inertia is shown by the fact that addition of the mass

with zero rotational inertia reduces the fundamental frequency from 42.1 Hz to 32.6 Hz, whereas inclusion of the inertia drops this to 11.7 Hz.

Modal data for the first 28 flexural modes of the unmodified structure was obtained from the analytical Euler-Bernoulli solution for a cantilever beam. Exact data was used in this case since the object was to compare the predictions based on exact rotations with those based on calculated rotations. The large number of modes was chosen in order to minimize modal truncation effects. The reduction in modal truncation effects was highlighted by the participation of nearly all the original modes in the formulation of the new mode shapes.

Theoretical estimates of the rotations at the 61 measurement points were obtained by curve fitting the original translational data using the interpolant which, as shown in Chapter 4, was the best approximant for error-free data. Figure 5.18a presents the comparison of the errors in the predicted frequencies from databases using exact and calculated rotations for a mass modification which included inertial effects. It must be noted that, in this case, the calculated and exact translations were equal and therefore had no bearing on the predictions. The particular form of the plots in Figure 5.18a is seen to be a result of the effect of the inertia alone as shown in Figure 5.18b where the effect of the mass was excluded.

The errors in the frequency predictions based on calculated rotations range from 0.7% for the first mode to 4% for mode 28. When these errors are compared with the errors in the calculated tip rotations which ranged from -2.5% to 13% (as summarized in Figure 5.19), the results are seen to be very good. Comparison of these results against those reported by Green et al [30] for the same modification shows an improvement in the estimates of the rotations and in the predictions. The similarities in the magnitudes of the error in the predictions from the exact and expanded databases and the over-prediction of the frequencies generally suggest that the errors in the predictions were largely due to modal truncation effects and not due to errors in the rotations. This was confirmed by the observation that the largest errors in the computed rotations were obtained for the higher frequency modes. The better accuracy seen in the predictions based on calculated rotations beyond mode 10 is explained by the relatively large over-estimation of the rotations in the higher frequency modes. As shown earlier, this over-estimation of the rotations would lead to an under-

prediction of the frequencies following a mass modification. However, in this case, because some of the tip rotations in the database were under-estimated which would lead to an over-prediction of the frequencies, the overall effect was to yield frequencies which were lower than those arising from the exact database and which, in turn, were closer to the exact solution for this modification. It is interesting to note that 18 of the tip rotations in the database were under-estimated while 7 were over-estimated, albeit with much larger magnitudes. The results therefore indicate the relative dominance of the under-estimated rotations over the over-estimated values on the frequency predictions which was not unexpected.

(b) Simulated Experimental Data

Predictions of the dynamic effects of mass modifications from simulated experimental data were performed in order to establish whether the optimum approximant of the rotations had to be mathematically accurate or whether an approximation in the 'ball-park' would suffice. In this regard and for the same model of the beam described in the previous section (17 point model), estimates of the rotations and the corresponding modal predictions of the effects of the 0.2 kg mass with and without the inertia of 0.3 kgm^2 at the tip were computed for a range of fits satisfying the boundary conditions at either the fixed end or the free end. Only the first five modes of the 1-0-1-0- (with error at the tip) and 0-1-0-1-databases (see Chapter 4) were used and in each case, the fit function was used to calculate translational as well as rotational displacements, the former to utilise the smoothing effect of the fit function on the original data. The results are summarised in Tables 5.2a and 5.2b.

For the test in which the moment of inertia was ignored, the differences between the different fits were small and very similar to the predictions based on the raw (unsmoothed) data (albeit with higher magnitudes for 0-1-0-1-data). This is however not surprising since the fits which satisfied the boundary conditions for the cantilever already satisfied the fitting criteria for the translations as was indicated in Chapter 4. Although the maximum errors in the smoothed translations were 0.8% for the root boundary condition and 1.8% for the tip boundary condition, the similarity of the predictions suggests that the predictions were relatively insensitive to the discrepancies in the translations. For the 1% bias error in this data, the benefits from smoothing are thus relatively small.

Significant variations are, however, apparent when the moment of inertia is included and the presence of rotational degrees of freedom is required. While errors of 13% in mode 5 may appear large, these should be contrasted with an error of around 30% which would result if the moment coupling were ignored. It will be recalled from the previous section that an attempt was made to determine the effects of a given level of error in the rotations on the errors in the frequency predictions. It was shown that a 10% error in the tip rotations of all the modes led to a maximum error of about 9% in the prediction of the frequency of the fundamental mode and a maximum error of about 1.5% for the fifth mode. In this case however, it is seen that much smaller error values in the rotations (less than 0.2%) yield errors of about 13 %. This has significant implications about the generality of applying the findings to different database sizes although the structures are the same. In the case of the FE data, a nine-mode database was used while in this case, a five-mode database was employed. Thus, it is not surprising that the results from the nine-mode database are superior although the errors in the rotations at the modification location were higher. This is further evidence that the predictions are less sensitive to the errors in the rotations than to the effects of modal truncation.

It was shown in Chapter 4 that the best fit function for estimating the rotations over the full length of the beam was that for which the root rotation was minimised (see Table 4.2 for 0-1-0-1-data). With regard to the SDM predictions of the mass modification, the expectation was that this fit would yield the best results. However, the results were surprising as they indicated that in fact superior predictions were obtained for the fit for which the second derivative at the free end was minimised. This might have been expected, since the modification site was at the free end. However, while the benefit in the quality of the predictions is relatively small, it will be appreciated that in applications where it is known at the outset that the modification site will be at the free end, the alternative fit criterion could be used with little loss of accuracy.

It may therefore be concluded that for this modification, there is no benefit in searching for a more accurate estimator of the rotations once the approximant for which the second derivative at the tip is minimised is found. This would reduce the time required for searching for the optimum estimator of the rotations.

It will also be noted from Tables 5.2a and 5.2b that the predictions from the two databases are very similar. This observation was however not surprising since the errors in the tip rotations from the two databases had the same signs and were of the same orders of magnitude. It is thus seen that for this modification, the predictions of frequency are not very sensitive to the pattern of the errors in the initial data and also indicates the benefit, albeit small in this case, which derives from smoothing.

(c) Real Experimental Data

A discussion of the accuracy of the SDM predictions based on a real experimental database for a cantilever beam is given in Appendix 3. Although the results are not intended to provide new insights, they provide further confirmation of the observation that the predictions of the mass modification at the tip are not very sensitive to the errors in the rotations. The results indicate that the errors in the predictions are less than 15% even for errors in the rotations which are in excess of 40%.

5.3.2 Bending Stiffness Modification

In this case study, the effect of error in the rotations was studied by adding a bending stiffness of 1 MNm/rad at the free end of the cantilever (see Figure 5.20). The effect of this modification was to increase the frequency of the fundamental mode from 42.1 Hz to 67.9 Hz. The database used was the 61-point, 28-mode database previously described in section 5.3.1.3a for which the rotations were estimated using an interpolating spline.

Figure 5.20 shows the variation of the errors in the predictions of frequency when the predictions based on interpolated rotations are compared with the predictions based on exact rotations. It is apparent that the errors in the predictions are less than 0.4%, the largest errors being for modes 21 to 25. When Figure 5.20 is seen in the light of Figure 5.19 which shows the variation of the errors in the tip rotations, it is immediately clear that for the high frequency modes (i.e., beyond mode 24), the errors in the predictions are seen to fall while the errors in the rotations rise from beyond 5% to 15%. It is thus clear that the predictions are not sensitive to the rising errors in the rotations. This is consistent with earlier observations. However, the relationship between the under-estimation and the over-estimation of the rotations shown in Figure 5.19 and the over-prediction and the under-prediction of the

frequencies seen in Figure 5.20 is not immediately obvious. The upward turn of the error plot in the figure is however consistent with expectation since, for stiffness modifications, an under-estimate of the rotations at the modification location would lead to a corresponding under-prediction of the frequencies.

5.3.3 Rib Stiffener Modifications

The steel cantilever beam used in the mass modification investigations was employed as the base structure in this analysis also. The beam was modelled with 61 equidistant measurement points. Ribs of the same width as the original cantilever but with various depths were added along the full length of the cantilever. Rib depths of 10%, 50% and 100% of the original beam were used to study the effect of the increase in the severity of the modification. The required modification mass and stiffness matrices were obtained from a finite element formulation in which the eccentricity of a stiffener is taken account of by using an offset transformation [80]. The details of the offset transformation are given in Appendix 2. For each modification, predictions were made using exact rotations and rotations calculated from the exact translations using the interpolating approximation on a 28-mode database. Since this modification linked all the rotations on the beam, it was envisaged that the study would provide different insights into the effect of errors in the rotations on the predictions. This modification also had the added advantage that it caused all the frequencies of the original structure to shift by the magnitude of the percentage increase in the depth without changing the resulting mode shapes. It was therefore envisaged that because the mode shapes were unchanged, the predictions should not suffer from truncation effects as the new mode shapes would be adequately represented by the original modal vectors.

Figure 5.21a presents the comparison of the modal prediction of the frequencies based on exact data with the exact solution. Although the results show a rise in the errors in the predictions with increase in the severity of the modification as would be expected, the distinct shape of the error plots was not consistent with expectation. At the very least, some over-prediction was expected as a result of truncation over the entire database. The plots show a distinct change over from over-prediction at low frequency to under-prediction at higher frequency. While the initial over-prediction is consistent with modal truncation effects (this was borne out by the relative modal contribution values which had significant off-diagonal

terms), it is clear that this effect was superseded by a more dominant effect which was responsible for the distinct shape of Figure 5.21a. Attempts to explain the behaviour were explored by performing FE analyses using the offset beam element. The results from these tests, which are discussed in Appendix 2, pointed to the theoretical formulation of the offset element as the probable cause for the distinct shape of the error plots. No further investigations were performed on this aspect but it is obviously an area which requires further attention.

Figure 5.21b presents the error in the modal predictions based on calculated rotations when compared with modal predictions based on exact rotations. The plots show increasing under-estimation of the frequencies from the expanded database with rise in the mode number. When this is viewed in the light of the errors in the rotations, the averages of the moduli of which are plotted in Figure 5.21c, it is seen that for the rib modification, under-estimation of the rotations leads to under-prediction of the frequencies. This observation is consistent with expectation since rib stiffener modifications are primarily governed by the stiffness matrix such that an under-estimation of the rotations will result in lower values of the stiffness matrix elements (when the eigen problem is transferred into modal space) thereby leading to a corresponding under-prediction of the modified frequency values. This finding has also been reported in published work involving rib-stiffener modifications [25,29].

Further examination of Figures 4.21b and 4.21c shows that the predictions of frequency are relatively more sensitive to the errors in the rotations than was the case for the lumped-mass and bending stiffness modifications which depended only on one rotation value (i.e., the value at the modification location). While a 14% error in the rotation yielded a 4% error in the frequency prediction for a lumped mass modification, an average error of 2.3% in the rotations yielded a 1.5% error in the frequency prediction for the rib modification. This is however not surprising since the error in the prediction is dependent on the estimates of rotations at every point on the beam.

Finally, it may be remarked that the predictions of frequencies do not seem to be very sensitive to the severity of modification. This is indicated by the relatively small increase in the maximum error from 0.6% to 1.5% when the depth of the added stiffener is increased

from 10% to 100% of the depth of the original beam. This is again not surprising since it is indicative of the fact that the modeshapes of the modified structure are not different from those of the base structure even with increased modification severity.

5.4 Modifications on Plate Structures

5.4.1 Free-Free Plate

For this test, a free-free mild steel plate, 152 x 300 x 5.5 mm was used. The plate was modelled using 16 thin plate finite elements on a 5 x 5 grid of measurement points. Modal data for the first 20 modes was obtained from an FE analysis of the structure. Rotations were also obtained from surface fitting using the interpolant. It should however be noted that the fitting results indicated that the spatial description of the structure did not allow for accurate representation of the last five modes in the database. This accounted for the significantly higher errors in the rotations for these modes, as shown in Table 5.3a.

5.4.1.1 Lumped Mass Modification

A mass of 0.2 kg with a moment of inertia of 0.3 kgm^2 about an axis parallel to the long side of the plate was added to one corner as shown in Figure 5.22. To give an idea of the effect of the large inertia applied, adding a mass of 0.2 kg with zero inertia reduces the fundamental elastic frequency from 328 Hz to 272 Hz, but with the inertia included, the value is 106 Hz, albeit with change in the resulting mode shape.

Table 5.3a gives the errors in the DMSM predictions with and without the mass using data sets based on calculated rotations when compared with modal predictions based on FE rotations (column (2) in the table). This excludes truncation effects in the comparisons. The errors in the modal prediction using FE rotations when compared with the FE solution are also included (column (1) in the table). The table also gives the error in the calculated in-plane rotation at the modification location. Since the interpolant was used to estimate the rotations, the discrepancies in the translations were insignificant and therefore did not affect the predictions. The errors in the calculated rotations range from less than 1%, for the rigid body modes, to about 130% for the tenth elastic mode. This large error was a result of a difference in the sign of the computed rotation from that of the FE value. It is however interesting to note that the error in the frequency prediction for this mode is only about 7%

and is the maximum over the entire set of predicted frequencies. While the comparison of the modal predictions based on FE rotations with the FE predictions (column (1)) indicates that the frequencies were over-predicted, it is clear from column (2) that the predictions based on interpolated rotations were, except for the first elastic mode, all under-estimated. It will also be seen that the errors in the predictions based on interpolated rotations were generally less than 1% except for modes 9, 10, 13, 16, 17 and 18.

An examination of the modeshapes following modification indicated that, as would be expected, the modes which exhibited the highest prediction errors when compared with FE predictions were the ones for which there was significant rotation at the attachment point about the axis parallel to the long side of the plate (modes 7, 9, 12, 14, 16 and 18, column (1) in Table 5.3a). These modes also exhibited large shifts in frequency after modification. The results in column (2) also confirm that of the modes with the relatively large errors in the rotations (modes 7, 9, 10, 13, 15, 16, 17, 18, 19, and 20), it was those modes with significant rotation about the axis parallel to the long side of the plate (modes 9, 16, and 18) at the attachment point which had the largest errors in the predictions (above 3%). Thus, it is seen that the other modes, particularly the high frequency modes (upwards of mode 15), were relatively insensitive to the errors in the rotations.

The lack of sensitivity of the predictions of frequency to the errors in the rotations is further highlighted by comparing the results in Table 5.3a (column (1)) with the predictions based on a relatively smoother approximation of the rotations (only one knot in each direction in the plane of the plate) (see Chapter 4), shown in Table 5.3b. It will be seen that although the errors in the computed rotations are higher than those given in Table 5.3a from interpolation, the errors in the predictions exhibit the same orders of magnitude. In addition, the errors in the predictions based on calculated translations and rotations in Table 5.3b are broadly similar to those seen for the predictions based on computed rotations only. This is indicated by the relative superiority of the predictions based on smoothed data (translations and rotation) to those based on calculated rotations only (compare (3) with (2)). It will also be noted that the under-prediction seen in Table 5.3a is also present in Table 5.3b. Comparison of the results in the two tables thus suggests that, for this modification, a relatively loose approximation yields rotations which are sufficiently adequate to produce comparable modification

predictions with those from a database expanded by interpolation. This is in agreement with the results obtained from the analysis on the cantilever beam using simulated experimental data in which a 'ball park' approximation (within 20% of the correct value) was seen to yield errors in the modification predictions which were under 10% . This is however not surprising since for the number of measurement points used in this case, the approximation using one internal knot in each direction actually had the same number of knots as the interpolating approximation would have except that the value of the smoothing factor was higher.

5.4.2 Cantilever Plate

A mild steel cantilever plate, 500 x 150 x 5 mm was modelled using 140 thin-plate elements on a 36 x 5 grid of measurement points as shown in Figure 4.27. Translations and rotations were obtained from an FE analysis of the structure. Rotations were also obtained from surface fitting using the interpolating approximation.

5.4.2.1 Lumped Mass Modification

A mass of 0.2 kg with a moment of inertia of 0.3 kgm^2 about an axis parallel to the long side of the plate was added to a free corner of the plate (see Figure 5.22). The mass without any inertia effects dropped the fundamental frequency of the plate from 18.7 Hz to 16.8 Hz. Addition of the inertia further dropped the fundamental frequency to 6.96 Hz without any change in the modeshape.

Table 5.4a summarises the results of the prediction for the case where the rotational inertia is not included. Comparison of the modal prediction with the FE prediction showed some very small discrepancies, the majority of which were less than 1% in magnitude. This was not unexpected as the modification was largely dependent on the translations at the modification site since no inertial effects were included. It should be understood that the effects of truncation, albeit small, are also present in this comparisons. However, this is not the main object of the study. The focal point is the inclusion of the inertial effects which paints a very different picture as shown in Table 5.4b. Here, even the modal prediction based on FE rotations predicted only 13 of the 20 modes predicted by the FE computation. While the frequencies of some of the rest of the modes were close to those predicted by the FE analysis, the mode shapes were significantly different. This was an indication that the

predictions had suffered from serious truncation effects and therefore that the DMSM computation was unable to form the new mode shapes from linear combinations of the original mode shapes. While the added mass was less than 10% of that of the plate itself, it was clear that the added inertial moment was sufficiently high to cause significant modal truncation. This was demonstrated by the Modal Assurance Criterion (MAC) comparison of the modal vectors of the unmodified structure with those of the modified structure. The severity of the modification was illustrated by the significant departure from unity of the values on the leading diagonal (only modes 1 and 3 had MAC values of 0.99 and 0.85 at the leading diagonal) which, in turn, suggested significant changes in the mode shapes. This was also buttressed by the observation that only 4 off-diagonal terms suggested any correlation between the modified and the unmodified modeshapes. These correlations had MAC values above 0.90 and occurred as follows: old mode 1 correlated with new mode 2 (MAC=0.99), old mode 6 correlated with new mode 7 (MAC =1.00), old mode 10 correlated with new mode 11 (MAC =0.97) and old mode 17 correlated with new mode 19 (MAC=0.94). It was therefore not surprising that the predictions were so seriously affected by the effects of truncation. Thus, it appears that the modification was so severe that the dynamic characteristics of the original structure had been significantly changed. The resulting failure to predict all the new modes was therefore not surprising [78].

The errors in the modal predictions of frequency based on the expanded database when compared with modal predictions based on FE rotations are summarised in Table 5.4b. The errors in the estimated rotations at the modification location are also given (column (1)). It will be seen that the errors in the frequencies of the modes which were successfully predicted are acceptably low (ranging from -5.98% to 2.28%). When these are viewed in the light of the errors in the rotations which are in excess of 100% for some modes, it is seen that the predictions are not sensitive to the errors in the rotations. It will also be noted that although the rotations at the modification location were, in the main, under-estimated (except for 3 modes), the frequencies were not correspondingly over-predicted. Five of the frequencies were under-predicted while the rest were over-predicted. This behaviour is consistent with that observed for the case of the mass at the free end of the cantilever in part (a) of section 5.3.1.3. That is, the relative mix of under-estimation and over-estimation of the rotations leads to a particular mix in the over-prediction and under-prediction of the frequencies. In

this case, the over-prediction of the majority of the frequencies is consistent with the under-estimation of the majority of the rotations at the modification location.

5.4.3 Simply Supported Plate

A mild steel plate of dimensions 600 x 400 x 5 mm was used as the third case study in this series. The plate was modelled using a 5 x 5 grid of measurement points thereby producing 16 four-noded plate elements (Figure 5.23). The plate was simply supported at the corners. Modal data was obtained from FE analysis. Rotations were also computed as previously described using the interpolating approximation.

5.4.3.1 Lumped Mass Modification

A mass of 0.2 kg with a mass moment of inertia of 0.3 kgm^2 about an axis parallel to the short side of the plate (i.e., about the y-axis) was added at the centre of the simply supported plate. The effect of this modification was to drop the fundamental frequency from 31.4 Hz to 25.2 Hz. It will be understood that this modification had different effects on different modes. For one mode, the modification had no effect at all (i.e., there was neither translation nor rotation at the centre) while for others the mass had rotation only. For the remainder, the mass had both rotation and out-of plane translation. An examination of the mode shapes, the plots of which are given in Figure 5.24, confirmed this and in fact indicated that this modification merely introduced a new fundamental mode while the frequencies and mode shapes of the original modes remained virtually unaffected. That is, for example, the frequency and mode shape of the new mode 2 were very similar to those of the old mode 1 and so on.

The results for this modification are summarised in Table 5.5a. The last column in the table shows the errors in the modal prediction using estimates of rotations from the interpolating spline when compared with the modal prediction based on FE rotations. It must also be understood that since an interpolating approximation was used, there were no discrepancies between the calculated and FE translations and thus the translations had no effect on the errors in the predictions.

It will be seen from the results that the predictions for modes 1, 3, 4, 6 and 9 were error-free whereas the predictions for the rest had appreciable errors, particularly modes 2 and 5. The error-free predictions were not surprising since there was little or no rotation about an axis parallel to the short side of the plate (i.e., the y-axis) at the modification location for these modes. This has to be seen in the light of the observation that there was a correlation between the new modes and the original modes as indicated above. It is thus interesting to note that although the original mode 3 had an error of around 7% in the rotation at the modification location, the prediction for mode 4, which correlated with it, was not sensitive to this error (0% error in the prediction).

The high errors in the predictions of modes 2 and 5 were attributed to the observation that these modes also had the largest shifts in frequency (59% and 36% respectively) as a result of the modification. It is however interesting to observe that there were no errors in the rotations at the modification location in the original modes with which they correlated (modes 1 and 4). Thus it is seen that these relatively large errors in the predictions were not due to the errors in the rotations but due to the absence of key descriptor modes required to form the new modes.

The 3% error seen in the prediction of mode 7 was attributed to the 39% error in the rotation at the modification location for the original mode 6 with which it correlated. While there was no error in the rotation at the modification location in the original mode 7, there was a 4.5% error in the frequency prediction of the new mode 8 with which it correlated. This mode also had the third largest shift in frequency (around 30%) as a result of the modification. Thus, the error in the prediction for this mode was not due to the error in the rotation but due to truncation effects.

5.4.3.2 Rib Stiffener Modification

If a central rib stiffener was to be placed across the plate, as shown in Figure 5.23, the connection could be idealised in one of two ways; namely by a substructuring approach or by the dual modal space procedure. This case was chosen in part to allow comparisons to be made between the two. Although the substructuring approach [70] gives good results when compared with the FE prediction, as shown in Table 5.5b (column (2)), it requires

separate modal data for both structures. If this is not readily available, it would be more convenient to link the shared translations and rotations using the dual modal space method. The required mass and stiffness matrices for the rib were, as before, obtained from the offset finite element formulation (see Appendix 2). While the DMSM results using FE rotations (column (1) in Table 5.5b) show good agreement with the substructuring results, the dual modal space method has the added advantage of being quicker and cheaper [12]. Examination of the mode shapes of the modified structure, which are shown in Figure 5.25, revealed that, except for mode 9, the new modes were similar to the original modes. Thus, it was not surprising that the largest error in the predictions was obtained for mode 9.

The last column in Table 5.5b summarises the comparison of the modal predictions based on rotations from an interpolating spline with the modal predictions based on FE rotations. It will be noted that the frequency predictions for modes 3, 4, 6 and 7 have little or no error. When these are viewed in the light of the errors in the rotations at the points of attachment (Table 5.5c), it is clear that these errors are a result of the very low error values in the rotations for these modes. It is also interesting to note that although the longitudinal axis of the stiffener had significant flexing for modes 4 and 7, this had little effect on the frequency predictions since the errors in the rotations about the x-axis were very small.

The relatively higher error values in the frequency predictions for modes 1, 2 and 8 (i.e., 0.3%, 0.1% and 0.4%) can be related to the relatively higher errors in the rotations at the attachment points for these modes which were 15.8%, 7.5% and 39% respectively. However, for the fundamental mode, the longitudinal axis of the stiffener does not flex.

The errors in the frequency predictions for modes 5 and 9 (which are the largest) are not due to the errors in the rotations since these were zero (Table 5.5c). However, the stiffener axis under-goes significant flexing for mode 9 (Figure 5.25) while this is not the case for mode 5. Thus the frequency predictions for these modes seem to suffer from truncation effects as highlighted by the comparison of the modal prediction based on FE rotations with the FE prediction of the modification.

It will finally be noted from Table 5.5b that the overall errors in the predictions were small (with a maximum value of 0.6%). This was not unexpected since the frequency shifts produced by this modification were not large (only up to 3%). Nevertheless, the predictions are seen to be relatively insensitive to the magnitudes of the errors in the rotations. However, the under-prediction of the frequencies is consistent with the under-estimation of the rotations about the x-axis as was observed in the case of the rib stiffener modification on the beam.

A comparison of the errors in the modal predictions (using the interpolated rotations when compared with FE predictions) against the results reported by Green and Williams [30] for the same modification indicated that the results from the present work were superior by an average of about 30%.

The accuracy of prediction for a more severe modification was investigated using a central rib stiffener with doubled cross-sectional dimensions (20 x 20 mm). The results are summarised in Table 5.5d. The last column presents the comparison between modal predictions based on calculated and Fe rotations. It should be understood that this modification produced larger frequency shifts than the previous case, the largest being for mode 7 (26%) and the smallest being for modes 3 and 8 (1% and 0.6%) respectively, with the rest averaging at around 9-11%.

In this case, modes 2, 4, 7 and 8 had significant rotation at the points of attachment about the x-axis, while modes 1, 3, 4, 5 and 6 had significant rotation at the points of attachment about the y-axis. The magnitude of the errors in the predictions of frequency for modes 1, 2, 4, 7, and 8 are not surprising since these modes also had significant errors in the rotations about the x-axis at the points of attachment. The 3.7% error in the prediction for mode 7, which was also the maximum, was not particularly surprising since this mode had the largest shift in frequency as a result of the modification. The very low error in the prediction for mode 3 was also not unexpected since, for this mode, there were no errors in the rotations about the x-axis at the points of attachment and the frequency shift as a result of the modification was very small. The errors in the predictions for modes 5 and 6 were attributed to the shifts of frequency which were 9 and 11%. In addition, while the mode shapes for modes 1 to 4 were similar to those seen for the less severe modification above, the shapes for modes 5 to

8 were different from those seen earlier. This explains the error levels in the predictions for modes 5 and 6.

Finally, it will be noted that although the rotations at the points of attachment were, in the main, under-estimated, half of the frequencies were over-predicted while the other half were under-predicted. Thus, it is seen that, in this case, the expected relationship between over-estimation or under-estimation of the rotations with over-prediction or under-prediction of the frequencies is not apparent. What is clear however is that the modes for which the frequencies were over-predicted (modes 3, 4, 5 and 6) were those for which the errors in the rotations were zero or nearly so.

5.4.4 L-Beam Plate Structure

Modifications on plate structures which have been presented so far are based on error-free databases. However, the technique for estimating rotations which is proposed in Chapter 3 and investigated in Chapter 4 is intended for use on real experimental databases. The data which was available for use in this case was not consistent with the findings on optimising the performance of the approximating technique as presented in Chapter 4. For this reason, the accuracy of the SDM predictions based on this experimental database is discussed in Appendix 3. The appendix provides further confirmation for the observation that, for a mass modification, the predictions are relatively insensitive to the errors in the estimates of the rotations at the modification location. The data also highlights the fact that the exclusion of rotational degrees of freedom results in very large errors in SDM predictions. In addition, the results illustrate the benefit which derives from smoothing the original data for SDM applications.

5.5 Effect of Seeding on the Accuracy of the Mode Shapes

One of the important considerations in a study such as this one is the determination of the magnitude of the effect of a given level of error on the overall accuracy of the modeshape vectors and hence on the predictions following a modification. While several techniques are available for quantifying the comparison between mode shapes from different sources, the Modal Assurance Criterion (MAC) is perhaps the most widely used.

In order to determine the effect of the addition of error to one degree of freedom in the modeshape vector in the original database on the modeshape vectors in the seeded database, the MAC comparison of the databases with 1%, 5%, 10%, 20%, 50% and 100% error in the tip rotation of the first mode of the cantilever against the error-free database was performed. This was compared with the results of the auto-mac analysis on error-free data and the results are presented in Table 5.6. While there was no change in the leading diagonal terms of the MAC matrix up to the 50% error level, the off-diagonal terms showed some appreciable discrepancy even for the case with the 1% error level. Departure from unity for the leading diagonal terms was observed for the 50% error level (down to 0.97) and the 100% error level (down to 0.91). When this is viewed in the light of the errors in the predictions of frequency based on the seeded databases, it is apparent that the MAC is not a good indicator upon which to gauge the effect of a given level of error in the rotations on the predictions of frequency. For instance, while Figures 5.4 and 5.9 indicate appreciable error in the predictions of frequency for a 10% error level in the tip rotation of the first and ninth mode, the comparison of the MAC values for the comparison of error-free and seeded (10% error in tip rotation) databases with the auto-mac computation on error-free data indicated no change in the leading diagonal term, 2.6% change in the off-diagonal term for the second mode, and discrepancies from 9% to 20% in the off-diagonal terms for modes 3 to 9. It is therefore apparent that while the errors in the predictions of frequency are greater for the mode with the noise in the tip rotation and the mode adjacent to it (modes 1 and 2 respectively), the MAC computation, on the other hand indicates that the corresponding MAC values for these modes are least sensitive to the noise in the tip rotation of the first mode. This feature was also observed for higher levels of seeding albeit with higher magnitudes of discrepancy. This was attributed to the fact that the MAC computation is an integrating type of computation and thus the effect of an error in a single mode would be insignificant in a large database. It may therefore be concluded that the MAC comparison is not a satisfactory indicator of the level of error in modeshape vectors for purposes of predicting the effect of such errors on the prediction of structural changes.

5.6 Closing Discussion

The efficiency and, thus, the success of a method of estimating rotations from translational data is measured by the success in using the expanded data in structural dynamics

modification work and the comparison of the results with those from existing techniques. In this regard however, it will be recalled from Chapter 2 that the majority of references cited are silent on the performance of the techniques in SDM work. Of those in which the matter is addressed [25,26,29,30], it was found that the errors in the prediction of structural changes were generally less than 10% for error levels in the rotations of up to 100%. However, with the exception of references [25] and [30], the rest did not provide a complete description of the structural and/or database details to enable direct comparisons to be made. Nevertheless, the analyses reported in this chapter have shown that the errors in the dual modal space method predictions have generally been of a similar order of magnitude. While this is a very welcome observation, it is however not surprising given that the errors in the prediction of structural changes are less sensitive to errors in the estimates of rotations than to the effects of modal truncation.

The work reported here has also provided valuable insights into the effects of errors in the rotations on the resulting predictions of structural changes. However, the work has also highlighted the limitations which present theoretical knowledge has in explaining the actual magnitudes and the manner (under-prediction or over-prediction) of the predictions which result from a given error mix in the modal vector components.

5.7 General Concluding Remarks

From the analyses reported in this chapter, it may therefore be concluded that:

1. the presence of error in a rotation vector component of a mode shape has an effect on the predictions following a modification. This 'contamination' effect of the mode with the error is, on the other hand, accompanied by a 'dilution' effect on the predictions from the error-free modes in the database (Figures 5.4 and 5.12).
2. errors in the rotation estimates do not necessarily translate to the same levels of magnitude in the predictions following modifications. The magnitude of the error in the predictions is, in the main, much lower than the magnitude of the error in the rotations (i.e., a 10% error in the rotation gives up to about 6% error in the predictions).

3. for a lumped mass modification on a cantilever beam, there exists a quantitative but unquantifiable relationship between the error in the rotation at the modification location and the error in the prediction of frequency (Figure 5.7).
4. for mass modifications, an under-estimation of the rotations has a 'stiffening' effect on the modified structure which leads to over-prediction of the frequencies. On the other hand, an over-estimation of the rotations leads to under-prediction of the frequencies (Figures 5.4 and 5.9).
5. for mass modifications, when errors are present in all the rotations at the modification location, predictions for the low frequency modes are more sensitive to errors in the rotations than are predictions for the higher frequency modes (Figure 5.15).
6. for rib stiffener modifications, an under-estimation of the rotations leads to corresponding under-prediction of the frequencies (Figure 5.21b, Tables 5.5b and 5.5c).
7. generally, the errors in the frequency predictions from the dual modal space method are less sensitive to errors in the calculated rotations than to the effects of modal truncation consequent upon the imposition of severe modifications.
8. a 'ball park' estimation of the rotations (within 20% of the correct value) is sufficiently accurate to yield predictions which have an error of less than 10% error following a modification (Table 5.2).
9. the Modal Assurance Criterion comparison is not a satisfactory indicator of the level of error in modeshape vectors for purposes of predicting the effect of such errors on the predictions of structural changes.
10. the proposed technique for expanding modal data to include the unmeasured freedoms provides data which enables predictions of structural dynamics modifications to within 5% of the correct value.

o0o

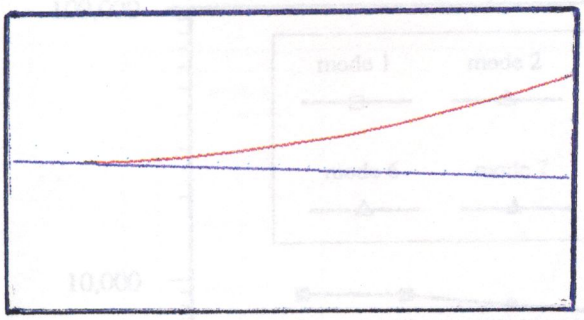

Mode 1, 3.96 Hz

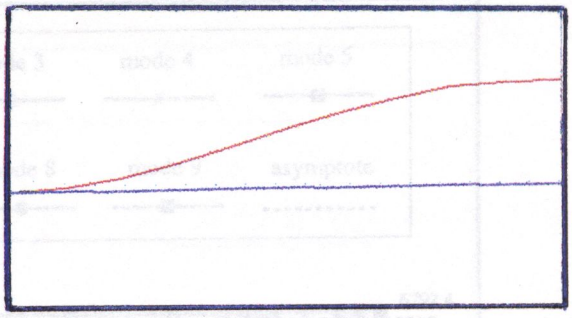

mode 2, 59.63 Hz

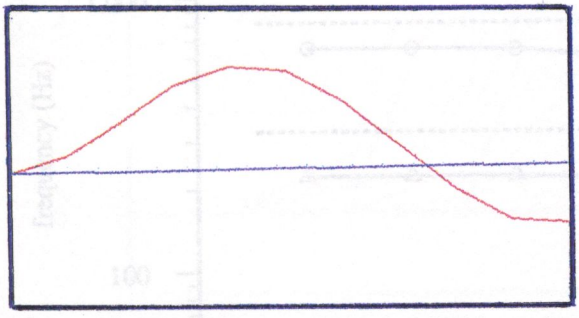

mode 3, 352.17 Hz

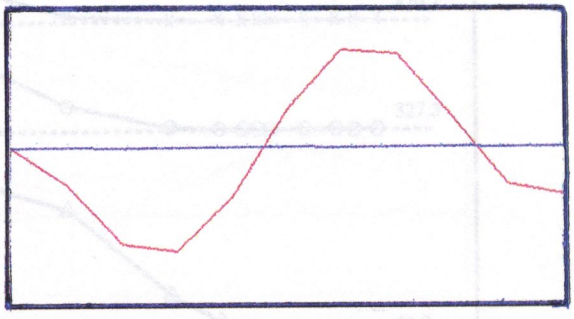

mode 4, 891.69 Hz

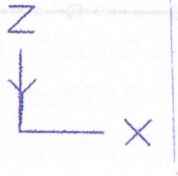

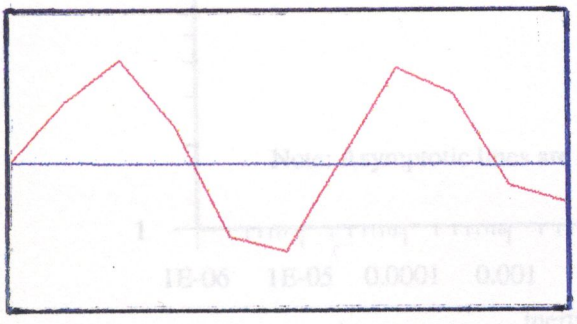

mode 5, 1693 Hz

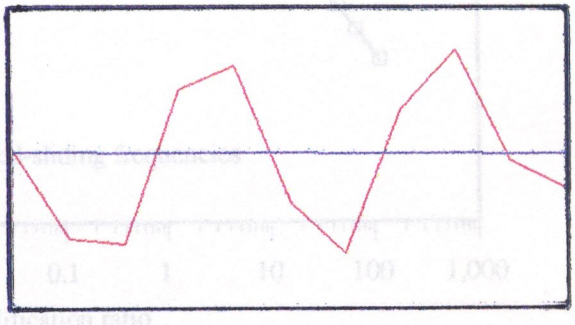

mode 6, 2763 Hz

Figure 5.2: **Predicted Modeshape Plots for the Steel Cantilever with a Tip Mass (m=0.2 kg, IMR=114.5)**

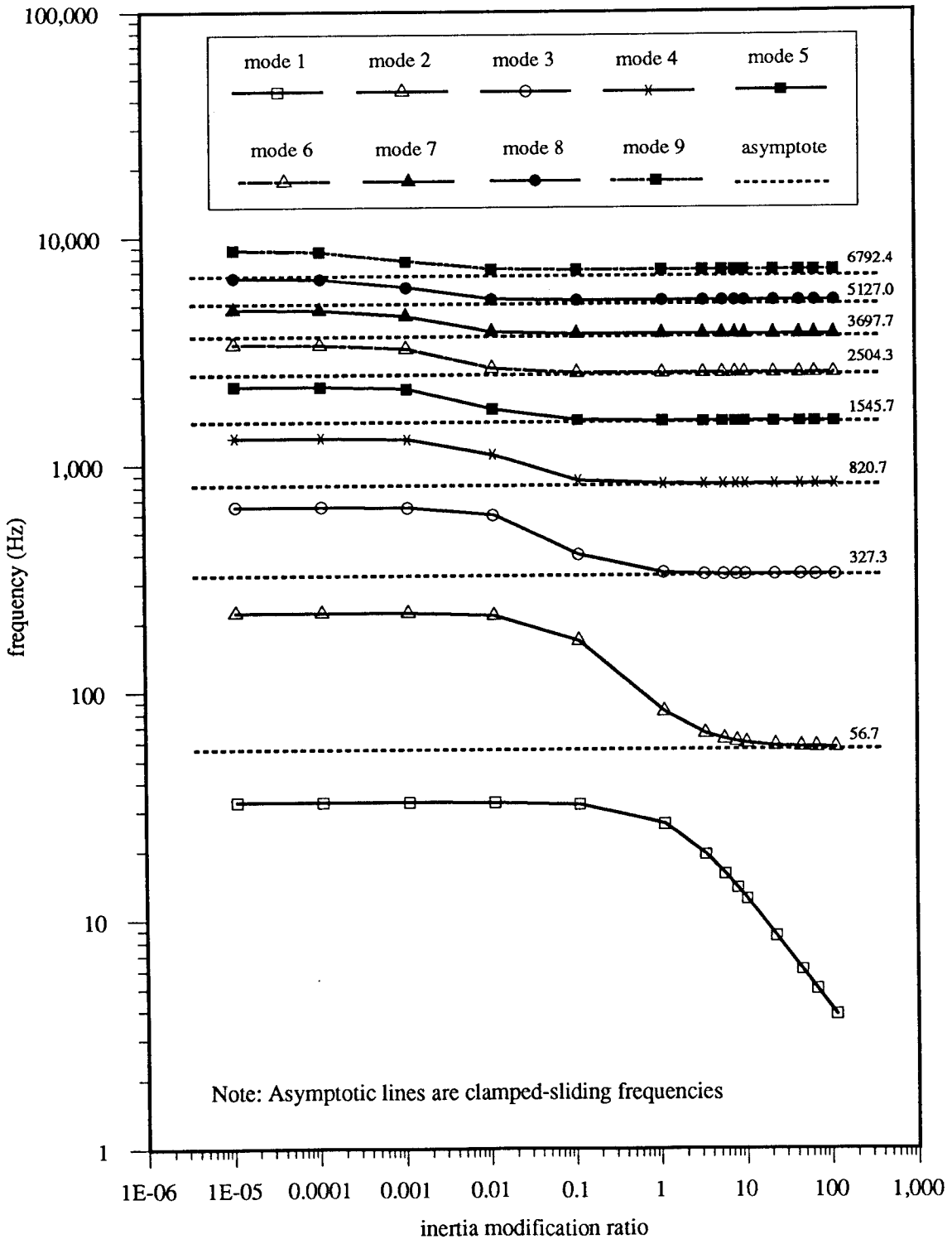

Figure 5.1: Behaviour of the Predicted Frequencies with increase in the IMR for the Steel Cantilever with a Tip Mass (mass = 0.2 kg)

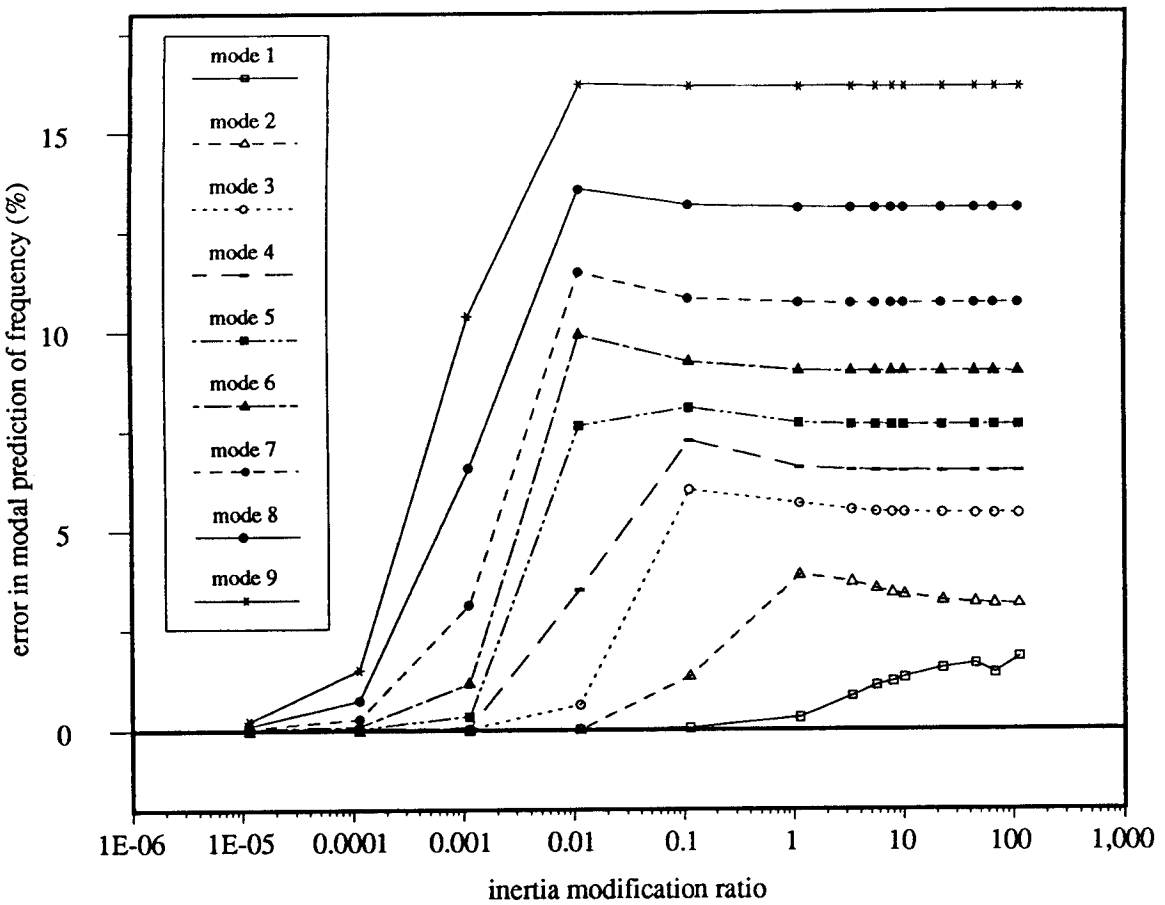

Figure 5.3: Comparison of the Modal Prediction with the FE Prediction of Frequencies for the Steel Cantilever with a Tip Mass (mass = 0.2 kg)

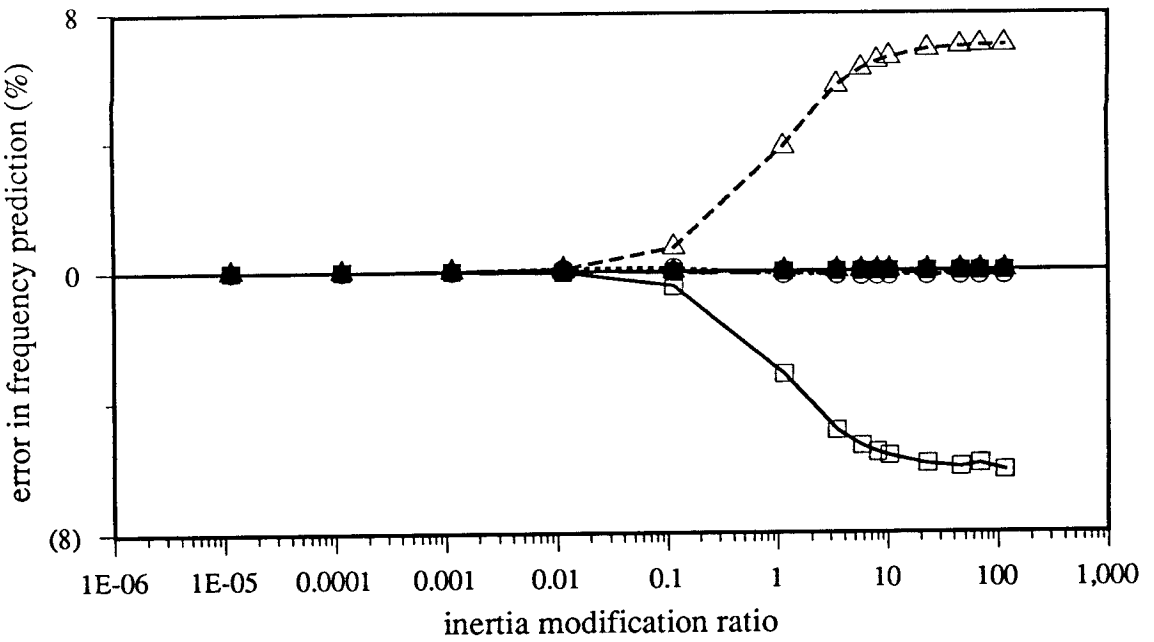

Figure 5.4a: Effect of a +10% error in the Tip Rotation for mode 1 on the Frequency Prediction of a Tip Mass Modification on the Steel cantilever (mass = 0.2 kg)

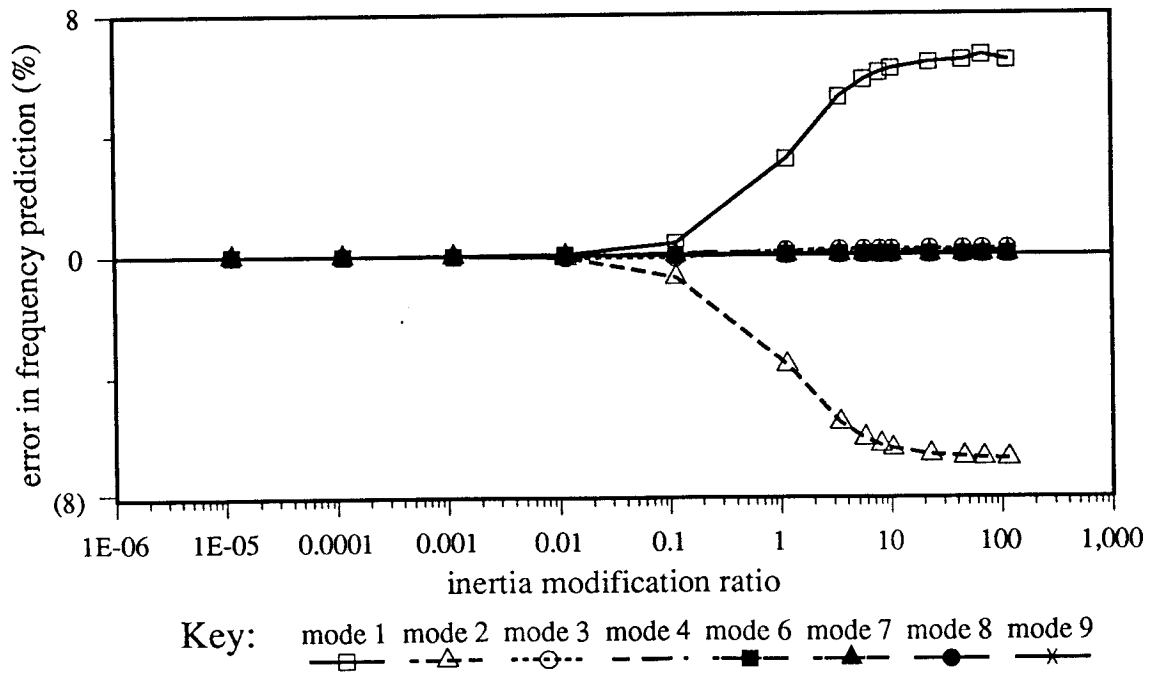

Figure 5.4b: Effect of a -10% error in the Tip Rotation for mode 1 on the Frequency Prediction of a Tip Mass Modification on the Steel cantilever (mass = 0.2 kg)

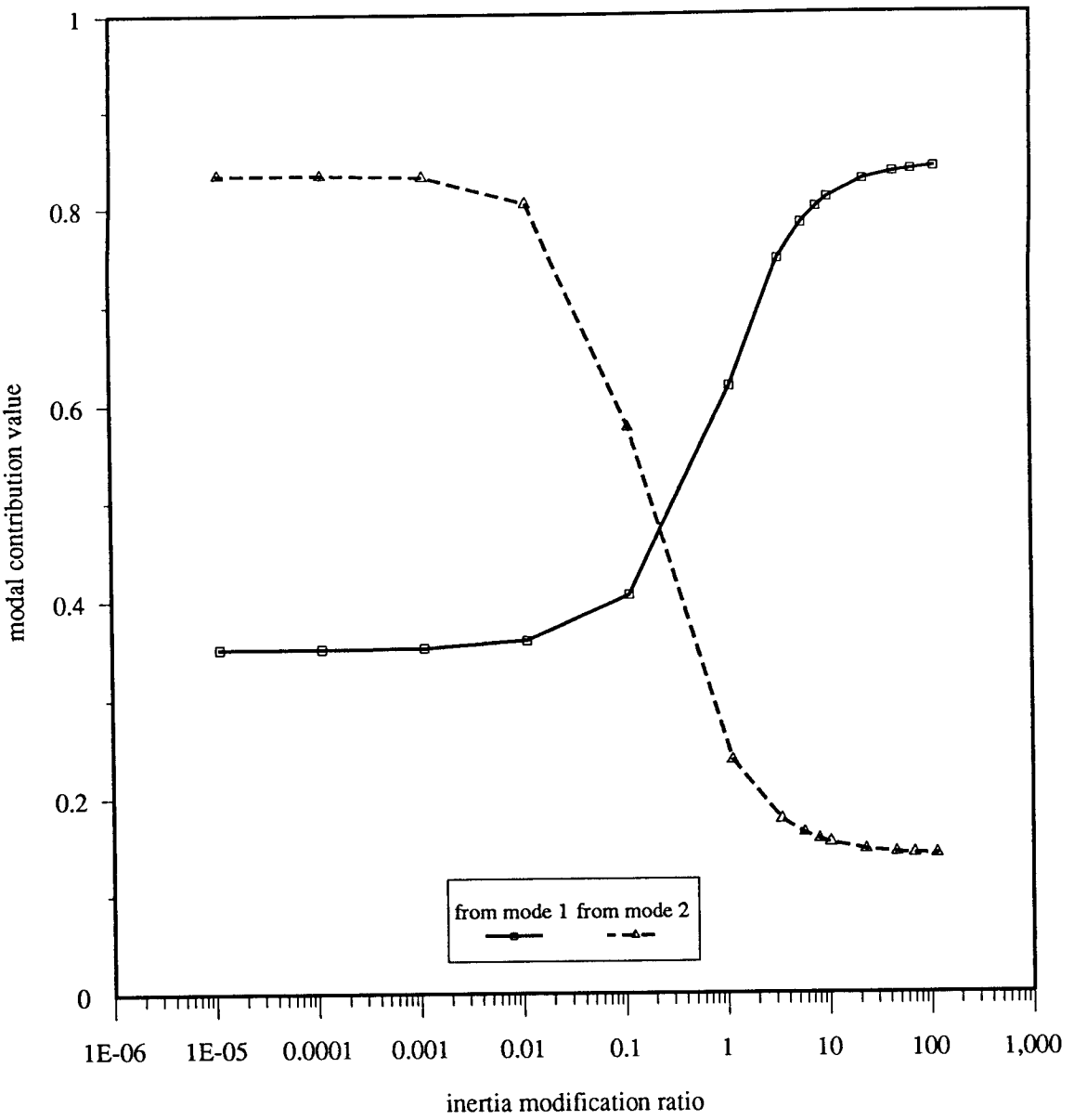

Figure 5.5: Modal Contributions to mode 2 for the case of the 10% error in the tip rotation of the first mode. Steel Cantilever with a tip mass (mass=0.2 kg)

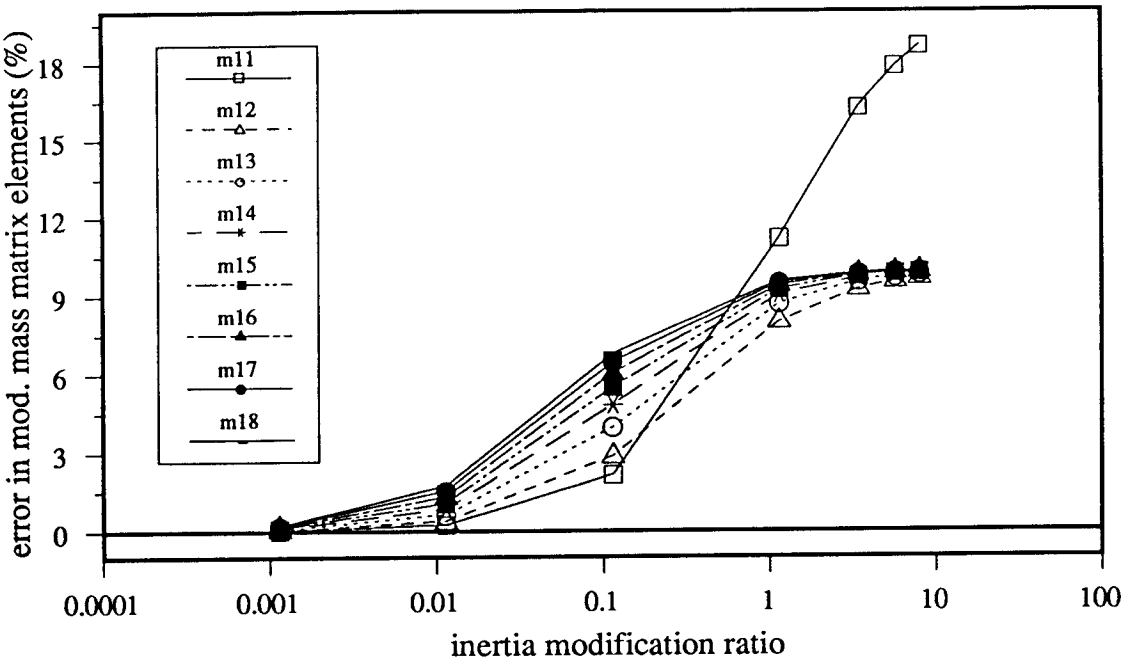

(a) -10% error in the tip rotation for mode 1

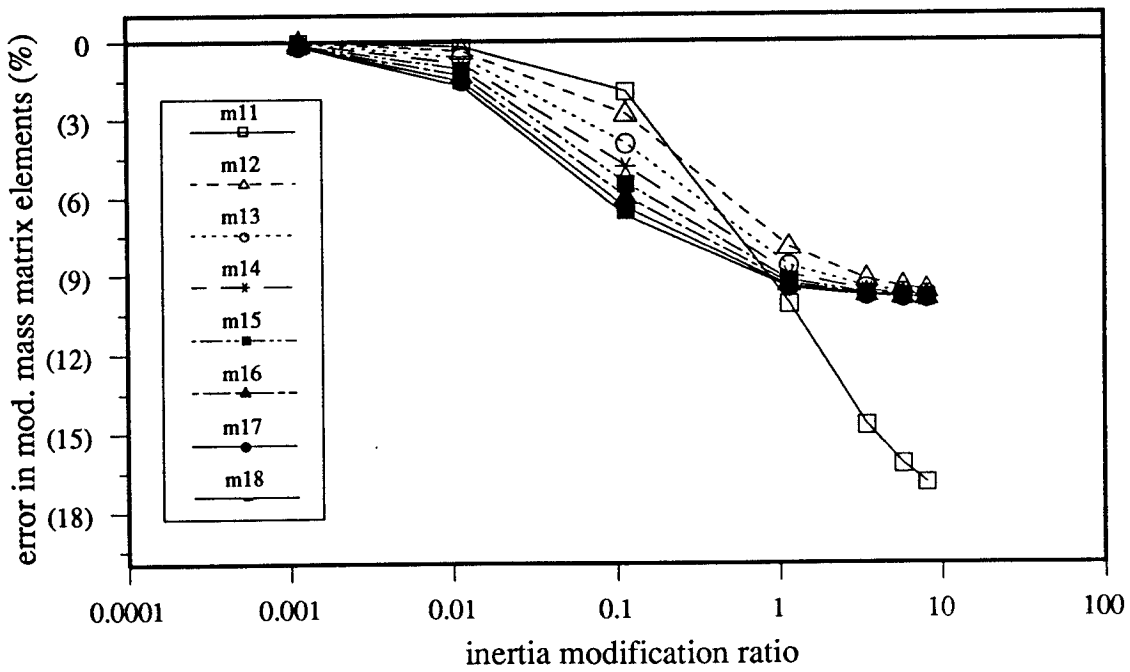

(b) +10% error in the tip rotation for mode 1

Figure 5.6: **Variation of the Errors in the elements of the Modification Mass Matrix for the Steel Cantilever with a Tip Mass (m=0.2 kg)**

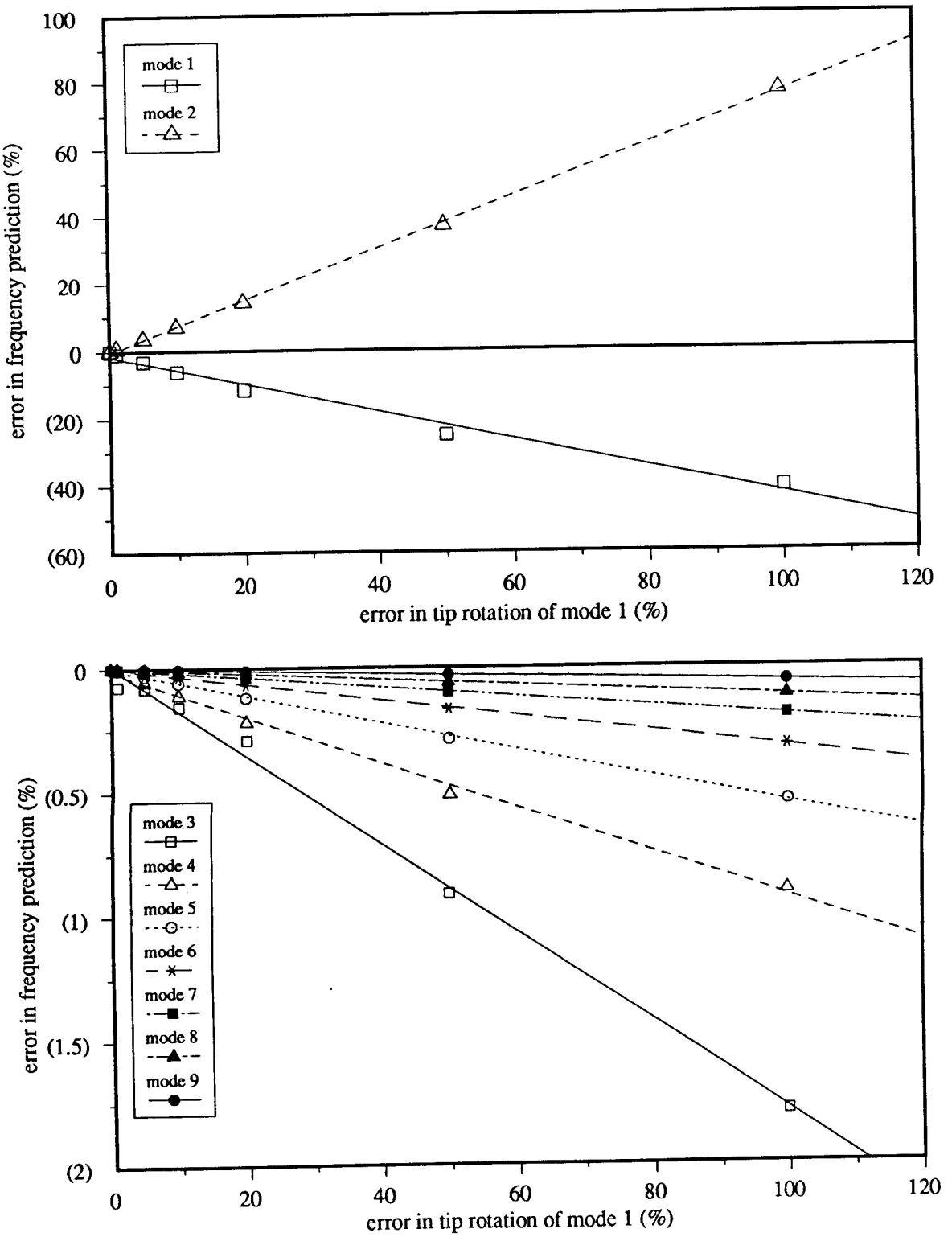

Figure 5.7: Relationship between the magnitude of the error in the tip rotation for mode 1 and the magnitude of the error in the modal frequency prediction for the Steel Cantilever with a Tip Mass (m=0.2 kg, IMR=114.5)

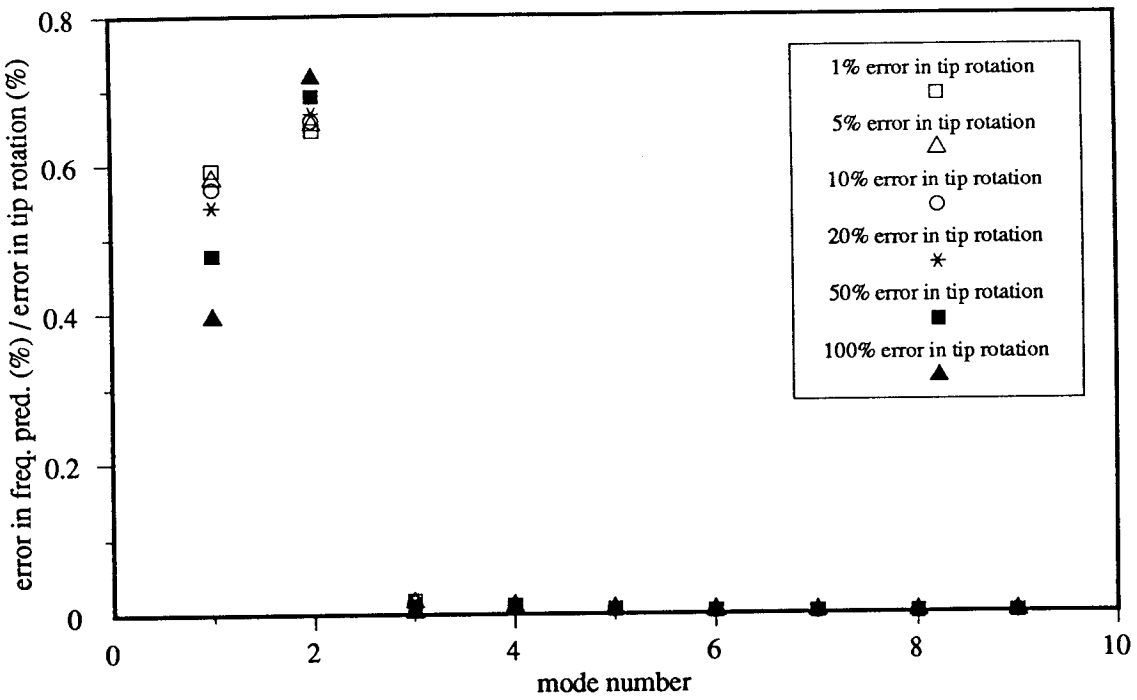

(a) m=0.2 kg, IMR=10.3

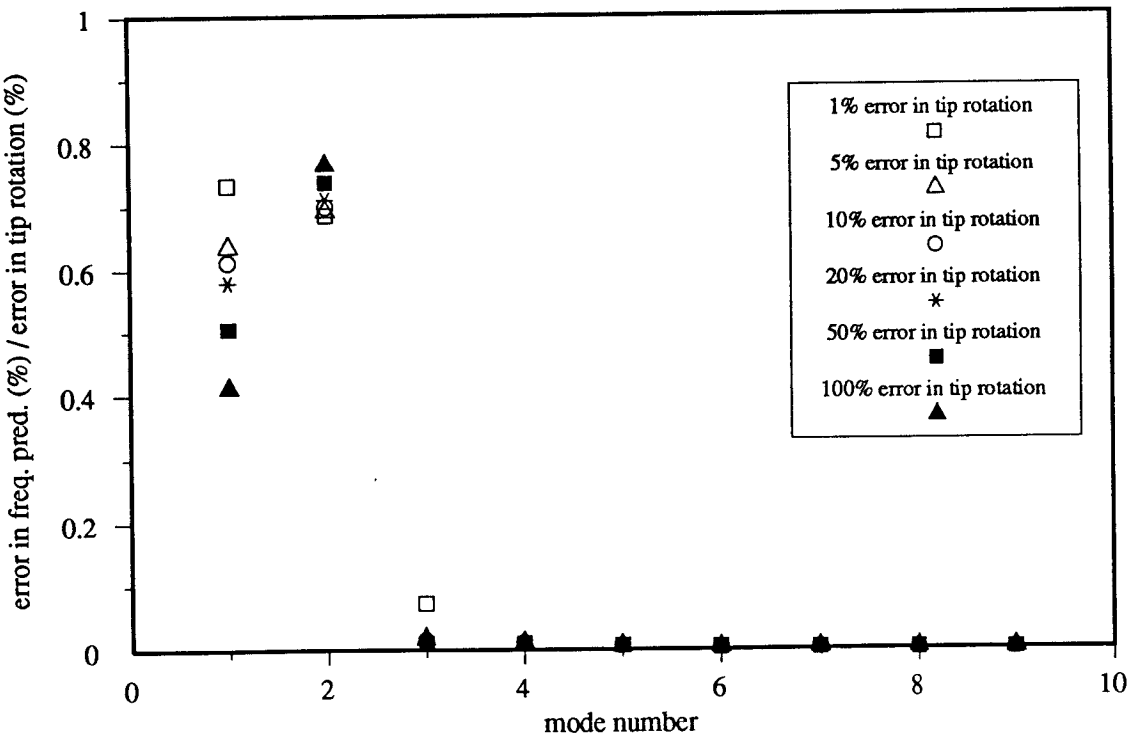

(b) m=0.2 kg, IMR=114.5

Figure 5.8: 'Contamination' and 'Dilution' effects on the Frequency Predictions for the Steel Cantilever with a Tip Mass for Various Levels of Error in the Tip Rotation of the First Mode

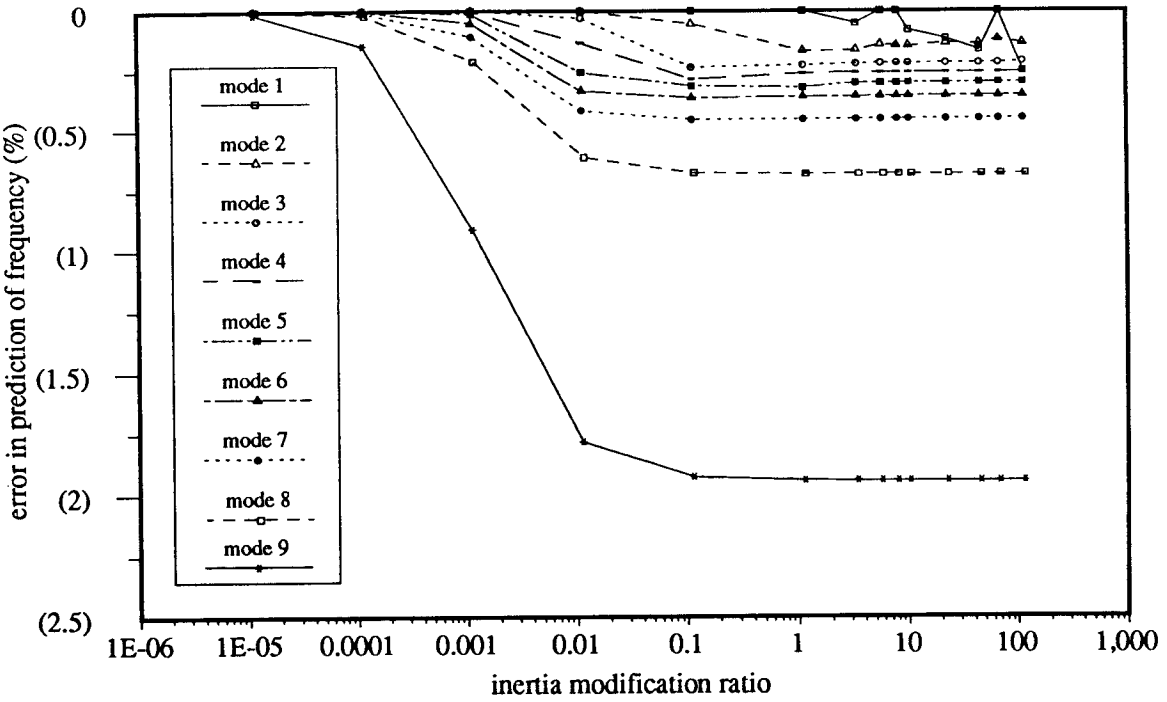

(a) +10% error in the tip rotation for mode 9

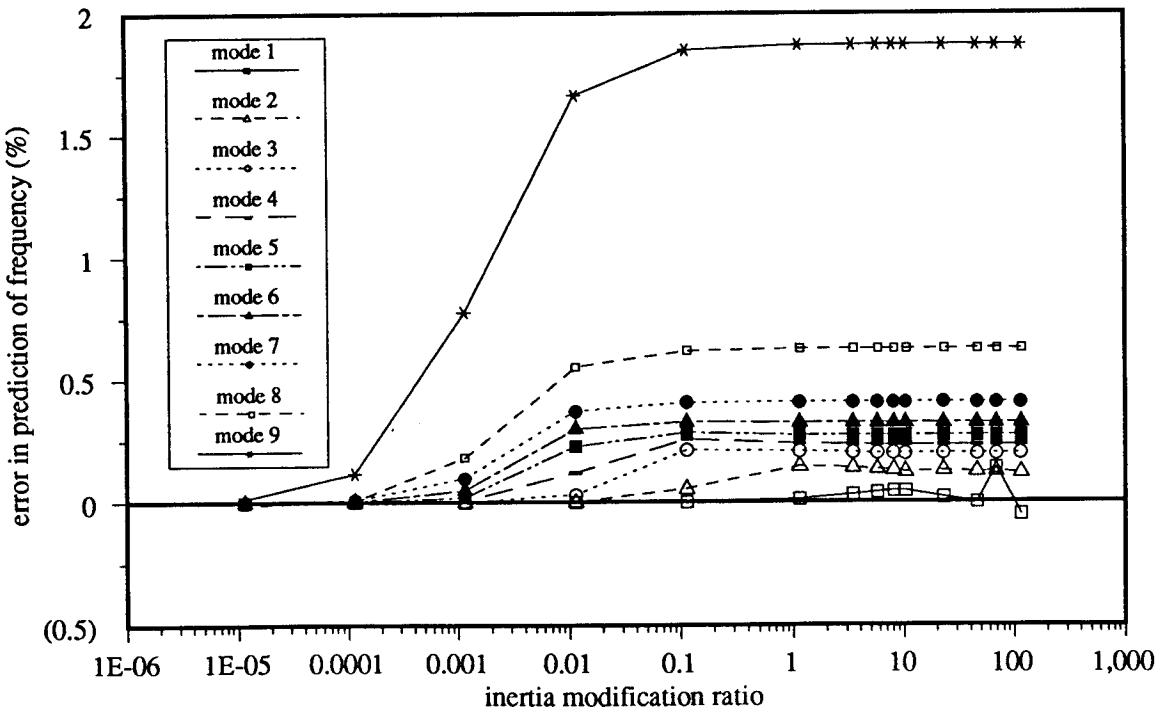

(b) -10% error in the tip rotation for mode 9

Figure 5.9: **Error in Modal Prediction of Frequency for the Steel Cantilever with a tip Mass for a given error in the tip rotation for mode 9**

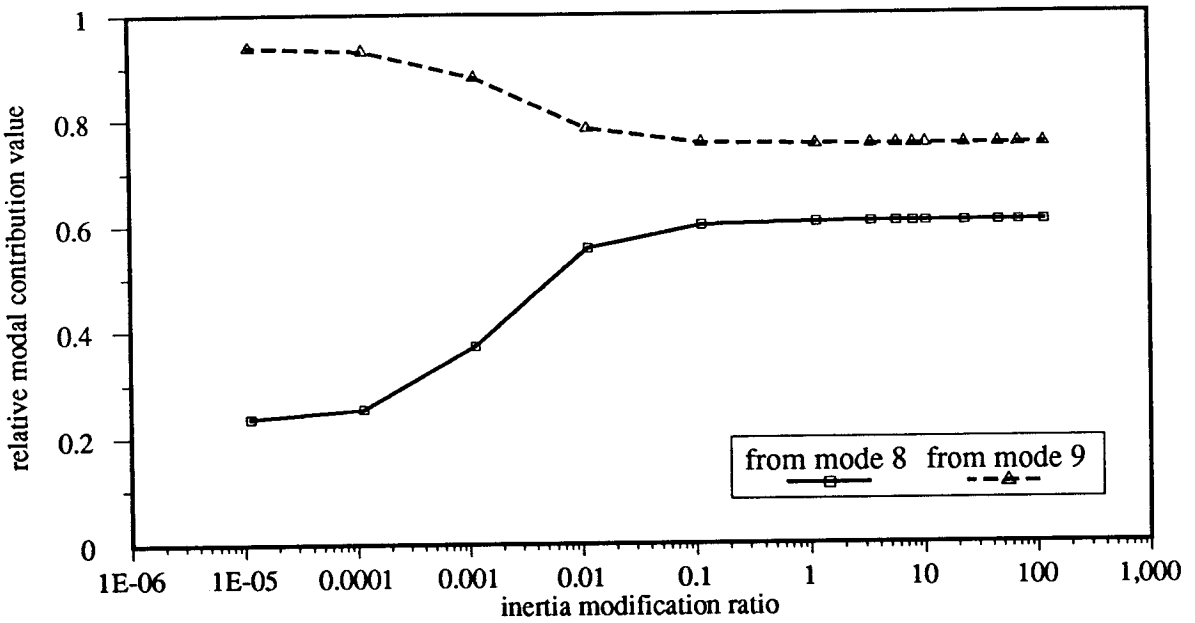

Figure 5.10: **Modal Contributions to mode 9 for the case of the 10% error in the tip rotation of the ninth mode. Steel Cantilever with a tip mass (mass=0.2 kg)**

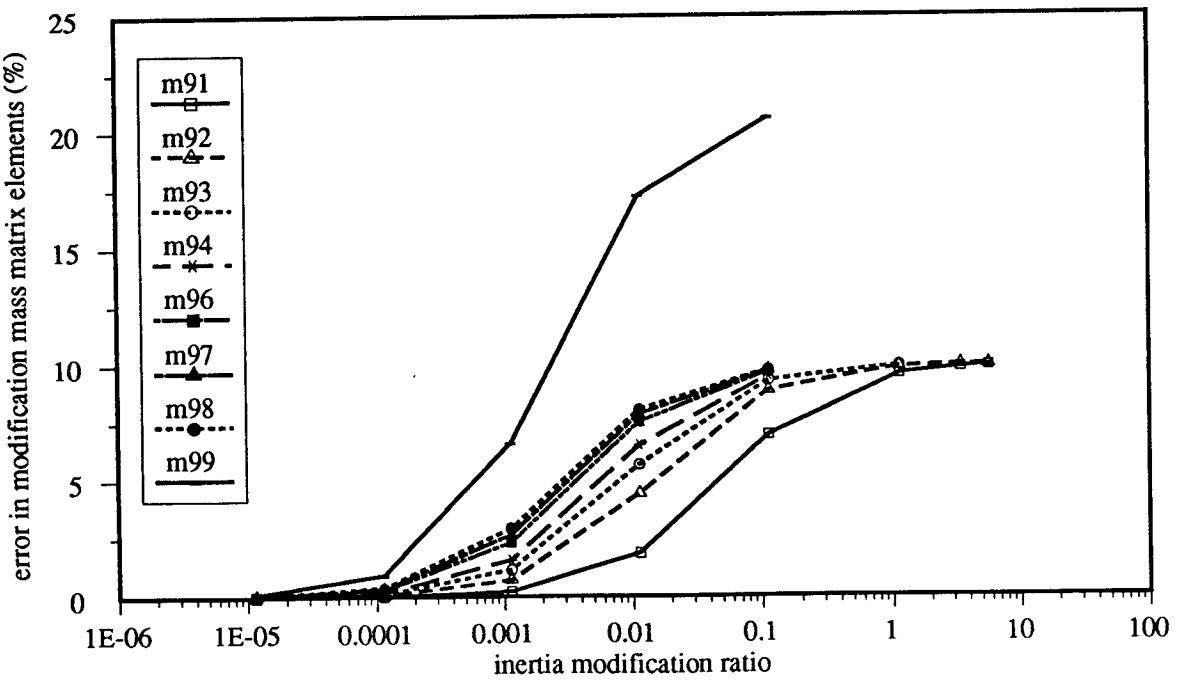

Figure 5.11: Errors in the Elements of the Modification Modal Mass Matrix for +10% error in the Tip Rotation for mode 9. Steel Cantilever with a Tip Mass (m=0.2 kg)

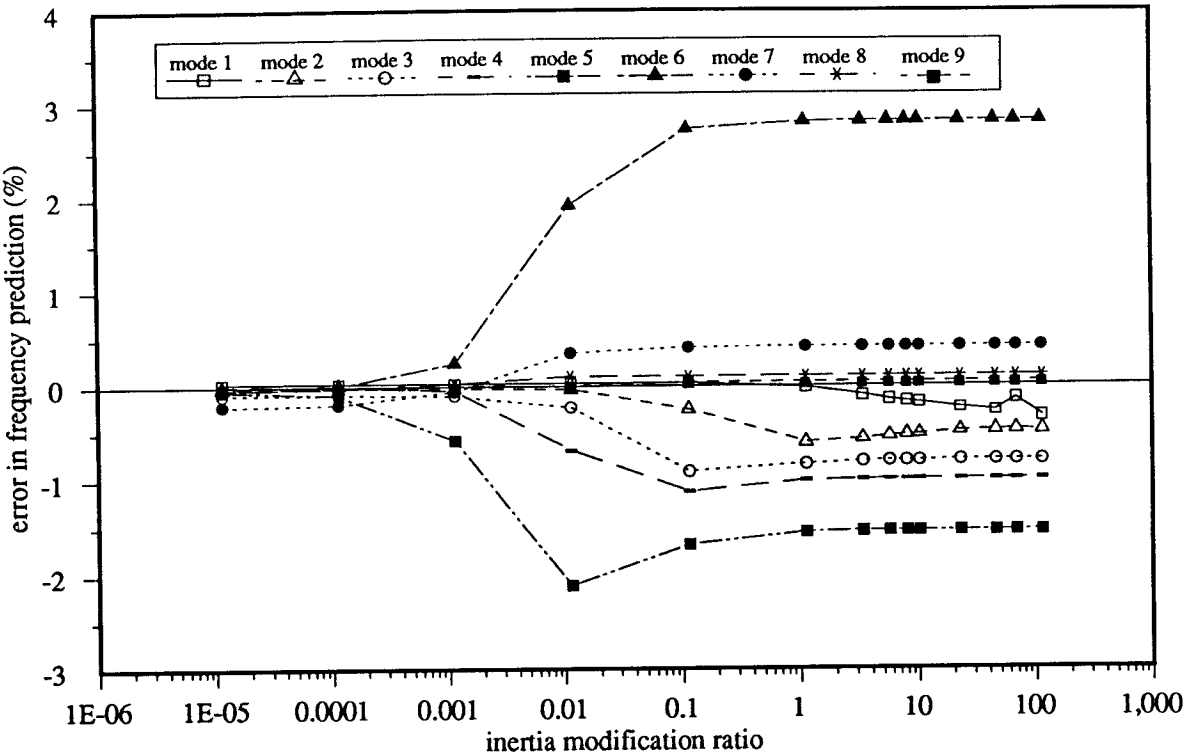

Figure 5.12: Effect of a +10% error in the Tip Rotation for mode 5 on the Frequency Prediction of a Tip Mass Modification on the Steel cantilever (mass = 0.2 kg)

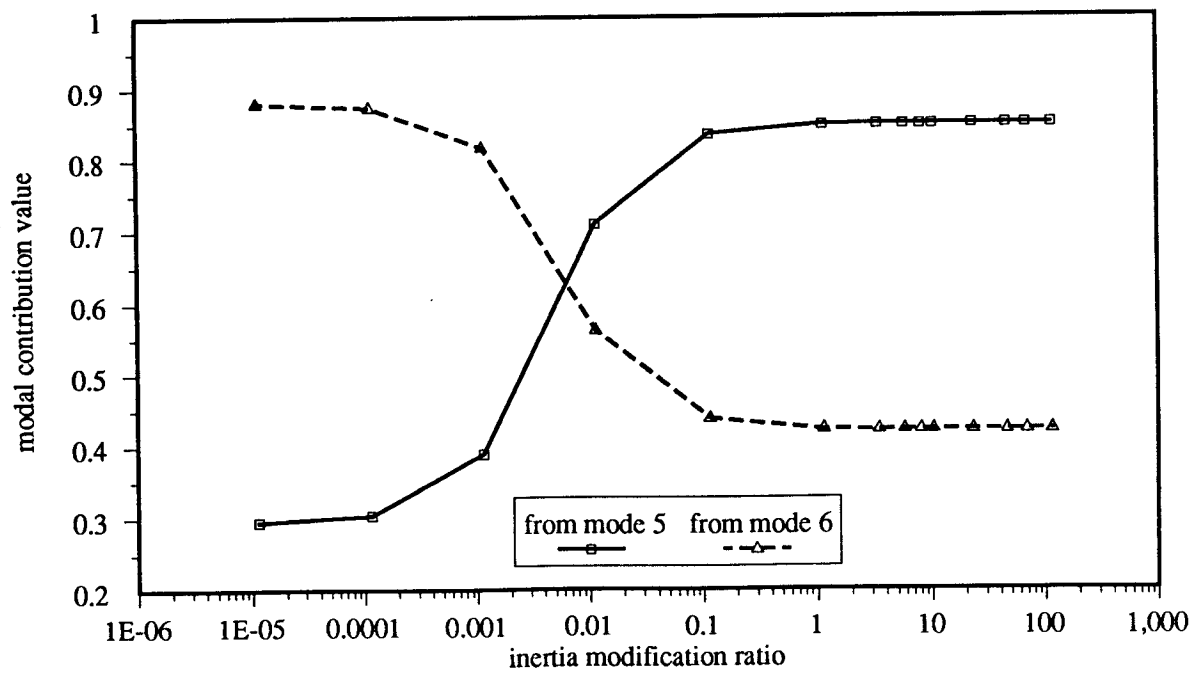

Figure 5.13a: **Modal Contributions to mode 6 for the case of the 10% error in the tip rotation of the fifth mode. Steel Cantilever with a tip mass (mass=0.2 kg)**

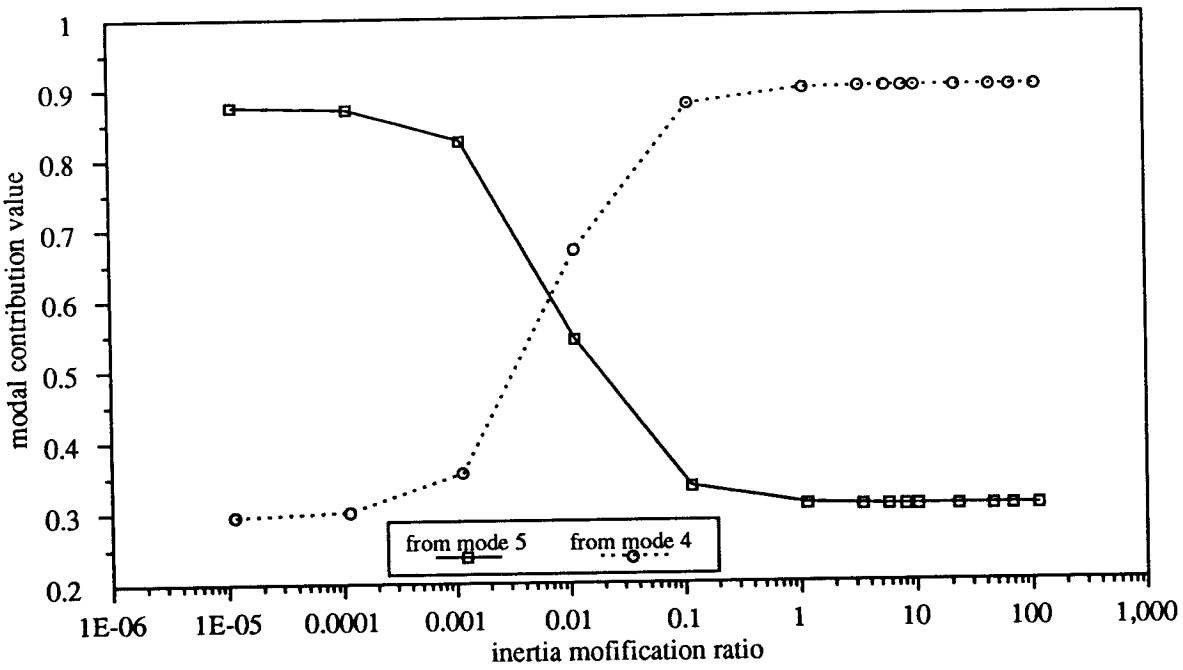

Figure 5.13b: Modal Contributions to mode 5 for the case of the 10% error in the tip rotation of the fifth mode. Steel Cantilever with a tip mass (mass=0.2 kg)

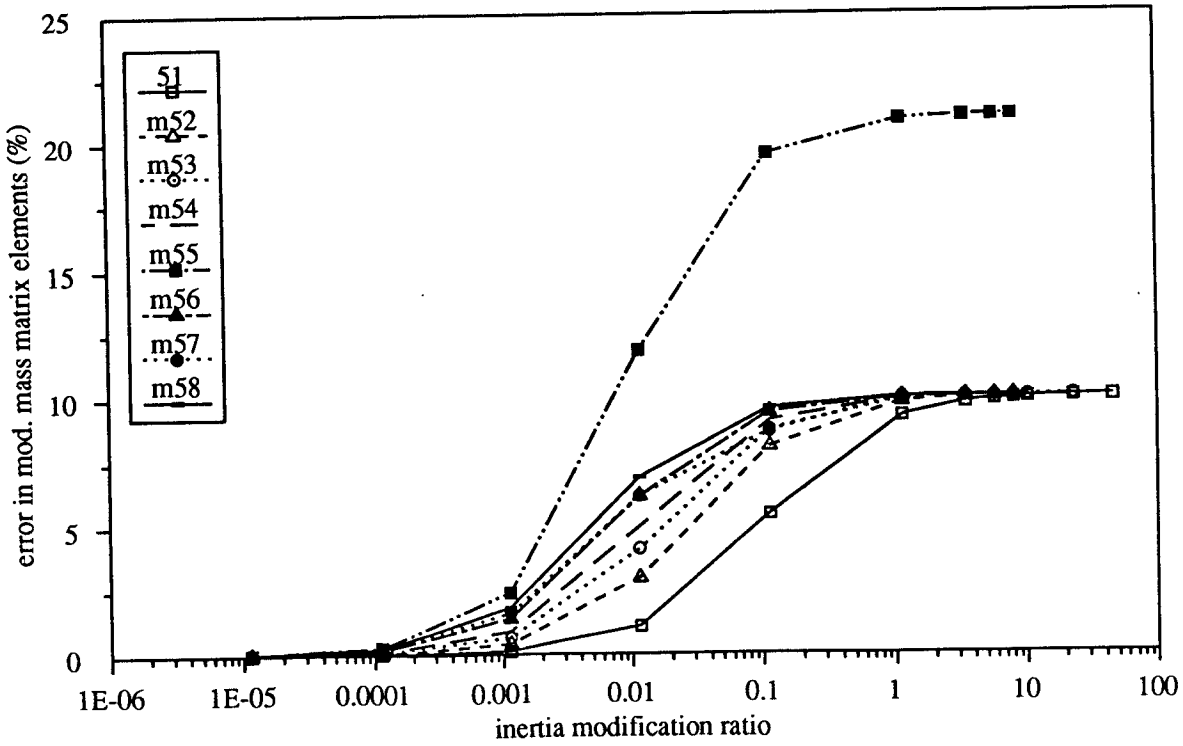

Figure 5.14: Errors in the Elements of the Modification Modal Mass Matrix for +10% error in the Tip Rotation for mode 5. Steel Cantilever with a Tip Mass (m=0.2 kg)

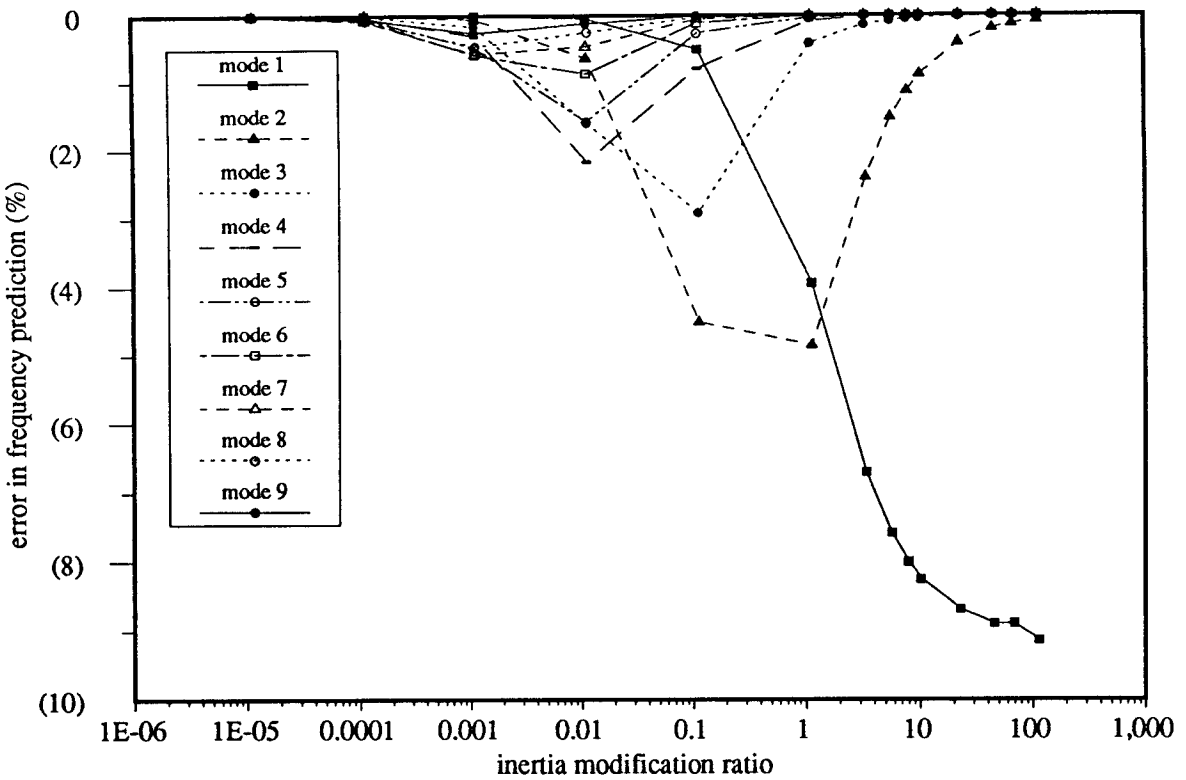

Figure 5.15: Effect of Introducing +10% error in the tip rotations of all the modes in the database on the Predicted Frequencies of the Steel Cantilever with a Tip Mass (mass=0.2 kg)

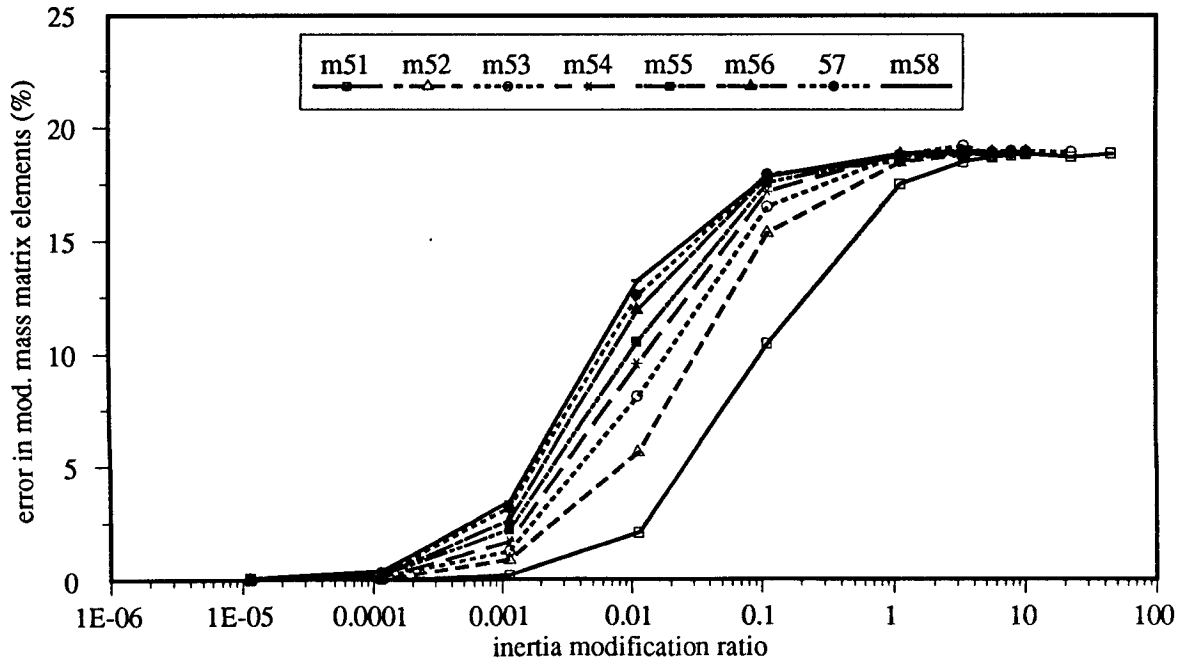

Figure 5.16: Errors in the Elements of the Modification Modal Mass Matrix for +10% error in the Tip Rotations for all modes. Steel Cantilever with a Tip Mass (m=0.2 kg)

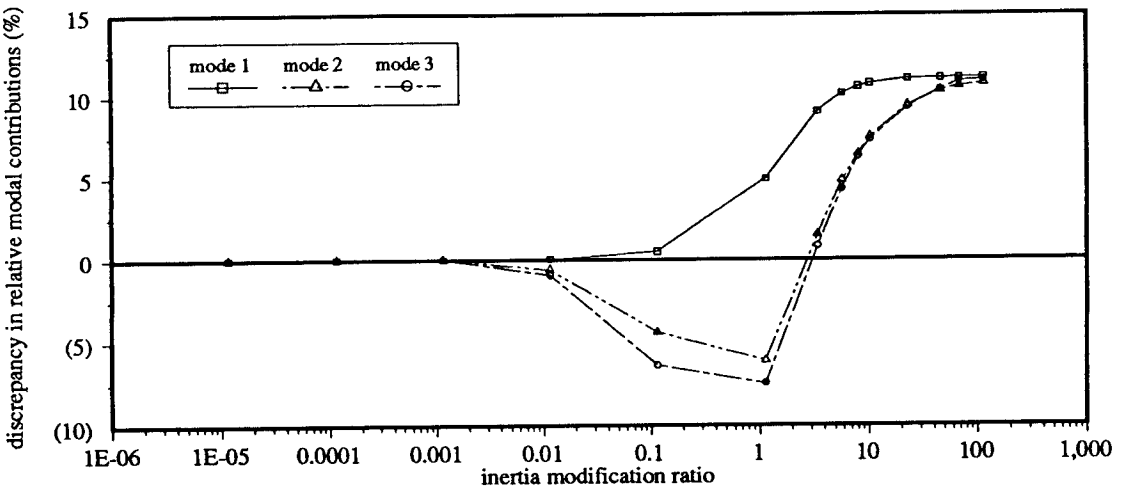

(a) contributions to mode 1

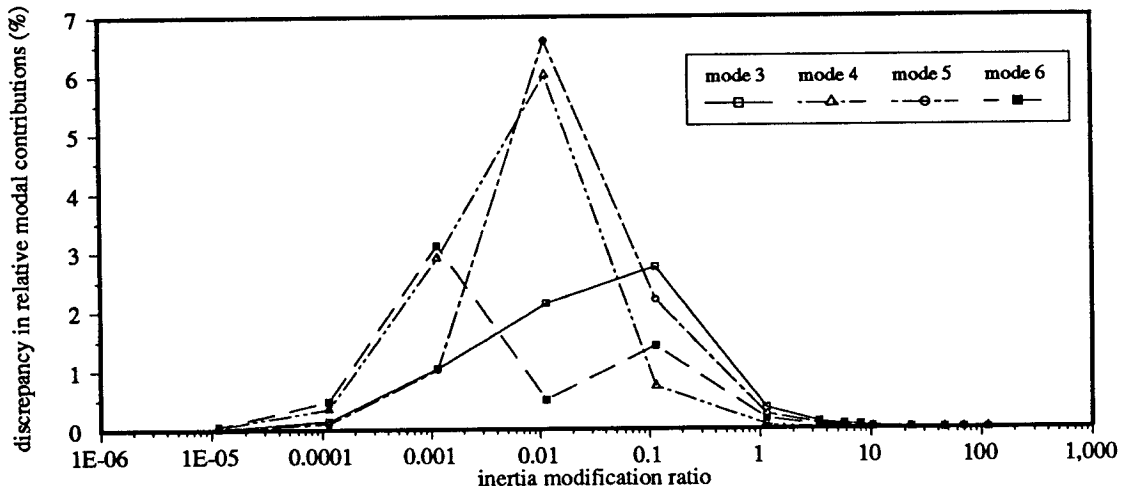

(b) contributions to mode 5

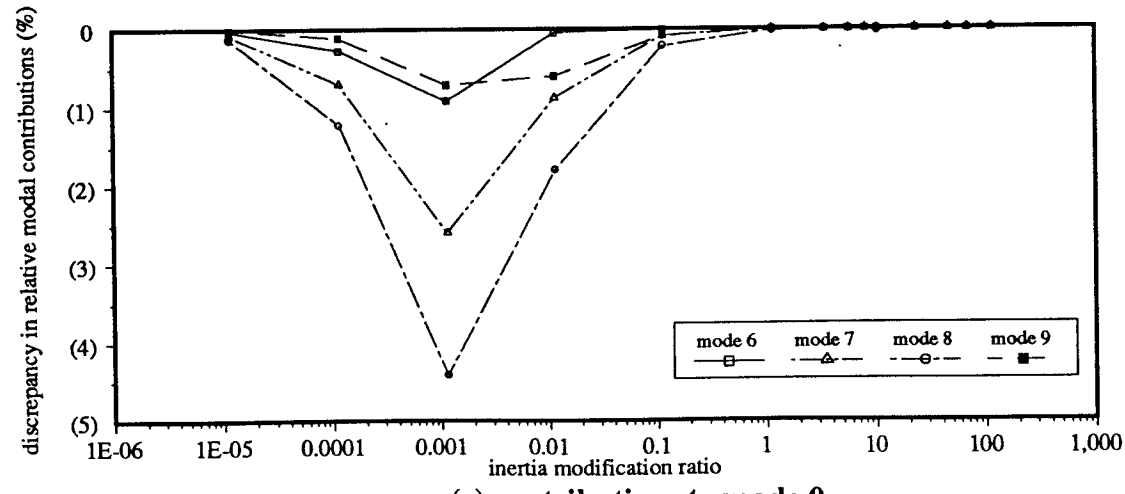

(c) contributions to mode 9

Figure 5.17: **Discrepancy in the Modal Contributions for the case of the 10% error in all tip rotations for the Steel Cantilever with a tip mass (mass=0.2 kg)**

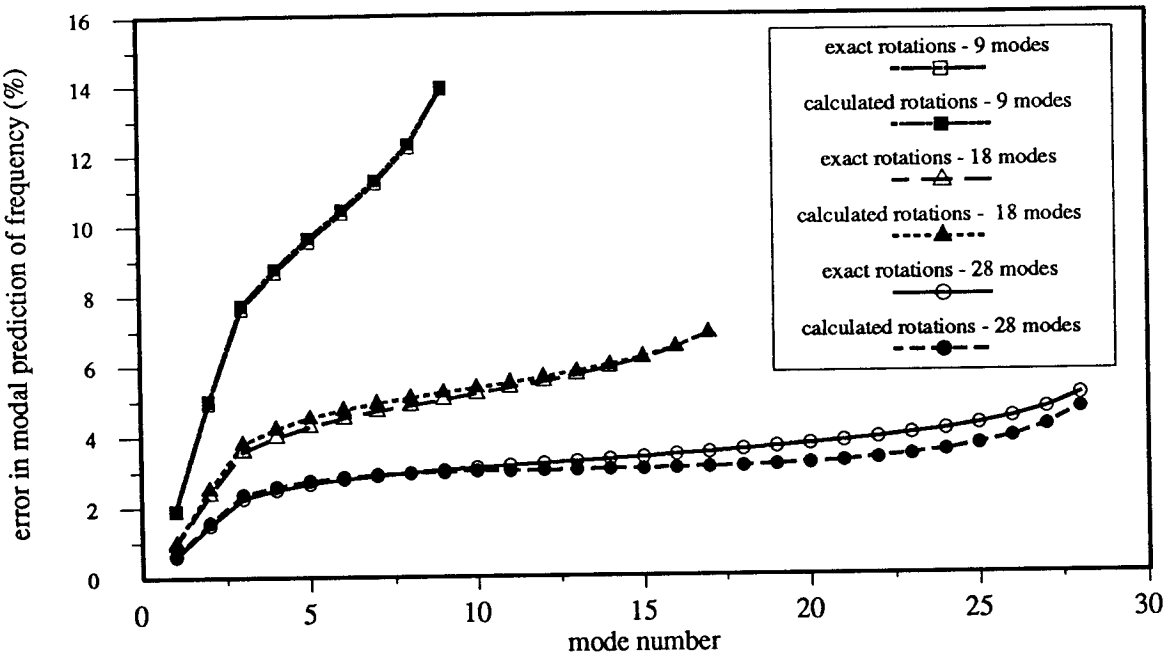

Figure 5.18a: **Comparison of the Modal Predictions using Exact and Calculated rotations against the Analytical solution for the Steel Cantilever with a Tip Mass (m=0.2 kg, IMR=11.4)**

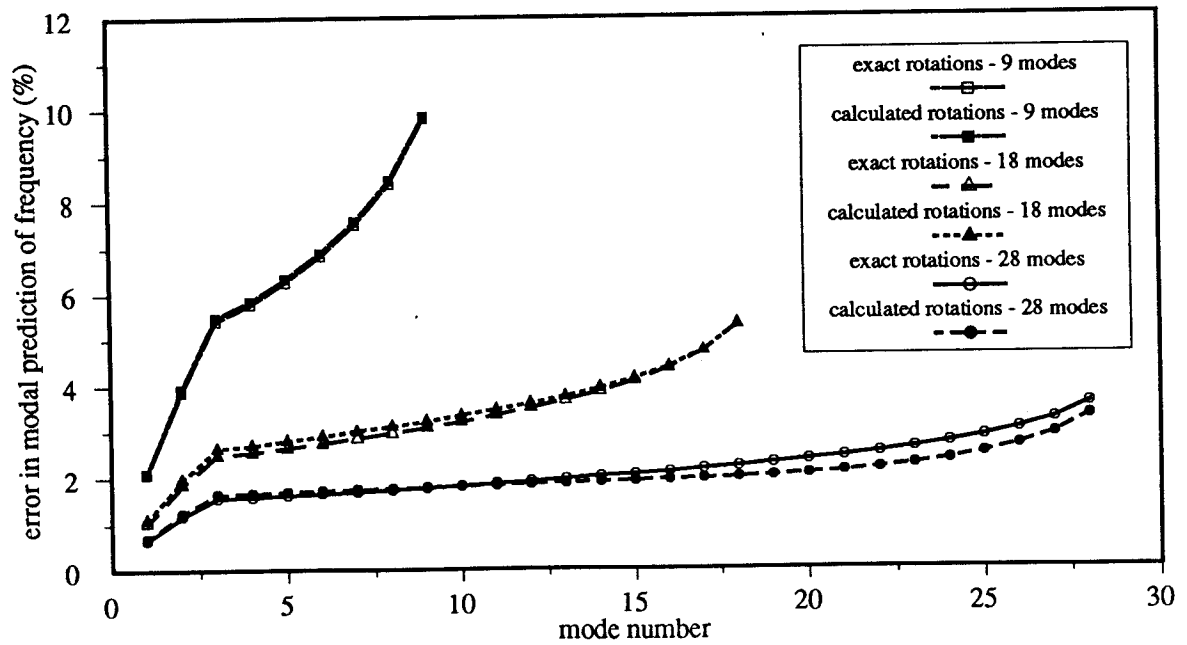

Figure 5.18b: **Comparison of the Modal Predictions using Exact and Calculated rotations against the Analytical solution for the Steel Cantilever with a Tip Inertia (m=0.0 kg, IMR=11.4)**

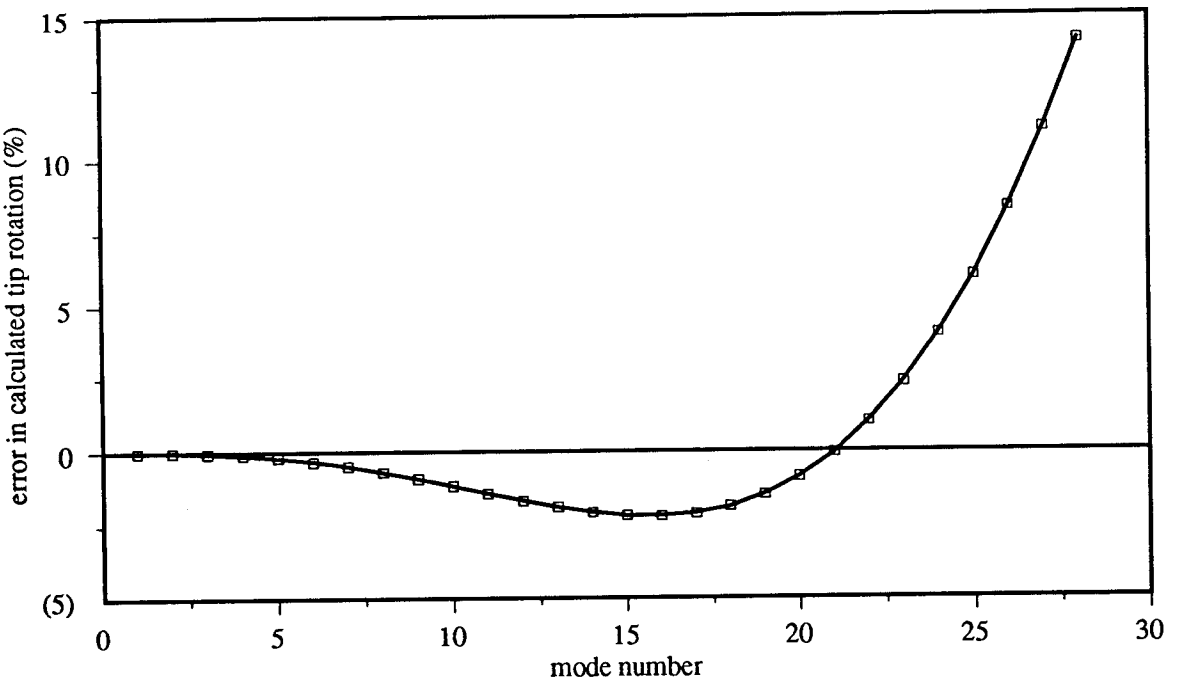

Figure 5.19: **Errors in the Estimates of the Tip Rotations from an Interpolating Spline Approximation on the Steel Cantilever**

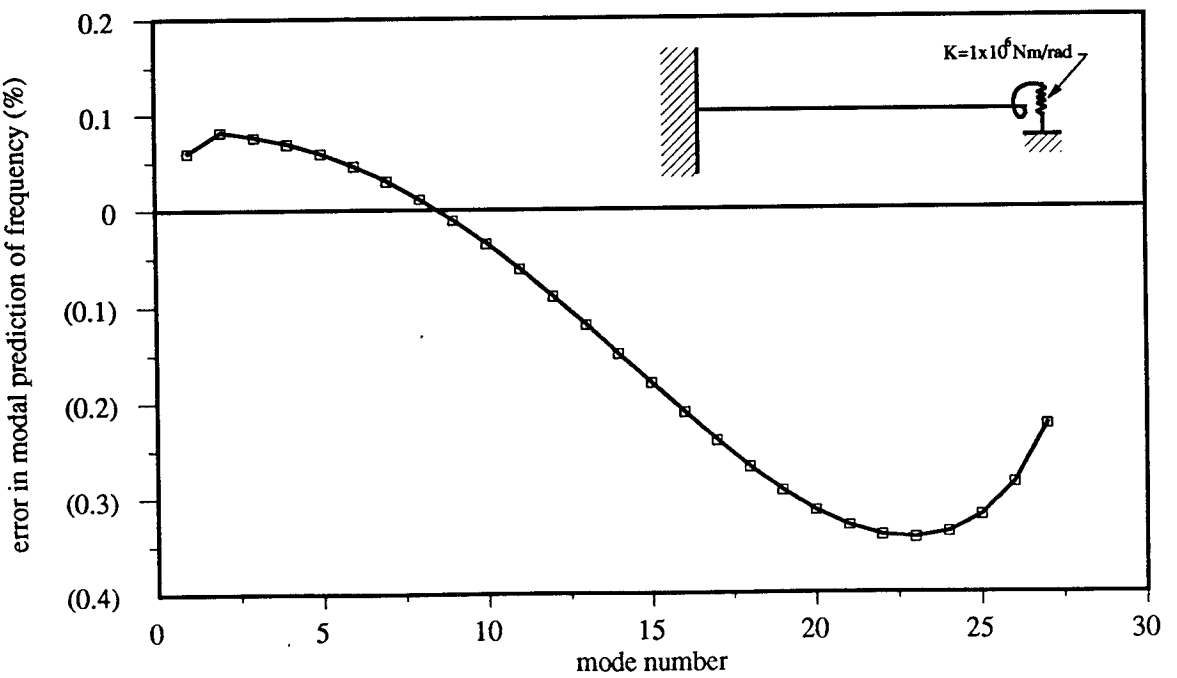

Figure 5.20: **Errors in the Predictions of Frequency for the Steel Cantilever with a Bending Stiffness at the Free end (K=1 MNm/rad)**

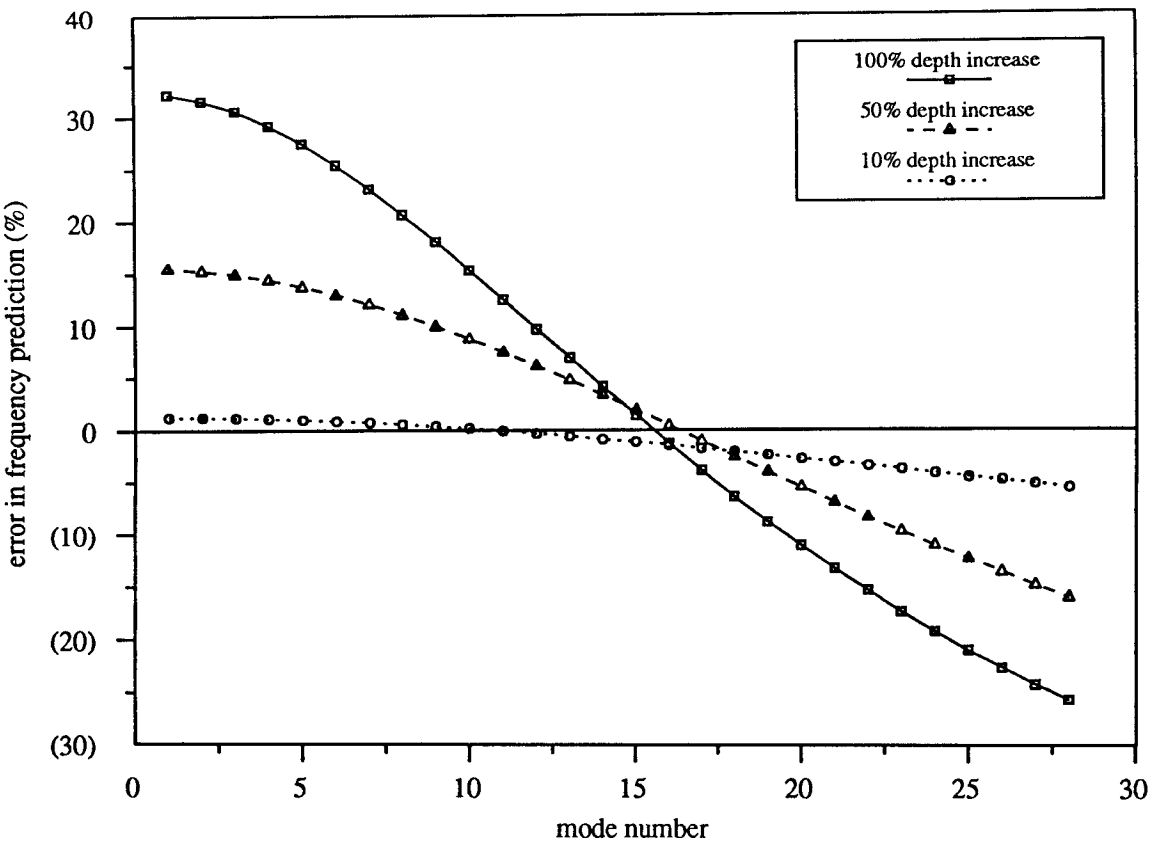

Figure 5.21a: **Comparison of Modal Predictions based on exact data with analytical solutions for full-length/full-width rib modifications on the Steel Cantilever**

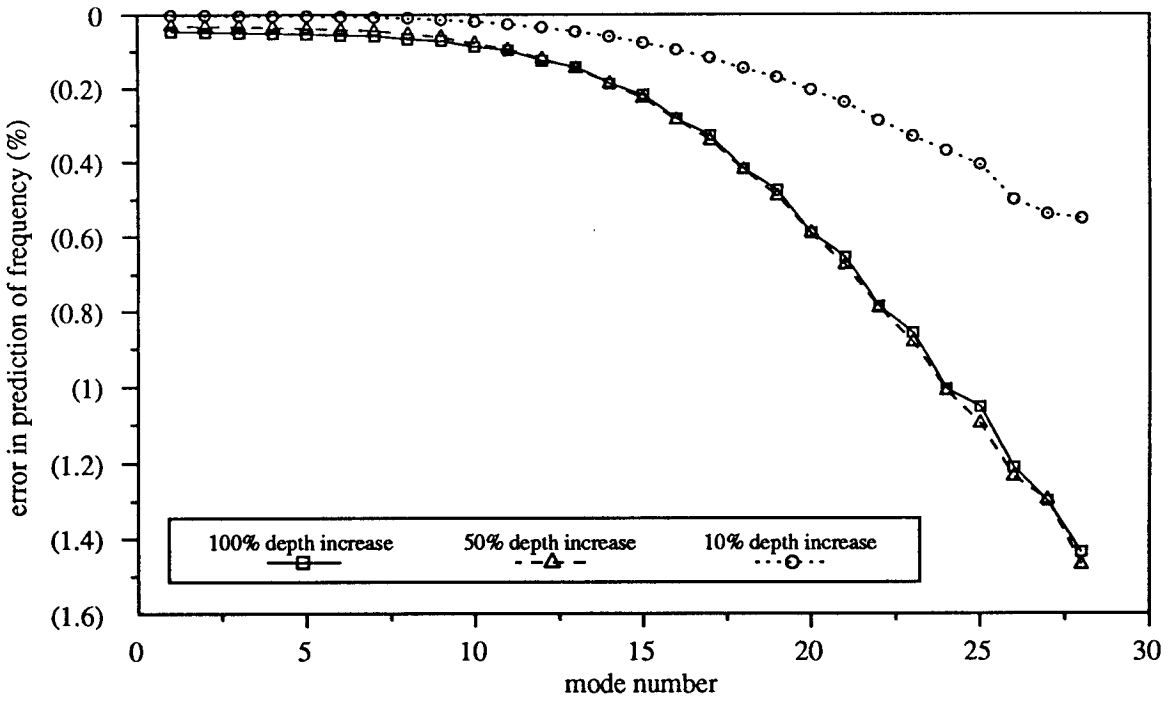

Figure 5.21b: **Error in the Modal Predictions based on Estimated rotations when compared with the predictions based on exact rotations for the full-length/full-width rib modification on the Steel Cantilever**

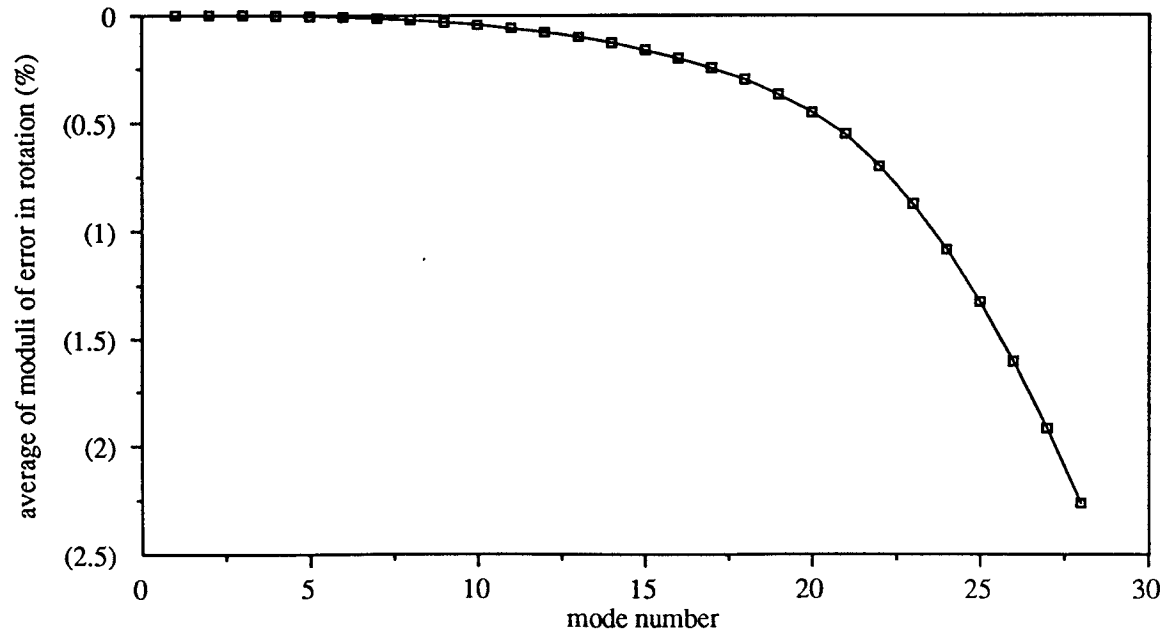

Figure 5.21c: **Variation of the averages of the moduli of the normalised errors in the rotation estimates from an interpolating spline for the Steel Cantilever**

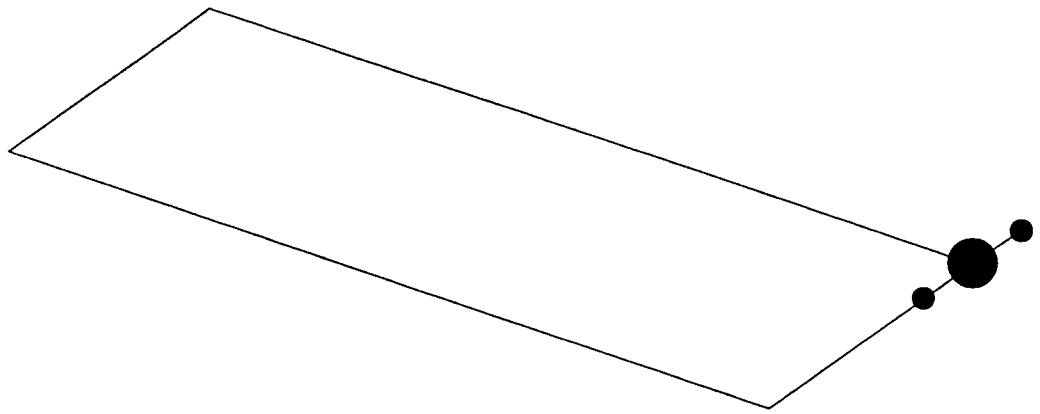

Figure 5.22: **Mass Modification on the Free-free Plate**

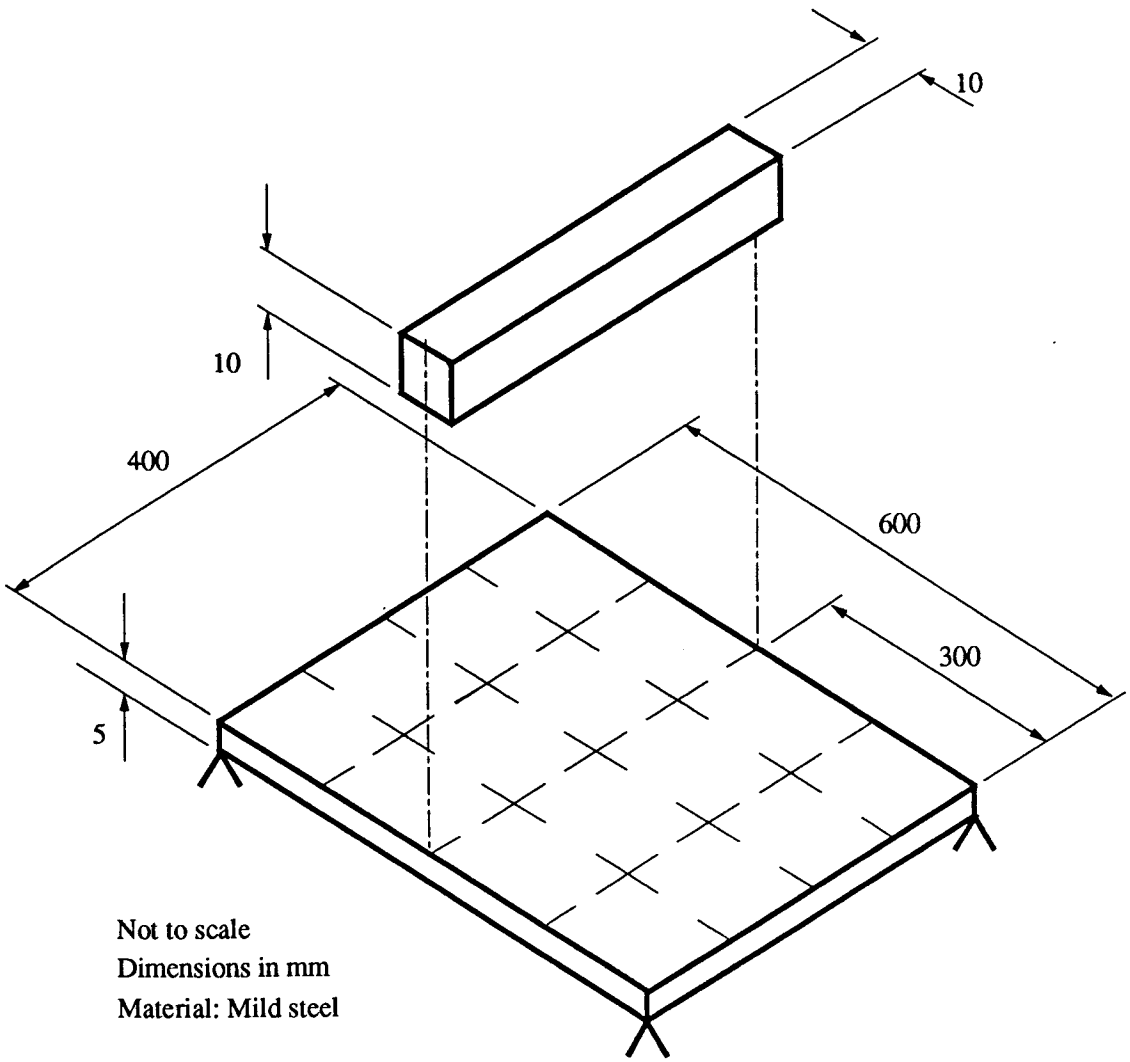

Figure 5.23: **Simply supported plate with a rib stiffener**

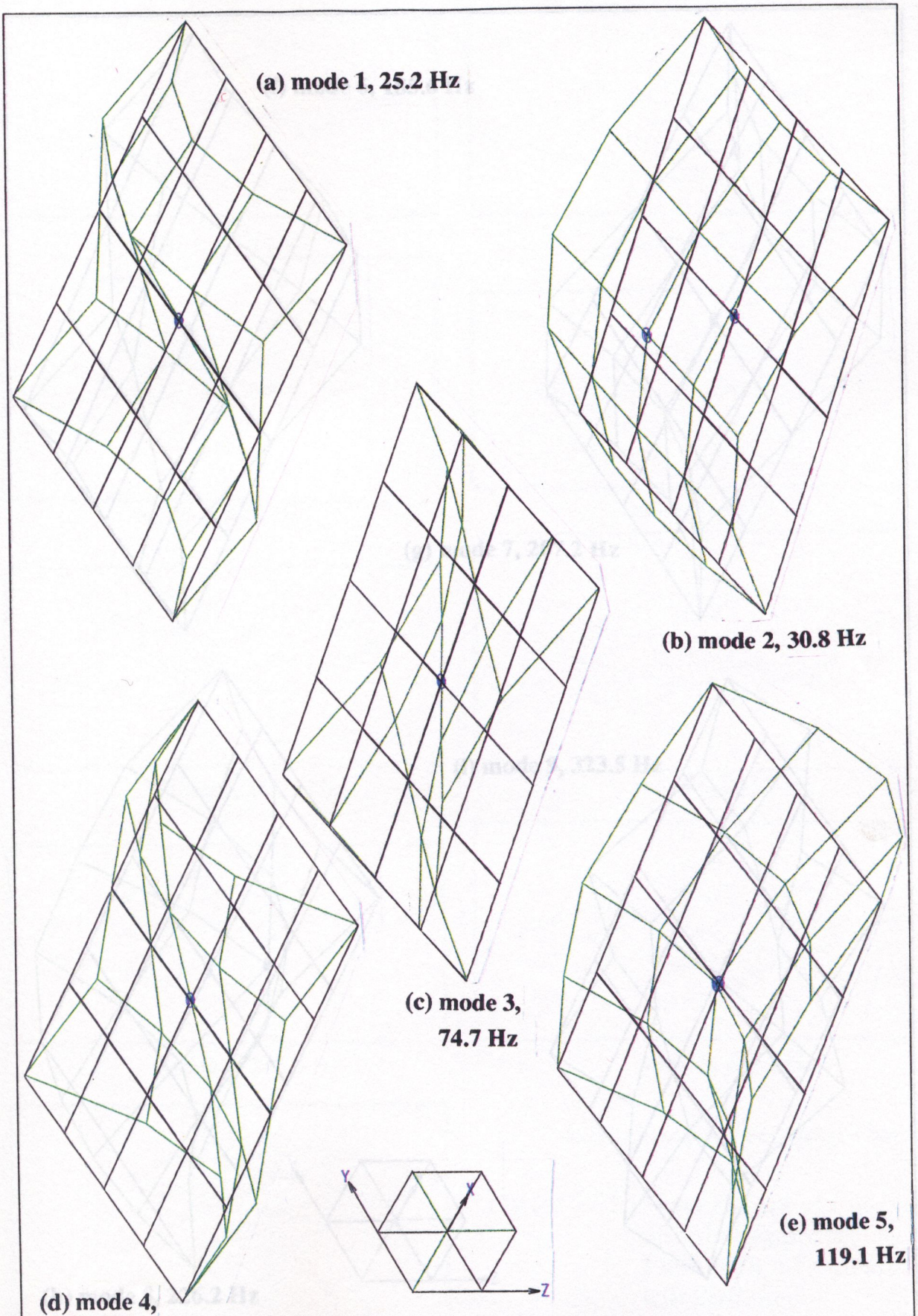

Figure 5.24: **Modeshapes of the Simply Supported Plate with a Central Mass**

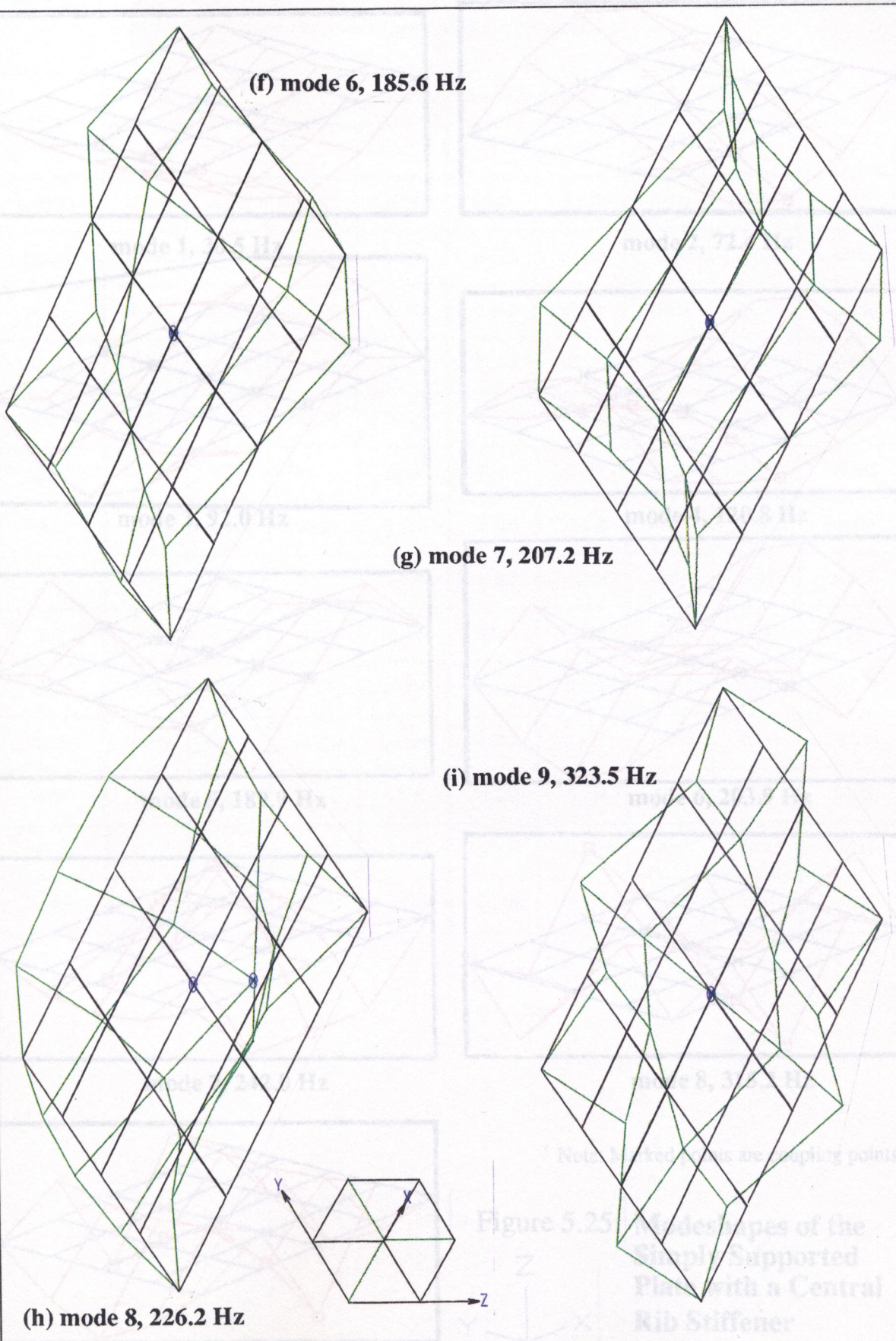

Figure 5.24: **Modeshapes of the Simply Supported Plate with a Central Mass**

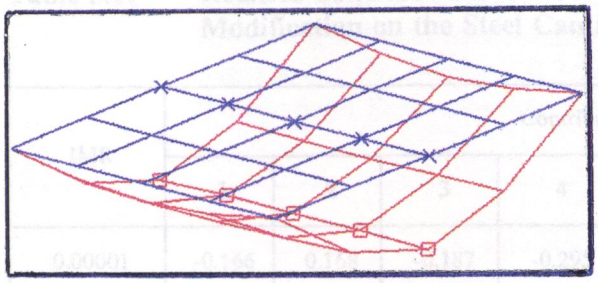

mode 1, 30.5 Hz

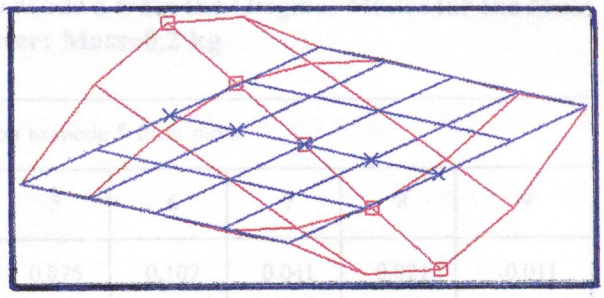

mode 2, 72.4 Hz

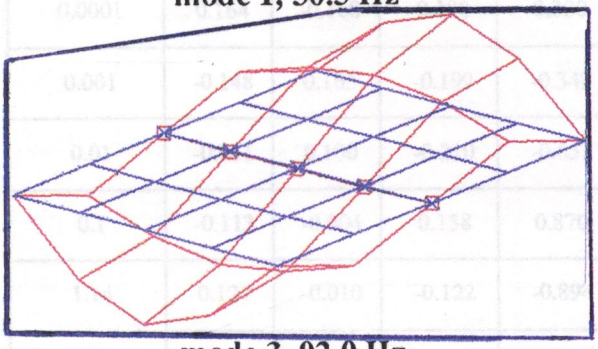

mode 3, 92.0 Hz

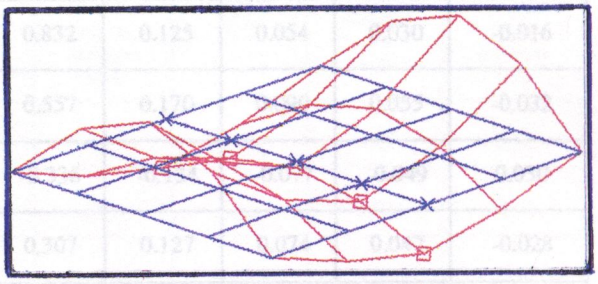

mode 4, 120.8 Hz

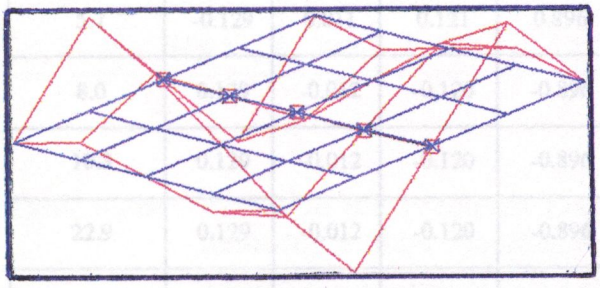

mode 5, 189.9 Hz

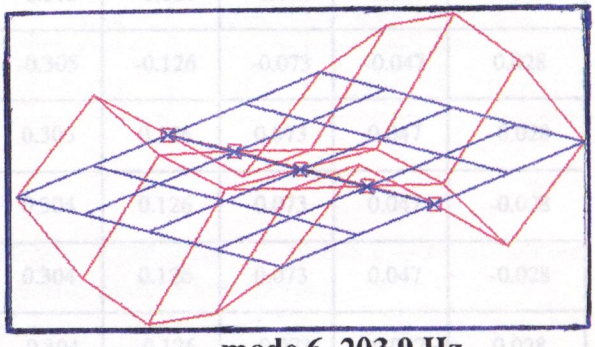

mode 6, 203.9 Hz

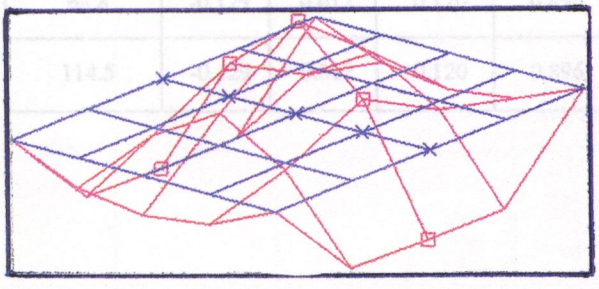

mode 7, 242.0 Hz

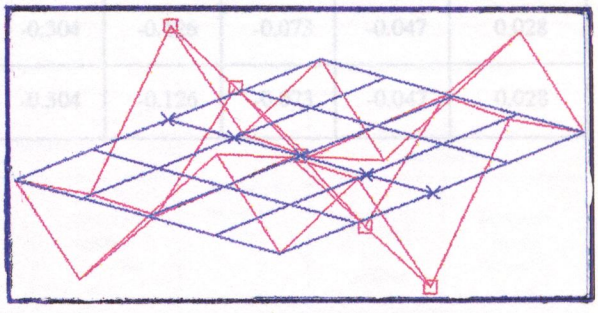

mode 8, 315.2 Hz

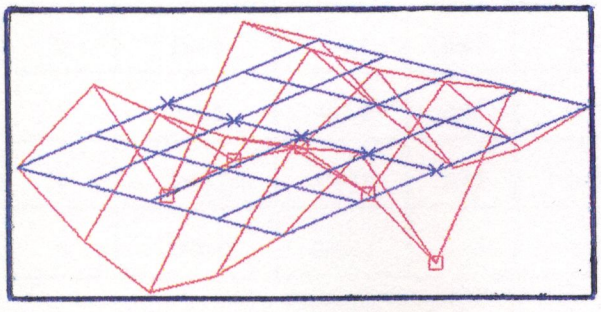

mode 9, 381.3 Hz

Note: Marked points are coupling points

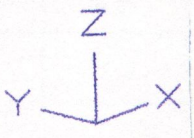

Figure 5.25: **Modeshapes of the Simply Supported Plate with a Central Rib Stiffener**

Table 5.1: **Relative Contributions to the New Mode 5 from the Original Modes for the Mass Modification on the Steel Cantilever; Mass=0.2 kg**

IMR	Contribution to mode 5 from mode								
	1	2	3	4	5	6	7	8	9
0.00001	-0.166	0.168	-0.187	-0.295	0.875	0.102	0.041	0.021	-0.011
0.0001	0.164	-0.168	0.188	0.300	-0.872	-0.104	-0.042	-0.022	0.012
0.001	-0.148	0.165	-0.199	-0.349	0.832	0.125	0.054	0.030	-0.016
0.01	-0.011	0.100	-0.210	-0.651	0.557	0.170	0.090	0.055	-0.032
0.1	-0.113	-0.004	0.138	0.870	-0.336	-0.134	-0.077	-0.049	0.030
1.14	0.127	-0.010	-0.122	-0.894	0.307	0.127	0.074	0.047	-0.028
3.4	-0.128	0.011	0.121	0.895	-0.305	-0.126	-0.074	-0.047	0.028
5.7	-0.129	0.011	0.121	0.896	-0.305	-0.126	-0.073	-0.047	0.028
8.0	0.129	-0.012	-0.120	-0.896	0.305	0.126	0.073	0.047	-0.028
10.3	0.129	-0.012	-0.120	-0.896	0.304	0.126	0.073	0.047	-0.028
22.9	0.129	-0.012	-0.120	-0.896	0.304	0.126	0.073	0.047	-0.028
45.9	-0.129	0.012	0.012	0.896	-0.304	-0.126	-0.073	-0.047	0.028
68.8	-0.129	0.012	0.120	0.896	-0.304	-0.126	-0.073	-0.047	0.028
114.5	-0.129	0.012	0.120	0.896	-0.304	-0.126	-0.073	-0.047	0.028

Table 5.2a: Errors in the Predicted Frequencies from Fits on the 1-0-1-0- database following a Mass Modification on the Steel Cantilever;
Mass = 0.2 kg, Inertia = 0.3 kgm^2.
Comparison Base: Predictions based on interpolation on exact data.

Mode	Unmodified Structure (Hz)	Mass alone (no added moment of inertia)				Mass and moment of inertia added		
		Modified structure (Hz)	Percentage error in prediction			Modified structure (Hz)	Percentage error in prediction	
			Raw data	Minimum root rotation	Minimum second derivative at tip		Minimum root rotation	Minimum second derivative at tip
1	42.3	33.0	-0.39	-0.19	-0.20	11.7	3.40	3.15
2	264.9	223.5	-0.13	-0.11	-0.33	59.3	2.31	-2.52
3	741.8	651.3	0.12	0.14	-0.10	327.9	8.17	5.34
4	1453.7	1309.9	0.50	0.41	0.55	821.0	9.35	8.32
5	2403.0	2203.7	1.21	1.23	1.23	1545.9	12.15	13.11

Table 5.2b: Errors in the Predicted Frequencies from Fits on the 0-1-0-1- database following a Mass Modification on the Steel Cantilever;
Mass = 0.2 kg, Inertia = 0.3 kgm^2.
Comparison Base: Predictions based on interpolation on exact data.

Mode	Unmodified Structure (Hz)	Mass alone (no added moment of inertia)				Mass and moment of inertia added		
		Modified structure (Hz)	Percentage error in prediction			Modified structure (Hz)	Percentage error in prediction	
			Raw data	Minimum root rotation	Minimum second derivative at tip		Minimum root rotation	Minimum second derivative at tip
1	42.3	33.0	-0.07	-0.11	-0.12	11.7	4.34	2.67
2	264.9	223.5	0.05	-0.15	-0.25	59.3	1.07	-2.96
3	741.8	651.3	0.26	0.17	-0.12	327.9	10.30	4.73
4	1453.7	1309.9	0.67	0.49	0.27	821.0	11.05	7.83
5	2403.0	2203.7	1.46	1.29	1.18	1545.9	12.03	12.99

Table 5.3a: Free Plate With Mass at Corner, Mass = 0.2 kg, Inertia = 0.3 kgm² Rotations Computed Using an Interpolant.

mode	unmodified (Hz)	Modified (Hz)	Error in Modal Prediction (%)		Error in Rotation at modification location (%)
			(1)	(2)	
1	-0.00028	-0.00034	0.0	0.00	0.01
2	-0.00018	-0.00019	0.0	0.00	-0.005
3	-0.00013	-0.0001	0.0	0.00	0.06
4	0.00019	-0.00004	0.0	0.00	-0.03
5	0.00023	0.00014	0.0	0.00	0.68
6	0.00035	0.00017	0.0	0.00	-0.24
7	328.5	106.3	45.62	0.72	10.70
8	401.0	278.0	1.29	-0.81	-4.53
9	886.1	403.7	16.62	-3.14	-19.89
10	921.4	734.3	3.81	-2.77	10.42
11	1309.9	922.9	2.17	-0.70	-1.14
12	1510.5	1285.8	5.69	-0.81	-3.98
13	1545.1	1354.4	4.39	-3.32	-52.30
14	1844.6	1563.4	8.56	-0.99	0.75
15	2064.5	1806.6	1.80	-0.05	-13.34
16	2450.4	1987.1	14.40	-7.19	-129.61
17	2866.3	2316.6	5.56	-1.50	-27.21
18	3409.4	2785.9	8.86	-6.16	71.90
19	3529.9	3220.2	3.96	-0.20	53.27
20	3632.3	3589.7	-1.62	0.00	49.29

Key:
(1) Comparison of modal prediction using FE rotations with FE predictions
(2) Comparison of modal prediction using interpolated rotations with modal prediction using FE rotations

Table 5.3b: Free Plate With Mass at Corner, Mass = 0.2 kg, Inertia = 0.3 kgm² Rotations Computed using a Smoothing Approximation

mode	unmodified (Hz)	Modified (Hz)	Error in Frequency Prediction (%)			Error in Translation at modification location (%)	Error in Rotationat modification location (%)
			(1)	(2)	(3)		
1	-0.00028	-0.00034	-	0.00	0.00	-1.60	7.27
2	-0.00018	-0.00019	-	0.00	0.00	-0.08	7.26
3	0.00013	-0.0001	-	0.00	0.00	-0.62	7.25
4	0.00019	-0.00004	-	0.00	0.00	0.60	7.12
5	0.00023	0.00014	-	0.00	0.00	1.01	7.32
6	0.00035	0.00017	-	0.00	0.00	0.27	7.23
7	328.5	106.3	43.27	-19.96	-19.96	-1.36	-22.10
8	401.0	278.0	1.31	-1.46	-1.17	-0.14	12.42
9	886.1	403.7	15.48	-12.80	-11.56	-3.92	24.52
10	921.4	734.3	3.81	-2.83	-2.40	0.27	-22.22
11	1309.9	922.9	1.99	-1.74	-1.77	-4.90	-25.72
12	1510.5	1285.8	5.92	0.18	-0.07	-1.08	-26.21
13	1545.1	1354.4	4.29	-2.53	-3.26	-0.63	60.52
14	1844.6	1563.4	8.39	0.02	-0.41	32.43	-23.52
15	2064.5	1806.6	1.92	-0.28	-0.97	-3.37	-39.39
16	2450.4	1987.1	13.75	-1.83	-2.75	18.22	148.21
17	2866.3	2316.6	3.46	0.96	0.59	-2.71	-34.67
18	3409.4	2785.9	7.43	-0.25	0.42	-0.89	203.70
19	3529.9	3220.2	3.11	0.08	0.20	1.97	-46.61
20	3632.3	3589.7	0.30	-0.01	0.00	-0.82	-48.90

Key: (1) Comparison of modal prediction using FE rotations with FE predictions
(2) Comparison of modal prediction using smoothed data with modal prediction using FE rotations
(3) Comparison of modal prediction using calculated rotations with modal prediction using FE rotations

Table 5.4a: Cantilever Plate With Mass at Corner, Mass = 0.2 kg, Inertia = 0.0 kgm²

mode	FE prediction		Error in Modal Prediction (%)
	Unmodified (Hz)	Modified (Hz)	
1	18.7	16.8	0.01
2	117.3	97.8	0.11
3	126.1	121.2	0.00
4	330.7	297.4	0.50
5	394.0	363.0	0.15
6	482.3	432.4	0.06
7	654.3	583.6	1.33
8	707.3	673.4	-0.15
9	1091.6	926.8	2.53
10	1095.3	1100.4	-0.60
11	1359.5	1228.1	1.30
12	1548.0	1444.4	0.73
13	1580.2	1566.2	-0.73
14	1687.2	1661.6	-0.33
15	1917.5	1823.6	1.06
16	2174.6	2077.1	0.40
17	2375.2	2308.8	1.82
18	2436.1	2376.3	-0.25

Table 5.4b: Cantilever Plate With Mass at Corner, Mass = 0.2 kg, Inertia = 0.3 kgm²

mode	unmodified plate (Hz)	Modified plate (Hz)	MAC comparison (mod. vs unmod.)	(1)	Modal prediction (Hz)		Error in Modal Prediction (%)
					FE rotations	Calculated rotations	FE rotations
1	18.7	7.0	0.99	-19.0	7.9	8.0	1.27
2	117.3	23.7	0.00	6.6	29.4	30.0	2.04
3	126.1	105.2	0.85	-0.7	108.3	108.3	0.00
4	330.7	131.6	0.00	5.6	153.8	157.3	2.28
5	394.0	325.3	0.29	-5.7	-	-	-
6	482.3	363.4	0.00	-100.0	357.9	357.6	-0.08
7	654.3	431.9	0.00	2.2	432.6	433.4	0.18
8	707.3	624.7	0.56	-15.4	-	-	-
9	1091.6	677.1	0.00	-20.0	661.5	660.9	-0.09
10	1095.3	966.0	0.01	-584.8	1020.4	1017.1	-0.32
11	1359.5	1117.8	0.00	-2.7	-	-	-
12	1548.0	1226.2	0.06	-3.8	1267.7	1288.5	1.64
13	1580.2	1465.2	0.11	-43.9	1482.3	1480.4	-0.13
14	1687.2	1593.4	0.04	-5.8	-	-	-
15	1917.5	1685.5	0.00	-8.3	-	-	-
16	2174.6	1845.6	0.02	-81.6	1836.9	1839.0	0.11
17	2375.2	2137.8	0.01	-18.0	-	-	-
18	2436.1	2368.7	0.55	-12.1	2329.0	2352.3	1.00
19	2891.1	2399.2	0.00	-385.9	-	-	-
20	3009.4	2527.4	0.67	-20.6	2907.0	2733.3	-5.98
				Others	385.2	393.2	
					738.9	751.9	
					1181.3	1184.0	
					1615.5	1641.2	
					1857.8	1888.1	
					2263.1	2300.5	
					2612.1	2656.2	

Key: (1) error in calculated rotation at modification location (%)

Table 5.5a: Simply Supported plate with Mass at Centre; m = 0.2 kg, I = 0.3 kgm².

mode	unmodified Plate (Hz)	Modified Plate (Hz)	Modal Prediction using FE rotations (Hz)	Error in rotation at modification location (%)		Error in Frequency. Prediction (%)
				θ_x	θ_y	
1	31.4	25.2	30.8	0.00	0.00	0.00
2	74.7	30.8	33.9	-0.95	0.00	25.37
3	91.7	74.7	74.7	0.00	-6.86	0.00
4	119.1	105.3	119.1	0.00	0.00	0.00
5	185.6	119.1	127.7	0.00	0.00	30.46
6	201.9	185.6	185.6	0.00	-38.92	0.00
7	237.9	207.2	219.2	0.00	0.00	3.28
8	323.5	226.2	226.4	-2.66	0.00	4.46
9	380.6	323.5	323.5	0.00	-39.86	0.00

Table 5.5b: Simply Supported Plate with Rib-Stiffener (Rib Stiffener cross-section: 10 x 10 mm)

mode	unmodified Plate (Hz)	Modified Plate (Hz)	Modal Prediction FE rotations (Hz)	Error in Frequency Prediction (%)		
				(1)	(2)	(3)
1	31.4	30.5	30.6	0.33	0.33	-0.33
2	74.7	72.4	72.5	0.14	0.56	-0.14
3	91.7	92.0	92.1	0.11	-0.33	0.00
4	119.1	120.8	120.9	0.08	-0.08	0.00
5	185.6	189.9	191.0	0.58	-2.32	-0.63
6	201.9	203.9	203.9	0.00	-0.98	0.00
7	237.9	242.0	242.8	0.33	0.00	0.04
8	323.5	315.2	317.7	0.79	0.00	-0.35
9	380.6	381.3	385.9	1.21	0.03	-0.49

(1) FE rotations, (2) substructure method, (3) Fe translations and calculated rotations

Table 5.5c: Errors in the Computed Rotations at the Points of Attachment of the Rib Stiffener on the Simply Simply Supported Plate

mode	Percentage error in calculated rotation at point									
	11		12		13		14		15	
	θ_x	θ_y	θ_x	θ_y	θ_x	θ_y	θ_x	θ_y	θ_x	θ_y
1	-15.77	0.00	39.50	0.00	0.00	0.00	39.50	0.00	-15.77	0.00
2	-7.32	0.00	2.17	0.00	-0.95	0.00	2.17	0.00	-7.32	0.00
3	0.00	-9.97	0.00	-8.73	0.00	-6.86	0.00	-8.73	0.00	-9.97
4	-0.45	0.00	-0.06	0.00	0.00	0.00	-0.06	0.00	-0.45	0.00
5	0.00	-12.50	0.00	-18.06	0.00	0.00	0.00	-18.06	0.00	-12.50
6	0.00	-18.17	0.00	-29.15	0.00	-38.92	0.00	-29.15	0.00	-18.17
7	-5.55	0.00	2.11	0.00	0.00	0.00	2.11	0.00	-5.55	0.00
8	-38.78	0.00	12.03	0.00	-2.66	0.00	12.03	0.00	-38.78	0.00
9	0.00	-4.99	0.00	-50.25	0.00	-39.86	0.00	-50.25	0.00	-4.99

Table 5.5d: Simply Supported Plate with Rib-Stiffener (Rib Stiffener cross-section: 20 x 20 mm)

mode	unmodified Plate (Hz)	Modified Plate (Hz)	Modal Predictions using FE rotations (Hz)	Error in Frequency Prediction (%)
				FE translations and calculated rotations
1	31.4	28.2	29.1	-1.72
2	74.7	66.4	67.5	-1.63
3	91.7	92.6	93.7	0.85
4	119.1	129.6	130.2	1.38
5	185.6	206.7	212.2	2.78
6	201.9	220.0	230.4	3.56
7	237.9	300.8	313.0	-3.71
8	323.5	325.3	317.6	-1.92

Table 5.6: MAC Comparisons of Modal Databases for the Cantilever with and without Error in the Tip Rotation of the First Mode

Mode Compared with mode 1	Error in the Tip Rotation of Mode 1						
	0%	1%	5%	10%	20%	50%	100%
1	1.00	1.00	1.00	1.00	1.00	0.97	0.91
2	0.39	0.39	0.39	0.40	0.41	0.43	0.46
3	0.08	0.08	0.08	0.09	0.10	0.12	0.16
4	0.11	0.11	0.11	0.12	0.13	0.16	0.20
5	0.06	0.06	0.06	0.06	0.07	0.10	0.14
6	0.07	0.07	0.07	0.08	0.09	0.12	0.17
7	0.05	0.06	0.06	0.06	0.07	0.11	0.16
8	0.07	0.08	0.08	0.08	0.10	0.14	0.21
9	0.07	0.07	0.07	0.08	0.10	0.15	0.23

CHAPTER 6

GUIDELINES FOR OPTIMUM PERFORMANCE, CONCLUSIONS AND RECOMMENDATIONS

6.1 Introduction

This study has endeavoured to contribute towards the development of a quick but effective technique of expanding experimental modal data to include the unmeasured degrees of freedom for structural dynamics modifications. To this end, the study has attempted to answer two important questions. These are:

1. **How accurate are the estimates of the rotations from the spline approximations?** This is an important consideration since errors in the modal vector values at modification sites affect the accuracy of the predicted effect of the modifications.
2. **What are the effects of errors in the rotations on the accuracy of the predictions of dynamic changes following structural modifications?** This is the true measure of success or failure since the suitability of an expansion technique is judged by its ability to predict the effects of structural modifications.

Detailed discussions and conclusions which were drawn from the analysis are given at the end of each relevant chapter and will not, therefore, be repeated here. Nevertheless, for completeness, the *main* points of the discussions are summarised here. Consequently, guidelines on the optimal use of the proposed technique of estimating rotational degrees of freedom are presented. Finally, the *major* conclusions of the work along with recommendations for further work are presented.

6.2 Summary of the Discussion of the Results and Implications

6.2.1 Estimation of Rotational Degrees of Freedom

In an attempt to provide an answer to the first question above, this work has identified and considered the effect of several parameters on the accuracy of spline curve and surface fitting. These include the density and distribution of the measurement points on the structure, the

smoothing factor which in turn controls the number of knots in the fit function and the level of error in the initial data.

While the analysis indicated that the interpolating spline was the best estimator of rotations from error-free data, it was apparent that interpolation was undesirable for noisy data and it was necessary to search for the optimum approximation using some suitable acceptability criteria. It was also shown that while the method was able to provide acceptable estimations of rotations away from the boundaries once the underlying mode shape function had been picked up, it was unable to truly represent the mode shape functions at and near the boundaries. However, it was shown that once the minimum number of measurement points between nodal lines was met (at least two), the inclusion of an additional point near the boundaries dramatically improved the estimates of the rotations there. Consequently, it was demonstrated that boundary conditions were suitable acceptability criteria for optimising the performance of the approximation method. Although the First-Order Difference computation was not included in the approximation algorithm, a separate analysis indicated that the computation was a useful indicator of the level of smoothing required (which in turn is a measure of the level of noise in the initial data) prior to fitting.

In the analysis, it was shown that the accuracy of the estimates of rotations is dependent on the spatial description of the mode shapes. The data indicated that the level of smoothing required increases with the amount of noise and with the complexity of the mode shape function, the resulting errors in the rotations from noisy data being generally under 10% provided there are at least two measurement points between nodal lines for the highest mode of interest. When this is compared with the results reported in the investigations which used polynomial or spline functions to estimate rotations [24,29,30] which yielded error levels of between 15% and 70% for comparable test cases, the present method is seen to be superior. Even when compared with the more accurate FE-based mapping, condensation and expansion methods [24,25,26] which offer errors of up to 5% for beam type structures, it is apparent that the present method is very attractive as it is much quicker and simpler. While the level of error in the original translational data affects the accuracy of the estimates of rotations, this work has shown that the precise pattern of the errors does not appear to influence the quality of the estimates obtained.

Surface fitting results indicated that the estimates of the rotations about the in-plane axes were dependent on the modelling of the structure with regard to the number of measurement points in each direction and the level of smoothing used. Thus the choice of axes during the formulation of the problem has to take account of the end-use of the required rotational entries. The study on noisy data (Appendix 3) has indicated that as in the case of curve fitting, the approximation which minimises the slope at the fixed end also minimises the overall error in the rotations. Although it was not specifically investigated for plate structures, it is envisaged that the requirements for measurement point distribution established for curve fitting will also apply for surface fitting. Where the cross-section of the plate structure demands treating the structure as separate planes, as in appendix 3, it has been shown that, at the intersection of the planes, where more than one entry of the rotation was generated, the entries to be retained were, where applicable, those from the planes with the larger cross-sectional dimensions. Finally, it has been shown that for the same controlling parameters, the estimates of rotations from curve fitting are superior over those from surface fitting.

6.2.2 Structural Dynamics Modification Predictions

The main finding from the SDM predictions performed in this work was that the errors in the predictions were generally less sensitive to errors in the estimated rotations than to the effects of modal truncation consequent upon the imposition of severe modifications. However, the analysis also highlighted the difficulty associated with attempts to establish the relationship between cause and effect with regard to the effect of errors in the estimates of rotations on the errors in the predictions of the effects of structural changes. This was especially pertinent in the situations where the modification was such that it linked several rotational degrees of freedom. Nevertheless, the analysis on mass modifications indicated that, an over-estimation of the rotation at the modification location leads to under-prediction of the frequencies following a modification with the reverse being true for an under-estimate of the rotation. For rib stiffener modifications, under-estimation of rotations leads to under-prediction of the frequencies. Thus it is seen that the effect of under-estimation or over-estimation of the rotations on the predictions of structural changes is dependent on the type of modification considered.

6.3 The Key Questions and Guidelines for Optimum Performance

From the foregoing, the approximation to be used for estimating rotations in a given situation will therefore depend on the answers to the following key questions:

(i) What is the level of error in the original data?

(ii) How many measurement points are available and where are they located on the structure? This limits the number of modes which can be acceptably expanded.

(iii) How many modes are there in the data base? This is closely linked to the number of available measurement points.

(iv) Is the original data real or complex?

(v) Is the measurement accuracy the same for all the data points in the data base?

(vi) What type of structure is being investigated? This determines the choice of the method of approximation to be used between curve or surface fitting.

(vii) What is the end-use of the expanded data? If the end-use of the data is structural dynamics modification, what type of modification is to be applied and where is it to be located?

It is apparent that answers to these questions provide guidance on the use of spline curve and surface fitting for estimating rotations from translational modal data. In this regard, the following guidelines thus emerge:

- The best estimator of rotations from error-free data is the interpolating spline.
- With real-world (noisy) data, interpolating should be avoided since it picks up all of the noise in the measured data.
- The general distribution of measurement points should reflect the shape of the highest mode of interest. In particular, satisfactory estimates (less than 10% error) can be expected if there are at least two measurement points between nodal lines.
- Additional measurement points should be located near the boundaries if there is an expectation that these regions will be required as modification sites.
- For structures with one or more clamped boundaries, the fit giving the best overall estimates of rotation is that which minimises the slope at the clamped boundaries. However, each clamped boundary will have its own optimum fit. Thus the fit to be used will be that which gives the best overall estimates.

Although this work has not investigated the applicability of this guideline to plates, it would be expected that this should hold for plate structures as well since the boundary conditions associated with rectangular plates are similar to those associated with beams.

- Where estimates of rotations are required at free or simply-supported boundaries, there is benefit (more than 5% improvement in the predictions) in setting the fitting criterion to minimise the second derivative of the displacement at the boundary.
- When the rotation is required at a point or at points in a line, curve fitting should take precedence over surface fitting as it provides better estimates of rotations.
- For plates, the orientation of the global axes should take account of the fact that the accuracy of the rotations is particularly sensitive to the density of measurement points in each in-plane direction and the level of smoothing used.
- Where the cross-section of a plate structure requires treating the structure as separate planes during surface fitting, the rotational entries to be retained at the lines where the planes intersect are those from the planes with, where applicable, the larger cross-sectional dimensions (Appendix 3).

6.4 Conclusions

6.4.1 Estimation of Rotations

1. While the use of cubic spline curve fitting for estimating rotational degrees of freedom had previously received some attention, its applicability on real experimental data had not been established. In addition, the use of bicubic surface fitting has not been hitherto investigated. This work has identified five parameters which control the accuracy of the estimates of rotations from translational data using spline approximations of the mode shape functions; namely the smoothing factor, the number and location of the data points on the structure, the level of error in the initial data and although it has not been investigated in this work, the weighting of the data points.

2. The results in the analysis have indicated that the proposed curve and surface fitting method using cubic splines provides a quick and simple, but versatile and effective method of estimating rotational degrees of freedom of structures for many engineering applications. It is however acknowledged that the application of the method to circular structures will require the use of polar coordinates and that in such applications, the tangential components of the displacements cannot be used in the fit. In the case of curved beams, it is envisaged that the technique will be applicable provided the out-of plane displacements are much larger than the in-plane displacements which are not usable by the method.

3. The ability to generate data for unmeasured freedoms (both translational and rotational) from the fit function is particularly attractive for structural modification applications. In addition and although this feature has not been investigated in this thesis, the capability of fitting through points which are arbitrarily located on the structure is particularly attractive as it provides the opportunity of analysing structures for which it is physically impossible to obtain measurements in straight lines or on a rectangular grid.

4. This 'modeshape' expansion approach presents a number of practical advantages over FE based expansion methods: there is no need to perform FE analyses of the structure thus CPU power (since smaller amounts of computational effort are required) and storage requirements are smaller. However, the relative computational costs still need to be established.

6.4.2 Structural Dynamics Modification Predictions

It will be acknowledged that the problem of relating the effect of errors in the rotations to the errors in the predictions is an extremely difficult task since several parameters are involved. These include the number of measurement points on the structure and the number of the modes of vibration which are of interest; the geometry of the structure and the associated boundary conditions and the type and location of the modification. In addition, it is an extremely difficult if not impossible task to trace the errors from source to effect. Therefore generalisations about the applicability of the expanded data to different types of structures and modifications should

be made and treated with great caution. In this regard, while some of the following conclusions (1, 2 and 5) may be universally applicable, it is prudent that all the conclusions are viewed in the light of the structures which have been used in the investigations unless otherwise stated.

1. Although it is well known that the accuracy of the predictions of the dynamic behaviour of a modified structure depends on the accuracy of the original modal data, the effect of the errors in the rotations on the predictions has not been hitherto well documented. It was, however, shown in Chapter 5 that structural dynamics modification predictions are more sensitive to the effects of modal truncation consequent upon the imposition of severe modifications than to the errors in the estimates of the rotations.

2. The investigations have established that predictions of the low frequency modes are more sensitive to errors in the computed rotations than are the predictions of the higher frequency modes. Typically, predictions of the low frequency modes for which the errors in the rotations were smaller (generally less than 7% when smoothing) had the largest errors in the predictions (generally greater than 10%). However, as one moved up the modes, the predictions of frequency were seen to be less sensitive to the errors in the rotations. This was evident in that errors in the rotations at the modification location which were in excess of 100% for these modes yielded errors in the predictions of frequency which were less than 10%.

3. The cases studied in this work have shown that the effect of under-estimation or over-estimation of the rotations is dependent on the type of the modification being investigated. While under-estimation of the rotations leads to over-prediction of the frequencies for a mass modification, for a stiffness modification, under-estimation of the rotations leads to under-prediction of the frequencies. This is consistent with reported findings in published work [25,29].

4. Since the main objective of expanding translational modal data to include the unmeasured rotations (and other required unmeasured translations) at specific locations on a structure is to allow for moment transfers which are needed in SDM applications,

the proposed technique provides data which is sufficiently accurate (up to 10% error in the rotations) for the structures investigated in this work (generally less than 5% error in the predictions).

5. From the beam analysis performed in this work, it has been shown that a 'ball park' estimation of the rotations (within 20% of the correct value) is sufficiently accurate to yield acceptable predictions (up to 10% error) following a modification. It must however be recognised that the magnitudes of the errors in the predictions are dependent on the severity of the modification.

6.5 Recommendations for Further Work

The result of the work carried out in this study was the development of an analytical technique capable of estimating the missing rotational degrees of freedom along with any unmeasured translations. The study has identified how the performance of the estimating technique can be optimised for the best performance in structural dynamics modification work. However, the following recommendations are seen as necessary extensions and logical developments of the work carried out in this study:

1. While the effects of measurement errors on the predictions are well documented and hopefully well understood, these errors cannot yet be quantified by analysis. The development of a method of determining the magnitude of the measurement errors present in a modal data base is a logical next step. When the magnitudes of these errors are known, they can be correlated with the errors in the predictions thereby making it possible to make corrections. However, it is acknowledged that this is a very difficult, if not impossible task. Thus, the alternative of improving existing measurement techniques or developing new, more accurate measurement techniques, such as current efforts with laser technology, seems to hold greater chance for success.

2. While this work has used only real modal data in the analysis, it is known that in the instances where mode shape data is markedly complex, expansion of such data to include the unmeasured degrees of freedom may lead to gross errors. An extension of the estimation method used in this work or the development of new techniques to

handle complex data would, to a great extent, enhance the range of applicability of complex modal data in structural dynamics modification work.

3. Although the proposed technique is capable of handling data with different measurement accuracy by applying variable weighting to the data points prior to fitting, this feature was not utilised in this work. Further investigation of this capability is therefore required in order to establish its validity boundaries.

4. The unexpected poor performance of the dual modal space method (and the FE method) in predicting the full-length, full-width rib-stiffened cantilever using the offset beam formulation suggests the need for further investigation of the offset beam formulation in order to enhance its utilisation.

5. Since rib stiffener modifications link several degrees of freedom on a structure, the errors in the predictions cannot be easily related to the errors in the rotation estimates. Development of a method of relating the errors in the rotations to the errors in the predictions for this and other related modifications such as substructuring would advance understanding of the effect of errors in the rotations on the predictions and would provide a platform for initiating corrective action.

6. The work reported in this thesis has mainly considered a cantilever beam and several plate structures. It is however acknowledged that the conclusions drawn from the analysis may not be universally applicable to the wide range of structural geometries and types of modifications. Further investigations on a wide range of structural geometries will enhance the range of applicability of the proposed technique and also provide a ready reference database to the user of the technique.

o0o

REFERENCES

1. Pal T.G. and Schmidtberg R.A., *Combining Analytical and Experimental Modal Analysis for Effective Structural Modelling*, Proceedings of the Ist International Modal Analysis Conference (Proc. IMAC-1), pp265-271, 1982.
2. Brown D.L., *Modal Analysis-Past, Present and Future*, Keynote Address, Proc. IMAC-1, 1982.
3. Ewins D. J., *Modal Testing : Theory and Practice*, Research Studies Press, pp146-147, 1984.
4. Ibrahim S.R., *Future Directions in Modal Analysis*, Keynote Address, Proc. IMAC-4, Feb 1986.
5. Richardson M.H., *Who Needs IMAC*, Keynote Address, Proc. IMAC-2, Orlando, Florida, Feb 6-9, 1984.
6. Allemang R.J., *Modal Analysis - Where do we go from Here?* Keynote Address, Proc. IMAC-10, Feb 1-4, 1993.
7. Snoeys R. and Sas P., *Reflections on Modal Analysis and its Applications*, Keynote Address, Proc. IMAC-5, 1987.
8. Ewins D.J., *Uses and Abuses of Modal Testing*, Keynote Address, Proc. IMAC-3, Orlando, Florida, Jan 1985,
9. Elliot K.B. and Mitchell L.d., *The Effect of Modal Truncation on Modal Modification*, Proc. IMAC-5, London, England, pp72-78, April 1987.
10. Weissenburger J.T., *Effects of Local Modifications on the Vibration Characteristics of Linear Systems*, Journal of Applied Mechanics, Vol 35, Trans. ASME, Series E. Vol 90, No. 2, pp327-332, 1968.
11. Formenti D. and Welaratna S., *Structural Dynamics Modification - An Extension to Modal Analysis*, Aerospace Congress and Exposition, SAE Paper No. 811043, October, 1980.
12. Luk Y.W. and Mitchell L.D., *System Modelling and Modification via Modal Analysis* Proc. IMAC-1, Orlando, Florida, pp423-429, 1982.
13. Chiaki Y., Riehle P.J., Brown D.L. and Allemang R.J., *An Estimation Method for Rotational Degrees-of-Freedom using a Mass Additive Technique*, Proc. IMAC-2, pp877-886, 1984.
14. Smiley R.G., *Rotational Degrees-of-Freedom in Structural Modification*, Proc. IMAC-2, pp937-939, 1984.
15. Sekimoto S., *A Study on Truncation Error in Substructure Testing*, Proc. IMAC-3, Orlando, Florida, pp1220-1226, Jan 1985.

16. Ceballos D.C. and Neto A.R., *Truncated Elastic Modes Coupling Effects Minimization Method by using Special Attitude Control Scheme*, Proc. IMAC-3, pp1227-1233, 1985.

17. Chung K.R. and Lee C.W., *An Efficient Method for Compensating Truncated Higher Modes in Structural Dynamics Modification*, Proc. Instn of Mechanical Engineers Vol 200, No. c1, pp41-48, 1985.

18. Braun S. and Ram Y.M., *On Structural Modifications in Truncated Systems*, Proc. IMAC-5, pp1550-1556, 1987.

19. Elliot K.B. and Mitchell L.D., *The Effect of Modal Truncation on Modal Modification*, Proc. IMAC-5, pp72-78, 1987.

20. Elnomrossy M., *Combined Modal Synthesis Techniques and Residual Flexibility for Large Structures*, Proc. IMAC-8, pp255-262, 1990.

21. Braun S.G. and Ram Y.M., *Predicting the Effect of Structural Modification: Upper and Lower Bounds Due to Modal Truncation*, Proc. IMAC-8, pp940-945, 1990.

22. Avitabile P., O'Callahan J. and Penchinsky F., *Understanding Structural Dynamic Modification Truncation*, Proc. IMAC-8, pp43-54, 1990.

23. Dagnitz D. and Snyder V.W., *Effects of Truncation of Modes on Eigenvalue Modification*, Proc. IMAC-8, pp77-82, 1990.

24. O'Callahan J.C., Lieu I.W., and Chou C.M., *Determination of Rotational Degrees of Freedom for Moment Transfers in Structural Modifications*, Proc. IMAC-3, Orlando, Florida, pp465-470, 1985.

25. O'Callahan J.C., Avitabile P., Lieu I.W. and Madden R., *An Efficient Method of Determining Rotational Degrees of Freedom from Analytical and Experimental Modal Data*, Proc. IMAC-4, Los Angeles, pp50-58, 1986.

26. Avitabile P., O'Callahan J.C., Chou C.M. and Kalkunte V., *Expansion of Rotational Degrees of Freedom for Structural Dynamic Modifications*, Proc. IMAC-5, London, pp950-955, 1987.

27. Lieven N.A.J. and Ewins D.J.; *Expansion of Modal Data for Correlation*, Proc. IMAC-8, Kissimmee, Florida, pp605-609, 1990.

28. Imregun M. and Ewins D.J., *An Investigation into Mode Shape Expansion Techniques*, Proc. IMAC-10, pp168-175, 1993.

29. Mitchell-Dignan M. and Pardoen G.C., *The Estimation of Rotational Degrees-of-Freedom using Shape Functions*, Proc. IMAC-6, Orlando, Florida, pp566-571, 1988.

30. Williams E.J. and Green J.S., *A Spatial Curve Fitting Technique for Estimating Rotational Degrees-of-Freedom*, Proc. IMAC-8, Kissimmee, Florida, pp376-381, 1990.

31. Haisty B.S. and Springer W.T., *A Simplified Method for Extracting Rotational Degrees-of-Freedom Information from Modal Test Data*, The International Journal of Analytical and Experimental Modal Analysis, Vol 1, No.3, pp35-39, July 1986.

32. Rorrer R.A.L., Wicks A.L. and Williams J., *Angular Acceleration Measurements of a Free-free Beam*, Proc. IMAC-7, Las Vegas, Nevada, pp1300-1304, 1989.

33. Cafeo J.A., Tretheway M.W., Rieker J.R. and Sommer III H.J., *Application of a Three Degree-of-Freedom Laser Vibrometer for Experimental Modal Analysis*, Proc. IMAC-9, pp1161-1167, 1992.

34. Lang G.F., *Including Rotational Terms in a Modal Model...An Experimental Prelude*, Sound and Vibration, pp24-32, Nov 1989.

35. Minas C. and Inman D.J., *Experimental Verification of the Theoretically Estimated Rotational Entries of Mode Shapes*, Proc. IMAC-8, pp1190-1194, 1990.

36. Minas C. and Inman D.J., *Model Improvement by using Substructure Modal Testing Results-Case Study*, Proc. IMAC-8, pp62-66, 1990.

37. Cafeo J.A., Tretheway M.W. and Sommer H.J., *Measurement and Application of Experimental Rotational Degrees-of-Freedom for Mode Shape Refinement*, The International Journal of Analytical and Experimental Modal Analysis, Vol 7, No.4, pp255-269, Oct 1992.

38. Cafeo J.A., Tretheway M.W. and Sommer H.J., *On the Use of Measured Rotational Degrees-of-Freedom in Structural Dynamics Modification*, Proc. IMAC-10, pp96-101, Feb 1-4, 1993.

39. Mitchell L.D., *A Perspective View of Modal Analysis*, Keynote Address, Proc. IMAC-6, 1988.

40. Tayeb M.M. and Williams E.J., *Rib Stiffeners for Use in Structural Dynamic Modification*, Proc. IMAC-6, Orlando, Florida, pp1094-1099, 1988.

41. Martinez D. R., Carne T. G., Gregory D. L. & Miller A. K., *Combined Experimental/Analytical Modelling using Component Mode Synthesis*, 25th Structures, Structural Dynamics and Materials Conference, Palm Springs, California. May 14-18, 1984.

42. Maleci G. and Young J. W., *The Effect of Rotational Degrees of Freedom in System Analysis (SA) via Building Block Approach (BBA)*, Proc. IMAC-3, Orlando, Florida, pp1040-1045, 1985.

43. Allemang R.J. and Brown D.L., *A Correlation Coefficient for Modal Vector Analysis*, Proc. IMAC-5, London, pp110-116, 1987.

44. Waters T.P. and Lieven N.A.J., *A Modified Surface Spline for Modal Expansion*, Proc. IMAC-12, pp66-73, 1994.

45. Furusawa M. and Tominaga T., *Rigid Body Mode Enhancement and Rotational DOF Estimation for Experimental Modal Analysis*, Proc. IMAC-4, Los Angeles, pp1149-1155, 1986.

46. Kitson, F. L., *An Algorithm for Curve and Surface Fitting using B-Splines*, Proc. International Conference on Acoustics, Speech and Signal Processing, Glasgow, May, Vol 4, IEEE, pp 1207-1210, 1989.

47. Daniel, C. & Wood, F. S. with the Assistance of Gorman, J. W., *Fitting Equations to Data*, 2nd Ed, John Wiley & Sons, New York, 1980.

48. Miquel, J. & Castells, F., *Curve Fitting Made Easy*, Hydrocarbon Processing, Volume 65 Number 11, pp 121-124, Nov 1986.

49. Lancaster, P. & Salkauskas, K., *Curve and Surface Fitting - An Introduction*, Academic Press, London, 1986.

50. De Boor C., *A Practical Guide to Splines*, Applied Mathematical Sciences, 27, Springer-Verlag, New York, 1978.

51. Cox, M. G. & Hayes, J. G., *Curve Fitting: A Guide and Suite of Algorithms for the Non-specialist User*, NPL, Division of Numerical Analysis and Computing, NAC Report NAC 26, December 1973.

52. Powell M.J.D., *Approximation Theory and Methods*, Cambridge University Press, Cambridge, 1981.

53. Tao T.M. and Watson A.T., *An Adaptive Algorithm for Fitting With Splines*, AIChE Journal, Vol 34, Number 10, pp 1722-1725, Oct. 1988.

54. Cox M.G., *Practical Spline Approximation*, National Physical Laboratory Report DITC 1/82, 1982.

55. Hermanski M. and Ostholt H., *Linking Finite Elements with Experimental Modal Analysis*, International Journal of Analytical and Experimental Modal Analysis, Vol 2, Part 3, pp144-147, 1987.

56. Lieven N.A.J. and Waters T.P., *The application of High Density Measurements to Dynamic Finite Element Reconciliation*, Proc. IMAC-13, Nashville, Tennessee, USA, pp185-192, 1995.

57. Blotter J.D. and West R.L., *Experimental Mechanical Intensity in Plates Using a Scanning Laser Doppler Vibrometer*, Proc. IMAC-13, Nashville, Tennessee, USA, pp1185-1191, 1995.

58. Dierckx P., *An Algorithm for Smoothing, Differentiation and Integration of Experimental Data using Spline Functions*, Journal of Computational and Applied Mathematics, Vol 1, No. 3, pp165-184, 1975.

59. Schoenberg I.J., *Contributions to the problem of Approximation of Equidistant data by analytic functions*, Quart. Appl. Math. 4, pp45-99, 112-114, 1946.

60. Curry H.B. and Schoenberg I.J., *On Polya Frequency Functions IV: The Fundamental Spline Functions and Their Limits*, J. Anal. Maths. 17, pp71-107, 1966.

61. Schoenberg I.J. and Whitney A., *On Polya Frequency Functions III*, Trans. Amer. Math. Soc. 74, pp246-259, 1953.

62. Reinsch C. *Smoothing by Spline Functions*, Num. Math., 10, pp177-183, 1967.

63. De Boor C., *On Calculating with B-Splines*, Journal of Approximation Theory, 6, pp50-62, 1972.

64. Cox M.G., *The Numerical Evaluation of B-Splines*, J. Inst. Math. Applics., 10, pp134-149, 1972.

65. Dierckx P., *A Fast Algorithm for Smoothing Data on a Rectangular Grid while using Spline Functions*, Siam J. Numerical Anal, Vol 19, No. 6, pp1286-1304, 1982.

66. Dierckx P., *An Algorithm for Surface Fitting with Spline Functions*, IMA Journal of Numerical Analysis, 1, pp267-283, 1981.

67. NAG Fortran Library Manual, Mark 14, Numerical Algorithms Group Limited, Oxford, 1990.

68. O'Callahan J.C. and Chou C.M., *Structural Dynamics Modification Using Generalised Beam Mass and Stiffness Matrices*, Proc. IMAC-3, Orlando, Florida, pp477-482, Jan, 1985.

69. Elliott K.B. and Mitchell L.D., *Structural Modification Using Beam Elements*, Proc. IMAC-5, London, England, pp956-965, April, 1987.

70. Tayeb M.M., *Implementation of the Dynamics Modification Theory for the prediction of the Modal Properties of Structures*, PhD Thesis, University of Nottingham, Nottingham, UK, pp51-97, 1987.

71. Richardson M., *Modal Analysis Using Digital Test Systems*, Seminar on Understanding Digital Control and Analysis in Vibration Test Systems, Shock and Vibration Information Centre Publication, Naval Research Lab., Washington D.C., May 1975.

72. Deel J.C. and Luk Y.W., *Modal Testing Considerations for Structural Modification Applications*, Proc. IMAC-3, Orlando, Florida, USA, pp46-52, Jan, 1985.

73. Bendat J.S. and Piersol A.G., *Random Data: Analysis and Measurement Procedures*, Wiley-Interscience, New York, 1981.

74. Wicks A.L. and Mitchell L.D., *A New Means of Estimation of FRF's in the presence of Uncorrelated Signals*, Part I, Proc. 1987 SEM Spring Conference on Experimental Mechanics, Houston, Tx, pp629-634, June 14-19, 1987.

75. Mitchell L.D., Codd R.E., Deel J.C., and Luk Y.W., *An unbiased FRF Estimator*, Proc. IMAC-5, London, England, pp364-373, April, 1987.

76. Allemang R.J., Rost R.W. and Brown D.L., *Dual Input Estimation of Frequency Response Functions for Experimental Modal Analysis of Aircraft Structures*, Proc. IMAC-1, Orlando, Florida, pp333-340, 1982.

77. Ulm S.C., *Investigations into the Effective use of Structural Modification*, Proc. IMAC-3, Orlando, Florida, pp1279-1286, January, 1985.

78. O'Callahan J.C. and Chou C.M., *Study of a Structural Dynamics Modification Procedure with Three Dimensional Beam Elements Using a Local Eigenvalue Modification Procedure*, Proc. IMAC-2, Orlando, Florida, pp945-952, Feb, 1984.

79. Meirovitch L., *Elements of Vibration Analysis*, McGraw-Hill Book Company, New York, pp256, 1975.

80. Davis R., *Advances in Beam Finite Elements and Applications to Stiffened Plates*, PhD Thesis, University of Nottingham, Nottingham, UK, pp81-106, 1972.

81. Green J.S., *Structural Dynamic Modification (Closing the Design Loop)*, Fourth Year Project Thesis, Department of Mechanical Engineering, University of Nottingham, Nottingham, UK, 1989.

82. Wilkes D., *Experiments in Dynamic Modification*, 3rd Year Project, Department of Mechanical Engineering, University of Nottingham, Nottingham, UK, 1993.

83. Warburton G.B., *The Vibration of Rectangular Plates*, Proc. I. Mech. E., Vol 168, No. 12, pp371-384, 1954.

APPENDIX ONE

SOFTWARE DESCRIPTION

A1.1 Introduction

This appendix provides a detailed description of the software which was developed for the work reported in this thesis. To begin with, a general overview of the system of computer programs, termed the Structural Dynamics Modification (SDM) system, is given. A discussion of the details of the individual procedures is then given. In each case, the flowchart is included.

The link between experimentation and curve fitting was an important consideration in this work. Experimental modal parameters were exported from the STAR software to the main-frame computer in Universal File Format (UFF). In order to facilitate this data transfer, the procedure UFFREADER was developed. The flowchart for this procedure is also included in this appendix.

A1.2 General Description of the Structural Dynamics Modification Software

The system of computer programs for expanding translational modal data to include the required rotations and solving the eigen problem of the modified structure consisted of three main computer programs, namely MODS, AUGFITTER, and EIGEN. The computer programs and the associated data files were held in four libraries named SDMFOLDER, WORKLIB, DATALIB and SDMMODLIB. SDMFOLDER held all the computer programs, WORKLIB held the intermediate files containing geometry and display sequence data and the modification matrices, DATALIB was the user's data area containing the initial and augmented modal data files. The general print file which held all the output data for the complete run was held in this library also. SDMMODLIB held all the modification files.

The three system programs were run successively beginning with the procedure MODS. MODS processed and formatted geometry and display sequence data for the fitting procedure and also generated the modification mass, damping and stiffness matrices.

AUGFITTER performed the expansion and therefore produced the required rotational entries at each point. The third program, EIGEN, solved the eigen problem of the modified structure and formatted the resulting data in Universal File Format in readiness for transfer to the STAR modal analysis system for display and further processing. The system was activated by the command SDM(PHIIN=libname.filename, PHIOUT=libname.filename, MODS=libname.filename, PRINTFILE=libname.filename) under which a series of machine commands for the sequential operation had been compiled.

Figure A1.1 shows the lay-out of the SDM system including the internal file manipulation. For completeness, the link to the STAR modal analysis package (and hence the test bed) is also included. The flowchart for the sequential operation of the SDM system is presented as Figure A1.2 while the commands for the sequential operation of the system are given in Listing A1.1.

Two input files were required upon entry into the system, namely the input modal data file, PHIIN, and the modifications file, MODSFILE (shortened to MODS in actual operation). PHIIN contained the number of modes in the database, the total number of measurement points, the number of degrees of freedom for which entries were available at each measurement location (3 or 6), the number of measurement points in the x and y-direction (not applicable for curve fitting), a tag to identify whether smoothing or interpolation was required and the actual modal data. The modification file contained the title of the job, structural geometry and display sequence data (connectivity), modification data stating the type (mass, damping, linear spring or rib stiffener) and location(s) of the modification and the associated parameters, the type of the modification material and the associated properties. This file also held information about whether augmentation was required or not, whether smoothed translations (where applicable) were to be retained or not, whether it was curve fitting or surface fitting required, whether in the case of curve fitting, motion was in two directions and the number and list of the fitting planes. In the display sequence data list, each measurement point was also assigned the number of the plane in which it was to be used during fitting. This information was especially useful in the case of surface fitting where a

measurement point might have to be defined in two fitting planes (if it was at a joint line, for example). Samples of the formats of the files PHIIN and MODSFILE are given in Listings A1.2 and A1.3 respectively.

The file PHIOUT was the main output file containing the eigen solution of the modified structure. A similar format to that used for the file PHIIN was used for this file to facilitate its use as an input file should the need arise.

A1.2.1 Procedure MODS

The procedure MODS, the format and philosophy of which were due to Green [81], was used to read and process the modifications file, MODSFILE. The information held in this file was processed using column headers and modules. The subroutine SPOT was used to identify whether the line contained module identifiers, column headers or numbers such as coordinates, display sequence data or modification details. For the preparation of the modification matrices and tagging of the points to be used in fitting and/or evaluation, the subroutine ACTION was used.

The output from this procedure, which was the processed coordinates with the associated tags, the display sequence data and the modification mass (DELTAM), damping (DELTAC) and stiffness (DELTAK) matrices, was separately stored in intermediate files. The coordinates and display sequence information were also written to the output UFF file for the modified structure. This file would later have the modal data from the solution of the eigen problem appended to it.

Figure A1.3 gives the flowchart for the procedure MODS.

A1.2.1.1 Coordinate Transformation

In the definition of the fitting problem, it was recognised that the line or plane of the fit may not always lie in the global x-direction for curve fitting or the global x-y plane for surface fitting. It was therefore necessary to transform the global axes to a local set of coordinates such that the line of curve fitting was always the local z-direction and the plane of surface fitting was always the local z-x plane. This transformation involved the rotation of the global

axes about the global x, y and z axes in turn, to produce the new set of local axes x', y' and z'. The angles required for the transformation were obtained using the structural geometry and trigonometric properties. These were then used to assemble the matrices for transformation to and from the local axes using the subroutine MATMAK. Fitting was carried out in the local axes to produce a set of local rotations which were then transformed back into the global coordinate system. The subroutine TRANS was used to effect the transformation from global to local axes and vice-versa.

The need to realign global axes into local ones also demanded that the modification matrices had to be assembled in local axes and then transformed into the global axes before storage. In the case of the rib modifications, the modification matrices were formulated using the offset beam element in local axes and were transformed to the structural points using the subroutine OFFTRANS.

A1.2.2 Procedure AUGFITTER

The procedure AUGFITTER was the main focus of the work reported in this thesis since the estimation of the rotations was carried out here. The expansion of the modal data was performed, a single mode at a time, in local axes using the NAG subroutines E02BEF for curve fitting and E02DDF (smoothing) or E02DAF (interpolating) for surface fitting. The transformation from global to local axes and vice-versa was done using the same subroutines as in the procedure MODS.

AUGFITTER required translational modal data and processed geometry and display sequence data (from MODS) as input data. The flags relating to whether augmentation was required, whether curve or surface fitting was required and whether, in the case of curve fitting, there were two directions of motion were contained in the file containing the processed geometry data.

The fit functions obtained from the subroutines E02BEF and E02DDF or E02DAF were differentiated and evaluated using the NAG subroutines E02BCF and E02DEF for curve and surface fitting respectively. The subroutine E02BCF evaluated and differentiated the curve fit function and also evaluated the derivative while the surface fit function was evaluated

using the subroutine E02DEF. Subsequent partial differentiation of the surface fit function and evaluation of the derivatives were performed by the subroutine E02BCF. It must be noted that the optimisation conditions were applied following the evaluation of the fit function and its derivative(s) but in local axes. The output from this procedure was stored in the file PHIINAUG. It must be remembered that PHIINAUG would not only contain modal entries at the measurement points, it would also include the entries for other non-modal points which may have been included in the geometry definition for purposes of locating modifications.

Figure A1.4 presents the flowchart for this procedure.

A1.2.3 Procedure EIGEN

The procedure EIGEN, based on a code by Green [81], was used to transfer the modification matrices to the modal space of the unmodified structure (modal space 1) and to formulate and solve the eigen problem for the prediction of the dynamic effects of structural changes to the original structure. The input data to this procedure was the augmented data file, PHIINAUG, and the modification matrices, DELTAK, DELTAC and DELTAM.

Transfer of the eigen problem to modal space 1 was effected by the subroutine MODAL while the NAG subroutine F02GJF solved the eigen problem. Since the output from the NAG eigen solver contained both negative and positive eigen values, it was necessary to sort the output such that only the positive eigen values and their associated eigen vectors were retained. It will be noted that at this stage, the solution vectors were in modal space 1. It was therefore necessary, for purposes of display and further processing (if required), to transfer this data into the physical space of the modified structure.

While the output from this procedure was stored in the file PHIOUT, it was also written to the UFF file (which at this stage already contained the coordinate and display sequence information from MODS) in preparation for transfer to the STAR package.

The flowchart for this procedure is given in Figure A1.5.

A1.3 Linking the Test Bed with the SDM System

In order to facilitate data transfer from the test bed to the main-frame computer, on which the SDM system was installed, the procedure UFFREADER was developed. This procedure was used to read the modal data from test, which was in Universal File Format, and to subsequently format this data for entry into the procedure AUGFITTER. Geometry and display sequence data was also formatted according to the MODSFILE format.

Development of the code for the procedure UFFREADER was based on the use of two copies of the input UFF file. From the first copy, all the data was read as characters. These were then used to identify and classify the various types of data lines in the line recognition subroutine SPOT using pre-defined records. The actual numbers were read from the second copy of the UFF file after they had been identified as such from the first copy.

This procedure was activated by the command UFF in which the command structure required to successfully run the procedure was compiled. The flowchart of the procedure is presented in Figure A1.6. The command sequence is also given in Listing A1.4.

o0o

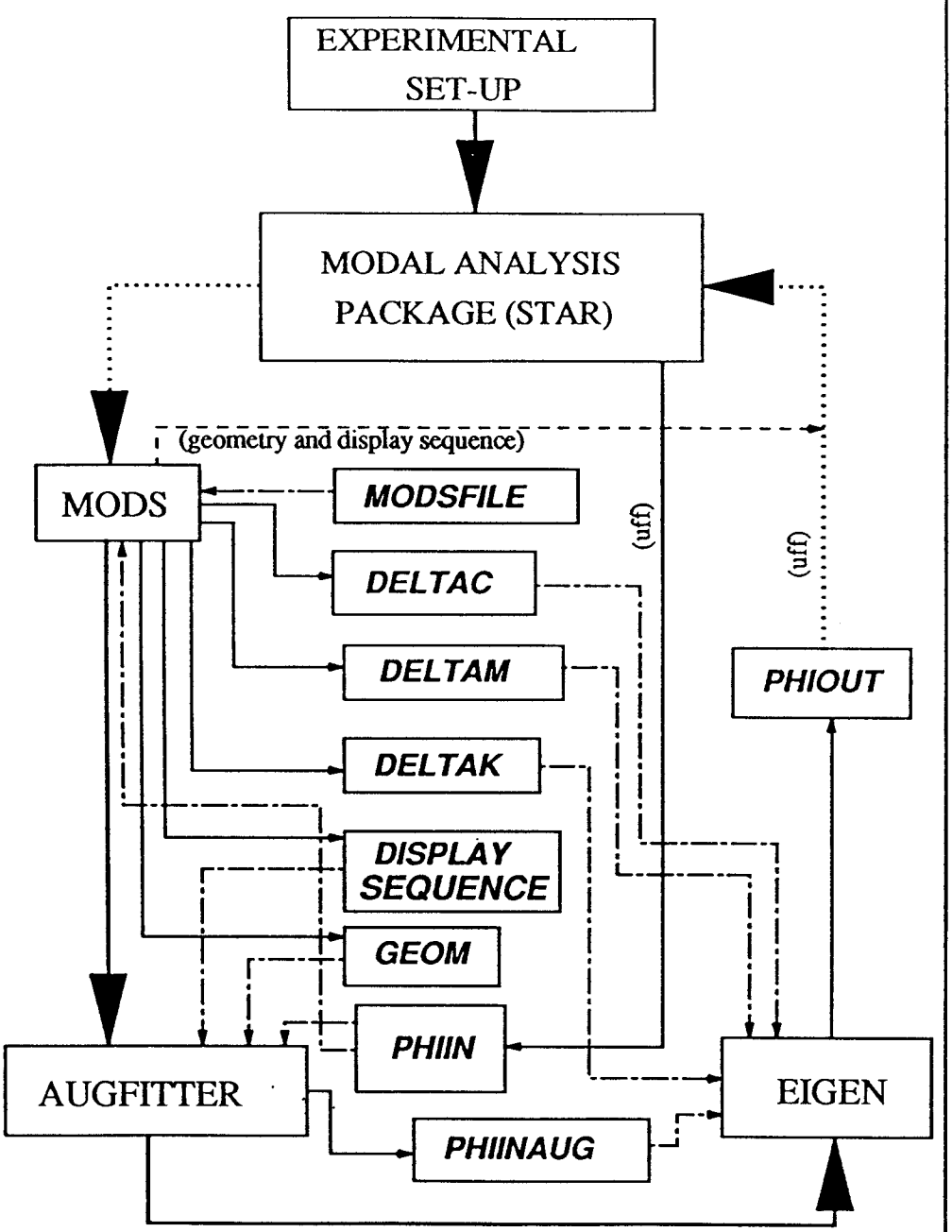

Figure A1.1: SDM System Layout including Internal File Handling

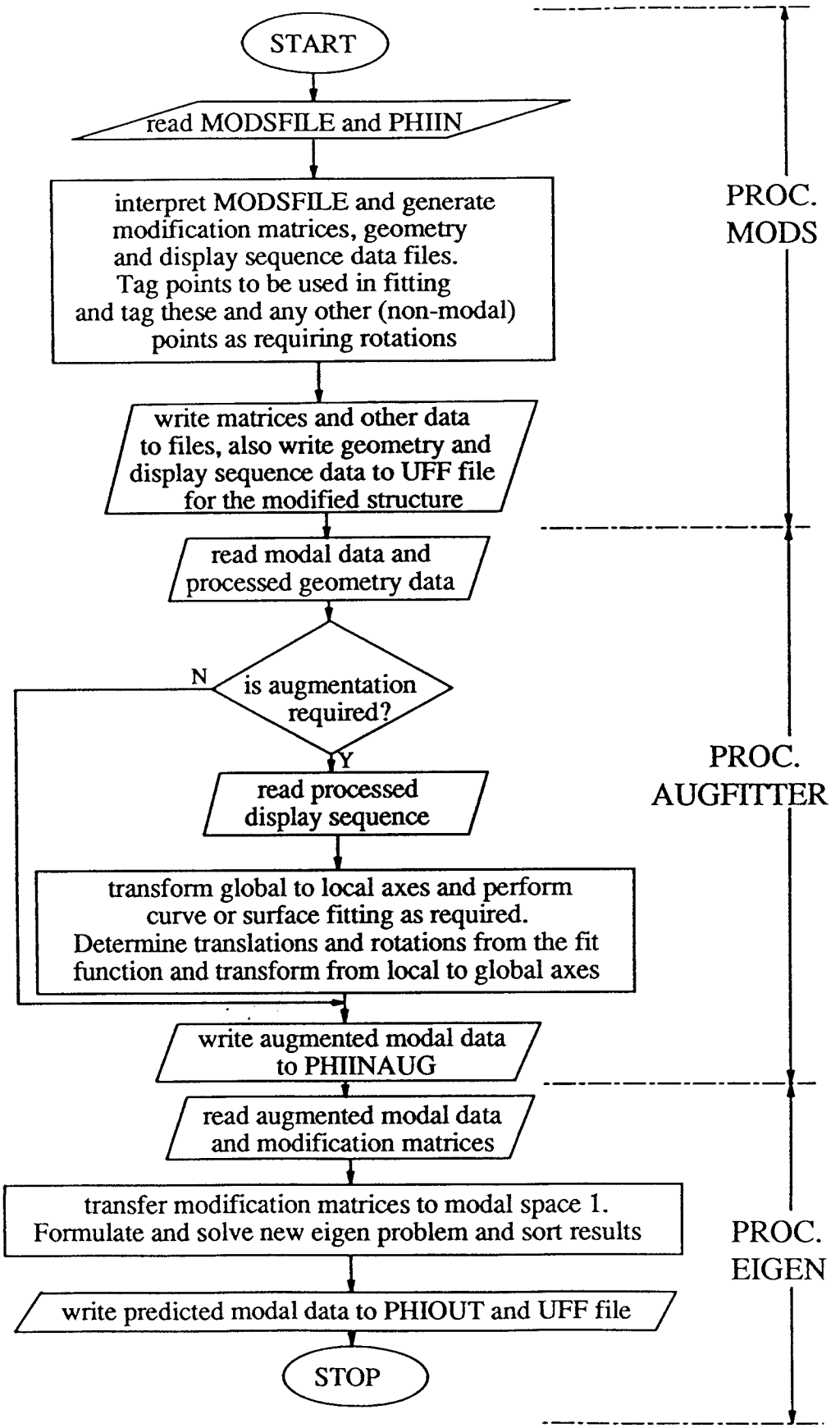

Figure A1.2: Flowchart for the Sequential Operation of the SDM System

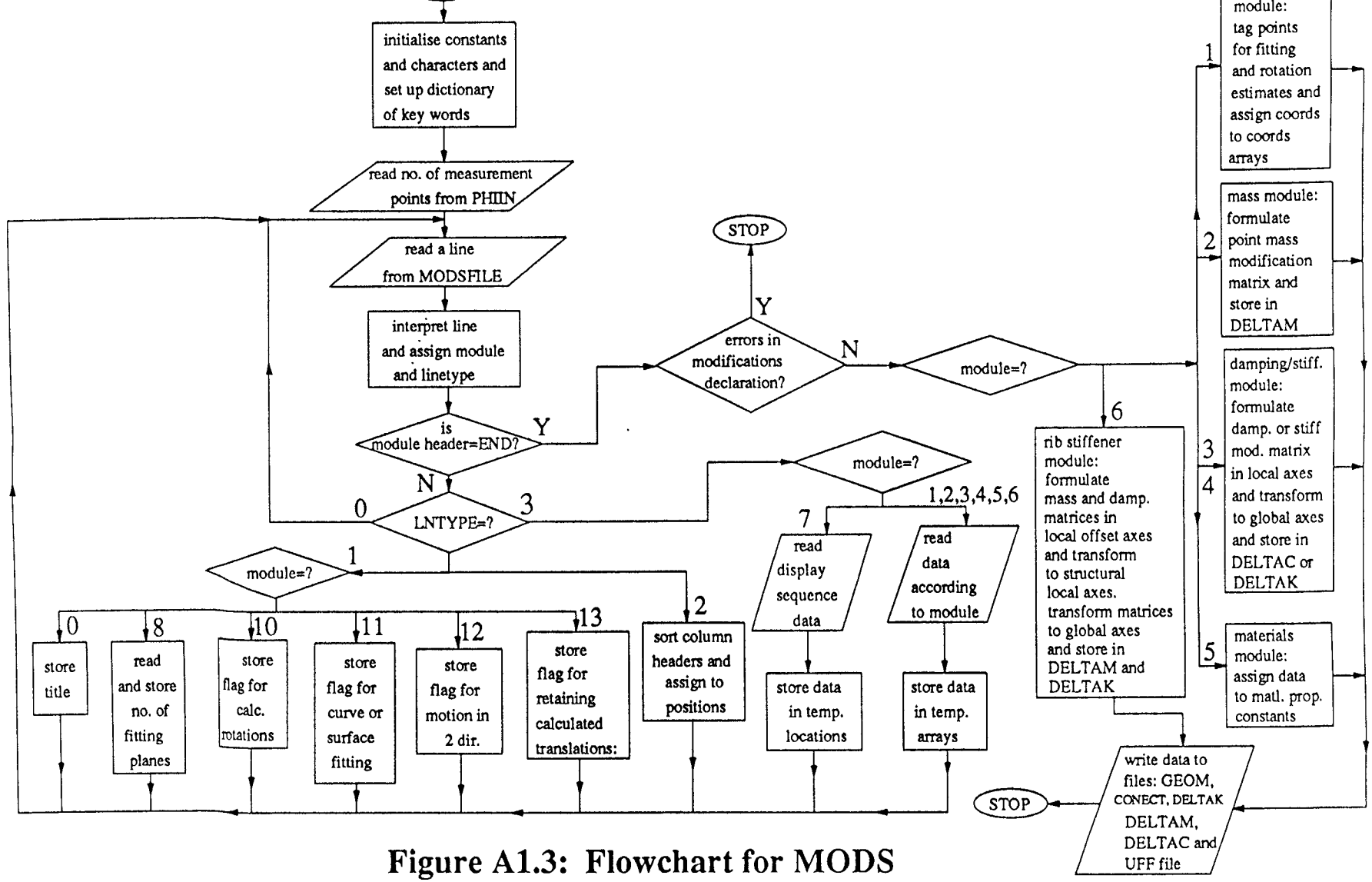

Figure A1.3: Flowchart for MODS

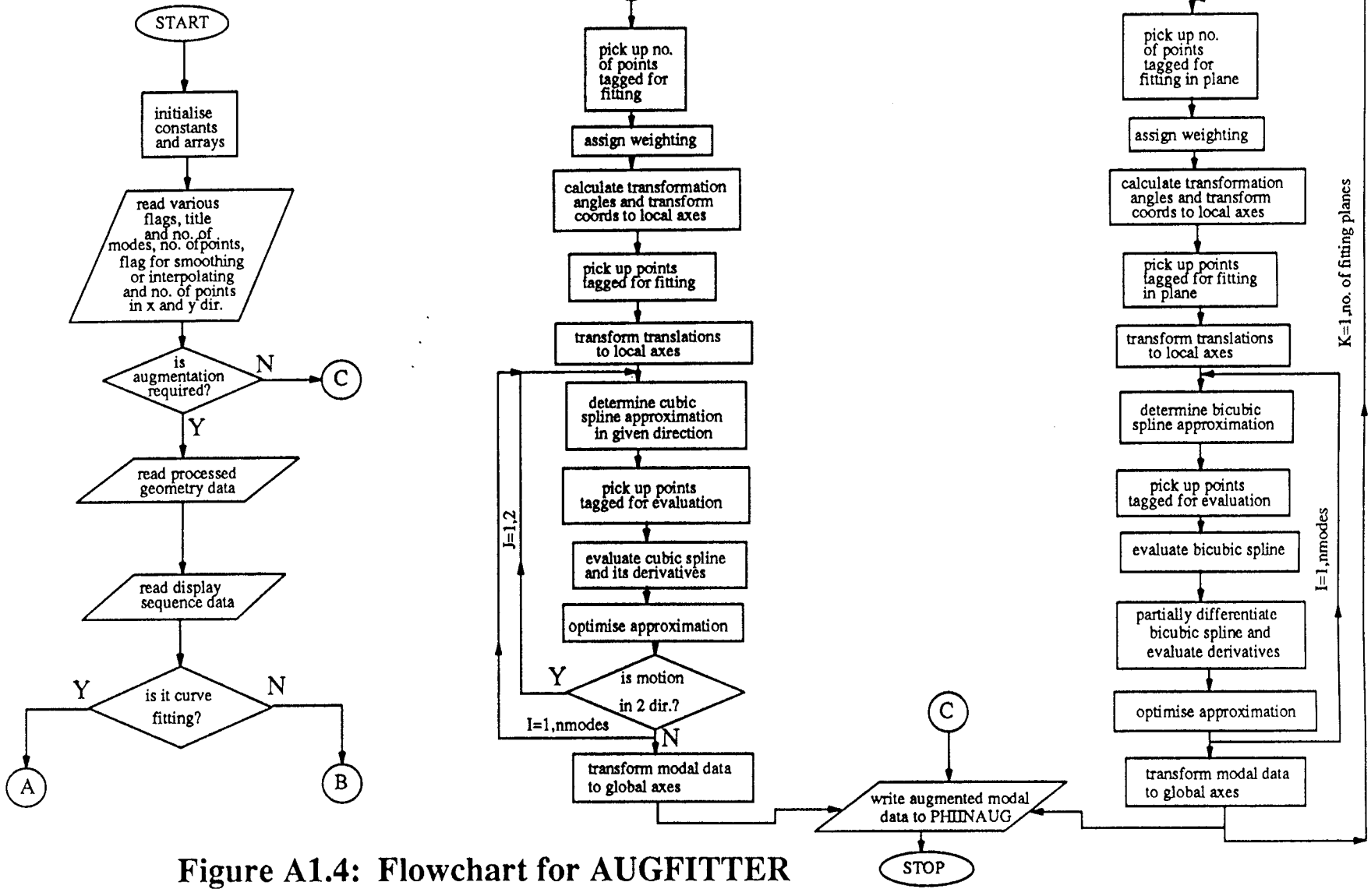

Figure A1.4: Flowchart for AUGFITTER

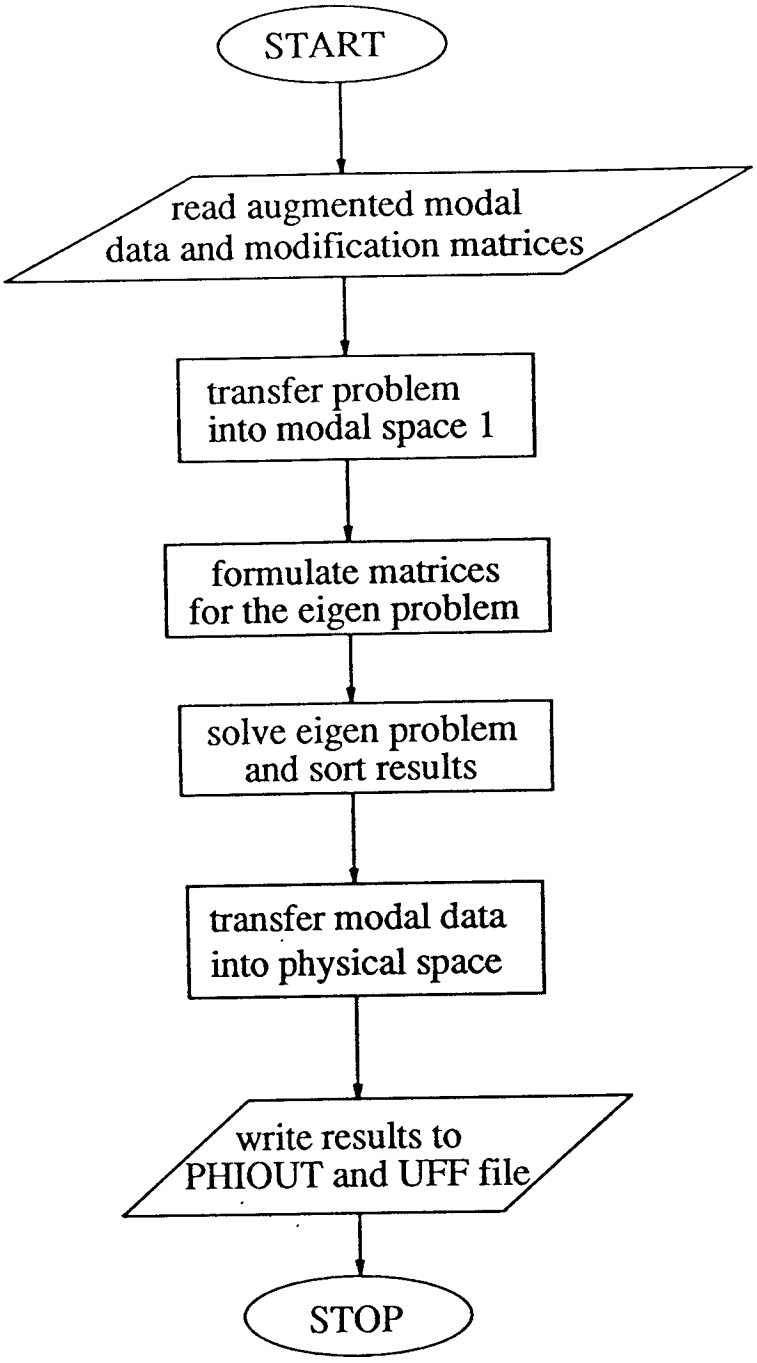

Figure A1.5: Flowchart for EIGEN

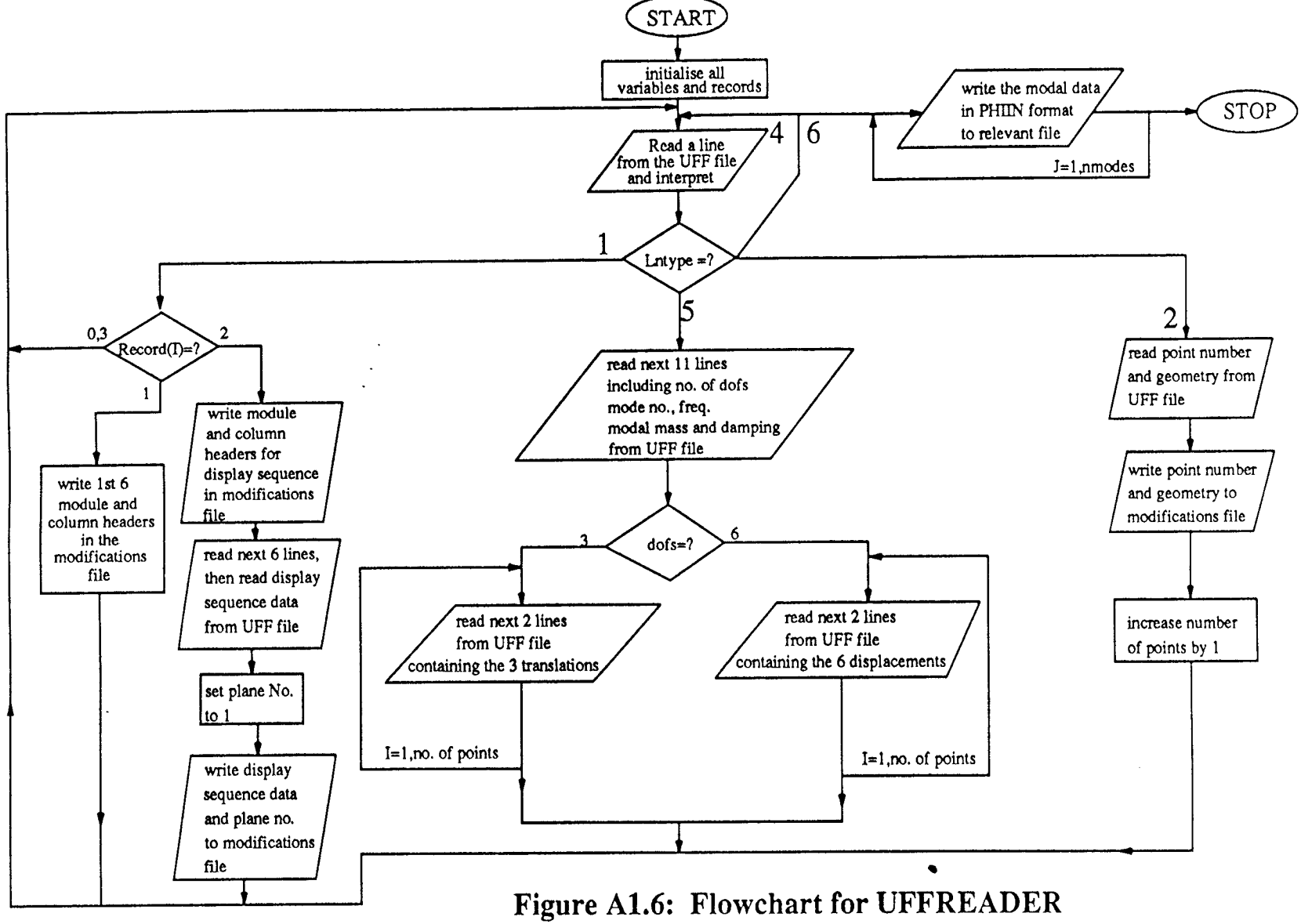

Figure A1.6: Flowchart for UFFREADER

Listing A1.1: Sequential Command Structure of the SDM System

```
PROC SDM IS (LITERAL PHIIN,LITERAL PHIOUT,LITERAL MODS,
LITERAL PRINTFILE:="WORKLIB.PRINT")
BEGIN
SEND_MESSAGE(" ")
SEND_MESSAGE("   STRUCTURAL DYNAMICS MODIFICATIONS")
SEND_MESSAGE("      Mechanical Engineering Dept.")
SEND_MESSAGE("         Nottingham University")
SEND_MESSAGE(" ")
ALBL(*NAGF)
STRING WORK:="WORKLIB.MODS",
      DC:=":.DELTAC",
      DK:=":.DELTAK",
      DM:=":.DELTAM",
      GEOM:="WORKLIB.GEOM",
      CONECT:="WORKLIB.CONECT",
      PHIAUG:=PHIIN+"AUG",
      PRINT:=PRINTFILE
      UFF:="UFFLIB.UFFFILE"
ULB(WORKLIB)
GWF(TEMP,INITSIZE=7168)
CNF(VAL PRINT,FUNIT=PRINT,INITSIZE=7168,MAXSIZE=7168,LIST=N)
CNF(VAL UFF,FUNIT=8,ACCESS=W,MAXSIZE=1024,LIST=N)

   BEGIN
   CNF(VAL MODS,FUNIT=1,ACCESS=R,LIST=N)
   ECCE(VAL MODS,VAL WORK,CONTROL)
   CNF(VAL WORK,FUNIT=2,ACCESS=R,LIST=N)
   CNF(VAL PHIIN,FUNIT=3,ACCESS=R,LIST=N)
   CNF(VAL DM,FUNIT=11,ACCESS=W,LIST=N)
   CNF(VAL DC,FUNIT=12,ACCESS=W,LIST=N)
   CNF(VAL DK,FUNIT=13,ACCESS=W,LIST=N)
   CNF(VAL GEOM,FUNIT=14,ACCESS=W,LIST=N)
   CNF(VAL CONECT,FUNIT=15,ACCESS=W,LIST=N)
   CF77(SDMFOLDER.MODS,LIST=NONE,SWCHECKS=NONE)
   RUN(SDMFOLDER.MODS,DFILE=WORKLIB.DIAG)
   SEND_MESSAGE("PHASE 1 COMPLETED")
   END
CNF(TEMP,FUNIT=PRINT,LIST=N,MAXSIZE=7168)

   BEGIN
   CNF(VAL PHIIN,FUNIT=3,ACCESS=R,LIST=N)
   CNF(VAL PHIAUG,FUNIT=4,ACCESS=W,LIST=N)
   CNF(VAL GEOM,FUNIT=14,ACCESS=R,LIST=N)
   CNF(VAL CONECT,FUNIT=15,ACCESS=R,LIST=N)
   CNF(DATALIB.THTXLP1,FUNIT=9,ACCESS=W,LIST=N)
   CNF(DATALIB.THTXLP2,FUNIT=10,ACCESS=W,LIST=N)
   CF77(SDMFOLDER.AUGFITTER,LIST=NONE,SWCHECKS=NONE)
   RUN(SDMFOLDER.AUGFITTER,DFILE=WORKLIB.DIAG)
   SEND_MESSAGE("PHASE 2 COMPLETED")
   END
APF(TEMP,VAL PRINT)
```

```
CNF(WORKLIB.UFF,FUNIT=8,ACCESS=W,LIST=N)

  BEGIN
  CNF(VAL PHIAUG,FUNIT=4,ACCESS=R,LIST=N)
  CNF(VAL DM,FUNIT=11,ACCESS=R,LIST=N)
  CNF(VAL DC,FUNIT=12,ACCESS=R,LIST=N)
  CNF(VAL DK,FUNIT=13,ACCESS=R,LIST=N)
  CNF(VAL PHIOUT,FUNIT=5,ACCESS=W,LIST=N,INITSIZE=1024,MAXSIZE=1024)
  CF77(SDMFOLDER.EIGEN,LIST=NONE,SWCHECKS=NONE)
  RUN(SDMFOLDER.EIGEN,DFILE=WORKLIB.DIAG)
  SEND_MESSAGE("PHASE 3 COMPLETED")
  END
APF(TEMP,VAL PRINT)
APF(WORKLIB.UFF,VAL UFF)
SEND_MESSAGE("SDM COMPLETED")
END
```

Listing A1.2a: PHIIN Input Data File - 3 DOF Format

```
nmodes          nnodes          ndof            inter           mmz             mmx

FREQ(1)         DAMP(1)
PHI(1,1,X)              PHI(1,2,X)              PHI(1,3,X)...           PHI(1,nnodes,X)
PHI(1,1,Y)              PHI(1,2,Y)              PHI(1,3,Y)...           PHI(1,nnodes,Y)
PHI(1,1,Z)              PHI(1,2,Z)              PHI(1,3,Z)...           PHI(1,nnodes,Z)

FREQ(2)         DAMP(2)
PHI(2,1,X)              PHI(2,2,X)              PHI(2,3,X)...           PHI(2,nnodes,X)
PHI(2,1,Y)              PHI(2,2,Y)              PHI(2,3,Y)...           PHI(2,nnodes,Y)
PHI(2,1,Z)              PHI(2,2,Z)              PHI(2,3,Z)...           PHI(2,nnodes,Z)
      .                       .                       .                       .
      .                       .                       .                       .

FREQ(nmodes)  DAMP(nmodes)
PHI(nmodes,1,X)  PHI(nmodes,2,X)  PHI(nmodes,3,X)...  PHI(nmodes,nnodes,X)
PHI(nmodes,1,Y)  PHI(nmodes,2,Y)  PHI(nmodes,3,Y)...  PHI(nmodes,nnodes,Y)
PHI(nmodes,1,Z)  PHI(nmodes,2,Z)  PHI(nmodes,3,Z)...  PHI(nmodes,nnodes,Z)
```

Listing A1.2b: PHIIN Input Data File - 6 DOF Format

```
nmodes          nnodes          ndof            inter           mmz             mmx

FREQ(1)         DAMP(1)
PHI(1,1,X)  PHI(1,1,Y)  PHI(1,1,Z)  PHI(1,1,θX)  PHI(1,1,θY)  PHI(1,1,θZ)
PHI(1,2,X)  PHI(1,2,Y)  PHI(1,2,Z)  PHI(1,2,θX)  PHI(1,2,θY)  PHI(1,2,θZ)
      .       .       .       .       .       .
      .       .       .       .       .       .
PHI(1,nnodes,X)  PHI(1,nnodes,Y)  PHI(1,nnodes,Z)  PHI(1,nnodes,θX)  PHI(1,nnodes,θY)
PHI(1,nnodes,θZ)

FREQ(2)         DAMP(2)
PHI(2,1,X)  PHI(2,1,Y)  PHI(2,1,Z)  PHI(2,1,θX)  PHI(2,1,θY)  PHI(2,1,θZ)
PHI(2,2,X)  PHI(2,2,Y)  PHI(2,2,Z)  PHI(2,2,θX)  PHI(2,2,θY)  PHI(2,2,θZ)
      .       .       .       .       .       .
      .       .       .       .       .       .
PHI(2,nnodes,X)  PHI(2,nnodes,Y)  PHI(2,nnodes,Z)  PHI(2,nnodes,θX)  PHI(2,nnodes,θY)
PHI(2,nnodes,θZ)
      .       .       .       .       .       .
      .       .       .       .       .       .

FREQ(nmodes)  DAMP(nmodes)
PHI(nmodes,1,X)  PHI(nmodes,1,Y)  PHI(nmodes,1,Z)  PHI(nmodes,1,θX)  PHI(nmodes,1,θY)
PHI(nmodes,1,θZ)
PHI(nmodes,2,X)  PHI(nmodes,2,Y)  PHI(nmodes,2,Z)  PHI(nmodes,2,θX)  PHI(nmodes,2,θY)
PHI(nmodes,2,θZ)
      .       .       .       .       .       .
      .       .       .       .       .       .
PHI(nmodes,nnodes,X)  PHI(nmodes,nnodes,Y)  PHI(nmodes,nnodes,Z)  PHI(nmodes,nnodes,θX)
PHI(nmodes,nnodes,θY)  PHI(nmodes,nnodes,θZ)
```

Listing A1.3: MODSFILE Input Data File Format

TITLE: (up to 60 characters in length)

ROTATIONS: NO/YES (only one space after the colon)

MOTION IN 2 DIRECTIONS? NO/YES (only one space after the colon)

SMOOTHED TRANSLATIONS REQUIRED? NO/YES (only one space after the colon)

SINGLE VARIABLE? NO/YES (only one space after the colon)

NUMBER OF FITTING PLANES = 1 (up to ten planes may be defined)

LIST OF PLANES
1

GEOMETRY (module header)

NODE	X	Y	Z	(column headers)
1	0.00000	0.00000	0.00000	(all dimensions in m)
2	0.02500	0.00000	0.00000	
3	0.05000	0.00000	0.00000	
4	0.07500	0.00000	0.00000	
5	0.10000	0.00000	0.00000	

Note: The number of nodes in this module will correspond to the number defined in PHIIN. Any node number greater than NNODES is considered a non-modal node, i.e.; one for which modal displacements are not available but are required for modification or otherwise. The required displacements are generated from the fit function.

CONNECTIVITY (Display Sequence)

NODE	PLANE	
1	1	(the start of a new line in the display sequence is indicated by 0)
2	1	
3	1	
4	1	
5	1	

MASSES

NODE	MASS	IX	IY	IZ

DAMPERS

FROM	TO	COEF	TORS

Note: COEF defines the damper coefficient while TORS is the torsional damping coefficient. A value of zero in either the FROM or TO columns specifies that the point is to be tied to ground.

SPRINGS

FROM	TO	STIF	TORS

Note: A value of zero in the FROM or TO columns indicates ground.
STIF and TORS are the linear stiffness (N/m) and the torsional stiffness (Nm/rad) of the spring respectively.

RIBS
FROM TO IN_PLANE OUT_PLANE AREA J MATERIAL EXOF EYOF

Note: AREA denotes the rib cross-sectional area. IN_PLANE and OUT_PLANE are the moments of area. EXOF and EYOF denote the offset of the rib and MATERIAL denotes the material number (should match the value in the MATERIAL module). J is the polar moment of inertia of the cross section.

MATERIAL
NUMBER E G RO

Note: NUMBER denotes the material number specified in the RIBS module. E, G and RO are the Young's modulus, Torsional modulus and density of the material.

END

Note: All values in the MASSES, DAMPERS, SPRINGS, RIBS and MATERIAL modules must be in SI units.

Listing A1.4: Command Structure for the UFF file Reading Procedure

```
PROC UFF IS (LITERAL INUFF)
BEGIN
SEND_MESSAGE(" ")
SEND_MESSAGE("   UFF FILE READING MODULE")
SEND_MESSAGE("   DEPT. OF MECHANICAL ENGINEERING")
SEND_MESSAGE("   Nottingham University")
SEND_MESSAGE(" ")
ULB(UFFLIB)
STRING WORK:="WORKLIB.INUF",
      PHIIN:="UFFLIB.PHIIN",
      MODS:="UFFLIB.MODSFILE"
CNF(VAL INUFF,FUNIT=7,ACCESS=R,LIST=N)
ECCE(VAL INUFF,VAL WORK,CONTROL)
CNF(VAL WORK,FUNIT=4,ACCESS=R,LIST=N)
CNF(VAL PHIIN,FUNIT=9,ACCESS=W,LIST=N)
CNF(VAL MODS,FUNIT=8,ACCESS=W,LIST=N)
CF77(UFFREADER,LIST=NONE)
RUN(UFFREADER)
SEND_MESSAGE("READING OF UFF FILE COMPLETED")
END
```

APPENDIX TWO

THE OFFSET BEAM ELEMENT

A2.1 Introduction

In his study of the vibration of eccentrically stiffened plates, Davis [80], took account of the eccentricity of a stiffener by using an "offset" beam element. This element is obtained by applying a transformation to the stiffness and mass matrices of the simple beam element. Three key conclusions ensued from his work:

(i) good agreement with exact frequencies was obtained for most modes of vibration,

(ii) special constraints did not have to be applied between the beam and the plate elements in order to take account of the offset of the rib,

(iii) large under-estimates were made in the frequency of vibration of the systems if the eccentricity of the stiffening beams was not taken into account (the error in the fundamental frequency when the stiffeners were taken as simple beams was of the order of ten times greater than when they were idealised with the offset beam).

For these reasons, the analysis involving rib stiffeners which is reported in this work used the offset beam element formulation for the mass and stiffness matrices.

This appendix gives a brief exposition of the theoretical background of the element and discusses aspects relevant to its application in this thesis.

A2.2 Development of the Element

In order to account for the eccentricity of beam stiffeners, it is necessary to find the effect of forces and displacements on a node of a beam which is some distance away from the node of interest. To do this, a transformation is performed on the simple two-node beam element mass and stiffness matrices. Details of the derivation of the transformation now follow.

Let point A (Figure A2.1) be a node on a structure. Point B is one end of a beam which is offset from point A in the y and z directions by e_y and e_z respectively. It is required that the

forces and displacements on the beam be referred to node A on the structure. The relationships between $\{P_i\}'$ and $\{P_i\}$ and $\{\delta_i\}'$ and $\{\delta_i\}$ at nodes B and A respectively can easily be shown to be

$$\{P_i\}'^* = [W]^* \{P_i\}^* \tag{A2.1}$$

and

$$\{\delta_i\}'^* = [Q]^* \{\delta_i\}^* \tag{A2.2}$$

(Matrices and vectors with a * refer to a single node and those without refer to a two-node system)

where

$$[W]^* = \begin{bmatrix} 1 & 0 & 0 & 0 & 0 & 0 \\ 0 & 1 & 0 & 0 & 0 & 0 \\ 0 & 0 & 1 & 0 & 0 & 0 \\ 0 & e_z & -e_y & 1 & 0 & 0 \\ -e_z & 0 & 0 & 0 & 1 & 0 \\ e_y & 0 & 0 & 0 & 0 & 1 \end{bmatrix}$$

and

$$[Q]^* = \begin{bmatrix} 1 & 0 & 0 & 0 & e_z & -e_y \\ 0 & 1 & 0 & -e_z & 0 & 0 \\ 0 & 0 & 1 & e_y & 0 & 0 \\ 0 & 0 & 0 & 1 & 0 & 0 \\ 0 & 0 & 0 & 0 & 1 & 0 \\ 0 & 0 & 0 & 0 & 0 & 1 \end{bmatrix}$$

The set of forces and displacements on the simple beam is related by

$$\{P_i\}' = [K] \{\delta_i\}' \tag{A2.3}$$

where [K] is the stiffness matrix for the simple beam.

Substituting equations (A2.1) and (A2.2) into (A2.3) gives

$$\{P_i\} = [W]^{-1}[K][Q]\{\delta_i\}$$

with

$$[W] = \begin{bmatrix} [W]^* & [0] \\ [0] & [W]^* \end{bmatrix}$$

and

$$[Q] = \begin{bmatrix} [Q]^* & [0] \\ [0] & [Q]^* \end{bmatrix}$$

Now

$$[W]^{-1} = [Q]^T$$

therefore

$$\{P_i\} = [Q]^T[K][Q]\{\delta_i\} \qquad \text{(A2.4)}$$

where $[Q]^T[K][Q]$ is the stiffness matrix of the offset beam. The element mass matrix must be similarly transformed using [Q].

A2.3 Application of the Element for Rib Stiffener Modifications on Beams

In the application of the element for modifying a beam (i.e., increasing the depth), it was indicated in Chapter 5 that the results (Figure 5.21a) showed an oddity which was not readily explainable. An attempt was therefore made to identify the source of the discrepancy. This involved FE analyses involving a free-free beam and a cantilever beam using the offset element. In the formulation of the problem, a rib of the same dimensions as the base structure was added to the original structure using the offset element. The base structure, with dimensions of 500 x 25.4 x 12.7 mm, was in each case modelled using 60 beam elements.

Figure A2.2 presents the comparison of the FE predictions with the exact solutions. The rigid body modes are omitted for the free-free beam and in both cases, only modes with displacement in the direction of the offset were considered. It will be seen from the plots that the FE solutions under-predicted the frequencies with increasing under-prediction as the mode number rises. These results were compared with physical space solutions using mass and stiffness matrices generated by the procedure MODS and solved using the procedure EIGEN. The comparison yielded no discrepancies. While no attempt was made to investigate the cause for the behaviour seen in figure A2.2, the results at least confirmed that the coding in the procedures MODS and EIGEN was correct.

Comparison of Figure A2.2 with Figure 5.21a shows that although the modal method initially over-predicted the frequencies with subsequent under-prediction, the characteristic shape of the error plot seen in Figure A2.2 is still inherent in Figure 5.21a. The initial over-prediction seen in Figure 5.21a is a manifestation of the shift of the error curve (i.e., higher errors in the modal predictions) due to the effects of truncation on the modal prediction and is therefore not surprising.

It will be noted that the offset element finds widespread use in work involving the stiffening of plates using rib stiffeners and does not seem to suffer from the anomalies seen in the application in this work. This may be attributed to the fact that in plate work, the rib does not undergo as much deformation as it does when it is attached to a beam (i.e., only the first or second flexural modes of the rib are excited at the most) and thus the stiffener largely experiences rigid body motion and the question of the motion of the neutral axis then becomes trivial. In modifications involving beam analysis, it would seem that the formulation does not account for any changes in the position of the neutral axis of the modified structure which the modification may impose. This makes the structure overly flexible thus leading to under-prediction of the frequencies.

Thus, it may be concluded that the use of the offset element in work involving beams requires further investigation in order to enhance its application.

o0o

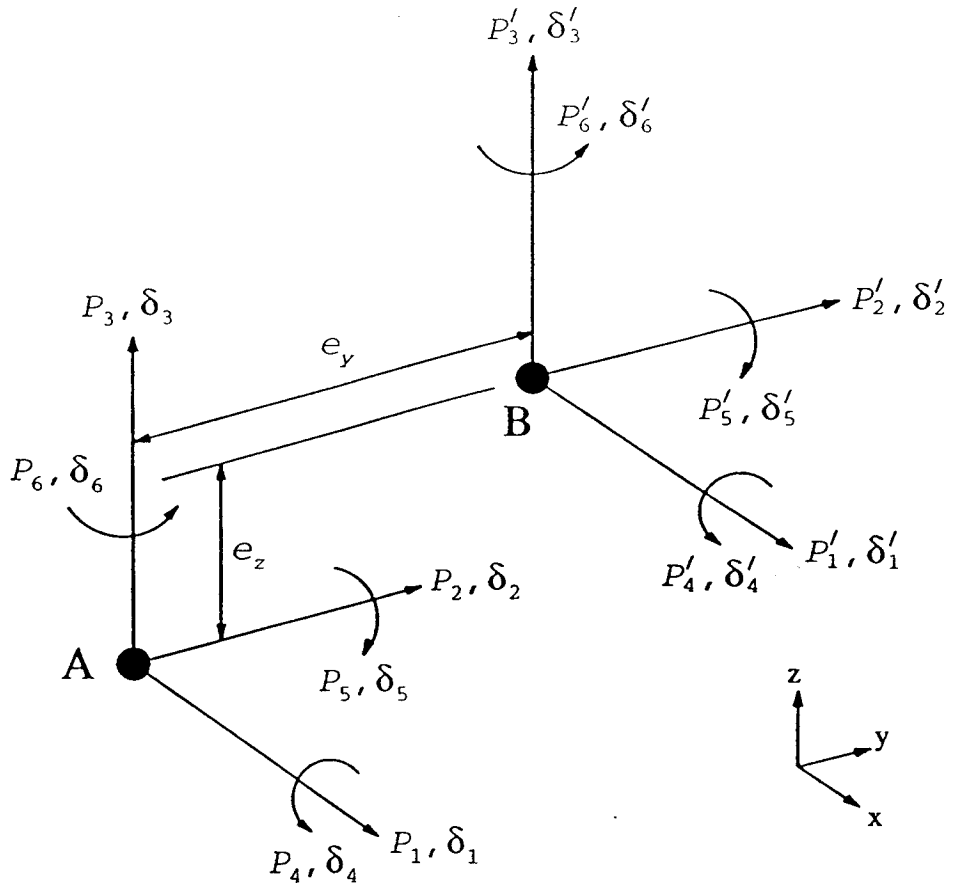

Figure A2.1: Force and Displacement system for an offset beam

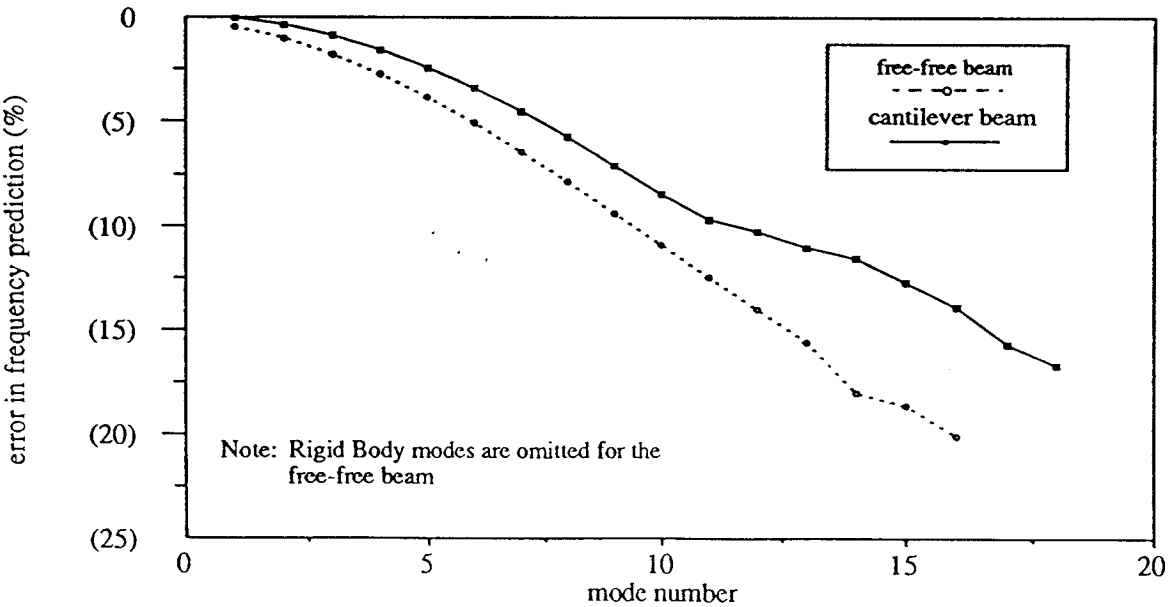

Figure A2.2: **Comparison of FE Predictions using the offset beam element with analytical solutions for full-length/full-width rib modifications (100% depth increase)**

APPENDIX THREE

ANALYSIS ON EXPERIMENTAL DATA

A3.1 Introduction

In this thesis, exact and simulated experimental data has been used to establish the performance of spline curve and surface fitting for the estimation of rotations. The analysis has presented key findings and conclusions along with guidelines for optimum performance of the proposed method. However, the real test of an approximation method is its ability to return acceptable estimates of rotations from real experimental data. In this regard, this appendix endeavours to demonstrate the performance of the proposed technique on real experimental data.

It must however be recognised that the use of real experimental data suffers from the basic limitation that the level of error in the initial data is unknown. Therefore conclusions from such studies must always be treated with caution. In addition, boundary conditions cannot always be truly reproduced in theoretical analysis and thus comparisons are difficult to make.

In the discussion which now follows, an attempt is made to illustrate the performance of the proposed technique on less-than ideal data. The databases used are less-than ideal because they do not follow the guidelines given in Chapter 6 with regard to the density and distribution of measurement points. It was envisioned that this limitation would serve to exaggerate any shortcomings of the proposed technique in less-than ideal conditions. The discussion considers the accuracy of the estimation of rotations with emphasis on the errors in the resulting structural dynamics modification (SDM) predictions. Of the two case studies which are presented, the surface fitting case provides new insights into the treatment of multi-surface structures at the joint lines.

A3.2 Perspex Cantilever Beam

In order to demonstrate the performance of the optimum estimator established from the analysis on simulated experimental data in Chapter 4, investigations were carried out on a Perspex cantilever beam, 575 x 25.4 x 12.7 mm. Frequency response functions (FRF's) were

measured at 24 structural points using the impact excitation test method. The data was captured using the PC-based Data Physics (DP420) multi-channel Fast Fourier Transform (FFT) analyzer for frequencies up to 2500 Hz. Each measurement was subsequently calibrated, for phase and magnitude, using a calibration FRF measurement obtained by the free-free mass technique [3], to ensure that the resulting modal parameters would be as accurate as possible. Modal parameters were extracted from the FRF measurements by global curve fitting for the first eight flexural modes of the cantilever beam using the PC-based modal analysis package called STAR and it was noted that the mode shape vectors were, in the main, real.

In order to assess the adequacy of the resulting modal vectors, the Modal Assurance Criteria (MAC) computation was performed on the experimental modal vectors. The results of the auto-MAC computation, shown in Table A3.1, reveal that, in general, the modal vectors were acceptably orthogonal.

A3.2.1 Estimation of Rotations

Estimates of the rotations were obtained by curve fitting the experimental data with the spline function which minimised the rotation at the fixed end with all the data points carrying the same weight on the assumption that all the measurements were of similar accuracy. Rotations were also computed from the Euler-Bernoulli solution of the classical cantilever equation.

One of the important considerations when working with experimental data is the quantification of the level of error in the initial data. In the absence of a proven method of determining the magnitude of the measurement errors present in a modal data base, a 'feel' of the extent of the error in the data used in this study was obtained by computing the percentage error in the translations when compared against exact data. This comparison, which is presented representatively in Figure A3.1 in the form of error plots for modes 2, 4 and 8 of the cantilever, indicated that the discrepancies were random. The magnitude of the error was largest at the free end. The effect of a point density which is not optimised is also particularly evident at the free end. Nevertheless, the level of error in the experimental translations was seen to be generally of the order of 4-7%.

The comparison of the computed rotations (using the optimum fit function as defined above) against the exact values is presented in Figure A3.2. It will be seen from the figure that even with this less-than ideal database, the errors in the estimates of rotations (normalised to the largest rotation for each mode) are, in the main, less than 10%. This very welcome observation demonstrates the capability of the proposed technique for smoothing noisy data. However, the real test is the accuracy of the resulting structural dynamics modification predictions.

A3.2.2 Modifications on the Cantilever Beam

The cantilever beam was modelled using 24 two-noded beam finite elements. Translational and rotational modal data for the first eight flexural modes was obtained from FE analysis. This was compared with the modal data derived from the modal test as described above. The comparison of the modal data from the two sources is given in Table A3.2. The table shows a very good correlation between the two data-sets although the FE solution slightly over-predicted the frequencies. This was attributed to the inability to experimentally create a perfectly clamped boundary condition which allowed some flexibility in the structure.

Rotations were also obtained from the FE data using an interpolating spline.

In the cases which are discussed below, a mass of 0.2 kg (representing approximately 91% of the mass of the beam) was added at a location 557.5 mm from the fixed end while the inertia associated with it was varied by changing the geometry of the modification as shown in Figure A3.3.

A3.2.2.1 Short Cylindrical Mass near the Free End.

A short cylindrical mass having a moment of inertia of 1.0457×10^{-4} kgm^2 was added near the free end of the cantilever. The effect of the combined modification is illustrated by the drop in the fundamental frequency from 11.6 Hz to 4.5 Hz, the mass being the dominant contributor to the reduction in frequency. The severity of the modification is understood better with the aid of the Modal Assurance Criterion (MAC) values computed from the unmodified and modified structural modal databases of the experimental data shown in Table A3.3. Although the first mode does not exhibit a large change in the mode shape as shown

by the MAC value of very nearly unity, it had the largest shift in frequency (in excess of 60%) due to the modification and would thus be expected to yield the largest error in the prediction. It will also be noted that because the value of the added inertia is small in comparison with the added mass, the modification is heavily dependent on the translation at the modification location although the rotation also plays a significant role.

Table A3.4 compares the Dual Modal Space Method (DMSM) predictions using FE translations and rotations and calculated translations and rotations from FE and experimental translations, with results from an experimental modal analysis of the modified structure. The FE prediction of the modification is also included ((1)). It must also be noted that the translation at the modification location was not measured. The value used in the computation was obtained from the fit function following expansion.

A cursory examination of Table A3.4 immediately reveals good agreement between the predictions from the various databases even though the errors in the predictions do not exhibit a regular trend with increase in mode number. The similarity in the errors of the predictions from FE-based databases ((2), and (3)) under-pins the good performance of the interpolant on supposed error-free data. It will also be noted that the frequencies are, in the main, over-predicted. This is consistent with the under-estimation of the rotations at the modification location as shown in column 4 of Table A3.4.

It is interesting to note that the magnitude of the error in the rotations was not directly related to the magnitude of error in the frequency predictions. Nevertheless, the large error in the prediction of the fundamental mode deserves special mention. While the error in the rotation derived from experimental data for the fundamental mode was about -51%, the error in the prediction of the frequency for that mode using experimental data was of the same order of magnitude as the FE-based predictions, albeit slightly lower. It will be noted that the error in the FE rotation at the modification location for mode 1 was less than 0.025% while that in the calculated rotation from FE translations was less than 0.4%. It would therefore seem that the error in the prediction of the fundamental mode was not due to the error in the rotations but due to some other effect. The results of the FE prediction of the modification suggest that, as would be expected, the physical clamping in the experimental set-up did not

completely constrain all movement at the supposed clamped end of the cantilever as was presumed in the modal predictions. This, therefore, introduced some extra flexibility into the experimental structure and is the reason for the modal over-prediction of the fundamental mode seen in all the databases used in the study.

The errors in the modal predictions for modes 4 to 8 were attributed to a combination of two effects. Firstly, these modes showed significant changes in the original mode shapes, as shown by the MAC values in Table A3.3, thereby pointing to the inability of the DMSM to form the new modes as combinations of the old ones. Therefore the degraded performance of the predictor for the higher modes was not surprising. Secondly, modes 4, 5 and 6 had, next to the first mode, the largest shifts in frequency (30%).

When the errors in the predictions are viewed in the light of the error in the rotations at the modification location, it is clear that the predictions are relatively insensitive to the errors in the modal vectors.

A3.2.2.2 Long Cylindrical Mass near the Free End.

In this case, a long cylinder having a moment of inertia of 2.6748×10^{-3} kgm^2 (about 25 times larger than the value used in the previous case and approximately 9 times smaller than that of the beam itself) was added at the same location as in the previous case. The effect of this modification is signified by the large drop in the frequency of the second mode from 77.8 Hz to 32.3 Hz compared to the reduction to 59.8 Hz in the previous case. The results of the MAC computation for the modal data of the modified structure against the modal data of the unmodified structure, shown in Table A3.5, confirm the relative increase in the degree of the severity of the modification when compared with the previous case. The MAC values for modes 3 to 7 show very little correlation between the mode shapes before and after the modification thereby suggesting significant changes in the mode shapes. This was further illustrated by the relative contributions of the modes in the original data set to the modes of the modified structure. Examination of the relative contributions revealed that all the original eight modes contributed to all but two (modes 1, and 2) of the new modes, with the relative contributions of the higher modes increasing with increasing mode number. Thus, for this relatively severe modification, large errors in the predictions would not be unexpected. This

expectation was also supported by the fact that the shift in the frequencies of the new modes were greater than those seen in the previous case although the magnitudes of the shift were seen to drop with increase in the mode number.

Table A3.6 gives the results using the four databases as described in the previous case. The results are once again seen to be broadly similar although the finite element prediction is distinctly better than the modal predictions. It will also be noted that using FE rotations in the analysis ((2)) yielded marginally poorer predictions than using calculated rotations from FE translations.

As would be expected, the results show a modest increase in the errors in the predictions due to the larger inertia applied in this case and once again show over-prediction which is consistent with the under-estimation of the rotations at the modification location. However, the errors in the prediction based on the experimental database (excluding that for the fundamental frequency), which range from 2% to 24% ((4) in Table A3.6), confirm the good performance of the DMSM while at the same time suggesting no correlation with the pattern or magnitude of the errors in the rotations. The rather high over-prediction of the fundamental frequency is once again evident. It is also interesting to note that the pattern of the errors in the prediction in this case is different from that seen in the previous case. This is attributed to a change in the mix of modes which were used to constitute the new modes. This is highlighted by the differences in the MAC comparisons as shown in Tables A3.3 and A3.5.

A3.3 L-Beam Plate Structure

In this case, a modal test was performed on a 10mm thick Perspex L-beam plate structure [82], 100 x 200 x 520mm, shown in Figure A3.4, using the impact excitation method. The measurements were taken at 118 points. Excitation was applied in both the x and y directions at the points along the joint line. This gave rise to 131 FRF measurements. The FRF's thus obtained were processed as previously described for the case of the cantilever beam and the modal parameters were extracted accordingly using a global curve fitter for the first 8 flexural modes of the structure and it was noted that the identified mode shapes were, in the main, real. The resulting mode shapes are presented in Figure A3.5.

A3.3.1 Estimation of Rotations

According to published work [83], if it is assumed that the waveforms of vibrating plates and beams are similar, the waveform of a plate can be obtained as the product of the characteristic functions for two beams with similar boundary conditions. The boundary conditions associated with rectangular plates will therefore be seen to be similar to those associated with beams. Thus for rectangular plates, a free edge supports neither bending moment nor shear while a clamped edge permits neither rotation nor translation. However, both the free and the simply supported boundary conditions for plates are considerably more complex than the equivalent beam boundary conditions. Based on this background therefore, the acceptance threshold for the surface approximation was set to be the fit which minimised the error in the rotations at the fixed end of the L-beam structure. Translations and rotations were also obtained from a finite element analysis of the structure modelled as in the test. This data was used as the comparison base in the discussion which now follows.

A3.3.1.1 Joint Line Considerations

It is important to understand from the outset that, in this case, two entries of rotational data about the z-axis (Figure A3.4) were generated at the joint line. Experience with this type of structure had indicated that because the planes of the structure are necessarily treated separately during the fitting process (since only one out-of-plane direction can be used for each fit), the resulting fit functions for each plane may not (and indeed did not) yield the same values of the rotations about the z-axis at the joint line due to the different parameters upon which the fit function depends for each plane. It was therefore necessary to pay attention to the following considerations in this regard:

(i) Which of the estimates about the z-axis at the joint line were to be retained in the final data and might the average of the two entries be a more accurate estimate?

(ii) in each plane, did the fit functions yielding the best estimates of the rotations about the z-axis also yield the best estimates of the rotations about the x and y axes? If not,

(iii) did the fit functions which yielded the best estimates of the rotations about the x and y axes in each plane also yield acceptable rotations about the z-axis?

Ideally, it was envisaged that the fit functions which produced the best rotations about the z-axis would also yield the best estimates of the rotations about the x and y axes. However, since the results clearly indicated that this was not the case, it became necessary to determine the ground rules to be used in order to obtain the best approximations. The comparison base was the FE database containing the rotations of the structure. Comparison of the results from the two planes indicated that the estimates of the rotations about the z-axis from the larger of the two plane surfaces (plane 1) were in the main more accurate than those from the smaller plane (plane 2). This was attributed to the better representation of the structure in the larger plane (more measurement points) than was the case in the smaller plane. The averages of the two entries were generally found to be less accurate than the values from plane 1. Table A3.7 summarises the results for mode 2 which is typical of the behaviour for the other modes. The estimates of the rotations about the z-axis from the fit on the larger plane were therefore retained in the final data set.

With regard to the second and third considerations, the fitting results indicated conflicting behaviour. In the case of the estimates of the rotation about the y-axis, the fit function which gave the best estimates of the rotations about the z-axis did not also yield the best rotations about the y-axis. The estimates of the rotations about the y-axis from the fit function which gave the best rotations about the z-axis were found to be generally unacceptably poor (Table A3.8). In this case, it was necessary to search for the fit function in plane 1 which produced the best estimates of the rotations about the y-axis. It must however be noted that this estimation did not satisfy the requirements for the rotations about the z-axis as illustrated in Tables A3.7. On the other hand, the fit function which gave the best estimates of the rotations about the z-axis in plane 2 in the main also produced the best estimates of the rotations about the x-axis (see Table A3.8). This suggested that in order to obtain the best estimates of the rotations about the x-axis it was necessary to search for the fit function which produced the best estimates of the rotations about the z-axis in plane 2 and to retain the estimates of the rotations about the x-axis from that fit function.

A3.3.1.2 The Fitting Results

The fitting results in the main confirmed the trends which were observed from the curve fitting analysis and the analysis on surface fitting using error-free data. Based on the

acceptance threshold of minimising the error in the rotations at the fixed end of the structure, the results revealed that generally, this criteria was also satisfactory at the joint line. Away from the joint line, the data was much more oscillatory. However, the results indicated that, generally, the error in the estimates of rotations was below 30%.

A3.3.2 Mass Modification on the L-Beam Plate Structure

The modification was physically performed after which a modal test was carried out to obtain the modal parameters of the modified structure [82]. Finite element analysis was also performed in order to provide a theoretical comparison base. Modal predictions were obtained from two sources; namely from the dual modal space method based on FE rotations and rotations computed from the experimental translations of the unmodified structure, and the SDM facility available on the STAR modal analysis system. The experimental measurements were used as the platform upon which the predictions were validated. It must be noted that the STAR system does not take account of rotations in the predictions.

A point mass of 0.51 kg (representing $^1/_4$ of the mass of the unmodified structure) having moments of inertia of 1.36×10^{-4} kgm^2, 8.5×10^{-5} kgm^2 and 8.5×10^{-5} kgm^2 about the x, y and z axis respectively was added to the structure at measurement point 23 as shown in Figure A3.6. Choice of this modification location was based on its proximity to the antinode of the third mode which is at point 8. It was envisaged that this modification would significantly reduce the frequency of the third mode. Table A3.9a summarises the results and confirms this expectation.

From the results in Table A3.9a, it is immediately clear that the predictions based on experimental data are superior to those based on FE data, an observation which was not unexpected due to the difficulty associated with reproducing the physical boundary conditions in the finite element model. This does not only highlight the good quality of the experimental data, it also suggests that for this modification, the predictions are relatively insensitive to the errors in the estimates of the rotations at the modification location (given in Table A3.9b). In addition, the results also highlight the benefit which derives from smoothing the original data. A comparison of columns (2) and (3) in Table A3.9a indicates that the predictions

based on the smoothed data are generally superior over those based on the unsmoothed translations.

When the errors in the SDM predictions are viewed in the light of the STAR predictions of the modification (Table A3.9a, (4)), it becomes clear that, except for mode 3, this modification does not in fact require the rotational entries at the modification location. However, mode 3 requires special attention as it exhibited the largest shift in frequency from the unmodified value to the modified value, which was the desired effect of the modification. Inclusion of the rotational entries at the modification location for this mode shows a marked improvement in the prediction (36% error in the prediction of frequency from STAR down to less than 0.3% from the DMSM). An examination of the mode shapes revealed that the seven other modes in the database had little or no slope across the modification location. However in the third mode, the modification location was in the proximity of the dominant antinode of the mode, an area in which significant bending across the modification location would be expected. Inclusion of the rotational entries at point 23 allowed the modal prediction to correctly model the behaviour of the structure at that point.

Table A3.9a also highlights relatively large errors in the FE and modal predictions (based on FE rotations) of the fourth mode. The errors in the translations at the modification location (compared to the FE values), given in Table A3.9b, show that the largest errors were in the translational data for the fourth mode. This indicated that the FE translational value at point 23 was responsible for the errors in the FE prediction and the modal prediction based on FE data.

A comparison of the errors in the predictions of the modifications with the errors in the computed rotations indicates that the errors in the predictions are not very sensitive to the errors in the rotations. In addition, there was no direct relationship between the pattern of the errors in the rotations and the pattern of the errors in the predictions of frequency.

A3.4 General Concluding Remarks

In this appendix, an attempt was made to show how the approximating technique performs in a less-than ideal environment. The results have shown that the estimates of the rotations

using structural boundary conditions as acceptability criteria are satisfactory for structural dynamics modification work. The results indicated that the errors in the predictions are generally less than 15% even with errors in the rotations which are in excess of 40%.

The analysis on the plate-like structure has shown that where the cross-section of a plate structure requires treating the structure as separate planes during surface fitting, the rotational entries to be retained at the joint lines are those from the planes with the larger cross-sectional dimensions.

It must however be recognised that in studies such as the one conducted in this case, interpretation of the results is very difficult since it is not easy to determine a comparison base which can take account of the various sources of error in the experimental database. In addition, the theoretical model only approximates the experimental model and does not always truly represent the experimental boundary conditions. The errors ensuing from such sources are not quantifiable.

Nevertheless, it may be concluded that the proposed method of estimating rotations performs satisfactorily on experimental data and that the resulting rotations are adequate for structural dynamics modification applications, even when the database used is less-than ideal.

o0o

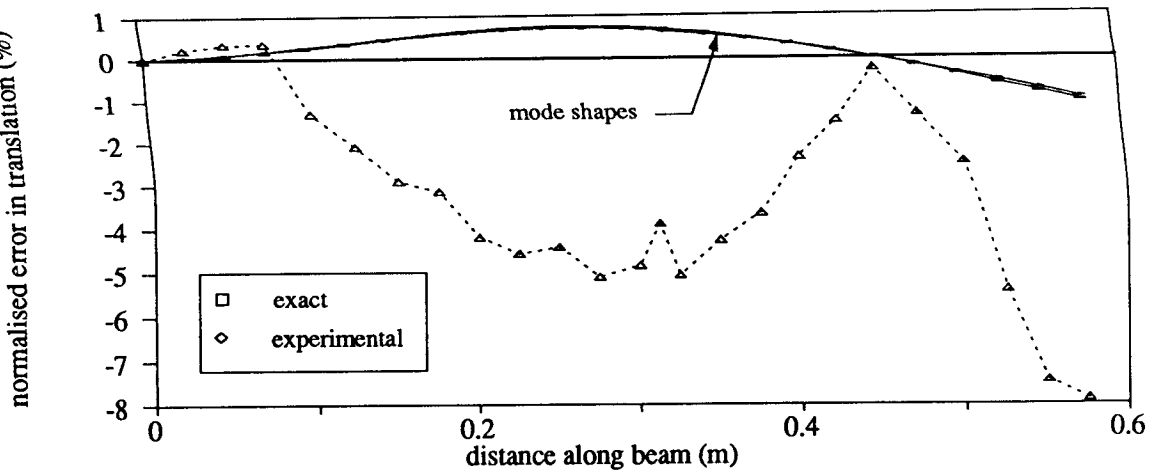

(a) mode 2

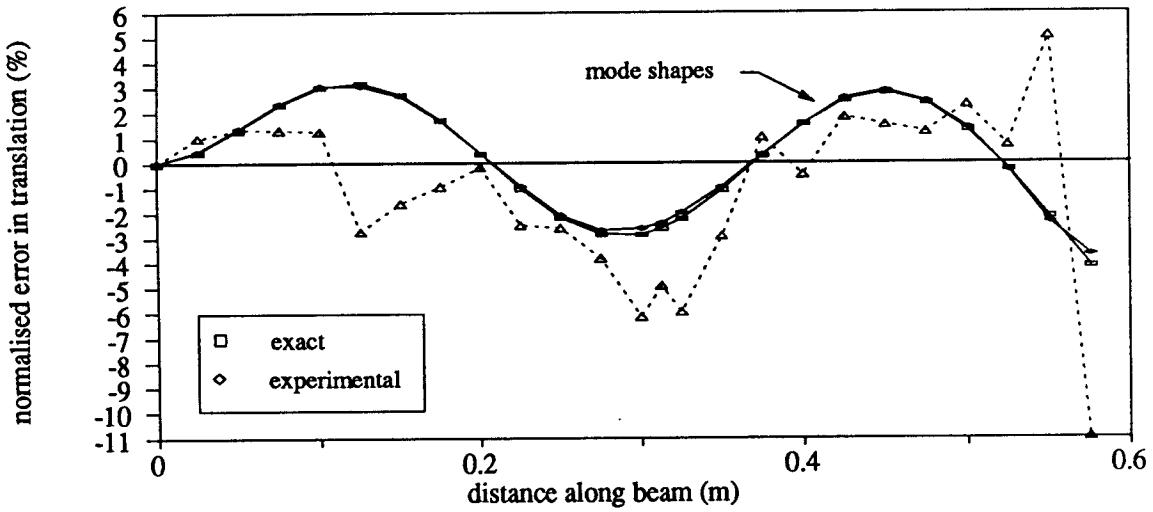

(b) mode 4

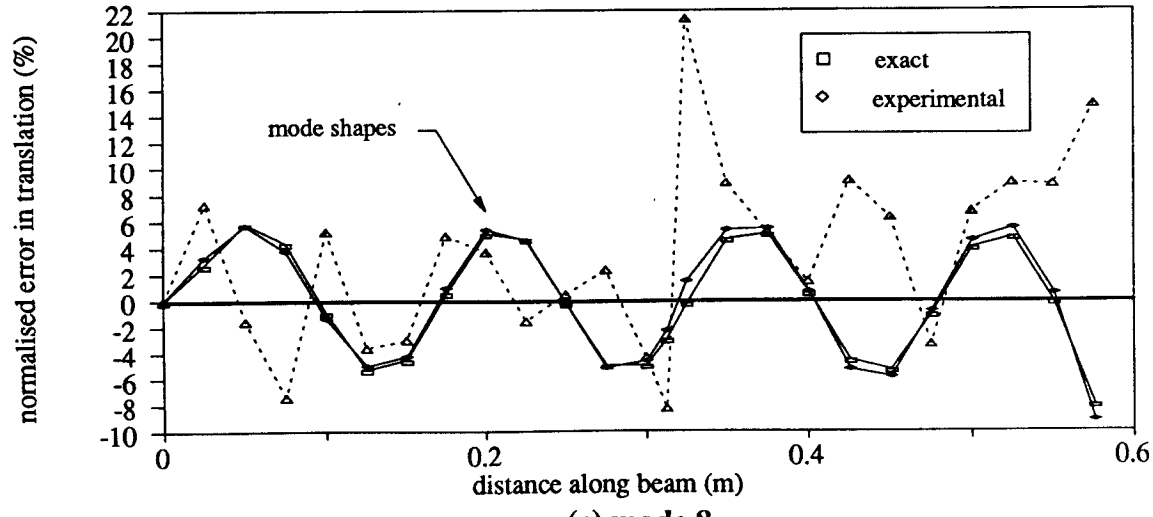

(c) mode 8

Figure A3.1: **Normalised Mode Shapes and Error in Experimental Translations for Selected Flexural Modes of the Perspex Cantilever**

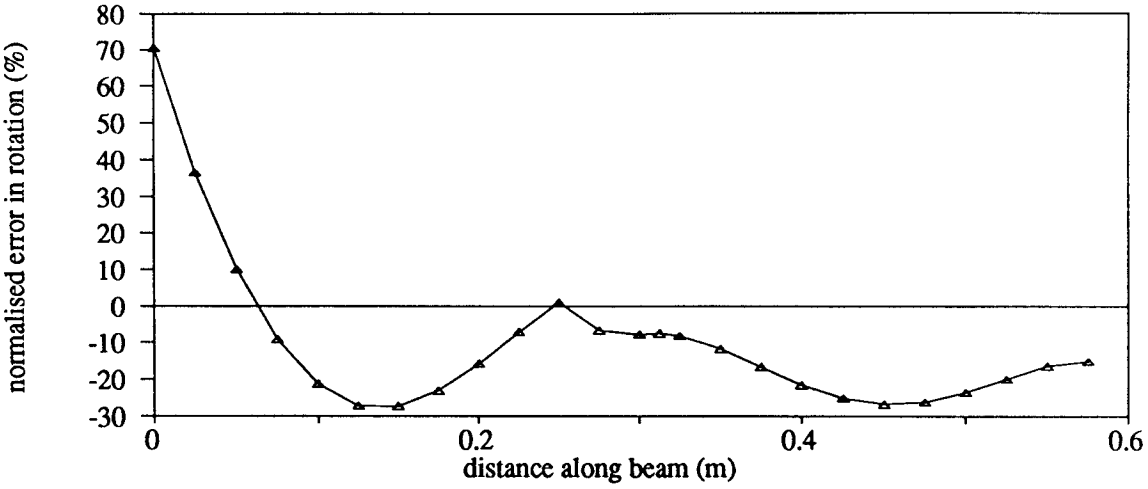

(a) mode 2

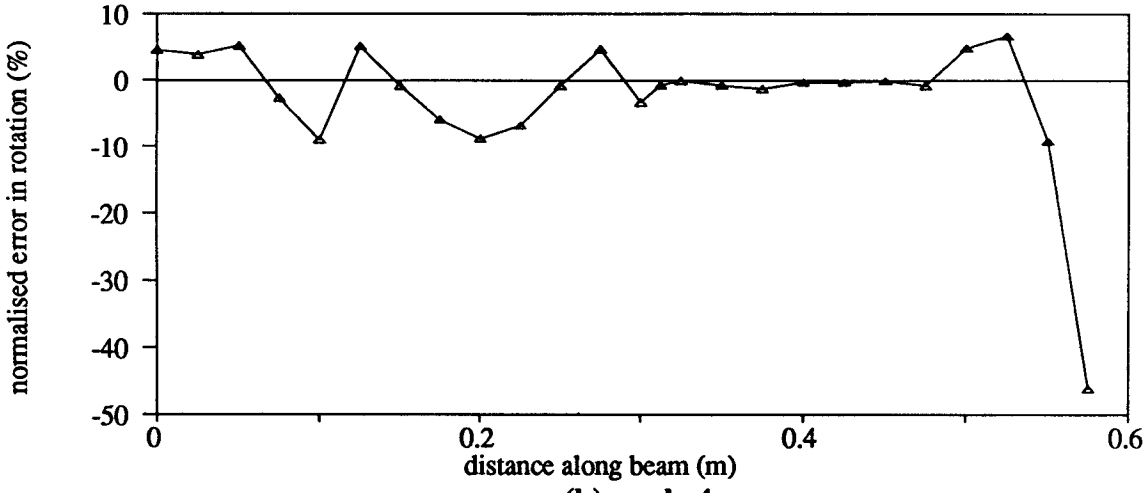

(b) mode 4

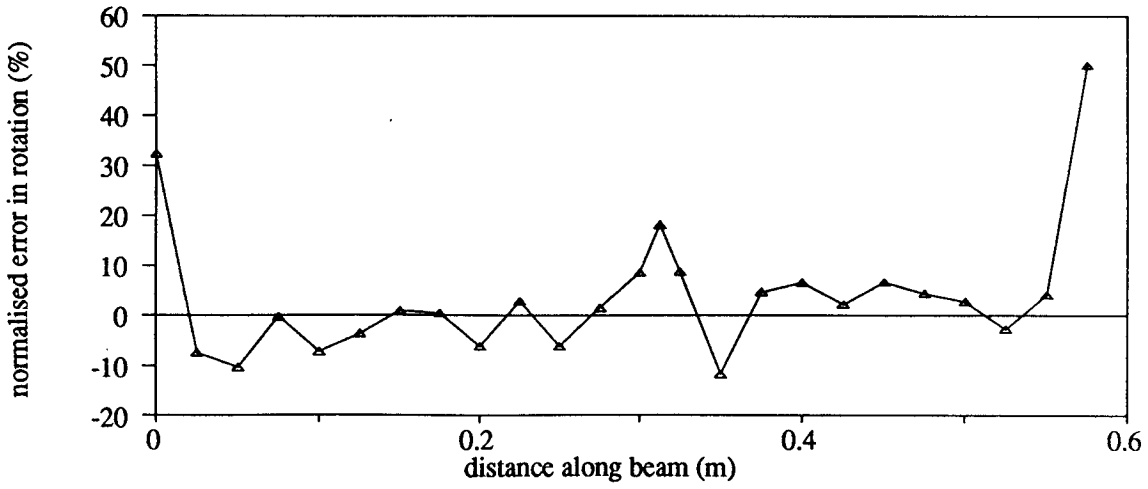

(c) mode 8

Figure A3.2: **Variation of the Normalised Error in the Calculated Rotations from Experimental Data Along the Length of the Perspex Cantilever**

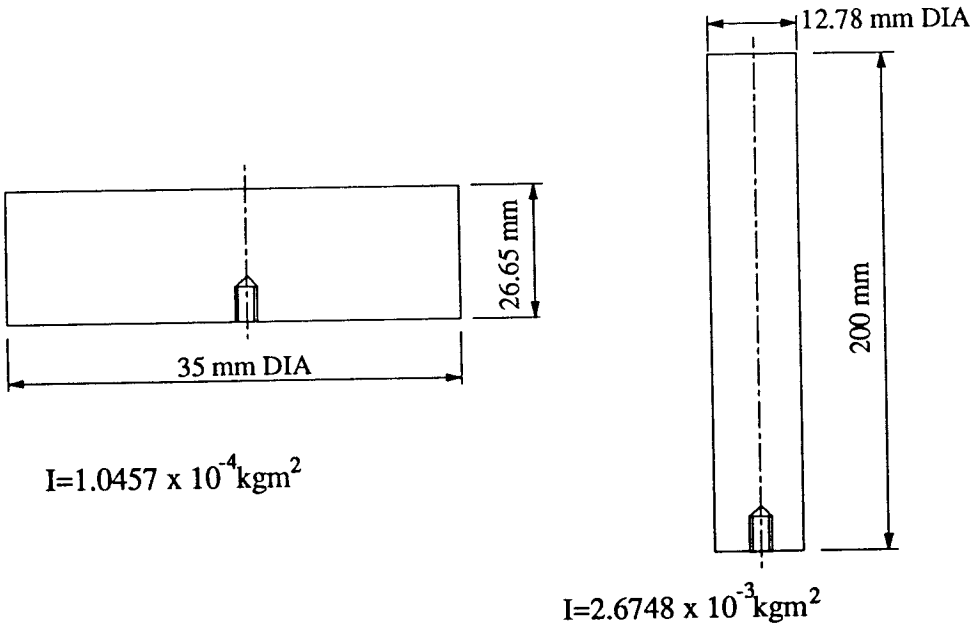

Figure A3.3: Dimensions of the Experimental Mass Modifications on the Perspex Cantilever

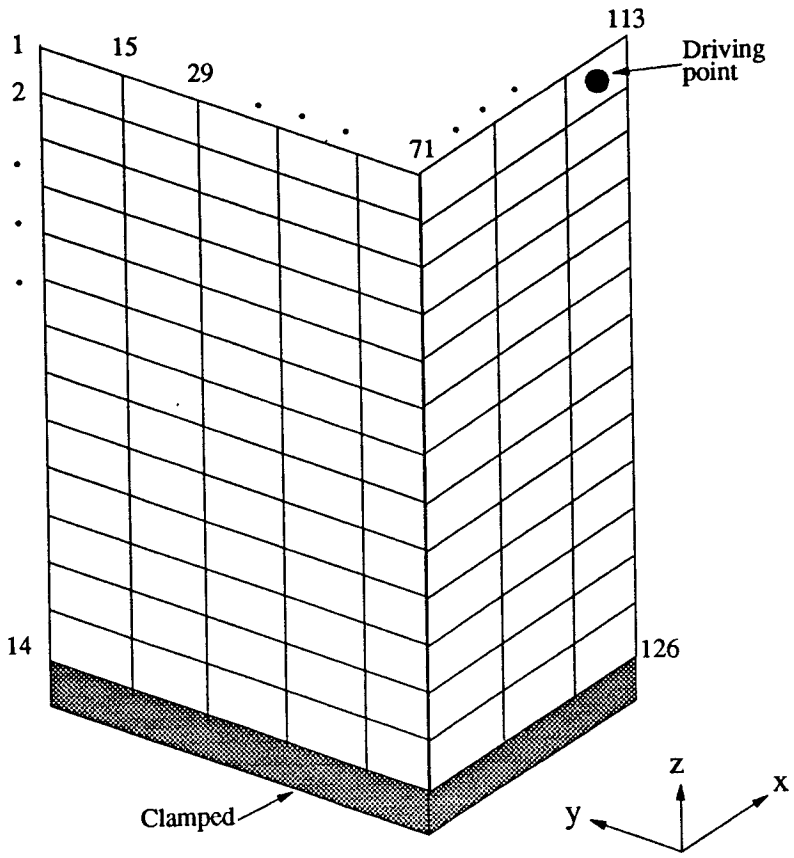

Figure A3.4: Idealisation of the L-Beam Structure

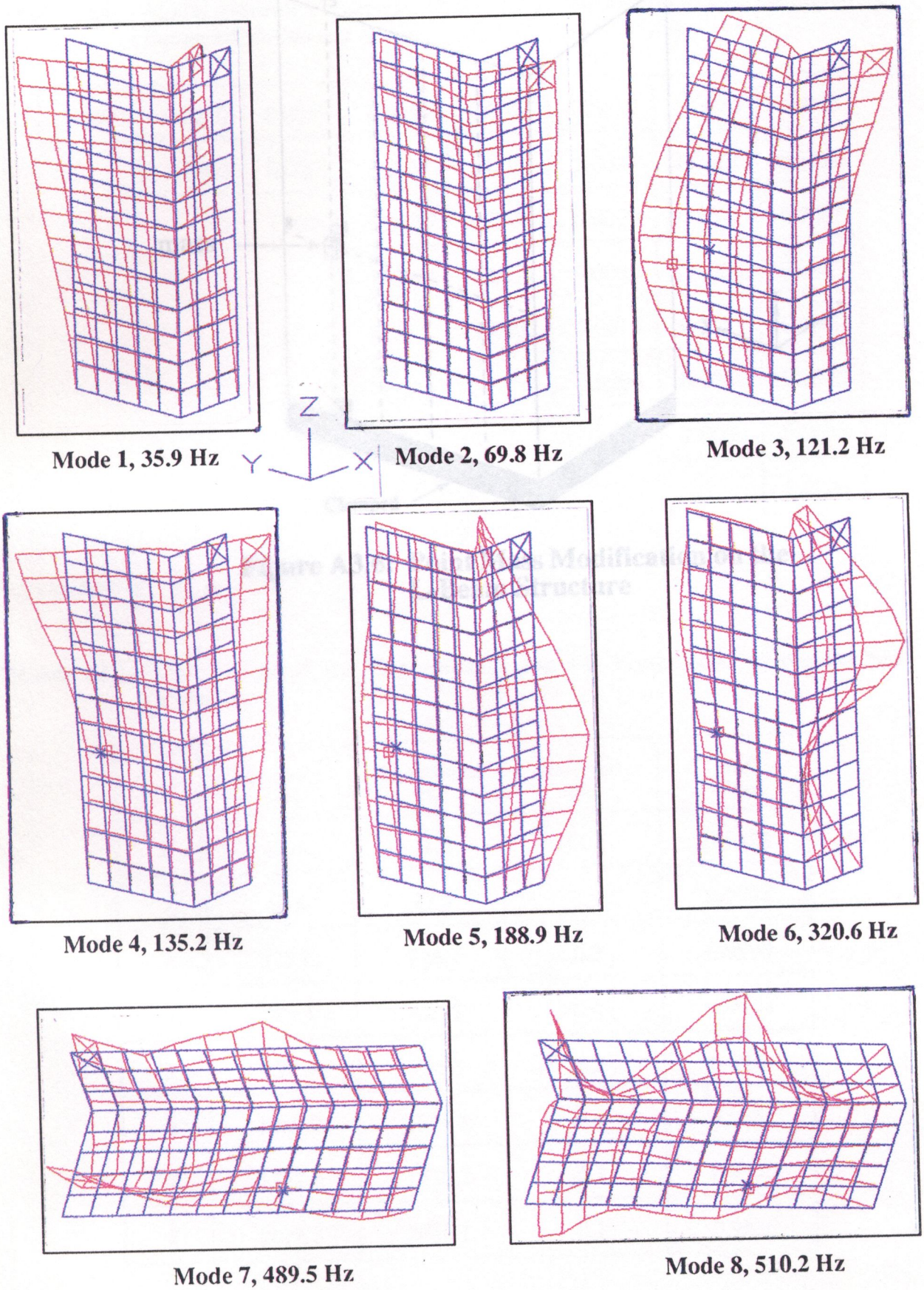

Figure A3.5: **Modeshapes of the Unmodified L-Beam Structure**

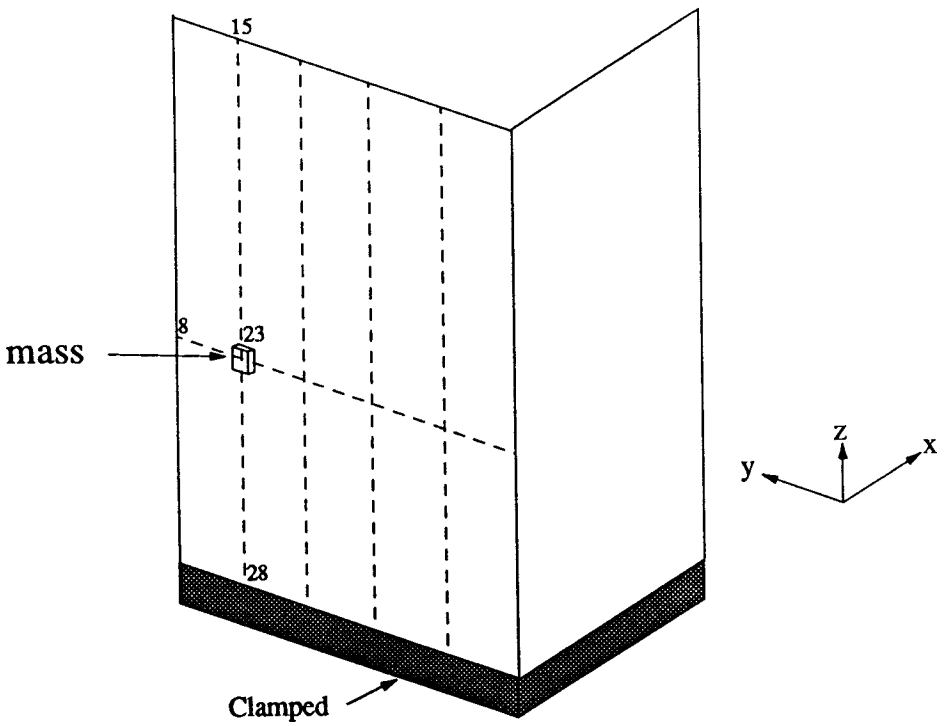

Figure A3.6: Point Mass Modification on the L-Beam Structure

Table A3.1: Modal Assurance Criterion Matrix for Experimental Modal Vectors of the Perspex Cantilever

1.0000	0.0000	0.0029	0.0066	0.0014	0.0010	0.0010	0.0035
	1.0000	0.0061	0.0012	0.0024	0.0047	0.0009	0.0090
		1.0000	0.0026	0.0038	0.0020	0.0001	0.0087
			1.0000	0.0051	0.0050	0.0008	0.0072
				1.0000	0.0013	0.0023	0.0060
					1.0000	0.0006	0.0072
						1.0000	0.0039
							1.0000

Table A3.2: Comparison of the Experimental and FE Frequencies of the Perspex Cantilever

mode	FE solution (Hz)	Experimental (Hz)	Discrepancy (%)	MAC Value
1	12.9	11.6	11.2	0.9972
2	80.5	77.8	3.5	0.9998
3	225.1	224.7	0.2	0.9990
4	441.3	439.5	0.4	0.9962
5	733.0	734.3	0.2	0.9928
6	1089.9	1094.8	0.4	0.9882
7	1522.8	1520.3	0.2	0.9553
8	2028.3	2030.1	0.1	0.9830

Table A3.3: Modal Assurance Criterion Matrix for the Comparison between the Unmodified Experimental Modal Vectors and the Modified Experimental Modal Vectors (Short Cylinder Modification)

0.9985	0.0277	0.1049	0.0131	0.0768	0.0026	0.0203	0.0047
0.0360	0.8929	0.0517	0.0077	0.0436	0.0003	0.0030	0.0006
0.0152	0.3861	0.8646	0.0000	0.0004	0.0015	0.0056	0.0181
0.0001	0.1273	0.2676	0.6803	0.1107	0.0108	0.0032	0.0004
0.0623	0.2628	0.1557	0.2693	0.5045	0.1101	0.0011	0.0000
0.0199	0.1238	0.0946	0.0880	0.1767	0.5096	0.2688	0.0370
0.0748	0.1295	0.0734	0.1145	0.1452	0.0281	0.3689	0.1187
0.0861	0.1687	0.1744	0.0748	0.1667	0.0205	0.2275	0.5028

Table A3.4: Perspex Cantilever with a short cylindrical mass near the tip

mode	Unmodified Beam (Hz)	Modified Beam (Hz)	Error in rotation at modification location (%)	Error in Frequency Prediction (%)			
				(1)	(2)	(3)	(4)
1	11.6	4.5	-51.2	35.6	35.6	35.5	33.3
2	77.8	59.8	-16.4	2.0	2.2	2.1	-3.2
3	224.7	175.9	-3.9	1.3	2.2	2.1	1.4
4	439.5	314.7	-9.2	4.3	9.2	9.1	12.8
5	734.3	477.6	-3.0	10.1	19.7	18.8	11.4
6	1094.8	732.2	-2.8	10.8	20.7	20.4	26.1
7	1520.3	1188.0	-28.1	0.6	9.9	8.9	9.8
8	2030.1	1620.0	4.2	1.2	11.8	11.8	7.3

Key:
(1) Finite Element Prediction
(2) FE translations and rotations
(3) FE translations and Calculated rotations from FE data
(4) Calculated translations and rotations from experimental data

Table A3.5: Modal Assurance Criterion Matrix for the Comparison Between the Unmodified Experimental Modal Vectors and the Modified Experimental Modal Vectors (Long Cylinder Modification)

0.9991	0.0238	0.0479	0.0042	0.0183	0.0004	0.0081	0.0013
0.0330	0.8543	0.2852	0.0357	0.0022	0.0041	0.0000	0.0000
0.0167	0.5008	0.1381	0.4708	0.0283	0.0010	0.0006	0.0109
0.0000	0.1952	0.1118	0.0437	0.5930	0.0282	0.0003	0.0019
0.0647	0.3166	0.0172	0.0646	0.0762	0.2875	0.0024	0.0027
0.0208	0.1541	0.0144	0.0126	0.0353	0.2923	0.4137	0.0493
0.0765	0.1498	0.0067	0.0252	0.0191	0.0061	0.2377	0.1796
0.0882	0.2058	0.0296	0.0003	0.0288	0.0033	0.1605	0.4170

Table A3.6: Perspex Cantilever with a long cylinder near the tip

mode	Unmodified Beam (Hz)	Modified Beam (Hz)	Error in rotation at modification location (%)	Error in Frequency Prediction (%)			
				(1)	(2)	(3)	(4)
1	11.6	4.4	-51.2	34.1	34.1	33.7	34.1
2	77.8	32.3	-16.4	6.2	9.3	9.0	-10.2
3	224.7	93.8	-3.9	7.7	14.4	14.2	24.3
4	439.5	240.4	-9.2	3.7	10.4	10.4	16.3
5	734.3	460.5	-3.0	3.8	11.1	10.9	2.1
6	1094.8	766.0	-2.8	2.4	10.4	10.1	16.5
7	1520.3	1209.0	-28.1	-3.5	4.8	4.8	4.4
8	2030.1	1581.0	4.2	2.9	13.5	13.4	8.9

Key:
(1) Finite Element Prediction
(2) FE translations and rotations
(3) FE translations and Calculated rotations from FE data
(4) Calculated translations and rotations from experimental data

Table A3.7: Joint Line Considerations for θ_z for the L - Beam Structure for mode 2

Measurement Point Number	FE estimate ($1/m.kg^{½}$)	Calculated Rotations about z-axis ($1/m.kg^{½}$)		
		best fit from P1	best fit for θ_y from P1	best fit from P2
71	6.42533	6.29215	5.87983	7.76126
72	6.76341	6.80441	6.19192	6.70045
73	7.09225	6.99000	6.35433	5.87479
74	7.41925	6.91783	6.37444	5.24123
75	7.56889	6.65685	6.25964	4.75673
76	7.50005	6.27597	6.01730	4.37825
77	7.11812	5.84345	6.65480	4.06205
78	6.47521	5.38434	5.17954	3.75726
79	5.56628	4.85508	4.59889	3.40898
80	4.32481	4.20773	3.92023	2.96225
81	2.94849	3.42164	3.15095	2.36211
82	1.55738	2.49789	2.29842	1.55361
83	0.44153	1.43814	1.37003	0.48180
84	0.00000	0.24407	0.37317	-0.90828

Table A3.8: Joint Line Considerations for θ_x and θ_y for the L - Beam Structure for mode 2

measurement point number	θ_y (1/m.kg^{½})			θ_x (1/m.kg^{½})	
	(1)	(2)	(3)	(1)	(2)
71	2.36839	1.57765	2.16181	-0.82210	-1.32368
72	3.00945	1.98472	2.18920	-1.45207	-1.12647
73	2.92447	2.21298	2.20948	-1.33199	-0.98597
74	2.87644	2.23704	2.22263	-1.33568	-0.90218
75	2.86905	2.42107	2.22866	-1.32829	-0.87510
76	2.82471	2.23649	2.22757	-1.30243	-0.90473
77	2.63073	2.21133	2.21936	-1.24516	-0.97104
78	2.44599	2.08965	2.20402	-1.13986	-1.01839
79	2.18735	2.04091	2.18156	-1.03825	-1.04350
80	1.88252	2.05467	2.15198	-0.90524	-1.04638
81	1.53521	2.08595	2.11527	-0.74820	-1.02703
82	1.09552	2.12961	2.07144	-0.55237	-0.98545
83	0.75560	2.18563	2.02049	-0.49326	-0.92163
84	0.00000	2.25403	1.96242	0.00000	-0.83558

Key:
(1) FE estimate
(2) Best fit for θ_z
(3) best fit for θ_y

Table A3.9a: Point Mass Modification on the L - Beam Plate Structure; Mass = 0.51 kg

mode	unmodified Structure (Hz)	Modified Structure (Hz)	Error in FE Prediction (%)	Error in Modal Prediction of Frequency (%)			
				(1)	(2)	(3)	(4)
1	35.9	31.6	-10.44	-0.13	-0.63	0.00	12.03
2	69.8	68.8	4.65	5.38	0.00	0.00	1.31
3	121.2	83.5	5.75	5.75	0.00	0.24	36.05
4	135.2	134.5	16.80	16.88	-0.22	-0.22	0.15
5	188.9	183.9	-1.09	-0.49	0.82	0.82	2.23
6	320.6	320.0	-4.50	-4.38	-0.31	-0.28	0.06
7	489.5	486.6	-1.81	0.62	-1.85	-1.77	0.39
8	510.2	507.8	-2.64	0.65	-0.55	-0.57	0.37

Key:
(1) FE rotations
(2) Calculated rotations from Experimental data
(3) Calculated translations and rotations from Experimental data
(4) STAR prediction

Table A3.9b: Error in the Translation and Rotation at the Point Mass Modification Location (measurement point 23) on the L - Beam Structure. Comparison base is FE data.

mode	% error in the translation		% error in the calculated rotation	
	measured	Calculated	θ_y	θ_z
1	-1.538	-3.553	-1.994	-16.962
2	-43.318	-49.156	95.596	-5.979
3	-0.555	-1.418	3.430	11.011
4	81.415	82.485	-49.018	87.549
5	-29.333	-29.762	7.634	-37.603
6	-31.594	-35.004	-41.225	-53.023
7	70.168	59.120	55.380	331.883
8	30.184	30.813	11.040	491.299